HELEN COOPER

# Regulating Mitochondrial Function

## The roles of SIRT3 as a mitochondrial protein deacetylase, and the functions of the Twinkle helicase in mitochondrial DNA maintenance

■

ACADEMIC DISSERTATION
To be presented, with the permission of
the Faculty of Medicine of the University of Tampere,
for public discussion in the Lecture Room of Finn-Medi 5,
Biokatu 12, Tampere, on December 5th, 2009, at 13 o'clock.

UNIVERSITY OF TAMPERE

ACADEMIC DISSERTATION
University of Tampere, Institute of Medical Technology
Tampere Graduate School in Biomedicine and Biotechnology (TGSBB)
Finland

*Supervised by*
Professor Johannes N. Spelbrink
University of Tampere
Finland

*Reviewed by*
Professor John M. Denu
University of Wisconsin
USA
Professor José Antonio Enriquez
University of Zaragoza
Spain

Distribution
Bookshop TAJU
P.O. Box 617
33014 University of Tampere
Finland

Tel. +358 3 3551 6055
Fax +358 3 3551 7685
taju@uta.fi
www.uta.fi/taju
http://granum.uta.fi

Cover design by
Juha Siro

Acta Universitatis Tamperensis 1481
ISBN 978-951-44-7923-6 (print)
ISSN-L 1455-1616
ISSN 1455-1616

Acta Electronica Universitatis Tamperensis 916
ISBN 978-951-44-7924-3 (pdf)
ISSN 1456-954X
http://acta.uta.fi

Tampereen Yliopistopaino Oy – Juvenes Print
Tampere 2009

*Du kan. Inget berg är för brant, om du tror blir det sant. Du kan!*
*(You can. No hill is too steep, have faith and you'll succeed. You can!)*
*Carolina Klüft, Swedish Olympic athlete*

*To my family*

# Table of contents

# List of original publications

This thesis is based on the following articles:

I. **Cooper HM** and Spelbrink JN.
The human Sirt3 protein deacetylase is exclusively mitochondrial.
*Biochem J.* 411(2): 279-85, 2008

II. Goffart S**, Cooper HM**, Tyynismaa H, Wanrooij S, Suomalainen A, Spelbrink JN.
Twinkle mutations associated with autosomal dominant progressive external ophthalmoplegia lead to variable enzyme defects and *in vivo* mtDNA replication stalling. *Hum Mol Genet* 18 (2):328-40, 2009.

III. **Cooper HM***, Huang JY*, Verdin E, Spelbrink JN.
A new splice variant of the mouse SIRT3 gene encodes the mitochondrial precursor protein *PLoSONE* 4:e4986, 2009.

IV. **Cooper HM**,* Wanrooij PH* & Spelbrink JN.
hSIRT3 deacetylates acetyl-coA acyltransferase 2 (ACAA2) and can stimulate acetyl-CoA production *Submitted to BBRC*

*Joint first-authorship

# Abstract

Mitochondria are responsible for many important cellular functions including energy production, the biosynthesis of cellular constituents, ion storage and programmed cell death. These events are controlled at several levels and are influenced by both the nuclear and mitochondrial DNA (mtDNA). This thesis presents a multifaceted study of the regulation of mitochondrial function from the point of view of enzymes involved in controlling metabolic pathways and enzymes that take part in mtDNA maintenance.

A recent discovery of the acetylation of mitochondrial proteins suggests that acetylation/deacetylation mediated control is an important way of influencing mitochondrial protein function. This notion is further supported by the presence of at least three mitochondrial SIR2-deacetylases, sirtuins (SIRT3-5). These enzymes are dependent on NAD and have been shown to influence the action of metabolic proteins. Especially SIRT3 has been shown to target components of the tricarboxylic acid cycle and the electron transport chain. SIRT3 can also promote acetyl-CoA production by activating the mitochondrial acetyl-CoA synthetase, AceCS2. In general, the highly conserved SIR2-deacetylases have been associated with the control of metabolism and cell survival in response to nutrient levels in several organisms. In this thesis work I set out to further elucidate the role of SIRT3 by investigating its potential targets among acetylated mitochondrial proteins. I here present evidence on the hSIRT3 mediated control of beta-oxidation enzymes of the mitochondrial fatty-acid oxidation pathway. And together with the finding that hSIRT over-expression can increase acetyl-CoA production in human cells the results presented here support the role of hSIRT3 in controlling nutrient flux and energy producing pathways.

I also addressed the question of the subcellular location of human SIRT3 as well as the possible length variant of its mouse homologue, mSIRT3. According to the studies described here, both full-length mouse and human SIRT3 are mitochondrial.

These observations clarify various discrepancies in the reported behaviour of the proteins and further demonstrate the strong conservation between the two proteins.

Mitochondrial function is dependent on its genome, which codes for components of the electron transport chain. The mitochondrial genome in turn is dependent on nuclear genes for its maintenance. Mutations to mtDNA maintenance proteins cause disorders, which involve impaired energy production. I have studied the molecular properties of various disease causing mutants of the mtDNA helicase Twinkle. These mutations cause autosomal progressive dominant opthalmoplegia (adPEO), which is a neuromuscular disease characterised by multiple mtDNA deletions in the post-mitotic tissues of patients. The results presented here show that Twinkle adPEO mutants are compromised in various biochemical properties including their ability to bind and unwind DNA. Expression of the mutants in human cells and mouse tissues result in a replication stalling phenotype. These studies shed light on the molecular mechanisms of mtDNA maintenance in health and disease.

# Abbreviations

| | |
|---|---|
| adPEO | autosomal dominant progressive external ophthalmoplegia |
| ADP | adenosine diphosphate |
| AMP | adenosine monophosphate |
| ATP | adenosine triphosphate |
| CNS | central nervous system |
| CPTI | carnitine palmitoyl transferase I |
| CPTII | carnitine palmitoyl transferase II |
| dNTP | deoxynucleoside triphosphate |
| dsDNA | double stranded DNA |
| ETF | electron transfer flavoprotein |
| FADH | flavin adenine dinucleotide |
| FADH2 | flavin adenine dinucleotide, reduced form |
| FAO | fatty acid oxidation |
| HEK | human embryonic kidney |
| IM | mitochondrial inner membrane |
| IIS | insulin/Igf signalling |
| mtDNA | mitochondrial DNA |
| mtSSB | mitochondrial single strand DNA-binding protein |
| NA | nicotinic acid |
| NAAD | deamido nicotinamide adenine dinucleotide |
| NAM | nicotinamide |
| NAMN | nicotinic acid mononucleotide |
| NAD | nicotinamide adenine dinucleotide (oxidised form) |
| NADH | nicotinamide adenine dinucleotide (reduced form) |
| Namprt | nicotinamide phosphoribosyl transferase |
| Namnt | nicotinamide mononucleotide adenylyl transferase |
| NMN | nicotinamide mononucleotide |
| OM | mitochondrial outer membrane |

| | |
|---|---|
| OXPHOS | oxidative phosphorylation |
| PDH | puryvate dehydrogenase |
| PDK | pyruvate dehydrogenase |
| PGC-1α | Peroxisome proliferator-activated receptor gamma, coactivator 1 alpha |
| POLG | polymerase gamma, the mitochondrial DNA polymerase |
| POLGA | the catalytic subunit of POLG |
| POLGB | the accessory subunit of POLG |
| QA | quinolic acid |
| SIR | silent information regulator |
| ssDNA | single stranded DNA |
| TCA | tricarboxylic acid |
| TFAM | mitochondrial transcription factor A |
| TSA | trichostatin A |
| Twinkle | the mitochondrial DNA helicase |

# 1. Introduction

Mitochondria are intracellular organelles, which are responsible for the majority of cellular energy production. Several catabolic and anabolic pathways converge and diverge within mitochondria, and it is the regulation of nutrient flow through these pathways that is required to maintain a balanced energy state and bodily functions. The regulation of energy production is complex and involves the action of proteins that respond to the presence or absence of metabolites. Among such regulators are the sirtuin deacetylases, which can influence the behaviour of target proteins in an NAD-dependent fashion. Sirtuins belong to the highly conserved SIR2-family of deacetylases, which is associated with responses to nutrient levels and stress stimuli and at least in lower eukaryotes, lifespan extension. Mammals have three mitochondrial sirtuins, which are of particular interest, as they can directly influence metabolic enzymes and may have a role in the development of conditions such as type 2 diabetes.

Mitochondria also contain their own DNA (mtDNA), which has an important influence on energy production, as mtDNA codes for components of the energy producing respiratory chain. Mutations in mtDNA impair energy production and underlie a number of neuro-muscular disorders. Secondary mtDNA mutations can be caused by defects in mtDNA maintenance, as is the case in autosomal dominant progressive ophthalmoplegia (adPEO), an adult onset disease of the ocular muscles.

In this thesis I have studied the targets of a human mitochondrial sirtuin, hSIRT3, in order to expand our understanding of how and in which situations it controls metabolism. I have also examined the subcellular localisation of hSIRT3 and its mouse homolog mSIRT3. Finally, I have addressed the mechanisms of mitochondrial maintenance in health and disease by studying adPEO causing mutants of the mitochondrial DNA helicase, Twinkle.

# 2. Review of the literature

## 2.1 Energy metabolism

The regulation of energy production and storage is vital for the survival of organisms. Inside cells key biochemical pathways are devoted to the conversion of food molecules into charged energy compounds that can drive reactions. These pathways are regulated and connected to each other through the action of small molecules that sense and convey changes in nutritional state, stress levels, developmental stages and other influences such as pathologies. This chapter describes the main energy producing pathways, major regulatory systems and highlights emerging mechanisms in controlling energy metabolism at the cellular level.

### 2.1.1 Energy producing pathways

#### *2.1.1.1 Glucose catabolism*

Glucose is the building block of sugars and the principal energy source of cells. The six-carbon carbohydrate can be broken down to yield a net total of up to 38 molecules of adenosine triphosphate (ATP), a charged compound that can donate its energy to cellular reactions. The catabolism of glucose begins in the cytosol, where it is broken down into two three-carbon pyruvate molecules in a process called glycolysis. Glycolysis yields two molecules of ATP, and when oxygen is limiting, such as in skeletal muscle during strenuous exercise, glucose catabolism doesn't proceed beyond glycolysis. Puryvate is then reduced to lactate by lactose dehydrogenase.

Under aerobic conditions pyruvate is oxidised and decarboxylated to acetyl-CoA and $CO_2$. In eukaryotic cells this and the following reactions take place in specialised compartments called mitochondria, which are double-membrane bound

organelles (Fig 2.8 and section 2.4). Acetyl-CoA transfers its two carbons to oxaloacetate to form citrate, which is oxidised by the enzymes of the tricarboxylic acid (TCA) cycle (Fig 2.1). Acetyl-CoA derived from the break-down of proteins and fatty-acids can also enter the TCA cycle. In the cycle, also known as the citric acid or Krebs cycle, a series of enzymes removes electrons from citrate and passes them onto the coenzymes NAD+ and FADH+ to form their reduced forms, NADH and FADH2, respectively. NADH and FADH2 then carry and transfer the electrons to the electron transport chain, which consists of four enzyme complexes (I-IV) embedded in the inner mitochondrial membrane (Fig 2.2). The electron transport chain passes the electrons to molecular oxygen to produce water, and simultaneously pumps protons from the mitochondrial matrix into the intermembrane space. The movement of protons creates an electro-chemical gradient across the membrane. Protons then flow down the gradient back into the matrix through ATP synthase, which uses the proton movement to phosphorylate ADP molecules to form ATP. This entire process, in which electrons flow to oxygen is coupled to ATP synthesis, is called oxidative phosphorylation and is the most efficient step in producing cellular ATP.

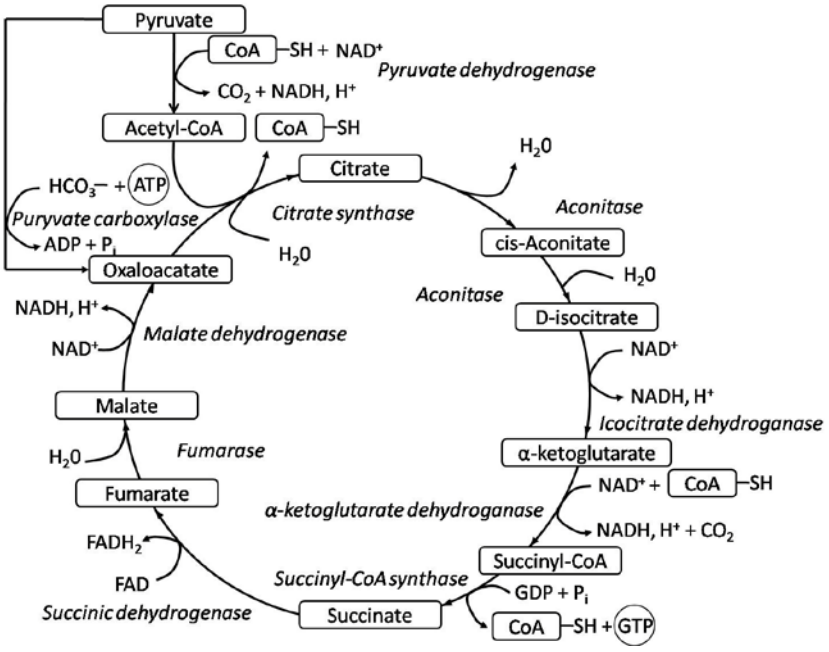


**Figure 2.1. TCA cycle**. Pyruvate is converted to acetyl-CoA, which enters the cycle and reacts with oxaloacetate to form citrate. A series of enzymatic steps then oxidise citrate, and the resulting electrons are transferred to the electron carriers NAD and FAD, which can feed them into the electron transport chain. The final step regenerates oxaloacetate to complete the cycle.

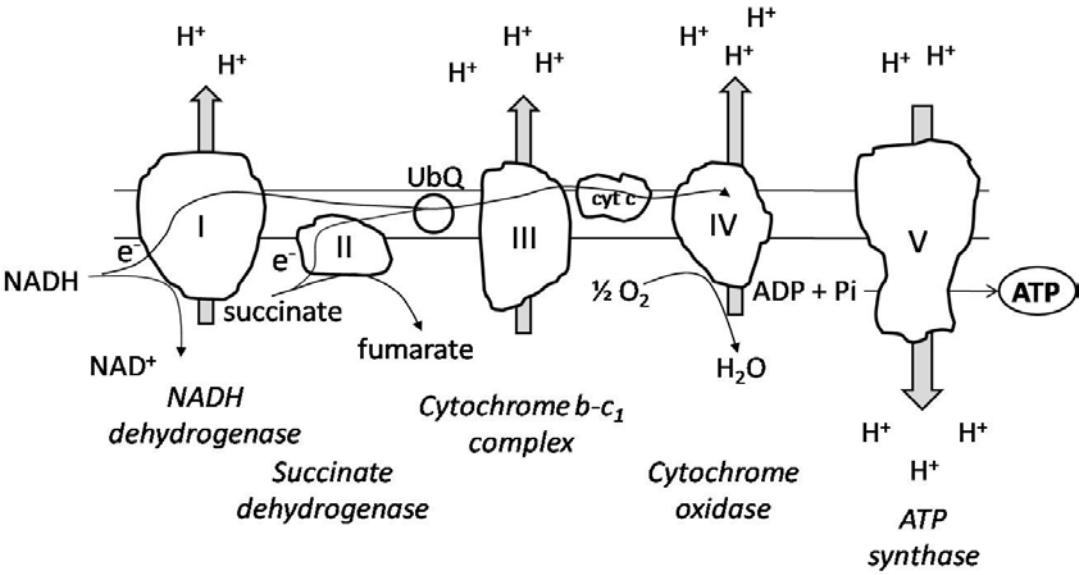


**Figure 2.2. Electron transport chain.** Electrons pass through the complexes (I-IV) in the inner mitochondrial membrane to molecular oxygen to form water. Simultaneously hydrogen ions are pumped from the matrix into the intermembrain space. This creates an electro-chemical gradient, down which the hydrogen ions flow back into the matrix through ATP synthase (V) enabling it to phosphorylate ADP to ATP.

#### *2.1.1.2 Beta-oxidation of fatty-acids*

Fat stores are an important source of energy, particularly for the cardiac and skeletal muscle. Long-chain fatty-acids are oxidised to produce energy primarily by the β-oxidation pathway, which resides in the mitochondrion (and peroxisomes, not discussed here). This multistep pathway was one of the first biochemical pathways to be described (Eaton et al., 1996)

When glucose is scarce, e.g. during periods of fasting, triacylglycerol stores in fat depot are hydrolysed into free fatty acids and released into the blood stream. Free fatty acids can be taken up and oxidised by most tissues, except for the central nervous system (CNS). The CNS has an obligatory requirement for glucose and by switching to a fuel economy based on lipolysis, other tissues allow the movement of any available glucose to the CNS. After they have entered the cell, fatty acids are activated to acyl-CoA esters by acyl-CoA synthetases. They can then be targeted to mitochondria to undergo β-oxidation for the production of energy. Acyl-CoA esters cannot enter the mitochondria directly; the acyl-group is transferred from CoA to carnitine by carnitine palmitoyl transferase I (CPTI) on the outer mitochondrial membrane, after which it can cross the membrane as an acyl-carnitine intermediate

through the action of the acyl-carnitine translocase (Fig 2.3). Inside the mitochondria palmitoyl transferase II (CPTII) then reconverts it back to acyl-CoA. Once the acyl-CoA ester has entered the mitochondrion it is committed to oxidation. This is accomplished by a series of four repeated enzymatic steps, which ultimately produce Acetyl-CoA. There are multiple enzymes for each of the constituent steps of the chain shortening pathway, which vary in their chain length specificity (Fig 2.4). The β-oxidation pathway produces reduced co-factors, which can directly feed electrons into the electron transport chain: the first dehydrogenation is linked to the electron transport chain through the flavoprotein ETF and and ETF-ubiquinone oxidoreductase, the second dehydrogenation step is linked to complex 1 of the respiratory chain via NADH. In most tissues acetyl-CoA enters the TCA cycle for the generation of ATP. In liver and other ketogenic tissues most of the acetyl-CoA is used to form ketone bodies (acetoacetate and 3-hydroxybutyrate), which can be exported for oxidation by e.g. the CNS.

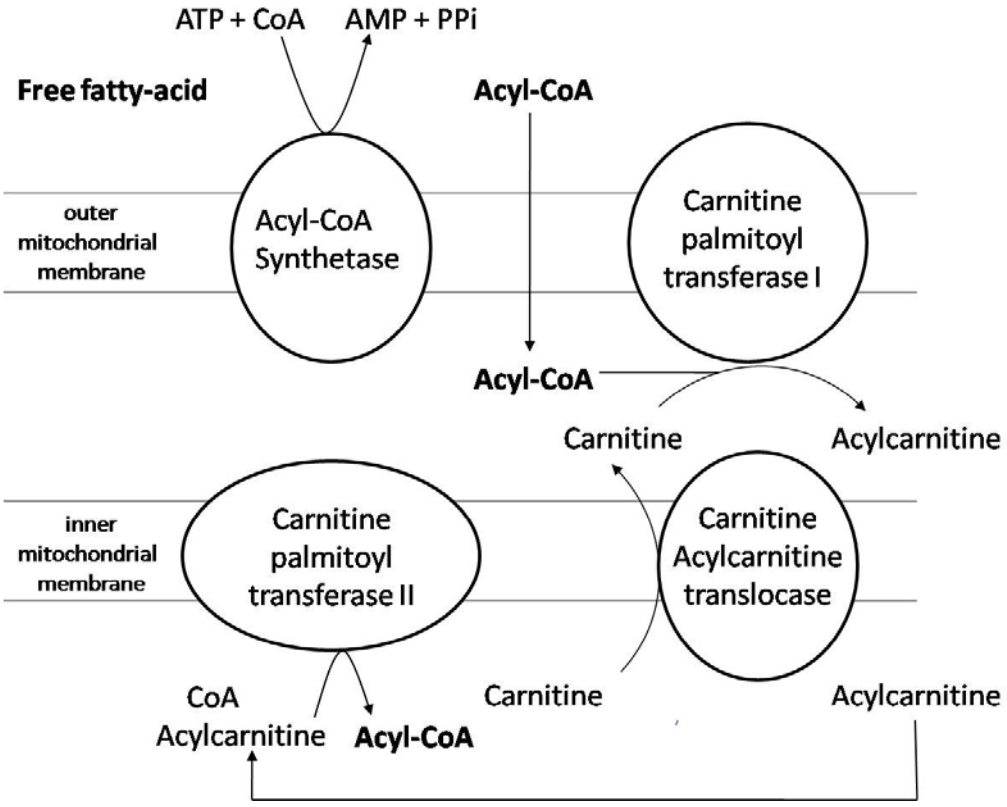


**Figure 2.3. Carnitine translocase shuttle**. Long-chain fatty acids cross the outer mitochondrial membrane bound to CoA. Carnitine palmitoyltransferase then swaps CoA for carnitine. The resulting acylcarnitine complex diffuses through the inner membrane into the matrix facilitated by the carnitine-acylcarnitine translocase. The acyl-cartinine complex is disrupted by carnitine palmitoyltransferase II and the fatty acid rebinds to CoA. Carnitine then diffuses back across the membrane into the inter-mitochondrial membrane space.

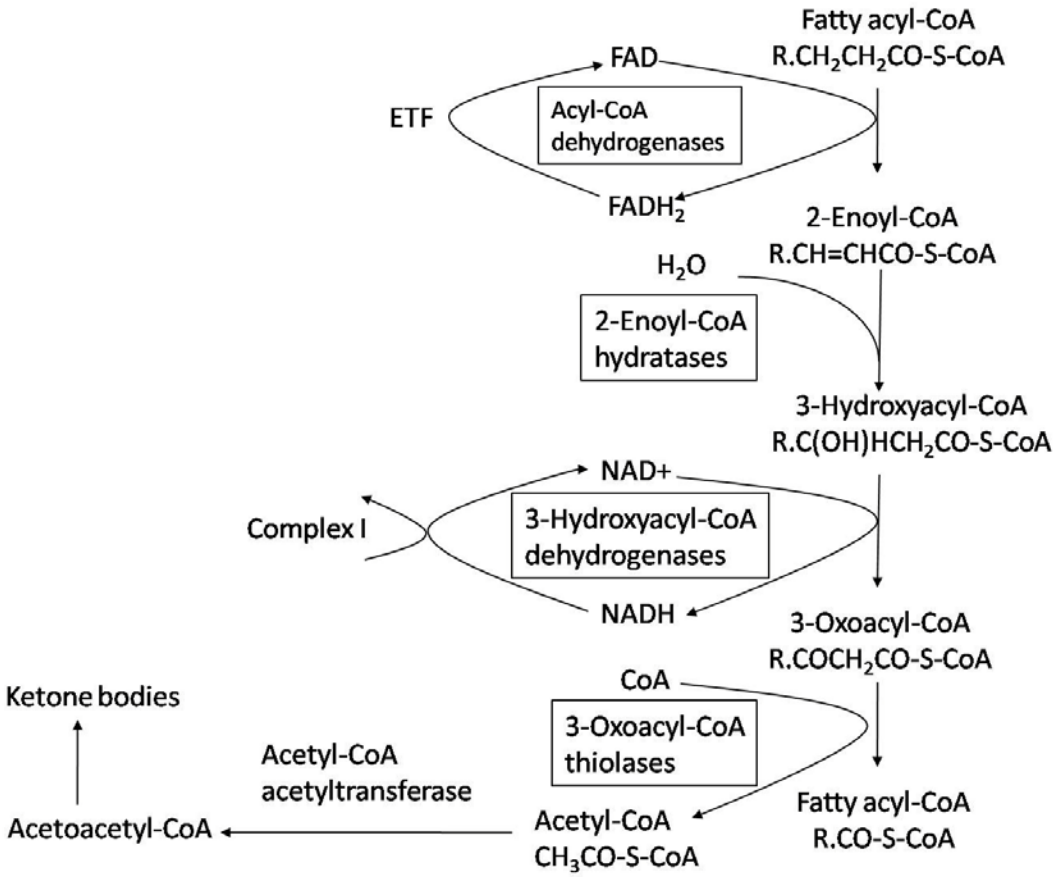


**Figure 2.4. Beta-oxidation of fatty acids**. Fatty acids, in the form of fatty-acyl-CoA molecules, are broken down in the mitochondrial matrix through four recurring enzymatic steps. For every cycle the acyl-CoA unit is shortened by two carbon atoms. The process continues until the entire chain is cleaved into acetyl-CoA units. Acetyl-CoA can be further converted into acetoacetyl-CoA, a precursor for ketone bodies. In addition to acetyl-CoA, one molecule and NADH and FADH are formed in each round. The electron transferring protein (ETF) passes electrons to ubiquinone in the electron transport chain.

## 2.1.2 Regulation of cellular metabolism

### *2.1.2.1 Insulin*

Insulin is a potent anabolic hormone, which promotes the synthesis and storage of carbohydrates, lipids and proteins and simultaneously prevents their degradation and release into the circulation. Insulin metabolism is of significant interest, since it plays a key role in type 2 diabetes and metabolic syndrome, and is a potential target for therapy. Insulin is secreted by pancreatic β-cells in response to a glucose containing meal. It promotes glucose uptake in muscle and adipose tissue. Insulin binds to its receptor, a heterotetrameric tyrosine kinase and through the activation of

signalling cascades stimulates the translocation of the glucose transporter GLUT4 from intracellular sites to the cell surface. This leads to glucose uptake primarily in skeletal muscle. Adipose tissue accounts for only a small fraction of the overall glucose uptake, but nevertheless plays an important role in insulin mediated glucose regulation, especially in the development of insulin resistance.

Insulin resistance is the inability of target tissues to respond to circulating insulin, and is thought to be the initial defect underlying the development of type 2 diabetes (Warram et al. 1990, Ferrannini 1998). Adipose tissue releases free fatty-acids, which can block insulin signalling pathways. This lipolysis is especially prominent in visceral fat, which is also insensitive to insulin. Adipocytes also secrete biologically active molecules (Shouldiner et al. 2001, Goldstein 2001) such as tumour necrosis factor α (TNF-α), leptin and adiponectin, which can influence insulin action. Although the order of events leading to type 2 diabetes is currently a matter of dispute and the mechanisms of action are somewhat unclear, it is evident that large amounts of body fat contribute to insulin resistance and subsequent hyperglycemia.

In the liver, insulin stimulates glucose storage as glycogen and lipid, and represses glucose synthesis and release. To accomplish this, insulin promotes the expression of genes encoding enzymes that are required for the synthesis of glycogen and fatty-acids, while repressing those needed in gluconeogenesis, the generation of glucose from non-carbohydrate sources. Hepatocytes, which do not respond to insulin normally, will keep on producing glucose via gluconeogenesis and release it into the blood stream, thus contributing to hyperglycemia.

At first pancreatic β-cells will secrete more insulin in response to high blood glucose, but when the hyperglycaemic condition persists, β-cells lose their ability to respond to glucose intake, and type-2-diabetic patients show a delayed early response to glucose and a progressive overall insulin defiency (Bergstrom 1990). In addition to glucose, the amino acids arginine and leucine are effective insulin secretagogues. Importantly, this amino acid stimulated (AAS) insulin response is maintained even if the response to glucose is lost (Palmer et al. 1976), and certain amino acid derivatives can be used to stimulate β-cells to produce insulin in diabetic patients.

#### *2.1.2.2 Regulation of glucose break-down*

In addition to its role in generating ATP, glycolysis also provides building blocks for cellular components. The rate of conversion of glucose into pyruvate is regulated to meet these two requirements. Glycolysis is inhibited by high levels of ATP and citrate which signal that the oxidative phosporylation is carried out and that biosynthetic precursors are abundant, respectively. Conversely, high levels of adenosine monophosphate (AMP), which indicate an energy deficit, up-regulate glycolysis. At the hormonal level, transcription of key regulatory enzymes, namely glucokinase, phosphofructokinase and pyruvate kinase are upregulated by isulin and glucagon over a period of hours to days, in reflection to general energy status. Also the redox state, i.e. the balance of oxidized NAD to its reduced form NAHD (see below), is a crucial regulator of glucose metabolism.

#### *2.1.2.3 Regulation of beta-oxidation*

Fatty-acid catabolism depends on the availability of glucose. During food deprivation, mitochondrial fatty acid oxidation is increased in peripheral tissues. In muscle cells, the major regulatory metabolic enzyme that allows the shift from glucose to fatty acid oxidation, is pyruvate dehydrogenase kinase-4 (PDK4). PDK4 inactivates pyruvate dehydrogenase and prevents the entry of puryvate into the TCA cycle. The activity of PDK4 is regulated by nutrient deprivation (Sugden 1993). PDK4 expression is induced by the common transcriptional co-activator PGC-1α. PGC-1α has a key role in fatty-acid utilisation (Puigserver &Spiegelman 2003) and it induces OXPHOS genes to promote complete oxidation of fatty-acids in mitochondria (Wu 1999).

The entry of fatty acids into mitochondrial via carnitine palmitoyltransferase I is the major regulatory point for beta-oxidation. CPT1 is inhibited allosterically by Malonyl-CoA, an intermediate of fatty-acid oxidation. During fasting Malonyl-CoA levels are low; this maintains fatty-acid oxidation by allowing the entry of long-chain fatty-acids into mitochondria. High-levels signal sufficient energy production, prevent entry and promote fatty-acid synthesis. In contrast to long-chain fatty acids, medium- and short-chain fatty acids can cross the mitochondrial membrane directly and be oxidized as their CoA esters (Roe 2001). These fatty acids bypass the

carnitine shuttle and have therapeutic application in some disorders of fatty acid oxidation (FAO).

Apart from their involvement in FAO disorders (Kompare 2008), little is known about the β-oxidation enzymes or their regulation. This thesis presents a potential mechanism of regulating beta-oxidation enzymes by post-translational acetylation.

### 2.1.3 NAD

Nicotinamide adenine dinucleotide (NAD) is a ubiquitious molecule that participates in many biological processes. It serves as a coenzyme in redox reactions, but is also used as a substrate by some enzymes.

In cells, NAD is produced by two major pathways (reviewed by Magni et al. 1999). In the *de novo* pathway NAD is synthesised from trypthophan, which is converted first, through several steps into quinolic acid (QA), which is then converted into nicotinic acid mononucleotide (NAMN). In the salvage pathway NAD is generated by recycling degraded NAD products, nicotinamide (NAM) and nicotinic acid (NA) being the main precursors. The formation of NAD from nicotinamide differs between mammals and lower eukaryotes. In yeast, nicotinamide is hydrolysed to nicotinic acid, by a nicotinamidase, encoded by *PNC1*. NA is then converted to NAMN, which is converted to deamido-NAD, NAAD. NAAD is converted to NAD. Importantly, the invertebrate specific *PNC1* is thought to mediate the lifespan extending effect of calorie restriction (discussed below) (Anderson et al. 2003). Vertebrates lack any obvious homolog of the nicotinamidase (Rongvaux 2003) and NAD is synthethised from NAM in only two steps: to NMN by Namprt, nicotinamide phosphoribosyl transferase (Fig 2.5), and then to NAD by Namnt, nicotinamide mononucleotide adenylyl transferase. Namprt is the rate-limiting component in mammalian NAD biosynthesis and (Revollo 2004) has been shown to act as an NAD boosting gene (Yang 2007).

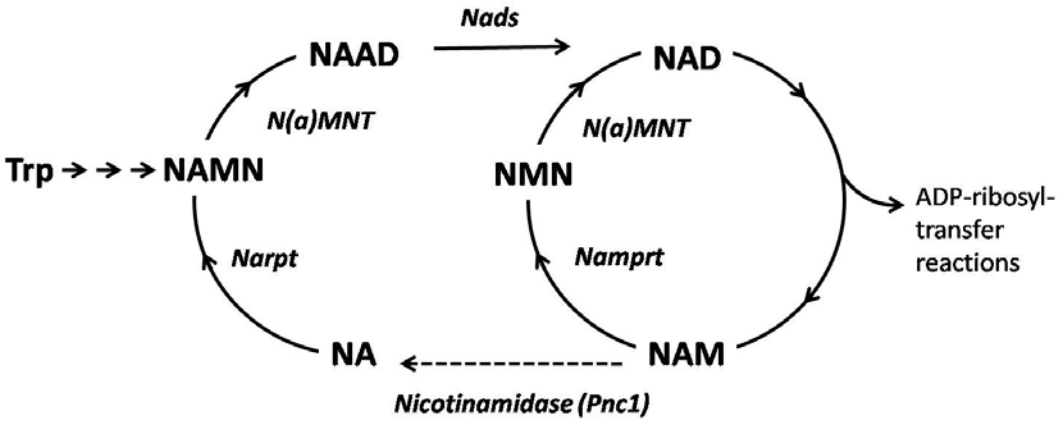


**Fig 2.5.** NAD synthesis. NAD can be produced either *de novo* from trypthopan or through the salvage pathway from nicotinamide (NAM). In vertebrates NAD is formed from NAM in two steps: nicotinamide phosphoribosyl transferase (Namprt) converts NAM to nicotinamide mononucleotide (NMN), which is then converted to NAD by nicotinamide mononucleotide adenylyl transferase, (Namnt). In yeast NAM is first hydrolysed by nicotinamidase to nicotinic acid (NA). Then the steps leading to NAD via nicotinic acid mononucleotide (NAMN) and deamido-NAD (NAAD) are catalysed by Narpt, Namnt and finally by NAD synthase (Nads). The last two steps of the yeast salvage pathway are shared by the *de novo* pathway in vertebrates and yeast.

NAD can carry electrons, and is converted to its reduced form NADH mostly in catabolic pathways such as glycolysis and the TCA cycle. NADH serves as a substrate for the NADH dehydrogenase of the mitochondrial respiratory chain, which transfers electron to coenzyme Q and re-oxidises NADH to NAD. Constant re-oxidation by the respiratory chain and other mechanism are vital for maintaining a proper redox balance, and the NAD:NADH ratio is considered a read-out of metabolic state. Many metabolic enzymes, such as the puryvate dehydrogenase complex, which produces acetyl-CoA from puryvate for the TCA cycle, are regulated by the NAD:NADH ratio. The term redox state is used to describe the balance of $NAD^+$/NADH and their phosphorylated forms $NADP^+$/NADPH in the cell. It is a reflection of the interconvertible oxidized and reduced forms of several sets of metabolites, such as lactate and pyruvate, β-hydroxybutyrate and acetoacetate. Accordingly, many metabolic, signalling and transcriptional events are influenced by the redox state. Maintaining sufficient amounts of available reducing equivalents is crucial in counteracting the potential damage by free radical intermediates, namely ROS (reactive oxygen species). The acute shift of the intracellular redox balance towards oxidation, known as oxidative stress, is due to increased production or insufficient degradation of ROS. The consequences of ROS to cellular damage and aging are discussed in section 2.5.

In addition to NADH dehydrogenase and other oxidoreductases, enzymes that use NAD as a substrate include NAD-dependant DNA ligases (Wilkinson 2001) and poly(ADP-ribose) polymerase (Bürkle 2001). Recent studies have linked NAD to transcriptional regulation, longevity and aging via the NAD-dependent SIR2-deacetylases.

## 2.2 SIR2-deacetylases

Members of the silent information regulator 2 (SIR2) family of genes encode NAD-dependent deacetylases, which are present in organisms ranging from archaebacteria to humans (Frye 2000), and are highly conserved between organisms (Brachmann 1995). SIR2-deacetylases can catalyse two reactions; deacetylation and ADP-ribosylation, both of which consume NAD. In the more common reaction, deasetylation of a lysine on the substrate protein, NAD is cleaved into nicotinamide and O-acetyl-ADP-ribose (Tanner et al. 2000) (Fig 2.6). This mechanism of action is unique and separates the SIR2-deactylases into their own group of class III deacetylases. The NAD-dependency suggests that SIR-activity is connected to metabolic state. In the yeast *Saccaromyces cerevisiae* Sir2p deacetylates histones thus silencing heterochromatin at telomeres, ribosomal DNA and mating type loci (Rusche et al. 2003). Sir2p suppresses the formation of extrachromosomal DNA circles in the nucleoli (Kaeberlein et al. 1999) thus extending replicative lifespan. Accordingly, an increase in Sir2p activity promotes longevity in yeast. The same lifespan extending effect is seen when the dosage of the homologous SIR2-gene is increased in *Caenorhabditis elegans* (Tissenbaum & Guarente 2001).

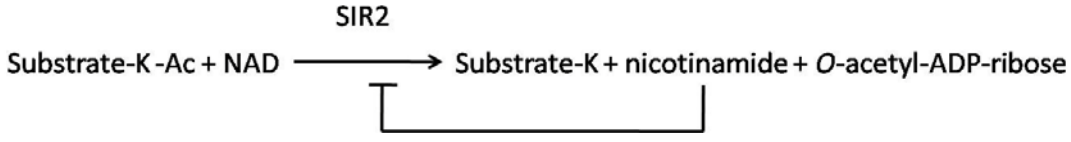


**Figure 2.6. SIR2-deacetylase reaction.**

A well known way of improving health and increasing the life-span of a wide range of organisms from yeast to mammals is calorie restriction. Reducing the daily calorie intake to about 60-70% of the amount an animal would eat *ad libitum*, can increase life span to up to twice that otherwise expected (MacCay et al. 1935, Richardson 1985, Lin et al. 2008). In addition to living longer, animals on a calorie restricted diet also have lower body temperature, lower blood glucose and insulin levels and reduced body fat (Koubova & Guarente 2003). They also appear to be more resistant to external stressors, such as heat and oxidative stress (Sohal & Weindruch 1996). Diluting the glucose in yeast growth media will also result in life span extension of the yeast i.e. the number of times the mother cells divide (Lin et al. 2002). This is dependent on the presence of SIR2, since CR did not expand life span in a SIR2-deficient yeast strain (Lin et al., 2000, 2002). Also, CR increased the silencing activity of Sir2p (Lin et al., 2002). The mechanism by which CR activated the Sir2-enzyme is unclear. Some studies have shown that CR boosts cellular respiration and shifts the NAD/NADH ratio in favour of NAD, which then increases Sir2p activity (Lin et al., 2002, 2004). Others have linked CR to the NAD salvage pathway, where the upregulation of the activity of the NAD synthesising enzyme Pnc1p reduces nicotinamide levels and thus relieves Sir2p inhibition (Anderson et al. 2002 &2003). However, since a yeast strain in which CR is independent of SIR2 has been described, possibly several pathways regulate CR in *S. Cerevisiaie* SIR2 (Kaeberlein et al. 2004). Nonetheless, it seems that a role for SIR2 in mediating CR has been conserved in metazoans, since several experiments indicate that CR activates the SIR2 ortholog Sir2 in Drosophila (Rogina et al. 2002, Rogina & Helfand 2004, Wood et al. 2004). The effect of CR in mammals is more complex and the connection between SIR2 and CR in mammals remains unclear. In mice, CR increases stress resistance (Sohal & Weindruchm 1999). Serum from CR mice enhanced the expression of SIRT1, the mammalian SIR2 ortholog in cultured fibroblasts (Cohen et al. 2004). Like Sir2p, SIRT1 is an NAD dependent deacetylase (Imai et al. 2000). However, it also targets many non-histone proteins (see below). Mammals have in fact multiple SIR2 –like proteins, sirtuins. The following section will review the known roles of SIR2 deacetylases in human and mouse.

### 2.2.1 Sirtuins

Humans have at least seven proteins (Sirt1-7), which share the catalytic domain with the yeast SIR2 (Blander & Guarente 2004, North & Verdin 2004). These sirtuins (from “sir-two-ins”) have been shown to act on different substrates and to localise to different cellular compartments (Michishita 2005). Human sirtuin deacetylases are emerging as important regulators of nutrient metabolism and cell survival; this links them to changes in metabolism and aging and related diseases such as cancer and type II diabetes.

**SIRT1** is a nuclear protein, with multiple reported targets. Of the seven human sirtuins it has the highest sequence similarity to Sir2 (Frye 2000) and is the most intensively studied sirtuin family member. SIRT1 has been shown to respond to changes in nutrient availability and stress by deacetylating several histone and non-histone targets. SIRT1 expression is induced by low levels of stress. Elevated levels of SIRT1 activity lead to deacetylation of p53, and repression of p53-dependent cell cycle arrest and apoptosis (Luo et al. 2001). SIRT1 epigenetically represses the expression and/or activity of many tumour proteins with DNA damage repair functions including Ku70 (Jeong 2007), and forkhead transcription factors (FOXO family (Motta et al. 2004, Brunet et al. 2004). And by deacetylating the heat shock factor 1 (HSF1) (Westerheide et al. 2009), SIRT1 positively regulates the transcription of heat shock proteins and activates the heat shock response. SIRT1 thus protects cells and promotes cell survival under low levels of stress. Extended survival responses during chronic stress may lead to tumour development. SIRT1 has been associated with several cancers, but having both oncogenic and tumor suppressive activities (see Deng 2009).

Over-expressing Nampt, the nicotinamide phosphoribosyl transferase of the NAD salvage pathway, increases SIRT1 transcriptional regulatory activity through the enhanced production of NAD (Revollo et al. 2004). NAD levels and the balance of NAD:NADH seem to be critical in controlling SIRT1 activity. Accordingly, SIRT1 can control nutrient metabolism by deacetylating key transcription factors and metabolic enzymes. And several lines of evidence suggest that SIRT tunes metabolism and stress resistance according to diet.

When glucose levels are low SIRT1 deacetylates and activates PGC-1α, the transcriptional co-activator, which promotes mitochondrial fatty-acid oxidation.

PGC-1α also upregulates the transcription of gluconeogenetic genes in the liver. Thus, when glucose is scarce SIRT1 promotes fatty-acid oxidation in extra hepatic tissues. And to provide glucose to the CNS, SIRT1 simultaneously promotes gluconeogenesis in the liver (Rodgers et al. 2005). The presence of SIRT1 is required for the increase in the rate of fatty-acid oxidation in response to low glucose, since knock-down of SIRT1 in muscle cells prevented this induction (Gerhart-Hines et al. 2007). SIRT1 thus functions as a regulator that drives the switch from glucose to fatty-acid based metabolism. SIRT1 is also able to deacetylate and activate the cytoplacmic acetyl-CoA synthetase, AceCS1 (Luong et al. 2000, Hallows et al. 2000). Acetyl-CoA synthetases convert free acetate into acetyl-CoA. It seems that the main activity of AceCS1 is to provide acetyl-CoA for fatty-acid synthesis (Skutches et al. 1979, Hallows et al. 2006). SIRT1 catalysed deacetylation leads to increased fatty-acid synthesis through acetate incorporation. Free acetate is produced by the liver under ketogenic conditions. Whe glucose is unavailable SIRT1 may allow the usage of free acetate as an energy source, by activating its uptake into fatty-acids, which can then be directed to mitochondria for oxidation. When glucose is available, newly synthesised fatty-acids are directed for storage. In mitochondria, AceCS2 (Fujino et al. 2001) provides acetyl-CoA to fuel the TCA cycle and links AceCS2 activity directly to energy production. AceCS2 is deacetylated by SIRT3 (Hallows et al. 2006, Schwer et al. 2006) (discussed below). This mode of AceCS2 regulation at the post-translational level is also found in *Salmonella enteriaca*, where CobB, the bacterial homolog of yeast SIR2 deacetylates and activates AceCS2 (Starai et al. 2002). The mechanism is thus conserved from bacteria to mammals.

In mice SIRT1 is highly expressed in pancreatic β-cells (Bordone et al. 2006). Knocking down SIRT1 expression in cultured β-cell lines prevents insulin secretion. This is due to a lowering of the ATP/ADP ratio because of increased mitochondrial uncoupling. SIRT1 promotes insulin secretion by inhibiting the mitochondrial uncoupling protein, UCP2. Accordingly, SIRT1 has been associated with insulin metabolism and glucose and fat tolerance. Moderate over-expression of SIRT1 in mice prevents high-fat-diet -induced insulin resistance (Pfluger et al. 2008).

A large proportion of SIRT1 deficient mice die during early postnatal period. Surviving animals are small and sterile and exhibit notable developmental defects of the heart and retina (McBurney et al. 2003, Cheng et al. 2003). Developmental

defects are accompanied with p53 hyperacetylation and increased thymocyte apoptosis upon DNA damage (Cheng et al. 2003). And although mammalian SIRT1 has not been shown to promote longevity as evidently as the yeast Sir2p, it is redistributed on mouse chromatin in an age-dependent manner (Oberdoerffer et al. 2008). This observation points to a conserved mechanism of aging in eukaryotes.

**SIRT2** is predominantly cytoplasmic (Afshar & Murnane 1999, Perrod et al. 2001). It localises with microtubules and deacetylates α-tubulin (North et al. 2003). SIRT2 has been associated with cell cycle regulation (Dryden et al. 2003). The abundance of SIRT2 is markedly increased during the G2/M transition in mitosis. Like other mitotic regulators, such as cyclins, SIRT2 turnover is regulated by ubiquitination and subsequent proteasomal degredation. Over-expression of the human SIRT2 in Saos cells prolonged the mitotic phase of the cell cycle. It is not known how SIRT2 regulates mitotic progression. This may be via α-tubulin deacetylation, since down-regulation of SIRT2 results in resistance to micro-tubule inhibitors (Inoue et al. 2009). SIRT2 has also been show to deacetylate Lys6 on H4 (Vaquero et al. 2006). Acetylation levels of H4 decrease during G2/M, and SIRT2 deficient mouse embryonic fibroblasts show elevated levels of acetylated H4Lys6. SIRT2 may thus be involved in the formation of facultative heterochromatin. However, since SIRT2 knock-out mice have no evident phenotype (unpublished observation reported in Vaquero et al. 2006), H4Lys6 deacetylation doesn't seem to be vital for progression through mitosis. By blocking chromosome condensation SIRT2 may be beneficial in preventing tetraploidy caused by mitotic slippage, subsequent aneuploidy and consequently cancer development (Inoue et al. 2007). SIRT2 may thus be a potential anti-cancer target.

**SIRT3** localises to mitochondria. This was first established in the studies that identified the enzyme and described its NAD dependent deacetylase activity (Schwer et al. 2002, Onyango et al. 2002, Michishita et al. 2005). However, one study later claimed human SIRT3 (hSIRT3) to be a nuclear protein that only translocates to mitochondria upon cellular stress and when over-expressed (Scher et al. 2007). But in experiments which are described in this thesis, and discussed later, we cleared the controversy that was piling up around the subject by showing the apparent nuclear localisation to be artefactual, and demonstrated that hSIRT3 is

exclusively mitochondrial (Cooper & Spelbrink, 2008). SIRT3 has robust NAD-dependent deacetylase activity on a histone substrate *in vitro*. In humans, it deacetylates the mitochondrial acetyl-CoA synthetase AceCS2 (Schwer et al. 2006, Hallows et al. 2006), found predominantly in heart, kidney and skeletal muscle. This activates AceCS2 to convert free acetate into acetyl-CoA, which is then targeted to the TCA cycle for energy production. hSIRT3 thus regulates the utilisation of free acetate produced and released by the liver as an energy source in extra hepatic tissues during glucose deprivation. By stimulating Acetyl-CoA production and by shifting the NADH:NAD balance by consuming NAD, hSIRT3 could promote gluconeogenesis by inhibiting the puryvate dehydrogenase complex. The resulting glucose would then be targeted to tissues that depend on it**.** hSIRT3 has also been shown to deacetylate and activate glutamate dehydrogenase (see below) and hSIRT3 can activate isocitrate dehydrogenase 2 (ICDH2), a key regulator of the TCA cycle, *in vitro* (Schlicker et al. 2008). Together, these findings point to a role for SIRT3 in regulating nutrient metabolism. Certain hSIRT3 polymorphisms have been linked to survivorship among the elderly (Rose et al. 2003, Bellizzi et al. 2005), but no experimental evidence for a molecular mechanism for SIRT3-mediated life span extension has been shown.

There is reason to believe, that at least in mouse, SIRT3 has multiple substrates. SIRT3 knock-out mice show hyperacetylation of mitochondrial proteins (Lombard et al. 2007, Ahn et al. 2008). Among these proteins are glutamate dehydrogenase (GDH) (Lombard et al. 2007) and NDUF1, a protein of Complex I of the electron transport chain (Ahn et al. 2008). GDH and NDUF1 were also shown to be mouse SIRT3 (mSIRT3) substrates *in vivo*. Over-expression of a truncated version of mSIRT3 in brown adipocytes resulted in a significant phenotype of up-regulated mitochondrial function through the activity of PGC-1α (Shi et al. 2005). However, as was shown by Jin et al. (Jin et al. 2009) and in experiments described in this thesis, this short isoform of mSIRT3 does not localise to mitochondria (Cooper et al. 2009). This and the identification of a longer mSIRT3 variant will be discussed later.

**SIRT4** localises to mitochondria and is highly expressed in pancreatic β-cells in human and mouse (Ahuja et al. 2007, Haigis et al. 2006). Neither human nor mouse SIRT4 displays detectable deacetylase activity, but instead they use NAD to ADP-ribosylate target proteins. hSIRT4 interacts with the ANT2/3 subunit of the

ATP/ADP translocase. Over-expression of hSIRT4 in β-cells suppresses insulin secretion, whereas knock-down enhances it. Insulin secretion is tightly linked to glucose derived ATP production in mitochondria. Therefore, Ahuja et al. proposed that by modifying the enzymatic activity of the ATP/ADP translocase, hSIRT4 can change the levels of insulin secreation in response to glucose (Ahuja et al. 2007). hSIRT4 was also found to interact with insulin degrading enzyme (IDE), a zink metalloproteinase that regulates plasma insulin and cerebral amyloid β-peptide levels *in vivo* (Farris et al. 2003, Miller et al. 2003). IDE has been linked to late onset Alzhaimer's and diabetes mellitus (Bertram et al. 2000, Cook et al. 2003), but little is known of its physiological functions and mitochondrial substrates. In mouse SIRT4 interacts with glutamate dehydrogenase (GDH) (Haigis et al. 2006), which coverts glutamate to α-ketoglutarate in mitochondria. ADP-ribosylation of GDH by mSIRT4 represses its activity and limits the break-down of glutamate and glutamine to produce ATP. Active SIRT4 inhibits insulin secretion in β-cells in response to these amino-acids. Accordingly, SIRT4 knock-out mice secrete insulin in response to glutamine (Haigis et al. 2006). Sirt4 thus mediates metabolic responses by regulating insulin secretion in mice and humans. SIRT4 and SIRT3 may have opposing effects on GDH, since SIRT3 has been shown to activate GDH (Schlicker et al. 2008). GDH activity is enhanced in CR mice (Haigis et al. 2006). CR may thus inhibit SIRT4 ADP-ribosylase activity and/or activate SIRT3 activity to allow the regulation of insulin secretion by amino acids rather than glucose in the setting of overall reduced carbohydrate metabolism (Haigis et al. 2006).

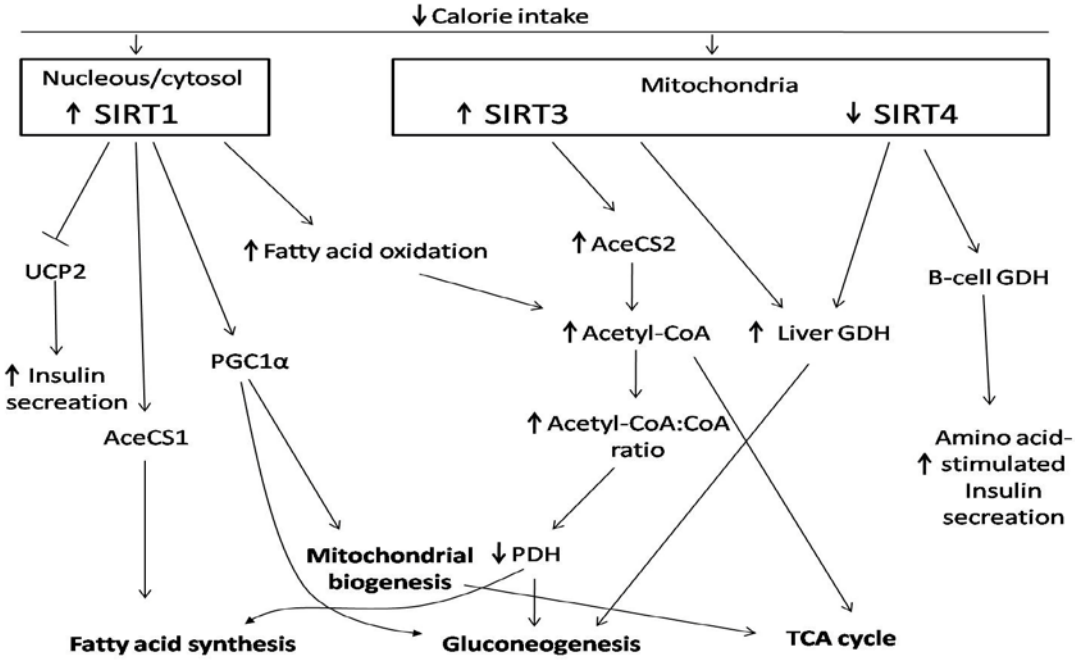


**Fig 2.7.** Complementing and opposing effects of SIRT1, SIRT3 and SIRT4 on energy producing pathways (adapted from North and Sinclair, 2006). AceCS, acetyl-CoA synthetase; GDH, glutamate dehydrogenase, PGC1α, UCP2, uncoupling proteins; PDH, puryvate dehydrogenase, PGC1α, Peroxisome proliferator-activated receptor gamma, coactivator 1 alpha

**SIRT5** localises to mitochondria, although according to one report the subcellular localisation of SIRT5 may change depending on the cell type (Pfister et al. 2008). In cerebellar granule neurons SIRT5 is predominantly in the nucleus and cytoplasm, and only a small proportion of cells show clear mitochondrial localisation. SIRT5 localisation to mitochondria in CNS has a pro-apoptotic effect (Pfister et al. 2008). Little is known about SIRT5 function and its substrates. Human SIRT5 has been shown to deacetylate cytochrome c *in vitro* (Schlicker et al. 2008). Recently, mouse SIRT5 was shown to deacetylate carbamoyl phosphate synthase 1 (CPS1) in the mitochondrial matrix (Nakagawa et al. 2009**)**. CPS1 is part of the urea cycle and needed to detoxify ammonia and SIRT5 knock-out mice have elevated blood ammonia levels during fasting (Nakagawa et al. 2009**)**.

**SIRT6** localises to the nucleus where it associates with chromatin (Mostoslavsky et al. 2006). Human SIRT6 has been shown to NAD-dependently deacetylate histone H3L9 and to modulate telomeric chromatin (Kawahara et al. 2009). SIRT6 depleted cells exhibit abnormal telomeric structures, telomere dysfunctions and

premature cellular senescence. Of all the sirtuin knock-outs, SIRT6 deficiency causes the most striking aging phenotype (Mostoslavsky et al. 2006). SIRT6 knock-out mice have lethally low levels of blood glucose, thin bones and spinal curvature, due to decreased Igf1 hormone levels, and drastic loss of lymphocytes; all hallmarks of premature aging. All SIRT6 knock-out mice die by one month of age. SIRT6 deficient cells grow slowly and are sensitive to genotoxic stress and show spontaneous genomic instability. SIRT6 may thus be directly involved in mediating DNA repair pathways on the level of chromatin. Alternatively or additionally, it may modulate the insulin/Igf signalling (IIS) pathway (Lombard et al. 2008). Recently it was shown that Sirt6 attenuates NF-κB signalling by modifying chromatin at NF-κB target sites (Kawahara et al. 2009). This SIRT6 mediated control of NF-κB prevents aging-associated NF-κB-dependent gene expression and inhibition of NF-κB can rescue the early lethality of Sirt6 knock-out mice. SIRT6 protein is stabilised upon nutrient deprivation in cultured cells, fasted mice and CR rats (Kanfi et al. 2008). This links SIRT6 to nutrient-dependent regulation. Intriguingly, at least mouse Sirt6 possesses intra-molecular ADP-ribosylase activity (Liszt et al. 2005). The significance of this self-modification remains unknown, but it led Liszt et al., to classify Sirt6 as a class IV deacetylase (Liszt et al. 2005).

**SIRT7** is nucleolar (Michishita et al. 2005), and is associated with rRNA genes (Ford et al. 2006). In mouse SIRT7 expression is high in metabolically active tissues such as liver and spleen, but not detected in skeletal muscle. SIRT7 is a part of the RNA polymerase I (Pol I) transcriptional machinery and stimulates Pol I transcription in cultured cells (Ford et al. 2006). However, the specific chromatin associated SIRT7 substrate remains to be identified. Surprisingly, the transcription activating effect of SIRT7 is opposite to the silencing effect of SIR2.

SIRT7-deficient mice develop progressive heart hypertrophy, accompanied by inflammation, decreased stress resistance and apoptosis (Vakhrusheva et al. 2008). This may be explained by the finding that SIRT7 deacetylates p53. The absence of SIRT7 would lead to hyperacetylation of p53 *in vivo* along with other apoptotic changes in the signalling network in cardiomyocytes. SIRT7 thus has a role in protecting the heart (Vakhrusheva et al. 2008).

## 2.3 Lysine acetylation

Lysine acetylation is a dynamic and reversible post-translational modification, which is now known to be a key regulator of many protein functions. Its initial discovery as a histone modification was made in the late 1960's. Acetylation of histones changes their affinity to DNA. This chromation remodelling is prerequisite to transcription and other DNA-templated processes.

But as can been seen from the sirtuin substrates, lysine acetylation can also target many non-histone proteins. And new discoveries of acetylation/deacetylation mediated regulatory events are constantly being made. Acetylation does not only regulate protein-DNA/protein-protein interactions, but can influence protein stability and localisation and enzymatic activity. The list of known acetylated proteins is extensive. The following will review some examples of proteins that are regulated by post-translational acetylation.

**p53** The tumor suppressor p53 maintains genome stability by activating a series of proteins involved in cell cycle regulation, senescence and apoptosis. In resting cells it is present at low levels, but becomes stabilised and active in response to DNA-damaging agents and stress stimuli. Once activated, p53 can either induce cell cycle arrest or lead cells into apoptosis. p53 is acetylated at several lysine residues in its C-terminus. Acetylation is thought to promote DNA binding and enhance p53's transcriptional activity at target promoters (Avantaggiati et al. 1997, Gu & Roeder et al. 1997). And as described in section 2.2.1, deacetylation by SIRT1 destabilises p53 and downregulates its activity. However, there are also contradictory reports on the requirement of acetylation/deacetylation of p53 at different promoters. For example, acetylation is not required for p53 binding at the p21 promoter (Espinosa & Emerson, 2001). It may be that the acetylation of p53 is promoter-, cell type- of stress type -specific. Acetylation has also been suggested to be a protective measure, since some of the acetylated lysine residues are also targets for ubiquitination and subsequent degradation by the proteasome (Li et al. 2002).

**The Werner (WRN) helicase** is a dsDNA unwinding enzyme (Gray et al. 1997) of the RecQ family with an additional exonuclease activity (Huang et al. 1998). The WRN helicase plays a role in damage-response. It is mutated in Werner syndrome, a

rare autosomal recessive premature aging disease (Yu et al. 1996). Under normal conditions the WRN protein is localised mainly in the nucleolus of human fibroblasts (Gray et al. 1998, Marciniak et al. 1998), but when cells are exposed to DNA damaging agents, it translocates to nucleoplasmic foci (Blander et al. 2002) interacts with numerous proteins, including p53 (Blander et al. 1999) and Pol δ (Szekely et al. 2000), (the major polymerase required for chromosomal replication) and has been proposed to resolve abnormal DNA structures (Bohr 2005). Translocation is enhanced by p300 mediated acetylation (Blander et al. 2002) and seems to be specific to DNA damage that requires recombination and base-excision repair (BER) (Karmakar & Bohr 2005). Acetylation has also been shown to stimulate the ATPase, helicase and exonuclease activities of the WRN helicase *in vivo* and *in vitro* (Muftuoglu et al. 2008). WRN interacts with Flap Endonuclease 1, **FEN-1**, to process branch-migrating structures at arrested replication forks. FEN-1 is a genome stabilising factor involved in the processing of single-stranded DNA structures (Liu et al. 2004). FEN-1 is acetylated upon DNA damage and this reduces its endonuclease activity (Hasan et al. 2004). Acetylation can thus regulate the replication and repair of DNA.

Furthermore, other repair enzymes known to be acetylated include **OGG1**, 8-oxoguanine-DNA glycosylase 1, and **NEIL2**: glycosylases involved in the base-excision repair of damaged DNA. Both have been shown to the acetylated by p300 (Bhakat et al. 2004, Bhakat et al. 2006). This, however, has opposing effects on the functions of the two proteins. Acetylation stimulates the glycosylation activity of OGG (Bhakat et al. 2006), but inhibits NEIL2 (Bhakat et al. 2004). Also **Polβ** is acetylated by p300 (Hasan et al. 2002). This inhibits its ability to cleave 5′-2-deoxyribose-5-phosphate (dRP) DNA ends generated during BER (dRP lyase activity), but has no effect on its polymerase or AP-lyase activities (Hasan et al. 2002). Taken together, these finding point to a role of actylation in controlling the activity DNA repair enzymes and maintaining genomic integrity, but the complexities of the regulation events are poorly understood.

## 2.4 Mitochondria

Mitochondria are the sites for the energy producing pathways described in the previous sections: the TCA cycle, the electron transport chain and beta-oxidation. In addition, mitochondria play an important role in the biosynthesis of steroids, iron-sulfur clusters and heme. The TCA cycle also provides intermediates for amino acid and fatty-acid synthesis. And some reactions of the urea cycle, which converts excess nitrogen into urea, reside in the mitochondrion. Additionally, mitochondria are involved in programmed cell death, apoptosis, and calcium storage. Importantly, mitochondria contain their own DNA.

### 2.4.1 Structure and dynamics

Mitochondria are double-membrane-bound intracellular organelles (Fig 2.8). The two membranes divide mitochondria into distinct compartments. Between the outer membrane (OM) and the innemembrane (IM) lies the intermembrane space. The inner membrane (IM) folds into christae and surrounds the mitochondrial matrix. Both the IM and OM are composed of a phospholipid bilayer containing embedded proteins. The electron transport chain is in the IM –and pumps electrons into the intermembrane space, from where they flow into the matrix. Both membranes contain specialised protein transporters to enable entry of proteins from the cytosol. Mitochondria are found in almost all cell types, and their amount depends on the energy requirement of the cell. Inside the cell mitochondria form a complex network are remodelled by fusion and fission, and they can move along microtubules (Frazier et al. 2006).

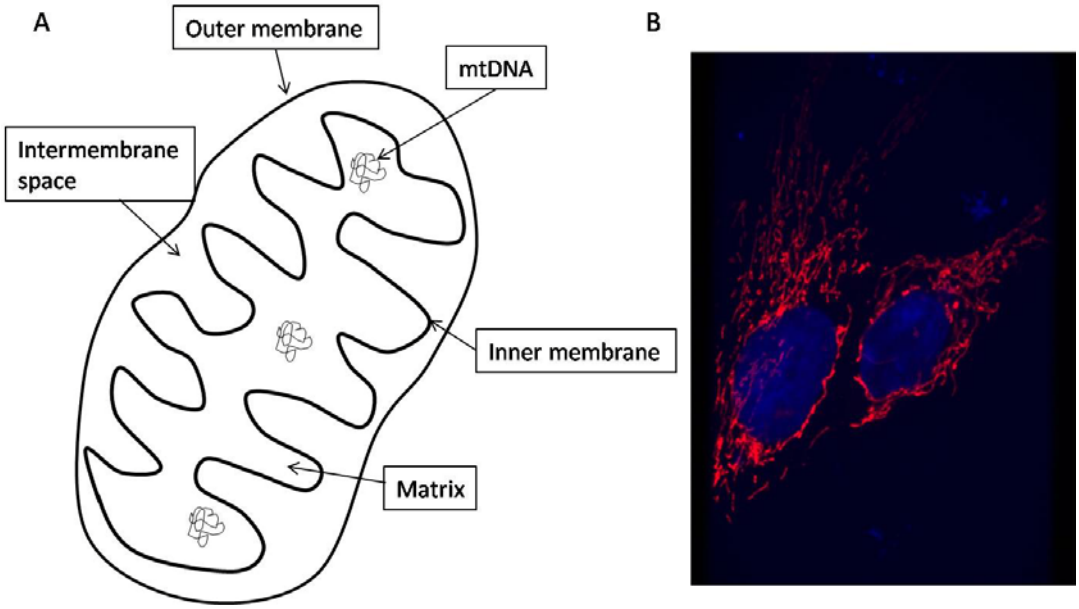


**Figure 2.8. A) Schematic representation of a mitochondrion. B) The mitochondrial network as seen by fluorescence microscopy.** Cytochrome c immunofluorescence with DAPI staining to show the nucleus (Image by J.N. Spelbrink).

### 2.4.2 The mitochondrial genome

Mitochondria have their own genetic material. According to the theory of endosymbiosis, mitochondria originate from respiring protobacteria, which were taken up by primordial eukaryotic cells about 1.5 billion years ago. In the course of evolution mitochondria either lost or transferred most of their genes to the nucleus thus losing their independence to nuclear control. The remaining mitochondrial genome in human cells is a circular molecule of 16, 569 base pairs (Fig 2.9) and codes for 37 genes: 13 polypeptides of the electron transport chain, 22 transfer RNAs (tRNAs) and 2 ribosomal RNAs (rRNAs) (Anderson et al. 1981, Andrews et al. 1999). The majority of the transcripts are derived from the so-called heavy-strand (HS). Transcription from the heavy-strand promoter (HSP) and light-strand promoter (LSP) produce polycistronic precursor RNAs, which are then cleaved into the individual rRNAs, tRNAs and the 13 protein coding messenger RNAs (mRNAs) (Ojala et al. 1981). The genes for all other mitochondrial proteins are in the nuclear genome. Many proteins that are destined to mitochondria have targeting peptides, most commonly at their N-terminus. These proteins enter mitochondria as precursors, which can then be proteolytically processed, folded and assembled into

complexes after import. The human mitochondrial DNA (mtDNA) contains only one major non-coding, regulatory sequence and no introns. It should be noted though, that the size, shape and coding and non-coding elements of the mitochondrial genomes of different species vary. For example the *Saccharomyces cerevisiae* mitochondrial DNA is over 60 kb in size and many plants have linear mitochondrial genomes. In mammals mitochondrial DNA is virtually always inherited maternally. Like the amount of mitochondria, the copynumber of mtDNA is proportional to the energy demand of the cell. However, due to the dynamic nature of the mitochondria, a mtDNA molecule cannot be assigned to a given mitochondrion, but is seen as part of the fluid mitochondrial network.

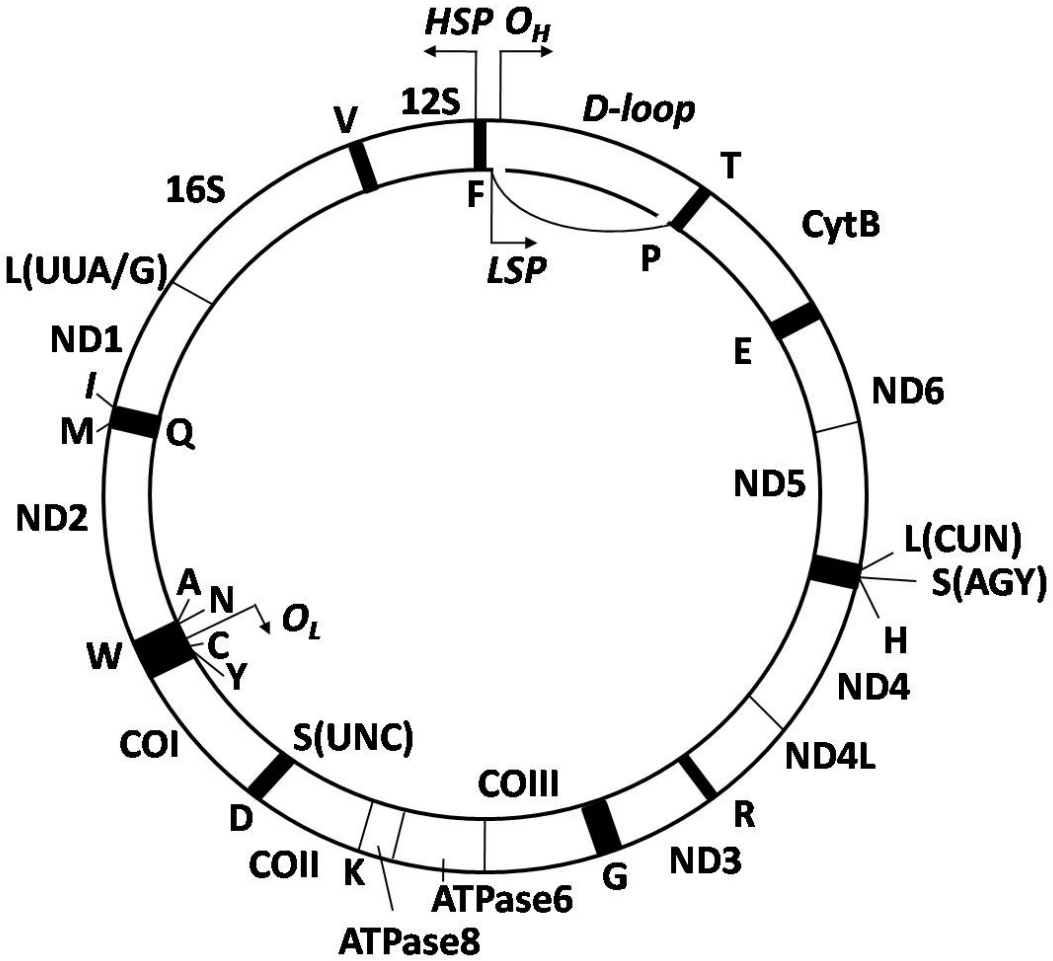


**Figure 2.9.** Map of the human mitochondrial genome. The outer circle represents the heavy strand, the inner represents the light strand. ND1-ND6 genes encode peptides of complex I; CO genes encode peptides of complex IV. tRNAs are represented by their their corresponding amino acid one-letter abbreviations. 16S and 13S are the mRNAs. The displacement (D)-loop contains the non-coding region.

### 2.4.3 Nucleoids

Although it was long thought that mitochondrial DNA exists “naked” in the mitochondria of human cells, it is now known that mtDNA is packed and organised with proteins to form complexes, known as nucleoids (Spelbrink et al. 2001) (Fig2.10). Nucleoids, which typically contain 2-10 copies of the mitochondrial genome, have been shown to segregate, and they possible mix with each other (Legros et al. 2004, Iborra et al. 2004, Garrido et al. 2003). Biosynthetic events take place in the context of the nucleoid. A layered model proposes that mtDNA replication and transcription take place in the core of the nucleoid, whereas RNA processing and translation occur in the peripheral zone (Bogenhagen et al. 2008). Several mitochondrial DNA maintenance proteins have been shown to be part of the nucleoid complex (Fig 2.10). And at least the mitochondrial transcription factor A (Tfam) seems to be required for DNA packaging (Alam et al. 2003, Garrido et al. 2003, Kaufman et al. 2007). However, no histones have been found in mitochondria, and little is known about the regulation of mitochondrial protein-DNA interactions.

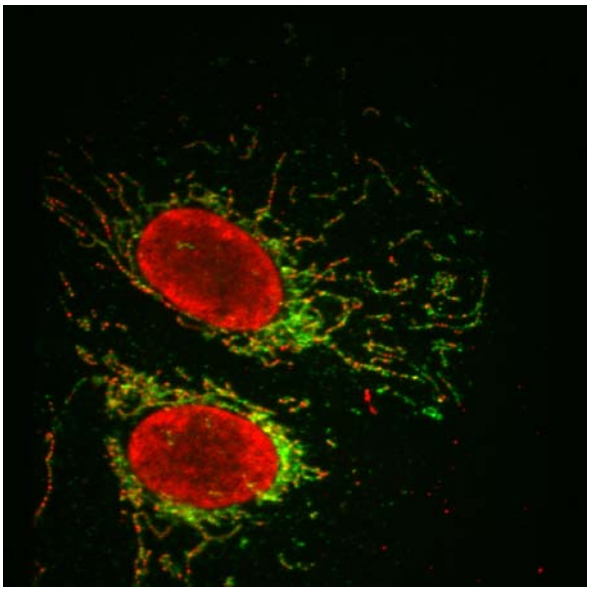

**Figure 2.10. Mitochondrial nucleoids.** A mitochondrial specific antibody showing the mitochondrial network in green and a DNA specific antibody showing mtDNA nucleoids and the nucleus in red (Image by J.N. Spelbrink).

### 2.4.4 Mitochondrial DNA maintenance

The replication of mitochondrial DNA was originally described as asynchronous (Robberson et al. 1972, Clayton et al. 1982). In this strand-displacement model replication starts from the heavy-strand origin and proceeds along two thirds of the genome length until the light-stand origin is exposed and can initiate light strand replication in the opposite direction. This theory was then challenged when evidence for conventional strand-coupled replication was obtained (Holt et al. 2000, Bowmaker et al. 2003). In addition, the discovery of stretches of RNA in the lagging-strand (Yang et al. 2002, Yasukawa et al. 2006) led to the proposal of yet another model of replication coined RITOLS (for ribonucleotide incorporation throughout the lagging strand) (Yasukawa et al. 2006). But the replication mechanism for mtDNA is not completely understood and may occur in different ways depending to the situation and tissue in question.

Like nuclear DNA, mitochondrial DNA is vulnerable to damage caused by ionising radiation, environmental toxins, alkylating agents and reactive oxygen species. Especially oxidative damage is considered a significant threat to mtDNA integrity, because of internal ROS generated by the electron transport chain. Previously, it was thought that damaged mitochondrial DNA molecules were simply degraded and replaced. However, an increasing amount of evidence supports the notion that the mitochondrion has dedicated DNA repair mechanisms. The major mitochondrial DNA repair pathway is base-excision repair (BER) and several DNA glycosylases have been found in mitochondria (for a review see e.g. Bogenhagen et al. 2001). On the other hand, mitochondria aren't able to repair the bulky lesions, which in the nucleus are repaired by nucleotide excision repair (NER). There are some reports on mitochondrial DNA repair by mismatch repair (Mason et al. 2003), homologous recombination (Thyagarajan et al. 1996) and non-homologous end-joining (Coffey et al. 1999). It is now evident that mitochondria possess DNA repair mechanisms, but the underlying molecular events and many participating proteins remain to be described in detail.

As mitochondria are almost exclusively inherited uniparentally from the maternal germline in metazoans, it was assumed that individuals generally possess only one mtDNA haplotype – a condition termed homoplasmy (Birky 2001). And since homoplasmy precludes recombination between heterogeneous molecules, mtDNA

used to be considered essentially non-recombining. The first evidence for mitochondrial DNA recombination in human cells came from studies on the muscle cells of an individual with a very rare case of paternal inheritance of mitochondrial DNA (Schwartz & Vissing 2002, Kraytsberg et al. 2004). Recombinant molecules were also found in hybrid cell lines containing two pathogenic mtDNA mutations (D'Aurelio et al. 2004, Zsurka et al. 2005) as well as in the skeletal muscle of patients carrying heteroplasmic mtDNA mutations. Recently, Pohjoismäki et al., found evidence of recombination in human heart, and proposed that recombination events initiate heart mtDNA replication. They were also able to induce recombination in transgenic mice thus demonstrating that mechanisms of recombination are conserved and have a physiological significance in tissues of high-energy demand and high levels in ROS production in mammals (Pohjoismäki et al. 2009).

### 2.4.5 Mitochondrial DNA maintenance proteins

All mitochondria DNA maintenance events depend entirely on nuclear encoded proteins. These proteins are transported from the cytosol into the mitochondria, where some associate intimately with the mtDNA and form the nucleoid complex. Yet all proteins that indirectly or directly participate in mtDNA maintenance events, whether or not they are part of the nucleoid, are considered mitochondrial DNA maintenance proteins. The following reviews the best described nucleoid associated mtDNA maintenance proteins.

**Polymerase γ** (POLG) is the replicative polymerase and the only known DNA polymerase in mitochondria (Lecrenier et al. 1997, Ropp & Copeland, 1996, Walker et al. 1997). The holoenzyme is thought to be a heterotrimer composed of a 140 kD core polymerase, POLGA and two 55 kD accessory subunits, POLGB (Yakubovskaya et al. 2006). The presence of POLGB stimulates the processivity of the polymerase and maintains the structural integrity of the holoenzyme (Farge et al. 2007, Yakubovskaya et al. 2007, Longley et al. 1998). In addition to the polymerase activity, POLGA possess a 3'→ 5' exonuclease activity, which allows efficient proofreading during DNA synthesis (Longley et al. 1998, Spelbrink et al. 2000,

Trifunovic et al. 2004) and a 5' deoxyribose phosphate lyase activity, which is required for POLGs role in base excision repair. POLGA also has reverse transcriptase activity on an RNA template (Murakami et al. 2003). The spacer region between the polymerase and exonuclease domain is thought to be involved in template positioning and the interaction with POLGB (Rewieved by Graziewicz et al. 2006). An interesting feature of the POLGA sequence is the presence of a polyglutamine repeat coded by CAG triplets. The prevailing length of the tract is 10 glutamines, and although the functional significance of the repeat is not understood, variations in repeat length have been associated with male infertility (Rovio et al. 2001, Jensen et al. 2004). POLG mutatations can cause mitochondrial syndromes (described in 2.4.6).

**Twinkle, the mitochondrial DNA helicase** shares considerable sequence homology with the T7 (gp4) primase/helicase (Spelbrink et al. 2001) (Twinkle is an acronym for T7 gp4-like with intramitochondrial nucleoid localisation.) Spelbrink et al. showed that Twinkle localises to mitochondria in "star-like" foci, which were identified as nucleoids (Spelbrink et al. 2001). Twinkle is thus an integral part of the mitochondrial DNA-protein complexes. Monomeric Twinkle is 684 amino acids and 77kD in size and in the presence of DNA, Mg2+ and a nucleotide co-factor six monomers are joined in a ring to form the active helicase. Under these conditions hexameric Twinkle can unwind double-stranded DNA with a single-stranded over-hang (Spelbrink et al. 2001, Korhonen et al. 2003). Together with POLG and the mitochondrial single-stranded binding protein (SSB), Twinkle forms the minimal mitochondrial replisome, which can synthesise a 16 kB DNA fragment *in vitro* (Korhonen et al. 2004). The Twinkle protein (Fig 12) is divided into a helicase domain containing conserved Walker A and Walker B helicase motifs and a domain with unknown function. In T7 gp4 this domain acts as a primase, but the Twinkle N-terminal domain carries no primase activity (Spelbrink et al. 2001, Shutt & Gray, 2006). The N- and C-terminal domains are connected by a linker region thought to be involved in subunit interactions in the hexameric form (Spelbrink et al. 2001). Twinkle is encoded by the *C10Orf2* gene, which also gives a splice variant Twinky, which lacks exon five, and has a unique C-terminal tail. Twinky does not form hexamers or localise with nucleoids, and its physiological role is unclear. Twinkle has been shown essential for mtDNA maintenance and to regulate mtDNA

copynumber (Tyynismaa et al. 2004). Mutations in Twinkle are associated with a number of mitochondrial diseases.

**The mitochondrial transcription factor A** (TFAM) enhances mitochondrial DNA transcription by POLRMT (Fisher & Clayton 1988, Parisi et al. 1993, McCulloch et al. 2002). TFAM contains two high-mobility-group boxes and has been shown to bind DNA in a sequence-independent fashion (Fisher & Clayton, 1988). It is thus thought, that in addition to promoting transcription, TFAM is involved in packaging mtDNA within the context of the nucleoid (Alam et al. 2003, Garrido et al. 2003). Over-expression and knock-down studies have shown that TFAM levels influence mtDNA levels (Larsson et al. 1998, Pohjoismäki et al. 2006).

**ATAD3** is a recently described component of many but not all nucleoids (He et al. 2007). It is an AAA+ protein and can bind DNA. ATAD3 is involved in maintaining the structure of nucleoids and preferentially binds the D-loop of mtDNA. It was suggested that ATAD3 promotes the formation and segregation of mitochondrial nucleoids.

### 2.4.6 Mutations in mitochondrial DNA maintenance proteins

Mitochondrial diseases are characterised by impaired energy production. They can arise from primary mutations to mtDNA or they can be due to defects in nuclear encoded components of the electron transport chain. A mitochondrial disease can also be the result of mutations in mtDNA maintenance proteins, which cause secondary mtDNA mutagenesis or instability. Primary mtDNA mutations (reviewed by Dimauro & Davidzon 2005) can be sporadic or maternally inherited and in most cases deleterious mutations are present in some, but not all of the mtDNA molecules of an affected individual in a state termed heteroplasmy. The relative proportions of normal and mutated genomes in different tissues contribute to the severity of the clinical expression of the disease. Mutations to nuclear encoded electron transport chain proteins and to mtDNA maintenance proteins can be sporadic or show X-linked or dominant or recessive Mendelian inheritance. Mutated genes known to

cause secondary mitochondrial DNA defects can code for either proteins functioning at the replication fork or proteins which supply mtDNA replication with deoxyribonuclotides. The following will focus on mutations to the mitochondrial replication proteins POLG and Twinkle.

#### *2.4.6.1 POLG mutations*

To date nearly 90 pathogenetic POLGA mutations have been described (Longley et al. 2005). The first mutation to be identified in the *PEO* locus was for autosomal progressive external ophthalmoplegia (PEO) in POLGA (Van Goethem et al. 2001). PEO, which can be recessive of dominant (arPEO or adPEO) is characterised by late-onset bilateral ptosis and progressive weakening of the eye muscles. Muscle weakness and exercise intolerance are also associated with the syndrome. Ragged red fibres and decreased respiratory enzyme activities are seen in the skeletal muscles of PEO patients. Mitochondrial dysfunction is due to the accumulation of deletions in the mtDNA of post-mitotic tissues (Zeviani et al. 1989, Hirano et al. 2001, Van Goethem et al. 2005). Most of the adPEO causing mutations are in the catalytic subunit POLGA, whereas arPEO mutations are also found in the exonucleous and spacer domains (POLG mutation database, http://tools.niehs.nih.gov/polg/). Only one disease causing mutation has been found in the accessory subunit, POLGB. (Longley et al. 2006). This G451E mutation, which causes PEO, renders POLGB defective in interacting with POLGA and as a consequence POLGB fails to stimulate processivity. Although it has been demonstrated that low catalytic activity leads to replication stalling, the actual mechanism of mtDNA deletion formation in PEO patients remains unknown. The prevailing hypothesis has been that since PEO patients also accumulate mtDNA deletions, errors in replication would lead to replication stalling and subsequent deletions (Wanrooij et al. 2004). And this is likely the case in proliferating cells, at least in cell culture models (Wanrooij et al. 2007). However, in a recent review article Krishnan et al., suggest –based on analysis of break points and the notion that replication rates are very low in post-mitotic tissues- that deletions arise from errors in DNA repair (Krishnan et al. 2008).

Since the discovery of PEO causing mutations in 2001, POLGA mutations have been linked with diverse other neuro-muscular disorders. Not all POLGA mutations lead to multiple mtDNA deletions and some cause mtDNA depletion. Clinically they are very heterogeneous and it is beyond the scope of this review to discuss all of them in detail. Pathogenic mutations have at least been associated with parkinsonism (Luoma et al. 2004), premature menopause (Luoma et al. 2004, Pagnamenta et al. 2006), Alpers syndrome (Naviaux et al. 1999), mitochondrial neurogastrointestinal encephalomyopathy (MNGIE) (Van Goethem et al. 2003), ataxia (Hakonen et al. 2005), sensory ataxic neuropathy, and ophthalmoparesis (SANDO) (Van Goethem et al. 2004).

#### *2.4.6.2 Twinkle mutations*

The gene for the Twinkle helicase was first isolated as a PEO locus on chromosome 10 (Spelbrink at al. 2001). All of the dominant Twinkle mutations including a 13 amino acid duplication (aas 352-364) cause autosomal dominant progressive ophthalmoplegia (adPEO) and the PEO phenotype can be augmented by features including muscle weakness, dysphagia, mild ataxia, peripheral neuropathy, psychiatric symptoms, parkinsonism, depression and avoidant personality features (Suomalainen et al. 1997, Spelbrink et al. 2001, Hudson et al. 2005, Baloh et al. 2007). Most of the adPEO causing mutations cluster in or in close proximity of the linker region, i.e. the region between the helicase and N-terminal domains (Fig 2.11). The linker is thought to mediate the formation of multimers, and *in vitro* studies have shown various degrees of defective hexamerisation of Twinkle adPEO mutants (Korhonen et al. 2008). Also, in many cases, the *in vitro* helicase activity of the enzyme is impaired (Korhonen et al. 2008, Holmlund et al. 2009). This thesis presents the further molecular characterisation of seven adPEO mutants including their ability to multimerise, bind and unwind helicase and hydrolyse nucleotides.

A recessive Twinkle mutation, Y508C, leads to infantile onset spinocerebellar ataxia (IOSCA) (Koskinen et al. 1994a), which is characterised by the loss of deep tendon reflexes, athetosis, hyptonia, ataxia, ophthalmoplegia and sensorineural hearing deficts. The first symptoms are detected at 10-18 month of age, and due to the progressive nature of the syndrome, patients are rendered wheelchair-bound and

deaf by adolescence. Severe epileptic attacks may develop in adolescence or adulthood (Koskinen et al. 1994a, 1995). The neuropathology of IOSCA shows atrophy of the brain stem, cerebellum and the spinal cord (Koskinen et al. 1995). However, IOSCA patients do not have mtDNA deletions or the muscle histology of PEO (Nikali et al. 2005), nor is the *in vitro* performance of Twinkle affected (Hakonen et al. 2008). A study of IOSCA brain revealed mtDNA depletion associated with a respiratory chain complex 1 deficiency (Hakonen et al. 2008). These findings suggest that IOSCA a cell-type specific DNA depletion syndrome.

Three recessive disease causing Twinkle mutation have been described. The T457I mutation impairs helicase activity and leads to hepatocerebral mitochondrial depletion syndrome (Sarzi et al. 2007). Twinkle mutations also underly a case of early onset encelopathy (Hakonen et al. 2007). The two described patients were both compound heterozygote for the mutations A318T and Y508, the latter of which lies in the helicase domain of Twinkle. Mitochondrial DNA was found to be depleted in the liver and to a minor extent in the muscle of the patients who suffered from symptoms resembling those seen in IOSCA, but manifesting in more severe form and at an earlier age (Hakonen et al. 2007).

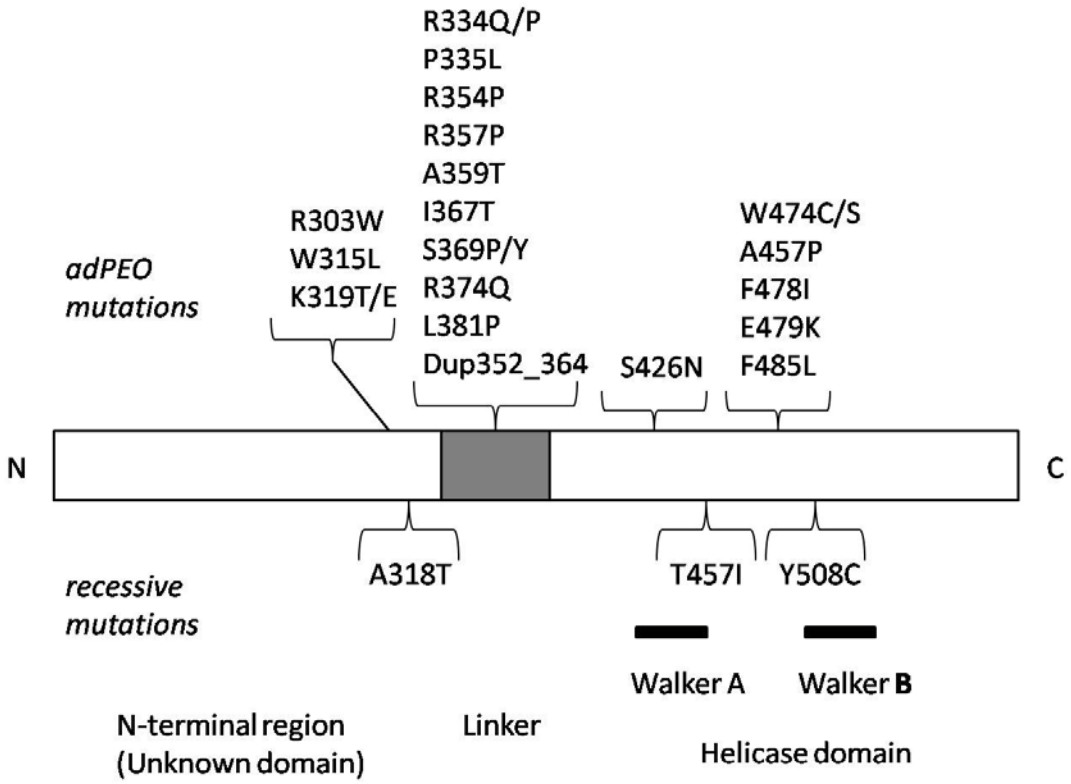


**Fig 2.11.** Twinkle mutations. A schematic representation of the Twinkle protein including sites for mutations which cause adPEO and recessive mutations causing IOSCA (Y508), early onset encelopathy (A318T/Y508) and mitochondrial depletion syndrome (T451I)

## 2.5 Aging

The lifespan of all organisms is limited. And as organisms approach this limit, they experience age-related diseases and loss-of-function. The cellular and molecular events underlying aging or the mechanisms, which under certain circumstances extend longevity and healthy lifespan, are unresolved. And as the lifespan expectancy of human increases, understanding the triggers of the aging process has become a popular goal for modern science. This chapter presents the prevailing theories on the biology of aging.

### 2.5.1 Reactive oxygen species

According to the free radical and oxidant theory of aging, coined by Denham Harman in the 1950, oxidative damage to proteins, lipids and DNA contributes to aging and age-related disease. Studies on different species have verified a negative correlation between longevity and the amount of reactive oxygen species (ROS), which are natural by-products of oxygen metabolism. Longer lived species exhibit decreased levels of oxidative damage, decreased susceptibility to oxidative stress, and decreased generation of reactive oxygen species. The largest amounts of ROS are generated in mitochondria during oxidative phosphorylation. Under normal circumstances a number of specialised scavengers act to remove ROS. But oxygen free radicals produced during abnormal respiration are thought to cause cumulative damage eventually leading to loss of functionality, diseases and ultimately death.

The importance of the detrimental effect of reactive oxygen species is underscored by the existence of anti-oxidants, compounds that non-specifically scavenge ROS. However, although anti-oxidants protect cells, they do not seem to be able to uniformly affect maximum lifespan potential. In some studies in invertebrates, an increase or over-expression of enzymes with anti-oxidant properties, such as catalase and superoxide dismutase, increased lifespan and delayed the aging process (Orr & Sohal 1994, Fleming et al. 1992, Parkes et al. 1998, Hari et al. 1998, Larsen 1993). However, results were strain and cell type specific. And in mammals, over-expression or feeding of anti-oxidants had little or no effect on longevity and did not delay aging (Sohal et al. 2002, Schriner et al. 2000, Holloszy 1998, Lipman et al. 1998, Andziak et al. 2005, Van Remmen et al. 2003). In fact, the overall

importance of ROS to aging has been since questioned and the theory challenged. While oxidative damage contributes to aging in many systems studied, it is likely that ROS are just one player in a complex set of cellular events that lead to the aging phenotype. So far, calorie restriction (CR) is the only regime known to prolong lifespan and longevity irrespective of the species. But it does seem that CR has an effect on ROS production. Long-term caloric restriction significantly decreased H2O2 production of rat liver mitochondria (Lopez-Torres et al. 2002). And in *in vivo* and *in vitro* analyses carried out by Lopez-Lluch et al. mitochondria under CR conditions showed reduced oxygen consumption, lower membrane potential, and less reactive oxygen species compared to controls, but were still are able to maintain sufficient ATP production. These observations suggest that CR produces very efficient electron transport through the respiratory chain with more ATP production under conditions of lower oxygen consumption and less ROS production. This increase in mitochondrial efficiency could attenuate molecular damage resulting from oxidative stress thus slowing aging at the cellular and organismic level (Lopez-Lluch et al. 2005).

### 2.5.2 Defective DNA repair

In order to avoid the detrimental effects DNA lesions have on cell function, eukaryotic organism have evolved five distinct mechanism to repair DNA damage. Single-strand lesions are repaired by base excision repair (BER), nucleotide excision repair (NER) and mismatch repair (MMR) (Lombard et al. 2005, Hsieh 2001). Double strand breaks (DSB) are repaired through homologous recombination (HR) and non-homologous end-joining (NHEJ) (Lombard et al. 2005). Despite the extensive investment in DNA repair pathways, DNA mutations persist to accumulate with time (Vijg 2000), and a vast amount of data supports the idea that unrepaired nuclear DNA is a significant cause of aging (Lombard et al. 2005). In both humans and mice, defects in DNA repair pathways accelerate some (but not all) aging events, resulting in progeroid phenotypes (Lombard et al. 2005, Martin 2005).

### 2.5.3 Mitochondrial DNA mutations

As mitochondria are the primary sites of ROS production, the mitochondrial genome is especially susceptible to oxidative damage. It has thus been proposed, that as mitochondrial DNA mutations disrupt the function of electron transport chain proteins, they will lead to deficient oxidative phosphorylation, which will lead to more ROS production, which will induce more mtDNA mutations, and that this vicious cycle will cause cellular aging. Although age dependent accumulation of mtDNA mutations can be detected in several tissues in humans, mice and rats, existing animal models do not unambiguously support the mitochondrial theory of aging. Attempts to prove the theory include decreasing mutations load indirectly. For example, transgenic mice that over-express the ROS scavenging enzyme, catalase, have a decreased frequency of mtDNA mutations (Schriner et al. 2005). Similarly, the frequency of mtDNA deletions is decreased in rats on a CR diet (Bua et al. 2004). Also, mutation rates have been specifically increased in the mutator mouse (Trifunovic et al. 2004, Kujoth et al. 2005). These mice harbour a proof-reading deficient version of the mitochondrial DNA polymerase, POLG. And not only do they accumulate mtDNA point mutations and deletions, but these mice also have a striking phenotype of premature aging, including weight loss, reduced subcutaneous fat, hair loss, osteoporosis, anaemia, reduced fertility and heart enlargement. However, excessive accumulation of mtDNA mutations was not associated with increased ROS production, but rather increased apoptosis (Trifunovic et al. 2005, Kujoth et al. 2005). Artificial animal models are, of course, subject to artefacts and phenomena that might not occur at all in wild-type conditions. Also, the accelerated aging events are likely distinct from those that happen over decades of exposure to moderate levels of ROS and other mutation inducing factors. Even though a causal relationship between mtDNA accumulation and aging is suggested by these and other models, and several hypotheses have been formulated, a definitive functional relevance of mitochondrial DNA mutations to the aging process remains to be demonstrated.

### 2.5.4 The insulin/IGF-1 signalling (IIS) pathway

When food is limited, juvenile *C. Elegans* worms enter a diapause state, called dauer, which is characterised by developmental arrest, reproductive immaturity, resistance to oxidative stress and longevity. The reappearance of food will then allow the worms to grow to adulthood and reproduce. Loss of function mutations in the insulin/IGF-1 signalling (IIS) pathway, either the receptor daf-2, or downstream components, cause dauer formation even in the presence of food. And weak mutations in the same pathway allow animals to grow to adulthood and increase their life-span to twice that of wild-types (Klass 1983, Friedman & Johnson, 1988). Lowered IIS does not only extend lifespan in worms, but has emerged as an important, evolutionarily conserved means of extending life expectancy also in fruit flies (Clancy et al. 2001, Tatar et al. 2001) and in mice (Holzenberger et al. 2003). Inhibition of specific components of the ISS signalling pathway also has several benefits to the overall health of these organisms as they age: interventions to ISS improve for example glucose homeostasis and immune profile and lower the incidence of age-related diseases such as osteoporosis and cataracts (Garsin et al. 2003, Selman et al. 2008, Libert et al. 2005). IIS starts with the insulin-like ligand binding to its receptor on the cell surface and the signal is transduced via phosphorylation of pathway components. Activation of a forkhead transcription factors results in its exclusion from the nucleus and thereby its inactivation. (For species specific pathway components see Broughton & Partridge 2009). Mutations that disrupt this pathway thus lead to the constitutive activity of the forkhead transcription factors, which are crucial regulators of cell fate (Sedding 2008). The biochemical mechanisms and tissues specify of the IIS mediated increase in lifespan are beginning to be understood and the pathway may offer the potential to attenuate functional senescence and age-related disease in humans.

# 3. Aims of the study

The aim of the research presented in this thesis was to elucidate the significance of acetylation and SIRT-mediated deacetylation to mitochondrial proteins.

More specifically I set out to

1. Unabigiously determine the subcellular localisation of the human and mouse SIRT3.

2. Identify novel acetylated mitochondrial proteins and substrates for hSIRT3.

3. Study the mitochondrial helicase Twinkle: its function and association to mitochondrial nucleoids in health and disease.

# 4. Materials and methods

The methods used in this study are briefly summarized here, and described in more detail in the original publications (I-IV). The experiments described in sections 4.6, 4.12-4.15 were carried out by Dr. Steffi Goffart.

## 4.1 Vector constructs

The full-length cDNAs of Twinkle variants and POLGB were originally cloned in the pcDNA3.1()/Myc-His A (Invitrogen), as previously described (Spelbrink et al. 2000, 2001). cDNAs for hSirt3, Δ1-142 hSirt3, AceCS2, HDAC7, ACAA2, ACADM, ACAT1 and SCEH were reverse transcribed from HeLa cell mRNA and cloned into the pcDNA3.1A and pcMV4A vectors. For the creation of the Flp-InTM T-RexTM 293 (Invitrogen) cell lines constructs were re-cloned into the pcDNA5/FRT/TO vector (Invitrogen) taking advantage of two PmeI restriction sites flanking the multiple cloning sites of the original pcDNA3 vector and the target vector. The resulting fusion proteins contained the sequence of the respective proteins followed by a Myc-His tag. Or, alternatively, to express Flag-tagged fusion proteins, genes were cloned directly into the pcDNA5/FRT/TO vector with the in-frame Flag tag sequence in the 3' primer. Mouse Sirt3 splice variants with 3' in-frame Flag-tag sequences were cloned from cDNA from NIH3T3 cells into the pcDNA5/FRT/TO vector. Yeast-two hybrid vectors were created using the Matchmaker 3 system (Clontech), supplied with pGBKT7 and pGADT7 plasmids, control plasmids (pGBKT7-53, pCL1, pGADT7-T and pTD1-1). The construct for hSirt3 was re-cloned from pCMV-Tag4.A vectors into pGBKT7 (=BD) and pGADT7 (=AD). The mitochondrial targeting signal was left out from this hSirt3 construct. All plasmid constructs were confirmed by DNA sequencing.

## 4.2 Cell culture systems

Stable, inducible cell lines were created as described (Wanrooij et al. 2007) using the Flp-In™ T-Rex™ 293 host cell line (Invitrogen), a HEK293 variant containing a Flip recombination site at a transcriptionally active locus. The resulting cells were grown in DMEM medium (Sigma) supplemented with 10% FCS (Sigma), 2 mM L-glutamine, 50 mg/ml uridine (Sigma), 150 mg/ml Hygromycin and 15 mg/ml Blasticidin in a 37°C incubator at 8.5% $CO_2$. To induce expression, the indicated amount of doxycycline (Sigma) was added to the growth medium.

Mouse hepatocytes were isolated from H129sv male mice according to a two-step collagenase perfusion technique described by LeCluyse et al. (LeCluyse et al. 1999)

HEK293EBNA cells were routinely grown in a 37°C incubator at 8.5% $CO_2$ in either DMEM medium (Sigma) supplemented with 10% FCS (Sigma) and 1 mM L-glutamine or in low glucose media (Gibco) supplemented with 0.9g/ml galactose, 10% FCS and 1 mM sodium pyruvate.

For transient transfections with DNA vectors HEK293EBNA cells or mouse hepatocytes were transfected with 3 µg of DNA per 10 cm plate using either Lipofectamine™2000 of TransFectin (BioRad) transfection reagent according to the manufacturers' instructions.

For immunofluoresence, cells were grown on coverslips and transfected with 2 µg of DNA per 6-well plate using either Lipofectamine™2000 or TransIT®-LT1 (Mirus).

For RNAi, HEK293EBNA cells were transfected with 420 pmol of siRNAs (Dharmacon) per 10 cm plate using Lipofectamine™2000.

## 4.3 Animals

In the mSIRT3 study, animal experiments were carried out under protocols approved by the Committee on Animal Research at the University of California, San Francisco.

In the Twinkle study, animal procedures were performed according to protocols approved by the ethical boards for animal experimentation of the National Public Health Institute and Helsinki University (agreement number STU575A/2004). The generation and the phenotypes of the Deletor and the wild-type Twinkle over-expressor mice have been previously described (Tyynismaa et al. 2004, 2005).

## 4.4 Yeast-two-hybrid library screen

For transformation, the S. cerevisiae strain AH109 was grown at 30 °C in YPDA medium (20 g/l peptone, 10 g/l yeast extract, 2% glucose and 0,003 adenine) and 0,1 μg of plasmid DNA was used for transformation by the LiAc-method. Transformants were plated on agar plates lacking tryptophan (-W) or leucine (-L) to select for the pGBKT7 or pGADT7 plasmids, respectively.

The BD-hSirt3 construct was tested for autoactivation of reporter genes in the Y2H system and for adverse effects on mating efficiency to ensure screening of a sufficient number of clones in the library screen.

Library screen: Cultures of AH109[pGBKT7-hSirt3] and Y187 pretransformed with a cDNA library from human skeletal muscle (# HY4047AH, Clontech) were incubated in 50 ml of 2 x YPDA/kanamycin for 22 hours at + 30 °C with gentle swirling (50 rpm). The mating culture was plated on plates lacking tryptophan, leucine and histidine (TDO) and incubated at + 30 °C for 8 days. Colonies were restreaked twice to plates lacking tryptophan, leucine, histidine and adenine and containing X-α-galactose (QDO/X-α-Gal). They were then restreaked twice to –L/-W plates containing X-α-Gal, thus only selecting for the presence of both types of plasmid, but allowing segregation and loss of multiple library plasmids from a

single clone. Colonies expressing the MEL1 reporter gene were once more restreaked to QDO/ X-α-Gal.

Plasmid was isolated from positive yeast clones by alkaline lysis and the library inserts were PCR-amplified from the pACT2 vector using a set of primers that flank the multiple cloning site (“3’ AD LD-insert”: 5’-gtg aac ttg cgg ggt ttt tca gta tct acg at-3’ and “5’ AD LD-insert”: cta ttc gat gat gaa gat acc cca cca aac cc-3’). PCR products were sequenced and sequences were analyzed by blasting the translated sequence (Translate tool of Expasy, www.expasy.org) against known protein sequences (BLASTp of NCBI, www.ncbi.nlm.nih.gov). Further information on the proteins, like subcellular localization and functions, was found in NCBI databases (GenBank, OMIM, RefSeq etc).

Interactions with hSIRT3 were confirmed using cotransformation of pGADT7-hSIRT3 and the pGBKT7-construct for the protein in question, ruling out false positives resulting from interaction of hSirt3 with the AD of Gal4.

## 4.5 Isolation and purification of mitochondria and nuclei

After detaching, NIH3T3 cells or HEK293 cells were isolated by centrifugation (1200 rpm for 2 min at +4°C) and washed once with ice-cold PBS. For isolation of crude mitochondrial fractions by hypotonic lysis and differential centrifugation, the cell pellet was resuspended by gentle pipetting in 2–3 vol of ice-cold homogenization buffer [4 mM Tris/HCl (pH 7.8), 2.5 mM NaCl, 0.5 mM MgCl2 and 0.1 mM PMSF], kept on ice for 6 min, then homogenized in a glass homogenizer with 20–25 strokes of a tight-fitting pestle. Disruption of the cells was monitored by microscopy. A one-ninth volume of 10×homogenization buffer was added following lysis and nuclei and cell debris were pelleted by centrifugation at 1200 ***g*** for 3 min at 4°C. Mitochondria from the post-nuclear supernatants were recovered by centrifugation at 12000 ***g*** for 3 min at 4°C. Mitochondrial pellets were washed once with 1 ml of ice-cold PBS and the mitochondrial pellet was lysed 15 min on ice in 50 mM Tris/HCl (pH 7.5), 150 mM NaCl, 1 mM EDTA and 1%Triton

X-10. For Western Blot analysis, an equal volume of 2× Laemmli sample buffer was added to the sample.

Nuclear pellets following hypotonic lysis were either extracted first by 0.5% Nonidet P40 in 50mM Tris-HCl (pH 7.5) and 150 mM NaCl, again pelleted and extracted with 20mM Tris-HCl (pH 7.9), 25% glycerol, 0.42M NaCl, 1.5mM $MgCl_2$, 0.2 mM EDTA, 0.1mM PMSF and 0.5M (DTT) for 20 min and centrifuged at 20 000 *g* for 30 min. Or, alternatively, the low speed pellet obtained from the hypotonic lysis was further purified on a 25%/30%/35% Optiprep™ (Iodixanol) (Axis-Shields) gradient according to the manufacturer's protocol and extracted with high salt as above.

## 4.6 Twinkle purification

Twinkle.MycHis was purified from Flp-In™ T-RexTM cells induced for 36 h. Cells were disrupted after a short cytochalasin treatment (Yasukawa et al. 2005); mitochondria were isolated using differential centrifugation and sucrose gradient purification and then lysed and sonicated in high salt buffer (50 mM KH2PO4, pH 7.4, 1 M NaCl, 0.05% Triton X-100, 10 mM Imidazol, 7 mM b-mercaptoethanol). The lysate was incubated with TALON Co2þ affinity resin (Clontech) for 1 h at 48C, the resin was washed twice with both high and low salt buffer (25 mM Tris pH 7.6, 200 mM NaCl, 100 mM L-arginine, pH 7.6, 40 mM Imidazol, 10% glycerol, 7 mM b-mercaptoethanol) and His-tagged proteins binding to the resin were isolated with elution buffer containing 25 mM Tris pH 7.6, 200 mM NaCl, 100 mM L-arginine, pH 7.6, 200 mM Imidazol, 50% glycerol. Protein extracts were aliquoted, shock frozen in liquid nitrogen and stored at –808C. The concentration of Twinkle in the eluate was judged by SDS–PAGE and Coomassie Brilliant blue staining using BSA as a reference. Typically 100 mg mitochondrial wet weight yielded 2–4 mg of Twinkle protein.

## 4.7 Immunoprecipitations

For Flag and Myc immunoprecipitations cells or mitochondria were lysed in 200 – 500 µl of 50mM TrisHCl pH 7.5, 150 mM NaCl, 1 mM EDTA, 1 % Triton X-100, including protease inhibitors and when stated, 50 mM NaBu and 5 mM nicotinamide, incubating for 30 min on ice. After a 5 min high-speed centrifugation the supernatant was collected. For Flag immunoprecipitation the lysate was transferred to a tube containing 250 µl of anti-Flag M2 agarose (Sigma) slurry (approximately 35 µl of resin in 50mM TrisHCl pH 7.5, 150 mM NaCl) prepared according to the manufacturer's instructions. 200-600 µl of lysis buffer was added and the tubes were rotated for 2 hours at +4°C. The resin was washed once in 50mM TrisHCl pH 7.5, 150 mM NaCl + 0.1% Triton X-100 and 2-3 times in 50mM TrisHCl pH 7.5, 150 mM NaCl according to the manufacturer's instruction. For SDS-PAGE, proteins were eluted by adding 50-100 µl of Laemmli sample buffer. For Myc immunoprecipitations the lysate was transferred to 50 µl of EZview™ Red Anti-c-Myc Affinity Gel (Sigma), pre-incubated in lysis buffer according to the manufacturer's instructions. Tubes were rotated for 1 hour at +4°C. The resin was washed with lysis buffer according to the manufacturer's instructions. For SDS-PAGE, proteins were eluted by adding 50-100 µl of Laemmli sample buffer.

For HA immunoprecipitations, cells were lysed in 50 – 500 µl of PBS + 1.5% Lauryl Maltoside or mitochondria were lysed in TrisHCl pH 7.5, 100-500 mM NaCl, 1.5% LM. Buffers routinely contained protease inhibitors, and when stated, 50 mM NaBu and 5 mM nicotinamide. The lysate was incubated for 30 min on ice and after a 5 min high-speed centrifugation the supernatant was collected. Protein A or G sepharose was prepared by pre-incubating 100mg of powder in 1 ml of PBS, 1mM EDTA, 0.15% LM rotating for 10 min at +4°C. The suspension was centrifuged at 5000rpm for 30 seconds and the supernatant was removed. The resin was washed once with 1 ml of PBS, 1mM EDTA, 0.15% LM and then resuspended in PBS, 1mM EDTA, 1 mg/ml BSA. The lysate was added to 50 µl of the sepharose slurry together with 10 µl of anti-HA antibody and tubes were incubated rotating for 2 hour at +4°C. Tubes were centrifuged at 5000rpm for 30 seconds and the supernatant was removed. The resin was washed once in 10 mM Tris/HCl pH 8.0, 1 mM EDTA, 0.5 M NaCl and 3 times in 10 mM Tris/HCl pH 8.0, 1 mM EDTA,

0.05% LM. For SDS-PAGE, proteins were eluted by adding 50-100 µl of Laemmli sample buffer.

## 4.8 Western blots

Mitochondrial lysates, nuclei or immunoprecipitates or deacetylase assay reactions all in sample buffer were denatured at 95°C for 5 min prior to SDS-PAGE. Western blot analysis by ECL enhanced chemiluminescence) was performed essentially as described previously (Spelbrink et al. 2000). Western blot analysis used pre-stained broad-range markers from Fermentas. Peroxidase-coupled secondary anti-mouse and anti-rabbit antibodies were obtained from Vector Laboratories. In some instances the Supersignal® West Femto Maximum kit (Pierce) was used for detection according to the manufacturer's protocol. Detection and quantification used a Bio-Rad Chemi Doc XRS system.

## 4.9 Immunocytochemistry

For immunofluorescent detection, cells were grown on coverslips in 6 well plates. Following transfection for 1-2 days and where indicated, leptomycin B (Sigma) treatment, cells were fixed using either 3.3% PFA (paraformaldehyde) in cell culture medium for 25 min or in methanol for 5 min at -20°C (Malka et al. 2007). This was followed by three washes in PBS and lysis for 10 min with 0.5% Triton X-100 in PBS/10% FCS after PFA fixation. No lysis step was performed after methanol fixation. Primary and secondary antibodies were incubated at recommended concentrations in PBS/10% FCS for 1 h or overnight. Mitotracker® Red CMXRos treatment was performed prior to fixation essentially as described previously (Goffart et al. 2007). Slides were mounted using ProLong® Gold antifade with DAPI (4_,6- diamidino-2phenylindole; Invitrogen). Image acquisition using confocal microscopy was carried out as described (Garrido et al. 2003), using

an Andor iXon DV885 EMCCD camera and the Andor iQ software (Andor). Images were further processed using Photoshop CS2.

## 4.10 In vitro assays

In vitro assays were carried out with purified Twinkle.mh. Helicase assays were performed with a radioactively end-labeled 60-nt oligonucleotide hybridized to M13 single-stranded (ss) DNA, forming a 20-nt double-stranded stretch with a 40-nucleotide 5'-overhang. Reactions were incubated at RT for 30 min in the presence of the indicated nucleotides. Products were separated on 10% TBE-gels, which were dried and exposed to autoradiography film.

The oligomerization of isolated Twinkle proteins was studied by crosslinking the protein with low concentrations of glutaraldehyde followed by separation on a sodium-dodecyl-sulfate (SDS)-polyacrylamide gel electrophoresis (PAGE) and Western Blotting. The stability of formed hexamers was also analyzed by gel filtration.

Affinity of Twinkle variants to ssDNA was analyzed using a previously described radioactive electromobility shift assay (EMSA) (Farge et al. 2008), but using used the following oligo nucleotide primer: CT TCC TGG CTT GCT TTG GCT GAG CCAAAA, instead of an oligodT primer. Reactions were run on 5% TBE gels, w which were dried and exposed to autoradiography film.

## 4.11 Acetyl-CoA measurements

Acetyl-CoA levels of hSIRT3 and vector control over-expressing cells were measured using the PicoProbe Acetyl-CoA assay kit from Biovision. TRex cells were induced with 3ng/ul doxycycline for 48 hrs. For each sample four full 10 cm plates were harvested and lysed in 1 ml PBS containing 1.5 % Lauryl Maltoside for

30’ on ice. Lysates were centrifuged for 5’ at 16,000 x *g* to pellet cell debris. Samples were deproteinized with perchloric acid (Biovision). 50 µl of sample was used for the reaction to produce NADH. Reactions were carried out in triplicate alongside an Acetyl-CoA standard according to the kit manufacturer’s instructions. Fluoresence at 535/589nm was measured with the Victor X$^{TM}$ Multilabel plate reader (Perkin Elmer).

## 4.12 Brewer-Fangman 2D neural/neutral agarose electrophoresis

Mitochondrial nucleic acids were extracted using cytochalasine (Sigma-Aldrich) as described (Yasukawa et al. 2005). Purified mtDNA was digested with HincII (human) or ClaI (mouse). The fragments were separated by 2DNAGE as described (Friedman and Brewer 1995, Brewer and Fangman 1987) and the gels were blotted and hybridized with a 32P-labelled DNA probe for human mtDNA nts 14846–15357 or mouse mtDNA nts 16356–136. The gels were blotted by capillary transfer and exposed to film and to a phosphorimager plate.

## 4.13 Quantitative PCR

The copy-number of mtDNA per cell was determined essentially as described (Wanrooij et al. 2007). Total cellular DNA was extracted by Proteinase K digest and isopropanolprecipitation, and copy-numbers of cytochrome b (mtDNA) and APP (nuclearDNA) were determined in a Taqman assay on an Abiprism7000 (Applied Biosciences, Foster City, CA, USA) using plasmids containing the amplicons as standards.

## 4.14 Southern blots

Total DNA was extracted from cells by proteinase K digest and Phenol–Chloroform extraction. mtDNA levels were analyzed by separating 2 mg of HindIII digested total DNA on a 0.6% agarose gel in TBE. For conformational studies, 1 mg of DNA was digested with BglII that does not cut mtDNA, and separated over a 0.4% agarose gel in TBE without ethidium bromide. All gels were blotted and hybridized with 32P-labelled DNA probes containing the D-loop region (nts 16341–151) or part of the cytochrome b sequence (nts 14846–15357) of human mtDNA. The signal was quantified by phosphorimager (Storm 840, Molecular Dynamics) and for mtDNA copy-number determination normalized against the signal for 18S rDNA.

## 4.15 Northern blots

RNA was extracted with Trizol (Sigma) using the manufacturer's recommendations. 4 mg of total RNA per sample was run on a 1% agarose MOPS/formaldehyde gel, blotted and hybridized using standard techniques (Church and Gilbert 1984). Blots were probed with ca. 500 bp double-stranded DNA probes radioactively labelled by random-primed labelling and exposed to a phosphorimager plate (Storm 840, Molecular Dynamics) for quantification.

# 5. Results

## 5.1 SIRT3 studies

### 5.1.1 The human SIRT3 deacetylase is exclusively mitochondrial

According to one report human SIRT3 is a nuclear protein, which translocates to mitochondria upon cellular stress and when over-expressed (Scher et al. 2007). However, we had only ever seen clear mitochondrial localisation of hSIRT3, when over-expressing it either transiently or stably in various human cell lines. These observations were in agreement with previous publications (Schwer et al. 2002, Michishita et al. 2005, Onyango et al. 2002). To clear this discrepancy we analysed the subcellular localisation of hSIRT3 by microscopy and subcellular fractionation.

We examined the distribution of the transiently over-expressed hSIRT3 protein in U2OS and HeLa cells and were able to demonstrate a clear mitochondrial localisation irrespective of epitope-tag or expression level (Fig 5.1A). To test for nuclear export we used leptomycin B (LMB) to prevent translocation from the nucleus. According to Scher et al., LMB treatment retains hSIRT3 in the nucleus by inhibiting CRM1 (chromosome region maintenance 1) (Scher et al. 2007). However, after addition of LMB to the hSIRT3 expressing cells we did not see a change in the intracellular distribution of hSIRT3 or any evidence of a fluorescence signal in the nucleus (Fig.5.1B). In contrast and accordingly, LMB prevented the nuclear export of HDAC7, which is known to translocate from the nucleus to the cytosol (Fig 5.1C). In HeLa cells occasional clustering of signal in the nuclear periphery complicated interpretation (Fig. 5.C). This phenomenon may have been mistaken for nuclear localisation in the previous study. We also transfected cells with an hSIRT3 variant lacking the first 142 amino acids. The missing region was suggested to be important for initial nuclear localisation. Removal by nuclear processing would then precede mitochondrial localisation. If this were true, the

deletion of the first 142 amino acids should result in a protein that is mainly mitochondrial. However, the truncated hSIRT3 could not be detected in mitochondria, but was present in the cytoplasm and the nucleus (Fig. 5.D). This is in accordance with the notion that an N-terminal sequence in the unprocessed form of hSIRT3 is required for mitochondrial targeting. LMB treatment did not affect this distribution (data not shown).

We also studied the intracellular distribution of hSIRT3 by isolating nuclei and mitochondria by hypotonic lysis and further purified the nuclei on an iodixanol gradient. The presence of various proteins was analysed by Western blot. This purification method resulted in pure nuclei devoid of any mitochondrial contaminants as could be seen by probing for POLGB, the accessory subunit of the mitochondrial DNA polymerase gamma (Fig 5.2A). Over-expressed and endogenous hSIRT3 were detected with commercial antibodies in the mitochondrial fraction, but neither could be detected in the nuclear fraction (Fig. 5.2B). The band tentatively assigned to be the endogenous hSIRT3 was verified by RNAi. Treating cells with hSIRT3 specific siRNAs resulted in a clear albeit modest decrease in the intensity of the band (Fig 5.2C). Hypotonic lysis combined with differential centrifugation is a common procedure for isolating mitochondria. But if the nuclear pellet resulting from the first low-speed centrifugation is not further purified, the nuclei will be contaminated by the unbroken cells that remain in the crude preparation. Accordingly, we could detect hSIRT3 and other mitochondrial proteins in such un-purified nuclei even when an additional Nonidet-P40 step was included in the isolation (Fig 5.2A.) This observation is of importance, since the claims for the nuclear localisation of hSIRT3 were based on results obtained from hypotonic lysis without a more rigorous nuclear purification step.

We thus demonstrate the unambiguous mitochondrial localisation of hSIRT3 and propose that previous, contradictory results are due to incomplete subcellular fractionation and misinterpretation of microscopy data

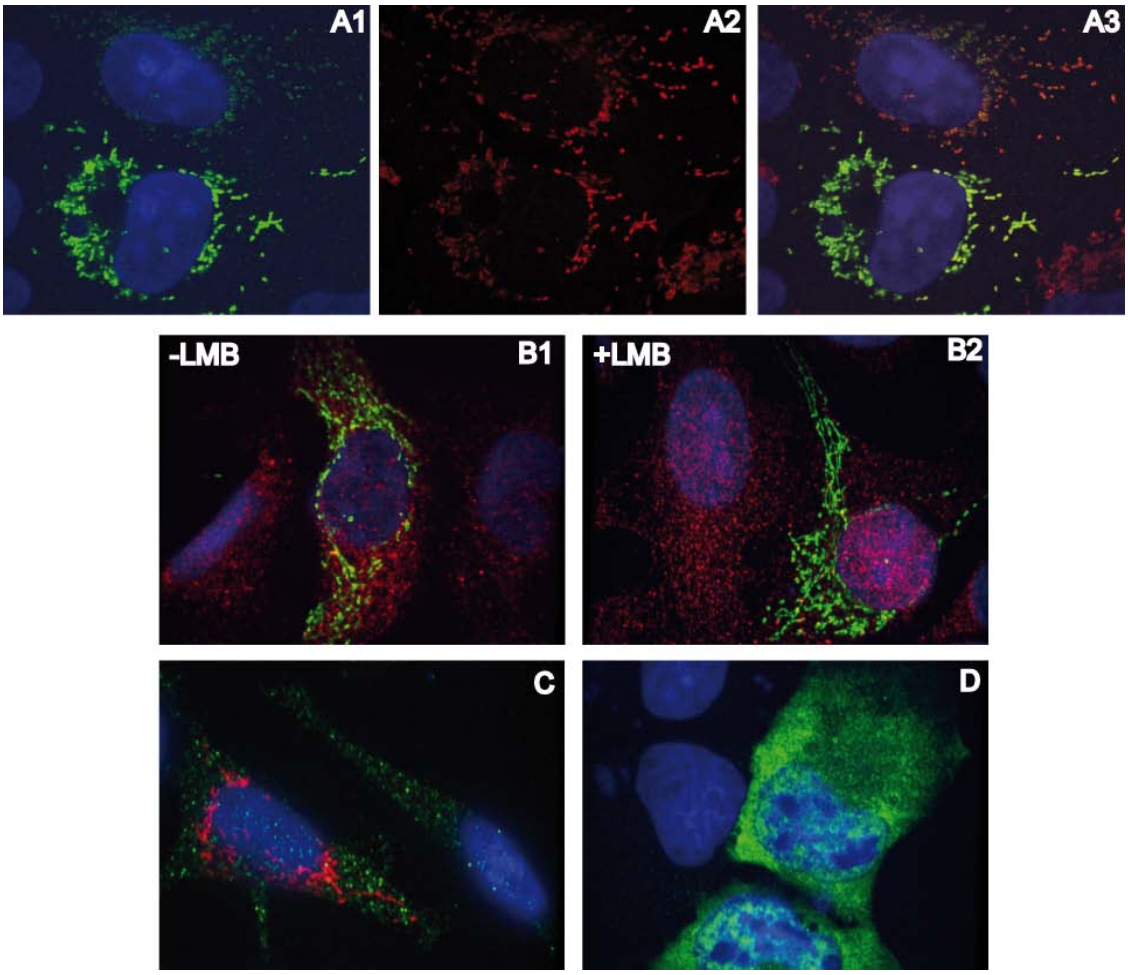


**Figure 5.1. Subcellular localisation of hSIRT3.**
U2OS cells were transiently transfected with hSIRT3-FLAG. 48 hours after transfection cells were probed for FLAG (A1) with a fluorescent antibody and stained with Mitotracker® Red (A2). The merge image (A3) demonstrates clear co-localisation of the two signals. U2OS cells transfected as in A were treated for 2-3 hours with 5ng/ml LMB. hSIRT3 localisation in LMB treated cells (B2) was indistinguishable from that in un-treated cells (green fluorescence). Co-transfected HDAC7, however, was retained in the nucleus by LMB (B2, red fluorescence). The same nuclear retention of HDAC7 by LMB was also seen in HeLa cells, altrough the effect was less clear (C, green fluoresence). hSIRT3 remained mitochondrial after LMB treatment in HeLa cells (C, red fluorescence), but in these cells the occasional clustering of mitochondia in the nuclear periphery gives the false impression of nuclear localisation. An N-terminal truncation hSIRT3Δ1-142-Myc was located in the cytoplasm and at high levels of expression, as shown in D, also in the nucleus. Over-expressed hSIRT localises to mitochondria irrespective of level of expression or LMB treatment.

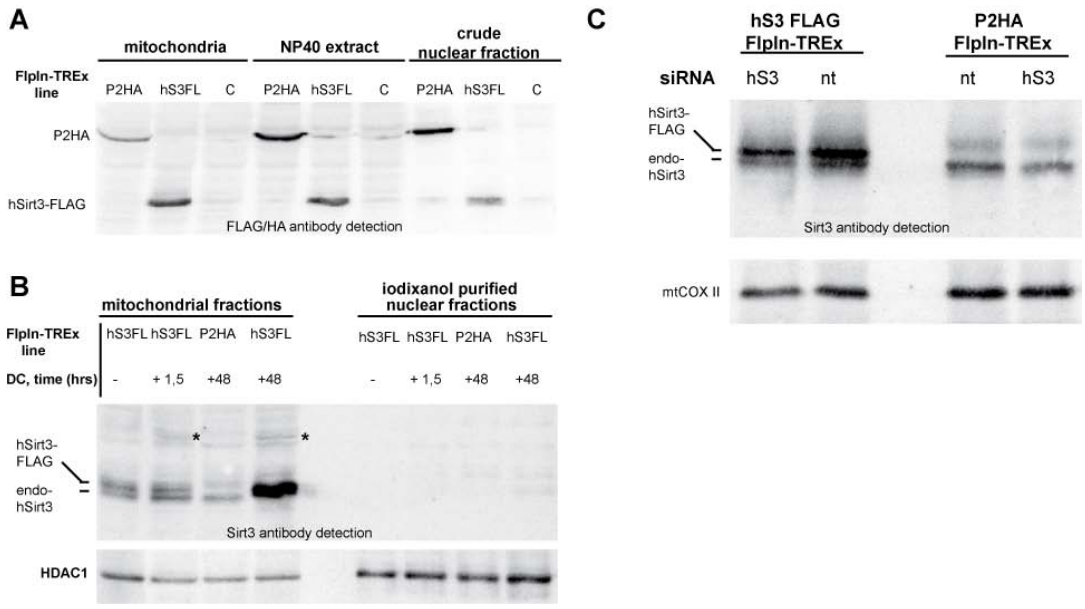


**Fig 5.2. Fractionation of hSIRT3 expressing cells.**
Stably transfected hSIRT3-FLAG (S3FL) and POLG2-HA (P2HA) were over-expressed in inducible TREx-HEK-293e cell by inducing with 5ng/ml doxicyclin (DC) for 48 hours. Crude mitochondrial fractions were prepared from over-expressing and non-expressing control (c) cells. The 'nuclear' pellet resulting from a low speed centrifugation of the total cell lysate was extracted with a small amount of NP-40 and the resulting pellet was subjected to a high-salt extraction. Despite the 2-step nuclear purification the well established mitochondrial protein POLGB-HA could be detected in the nuclear fraction (A). The presence of hSIRT3 in this fraction cannot thus be interpreted as nuclear localisation. Only after purification on an iodixanol gradient was the nuclear fraction devoid of mitochondrial contaminants (B). And after this step hSIRT3 could no longer be detected in the nuclear fraction either. The asterix denotes the hSIRT3-FLAG precursor protein, which could be detected in mitochondrial fractions already after 1.5 hrs of transgene induction, but never in the nuclear fraction (B). siRNAs against hSIRT3 modestly but reproducibly decreased the amount of both over-expressed hSIRT3 in TRex-hSIRT3 cells and endogenous hSIRT3 in TRex-POLGB cells (C**).** Both the precursor and the processed forms of over-expressed hSIRT3 as well as endogenous hSIRT3 are exclusively mitochondrial.

### 5.1.2 Identification of a longer splice variant of mSIRT3 confirms conservation between species

Sirtuins are highly conserved between species. However, the mouse SIRT3 -protein was reported to be markedly shorter than its human counterpart and to lack the N-terminal mitochondrial targeting signal present in the human protein. Therefore, we set out to look for longer transcripts of mSIRT3. An *in silico* analysis of mSIRT3 cDNA sequences predicted the presence of a splice variant that introduces two potential translational start site upstream of the previously described coding sequence (Cooper and Spelbrink 2008). These potential start sites, Met1 and Met15, correspond to Met1 and Tryp15, respectively, in the human SIRT3 gene (Fig 5.3).


**Fig 5.3. Mouse SIRT3 cDNA based on 'Celera ab initio RNA'Gnomon prediction Chmm195886.** Grey arrows denote EST starting positions with Genbank accession numbers, covering the exon 1b/2 boundry. Exon 2 has been originally predicted to harbour an 8 bp 5' extension resulting in a frameshift. Two new start sites are denoted with single red lines. The red double-line marks the terminal stop –codon.

We used a specific oligo that overlapped with the mSIRT3 stop codon, to make cDNA from polyA RNA isolated from mouse NIH3T3 fibroblasts. We then used the same reverse oligo and a forward oligo complementary to the region of exon 1B (Fig 5.4), which contains the predicted M1 start codon, to PCR amplify and clone, what turned out to be two cDNAs, which are distinguished by the insertion of an additional 8 bp at the 5' extremity of exon 2 in splice variant 2 (Fig 5.4). This 8 bp sequence is present in the originally reported major mRNA/cDNA (Shi et al. 2005). Theoretically, the insertion would induce a frameshift in mSIRT3 translation at the level of either Met1 or Met15. This would then result in the termination of translation at codon 66. In our hands nine out of 17 randomly selected cDNA clones did not contain the 8 bp insertion. These clones coded for the predicted full length protein, while the remaining 8, which did have the insertion, were predicted to cause

premature translation termination at codon 66. These findings suggest that at a longer SIRT3 variant, corresponding in size to the full-length human SIRT3, is present in mouse cells, and that at least in 3T3 cells both splice variants are present in roughly equal proportions.

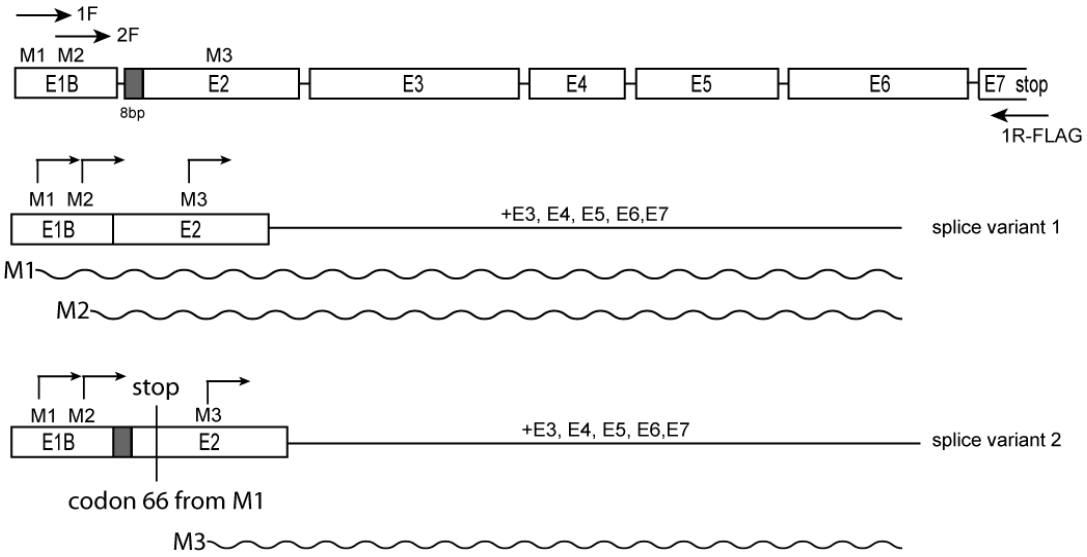


**Fig 5.4. Schematic representation of the mSIRT3 splice variant constructs, which produced the protein variants M1, M2 and M2.**

## 5.1.3 The longer mSIRT3 variant localises to mitochondria

To further study the properties of the proteins encoded by the different mSIRT3 cDNAs, we generated three constructs: Two distinct constructs, M1 and M2 were generated from splice variant 1 using in the first case Met1, and in the second case Met15 as the initiation codon (primers 1F and 2F, Fig 5.4). The third construct, M3 was generated from splice variant 2 but using primer 1F (see Fig 5.4). M3 included the Met1 and Met15 initiation codons, but also the 8 bp frameshift sequence predicted to lead to translation termination at codon 66. In all three constructs the coding sequence was followed by a 3' in frame sequence for the FLAG epitope tag (Fig 5.4)

We used immunofluoresence in transiently transfected cells to determine the subcellular localisation of the three mSIRT3 constructs. Both M1 and M2 showed clear mitochondrial localization in 3T3 cells. (Fig 5.5). This was further confirmed

by co-staining with Mitotracker® Red (Fig 5.5). Although translation from Met and Met15 was predicted to end at the stop codon at position 66, the M3 construct generated a protein, which was detected using the FLAG antiserum. This indicates that the cDNA encoded a protein starting at the third methionine, Met143. The M3 protein showed a non-mitochondrial uniform cytosolic and sometimes nuclear staining with some clusters in case of (rare) high levels of over-expression (Fig 5.5). Based on the immunofluorescence, M3 was generally expressed at lower levels than M1 and M2 and a much lower number of cells could be identified as clearly positive.

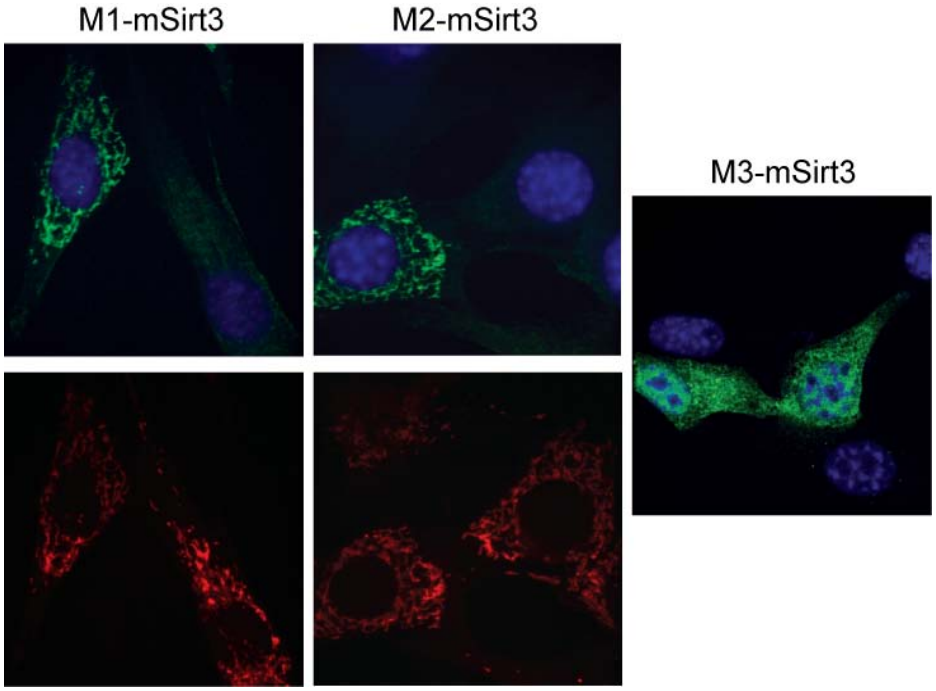


**Fig 5.5. Localisation of mSIRT variants**
Mouse 3T3 cells were transiently transfected with the FLAG-tagged mSIRT variants M1, M2 and M2. 4hrs after transfection cells were detected for immunofluoresence with an anti-FLAD antibody and stained with Mitotracker®Red. M1 and M2 co-localise with the mitochondrial network, whereas the shorter form M3 gives uniform cytosolic staining.

We then studied the expression profile of the mSIRT3 isoforms by Western blot using either an antibody against the FLAG epitope tag for the detection of over-expressed FLAG-tagged variants or an antibody specific for mouse SIRT3 for the detection of endogenous and over-expressed proteins. The human SIRT3 precursor protein has previously been shown to be cleaved into a significantly shorter, enzymatically active form upon entry into mitochondria (Schwer et al. 2002). The protein products of both the M1 and M2 construct could be detected as two major forms: an uncleaved precursor (indicated by arrows ‘M1’ and ‘M2’, respectively)

and a processed form (indicated by ‘proM1–2’), which corresponded in size with the endogenous mSIRT3 protein (including the epitope tag). This pattern of over-expression was seen in 3T3 as well as in mouse hepatocytes (Fig. 5.6). Comparison of the ratios of the cleaved protein versus the uncleaved precursor suggests that the M2 variant is processed more efficiently than M1. Especially in 3T3 and HEK293 cells, the precursor protein from the M2 construct was often barely visible (Fig.5. 3A and C) unless expression was boosted by replacing the endogenous sequence upstream of the start codon by a consensus Kozak sequence. The full-length M1-encoding vector rise to a protein, which was the same size as the precursor protein expressed from the M2-encoding vector. This observation suggests that translation also initiated at Met15 in the M1 construct. Detection of the shorter variant (M3) in total lysates and mitochondrial fractions from 3T3 cells was weak at best (Fig 5.6A). This is in agreement with the poor expression observed by immunofluorescence. Detection of M3 was clearer in total lysates from mouse hepatocytes and HEK293 cells (Fig 5.6B and C) The FLAG-tagged mSIRT3 M3 protein in mouse hepatocytes migrated on SDS-PAGE as a single band which was, despite the tag, smaller than endogenous (untagged) mSIRT3 (Fig 5.6B), while over-expression of non-tagged versions of M1 and M2 in 293T cells showed processed proteins larger than the FLAG-tagged M3 but identical in size with endogenous mouse liver SIRT3. The non-mitochondrial localisation of M3 is enforced by the observation that a variant of the human SIRT3 (Fig 5.1D), corresponding in size to the mouse M3 protein, was not enriched in mitochondrial fractions (data not shown).

We conclude that the proteins M1 and M2, starting from translational start sites at Met1 and Met15, respectively, yield proteins that are mitochondrial, whereas the shorter M3, which is the previously predicted full-length mouse SIRT3 protein, is not targeted to mitochondria. The low-expression levels of M3 compared to M1 and M3 also raise doubt about its physiological significance.

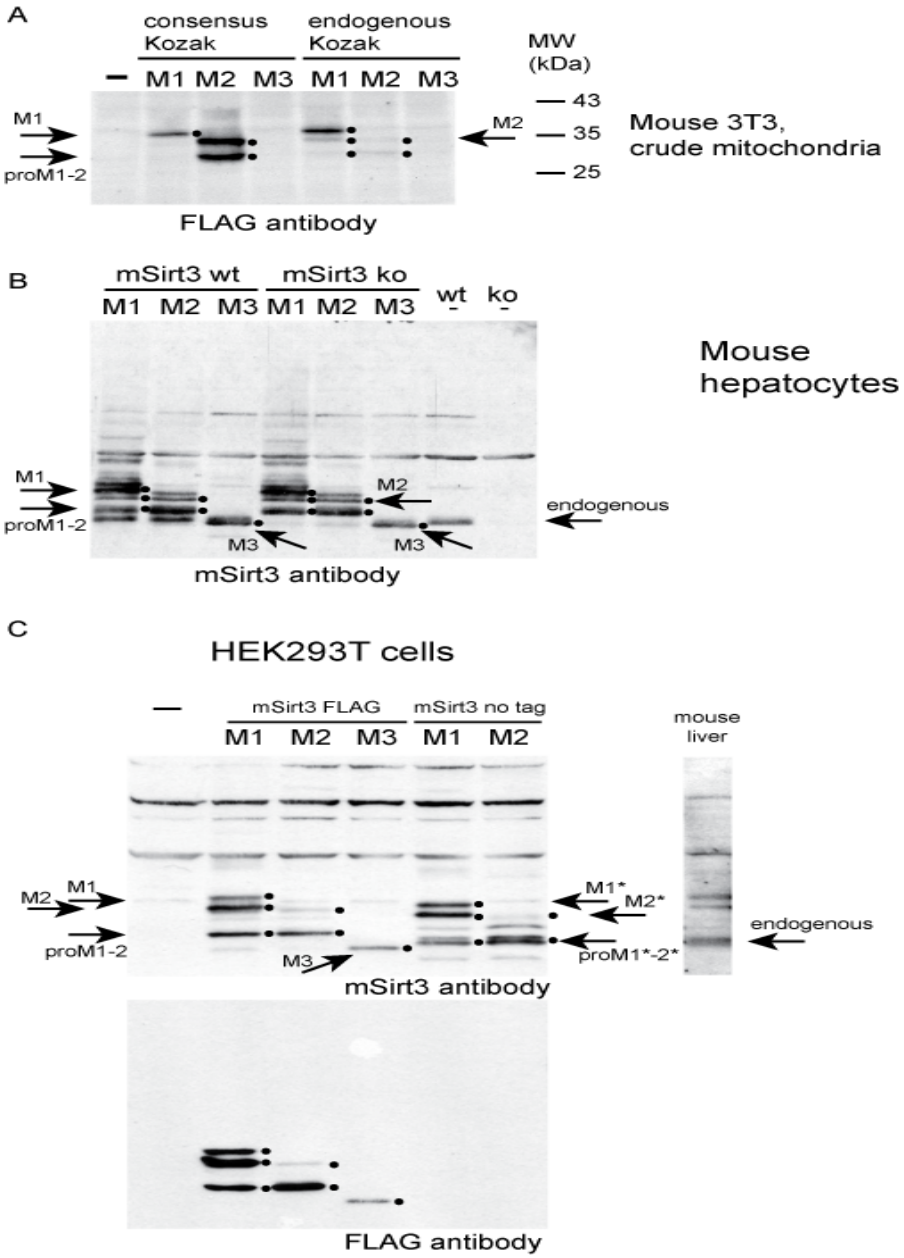


**Fig 5.6. Over-expression of mSIRT3 variants.**
FLAG-tagged mSIRT3 variants M1, M2 and M3 were expressed in mouse 3T3 cells (A) and primary mouse hepatocytes from both wt and ko-mice (B) while both FLAG-tagged M1-3 and untagged M1 and M2 were expressed in HEK293e cells. Total cell lysates or crude mitochondrial lysates were probed for the mSIRT3 variants on western blot with either an anti-FLAG antibody or with an antibody against mSIRT3. A consensus Kozac sequence was cloned into constructs to boost expression (A). To denote the size of endogenous mSIRT3 a mouse liver extract was run alongside the HEK293T derived samples (C). And to clearly detect the endogenous protein lysates from non-transfected wt and mSIRT3 ko mouse hepatocytes were run along transfected samples (B, R'endogenous'). Detected proteins are denoted by small dots. The mSIRT3 variants M1 and M2 appeared in two forms when over-expressed. M3 expression is weak. M3 was only weakly expressed.

### 5.1.4 New hSIRT3 interacting partners were identified in a yeast-two-hybrid library screen

The Matchmaker 3 system (Clontech) was used to search for interacting partners for hSIRt3. The AH109[BD-hSirt3] yeast strain was mated with a Y187 strain pre-transformed with a cDNA library from skeletal muscle (Clontech). Mating efficiency was calculated as 6,0%, which is high enough for a representative screen and corresponds to about 8,2 milloin library clones screened. Over 1000 positive clones grew on the TDO/X-α-Gal plates in the first round of selection, where only yeast clones carrying both plasmids and showing activation of the HIS3 reporter could grow. The resulting colonies were re-streaked to QDO/X-α-Gal plates for a more stringent selection, after which about 900 colonies survived. Blue growth on QDO/X-α-Gal plates indicates expression of all three reporters (HIS3, ADE2 and LacZ). Blue colonies were then re-streaked on to DDO/X-α-Gal plates three times, in order to allow segregation i.e. to retain only a single unique plasmid in each clone. As the DDO/X-α-Gal medium does not exert selective pressure for colonies with a two-hybrid interaction, segregation is possible. The presence of X-α-galactosidase, however, allows detection of colonies, which do contain a two-hybrid interaction. Only colonies which were blue and thus positive for a two-hybrid interaction were maintained. Finally, the preservation of the interaction after segregation was verified by streaking the colonies back onto the most stringent selection medium, QDO/X-α-Gal.

Plasmids from positive clones were purified and the library insert was PCR-amplified and sequenced. A total of 759 different clones were successfully sequenced and indentified using the Blastp program from NCBI (Altschul et al. 1990). A vast majority of clones analysed represented one of a small group of recurring proteins including and a total of 144 different proteins were identified to interact with hSirt3, 29 of which, according to reports in the literature, were mitochondrial. The mitochondrially localised proteins are presented in Table 1 while all interacting proteins are listed in Appendix 1.

### 5.1.5 The majority of the hSirt2-interacting proteins identified in the yeast-two-hybrid library screen are metabolic enzymes

Included in our YH2 screen results were several proteins involved in metabolic pathways such as enzymes of the citric acid cycle, electron transport chain and the beta-oxidation of fatty acids. These findings are consistent with the notion that hSIRT3 targets metabolic enzymes. NDUFA9, one of the proteins of Complex 1 of the respiratory chain has been shown to be a SIRT3 substrate in mouse. And accordingly, we found the hSIRT3 interacts with three members of the NADH dehydrogenase complex. And the hSIRT3 interaction with the alpha subunit of the ATP synthetase (complex V) has been reported previously in a cell based screen (Law et al. 2009), further validating the results of our Y2H screen.

### 5.1.6 Several of the hSIRT3 interacting proteins are known to be acetylated.

Since hSIRT3 is a deacetylase it is plausible to assume that many of its interaction partners are acetylated. Two recent proteomics studies have listed acetylated cellular proteins, including mitochondrial ones (Kim et. 2006, Choudhary et al. 2009). We compared our list of hSIRT3 interacting proteins to the results of these screens and came up with 13 and 5 proteins that were shared between our list and the list of Kim et al., and our list and that of Choudhary et al. respectively. Four proteins, fumarate hydratase, malate dehydrogenase, the alpha subunit of the mitochondrial ATPase, and acetyl-coenzyme A acetyltransferase were common to the two acetyl-lysine screens and our screen. We determined the significance of the overlap by determining that the probability of randomly selecting 13 of our 29 proteins from the group of 133 included in 600 acetylated proteins (Kim et al. 2006) is highly unlikely with a p value for acumulative hypergeometric probability of $\leq 0{,}0045$.

| **Interaction partners reported to be acetylated** | **Ref.** |
|---|---|
| Acetyl-coenzyme A acetyltransferase 1 | Kim et al., Choudhary et al. |
| Acetyl-coenzyme A acyltransferase 2 | Kim et al. |
| Adenylate kinase 2 | Kim et al. |
| ATPase, mitochondrial F1 complex, alpha subunit | Kim et al., Choudhary et al. |
| Electron-transfering-flavoprotein dehydrogenase | Kim et al. |
| Enoyl coenzyme A hydratase 1,short chain, mitochondrial | Choudhary et al. |
| Fumarate hydratase | Kim et al., Choudhary et al. |
| Hydroxyacyl dehydrogenase, subunit B | Kim et al., Choudhary et al. |
| Malate dehydrogenase | Kim et al. |
| NADH dehydrogenase ubiquinone 1alpha subcomplex 10 | Kim et al. |
| Solute carrier family 25 member 3 | Kim et al. |
| Thiosulfate sulfurtransferase | Kim et al. |
| Ubiquinol-cyt c reductase core protein I | Kim et al. |
| Voltage-dependent anion channel 1 | Kim et al. |
| Acyl-coA dehydrogenase, c-4 - c-12 straight chain | (Kim et al.)[1)] |
| | |
| **Interaction partners not been reported to be acetylated** | |
| Cytochrome c oxidase deficient homolog 1 | |
| Cytochrome c oxidase subunit III | |
| Deoxyguanosine kinase | |
| Electron-transfer flavoprotein, alpha | |
| GRIM19 (NADH dehydrogenase complex) | |
| Guanylate kinase 1 | |
| N-acylsphingosine amidohydrolase 2 | |
| NADH dehydrogenase ubiquinone 1 alpha subcomplex 7 | |
| NADH dehydrogenase (ubiquinone) Fe-S protein 3 | |
| NADH dehydrogenase (ubiquinone) Fe-S protein 8 | |
| NADH dehydrogenase ubiquinone 1 β subcomplex 10 | |
| Pyruvate dehydrogenase | |
| Succinate dehydrogenase complex, subunit B | |
| Sulfide dehydrogenase like | |

**Table 5.1**. 29 mitochondrial proteins were identified as hSIRT3 interacting partners found in a Y2H screen. A comparison of the YH2 screen results with two lists of known acetylated mitochondrial proteins. [1)] Different isozyme, with different chain length specificity found by Kim et al.

### 5.1.7 At least three of the hSIRT3 interacting beta-oxidation enzymes are acetylated.

As hSIRT3 has been shown to influence acetyl-CoA production via the deacetylation and activation of the mitochondrial acetyl-CoA synthetase, AceCS2 (Schwer et al. 2006, Hallows et al. 2006), we chose to further study the acetylation and hSIRT3 mediated deacetylation of the enzymes of the acetyl-CoA producing beta-oxidation pathway. We cloned and expressed the FLAG-tagged variants of medium chain acyl-coA dehydrogenase (ACADM), acyl-coA acyltransferase 2 (ACAA2), acetyl-coA acetyltransferase 1 (ACAT) and short chain enoyl-coA hydratase (SCEH) in HEK293e cells by transient transfection. The proteins were immunoprecipitated and analysed them by western blot using acetyl-lysine specific antibodies. Three of the four beta-oxidation proteins, ACAA2, ACADM and SCEH, were detected with different anti-acetyl-lysine antibodies from Cell Signalling Technologies (Fig 5.7A). We could not detect ACAT1 acetylation, although it was reported to be acetylated by both Kim et al., and Choudhary et al.

### 5.1.8 hSIRT3 influences the acetylation and stability of ACAA2 *in vivo*.

We then studied the effect of co-expressed hSIRT3 on the acetylation status of over-expressed ACAA2, ACADM and SCEH. HEK293e cells were transfected with the FLAG-tagged beta-oxidation genes together with hSIRT3 and a LacZ expressing vector to control for transfection efficiency. Cells were grown in low glucose media with supplementary galactose, since this enhanced the expression of the beta-oxidation enzymes. Proteins were immunoprecipitated and analysed by western blot for changes in acetylation levels. The co-expression of hSIRT3 resulted in a decrease in the acetylation of ACAA2 (Fig 5.7C). Interestingly, this was consistently accompanied by a decrease in overall protein levels. To test that this was not an immunoprecipitation artefact or due to the FLAg-tag, we expressed myc-tagged ACAA2 with hSIRT3 and histone deacetylase 7 (HDAC7) and prepared whole cell lysates. hSIRT3 influenced, but not HDAC7 influenced ACAA2 protein stability. In contract, the amounts of ACADM and AceCS2 were the same in the

presence of both hSIRT3 and HDAC7 (Fig 5.7C.). Quantification of the anti-acetyl-lysine signal and anti-FLAG signal from three different experiments showed that the reduction in acetylation was grater than the decrease in protein levels.

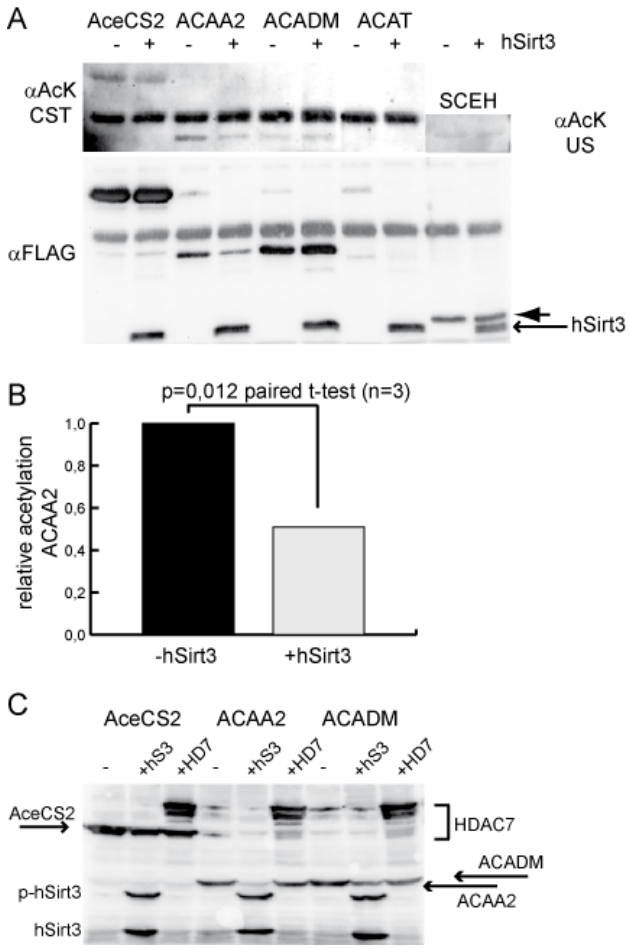


**Figure 5.7. Anti-acetyl-lysine antibodies recognise beta-oxidation proteins**. A) FLAG-tagged beta-oxidation proteins were over-expressed in HEK293 cells and immunoprecipitated. ACAA2, ACADM and the positive control AceCS2 are recognised by an anti-actyl-lysine antibody by Cell Signalling Technologies. SCEH is recognised by an anti-body from Upstate (Note that in the upper panel the SHEC signal is inserted into a higher position for convenience. In reality the protein runs at the position depicted in the lower panel). Co-expression of hSIRT3-FLAG resulted in a decrease in ACAA2 acetylation and protein amount. B) ACAA2 acetylation and protein levels were quantified from blots and acetylation levels were found to be decreased more than overall protein levels. Experiments were controlled for transfection efficiency. C) To rule out the possibility that the observed decrease in ACAA2 protein levels is an immunoprecipitation or epitope-tag artefact, whole cell lysates from differentially co-expressed cells were prepared. Here, ACAA2-Myc levels are less in the presence of co-transfected hSIRT3-FLAG, but unchanged in the presence of HDAC7-FLAG. AceCS2-FLAG and ACAA-FLAG levels are similar in the presence of the co-expressed deacetylases.

## 5.2 hSIRT3 influences acetyl-CoA levels

To investigate how hSIRT3 could regulate the function of beta-oxidation proteins we measured acetyl-CoA levels in doxycycline-inducible cell lines expressing hSIRT3. We used a fluoresence based assay kit (Biovision), in which free acetate is converted to CoA and the CoA reacts to form NADH, which interacts with a probe to generate fluoresence. Acetyl-CoA levels of hSIRT3 expressing cells that had been induced with 3ng/µl doxycycline for 48hrs were about 4-fold higher than those of induced vector-only expressing control cells (Fig. 5.8) We also noted that high levels of doxycycline depleted acetyl-CoA pools in both hSIRT3 and control cells (data not shown).

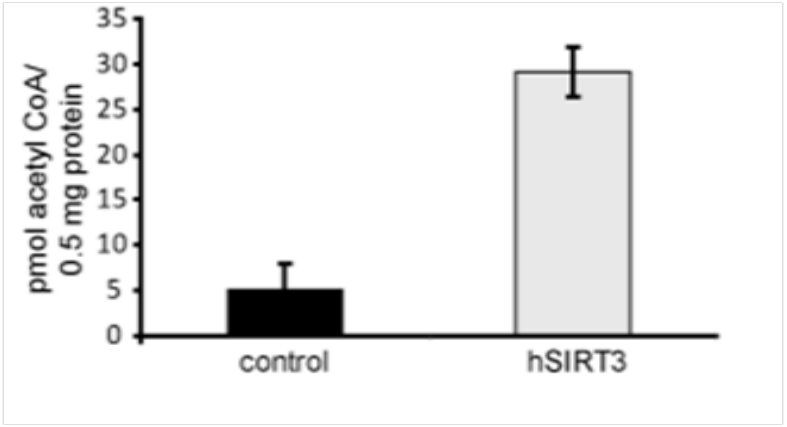


**Figure 5.8. Acetyl-CoA levels in hSIRT expressing cells.** hSIRT3 expression was induced in stable cell lines with low amounts of doxycycline for 48hrs, after which acetyl-CoA levels were measured from cell lysates. hSIRT3 cells had a 4-fold increase in acetyl-CoA levels (pmol/0,5mg of protein) compared to induced vector-only control cells.

## 5.3 Twinkle studies

### 5.3.1 Twinkle adPEO mutations affect in vitro DNA binding, helicase activity and oligomerisation

Seven adPEO-related Twinkle mutations, causing mild to severe symptoms, were cloned in to the pcDNA5 vector for stable inducible expression in human HEK293 Flp-In™ T-REx™ cells. The mutations chosen were: four mutations in the linker region of Twinkle (dup352–364, A359T, S369P, R374Q), two mutations located in the N-terminal domain in close proximity to the linker region (W315L, K319E) and one mutation in the helicase domain (W474C). For *in vitro* activity assays proteins were purified from crude mitochondrial lysates in one step using TALON® affinity $CO^{2+}$ resin and stored in small aliquots at -80°C. The *in vitro* DNA binding activity on a single stranded substrate was measured as described previously (Korhonen et al. 2008) The G575D mutant was used as control, since it was predicted to have, and indeed showed, weak DNA binding compared to wild-type Twinkle. The binding affinities of dup352-364, K319E and W315L were found to be reduced, A359T and R374Q showed near to normal ssDNA binding and the S369P mutant showed moderately increased binding (Fig 5.9B). (The W474C mutant was not included in the summary, since it repeatedly gave spurious results.)

*In vitro* helicase activities roughly agreed with the DNA binding levels of the mutants. In our hands Twinkle prefers UTP as its energy source. But we also used ATP, GTP and dGTP to drive the helicase reaction on a partially single-stranded substrate as described previously (Wanrooij et al. 2007), but with the exception that we carried out the reaction at 37°C. The helicase activity of K319E and R374Q was reduced to <20% for all nucleotides and the W474C and W315L showed an approximately 70% reduction in helicase activity irrespective of the nucleotide used. The dup 352–364 mutant had 70% remaining helicase activity, when GTP was used as an energy source, but the relative helicase activity was considerably lower with dGTP and UTP. S369P showed a marked reduction in

helicase activity despite its high DNA binding affinity. (Fig 5.9A) However, the S369P mutant also had only a mild effect on mtDNA copy-number (see below).

To investigate whether impairments in DNA binding and helicase activities were due to defective hexamerisation, we studied oligomerisation of the mutants using a previously described chromatographic approach (Korhonen at al. 2008). Wild-type Twinkle forms hexamers even under high ionic-strength conditions and in the absence of any nucleotide. Under similar conditions, all mutant protein also formed hexamers, but differences in the degree of oligomerisation could readily be detected. A359T, W474C, W315L and S369P showed multimer stability comparable to wt Twinkle. The mutants R374Q, K319E and dup352–364 appeared less stable, but in all three cases high molecular weight multimers could still be detected. (Fig 5.10).

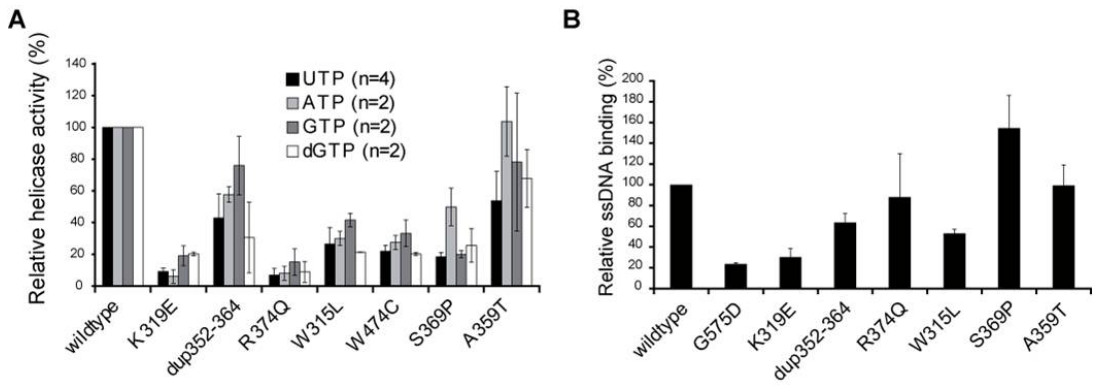


**Figure 5.9. Helicase activities and DNA binding affinities of the adPEO mutants.** Helicase activities of purified variants were measured in the presence of different nucleotides on a partially single-stranded substrate (A). And their binding affinities were measured on a single-stranded substrate (B). adPEO mutations affect both the unwinding and ssDNA binding activity of Twinkle.

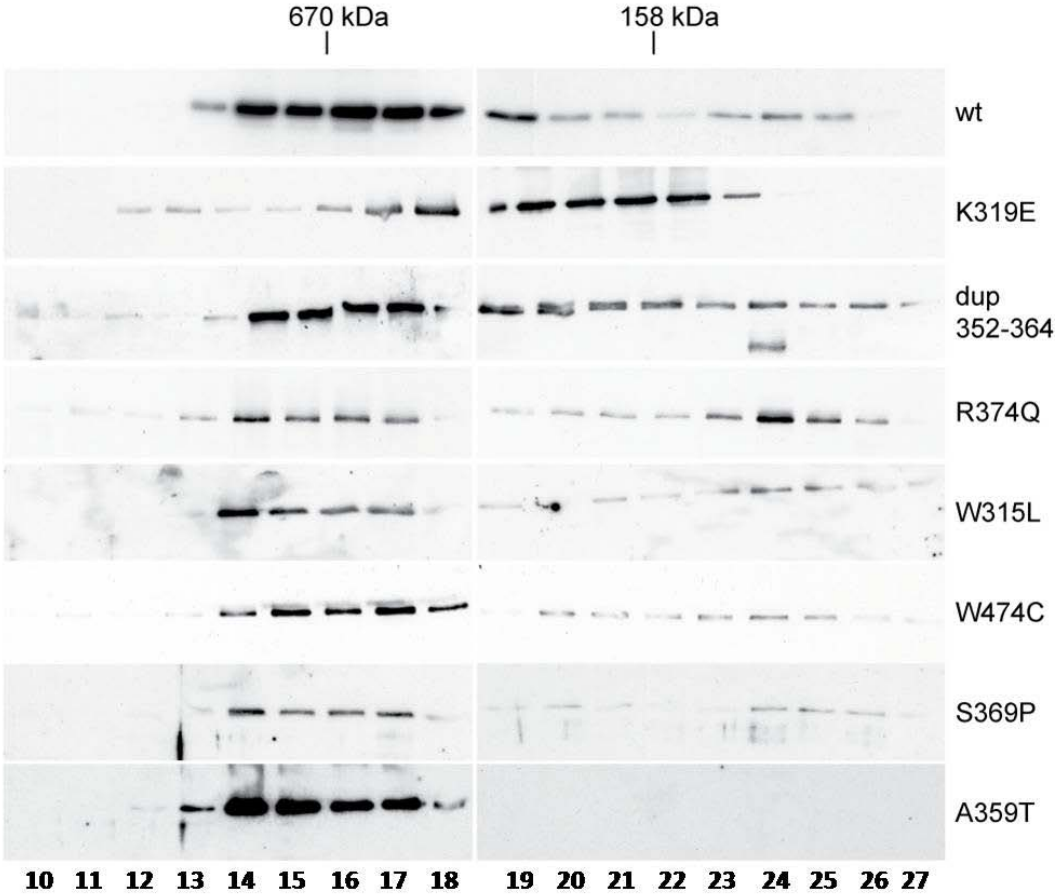


**Figure 5.10. Oligomerisation of the adPEO mutants.**
Proteins were purified and their ability to form multimers was measured by gel filtration chromatography. Twinkle proteins eluted in fractions 10 to 27. Some adPEO mutations decrease the stability of Twinkle hexamers.

### 5.3.2 Twinkle adPEO mutatants affect nucleoid localisation and mtDNA copynumber levels

A cell culture model based on the Flp-In™ T-REx™ system was used to study the *in vivo* effects of Twinkle adPEO mutants. The system allows tetracycline (doxycycline) inducible expression of a gene, from a defined insertion site in the genome of human HEK293e cells. Since the expression of the endogenous Twinkle is not affected, low induction of mutant gene expression resembles the heterozygous condition of PEO patients. Myc-His tagged Twinkle adPEO mutants were expressed for 2-3 days using 3 ng of doxycycline. This level of induction gave expression levels of about 10-fold compared to endogenous Twinkle.

MtDNA copynumber was measured with qPCR. Over-expression of wild type Twinkle resulted in a slight, but statistically significant elevation in mtDNA

copy-number. In contrast, expression of all mutants led to mtDNA depletion. The level of depletion varied between the different mutants. K319E and R374Q caused mtDNA levels to drop to 25% within three days. The 13 aa duplication reduced mtDNA levels more than 50%, and the rest of the point mutations lead to a 60-70% reduction in mtDNA copynumber. Intrestingly, Twinkle mutations also affected mitochondrial transcript levels (data not shown). This reduction of transcripts was stronger than the observed mtDNA copynumber depletion after two days of expression, indicating that the negative effect of Twinkle dysfunction on transcription precedes the depletion of mtDNA and is not due to reduced mtDNA template levels.

Nucleoid morphology of the Twinkle expressing cells was examined using immunocytochemistry and confocal microscopy. Wild type Twinkle and the W315L mutant showed spot-like co-staining with mtDNA, which is indicative of nucleoid localisation (Spelbrink et al. 2001). The variants K319E, R374Q and dup352-364MtDNA as well as A359T, but to a lesser extent, showed a more uniform staining of the mitochondrial matrix, but also clear punctuate co-localisation with mtDNA. The nucleoid spots in the K319E, R374Q and W474C and dup352-364 expressing cell lines appeared larger in size and fewer in number compared to wild-type. The S369P mutation showed good co-localisation with mtDNA. (Fig 5.12.)

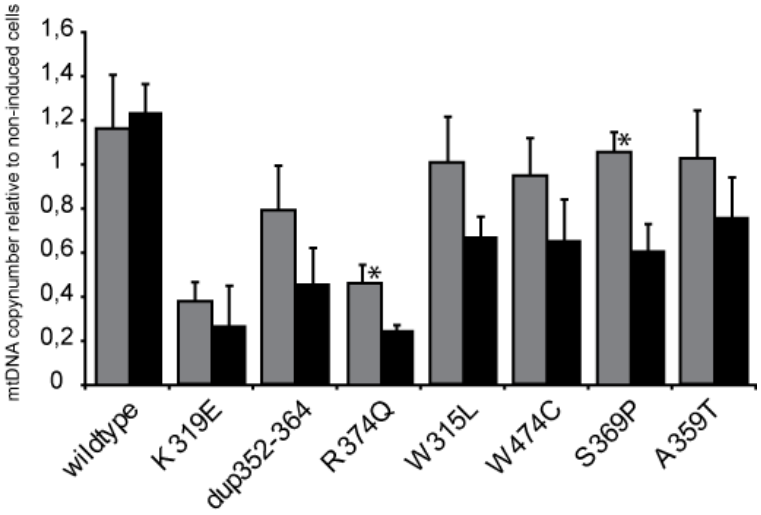


**Figure 5.11. Mitochondrial DNA copynumber of adPEO mutant expressing cells.**
MtDNA levels of cells induced with 3 ng/ml doxycycline for two days (grey bars) or three days (black bars) were quantified by duplex Taqman PCR and normalized to non-induced cells of the same cellline. Four to six independently isolated samples were measured in triplicate with the exception of the two samples indicated with an asterisk that were isolated twice and measured in triplicate. Mutant expression causes a rapid depletion of mtDNA.

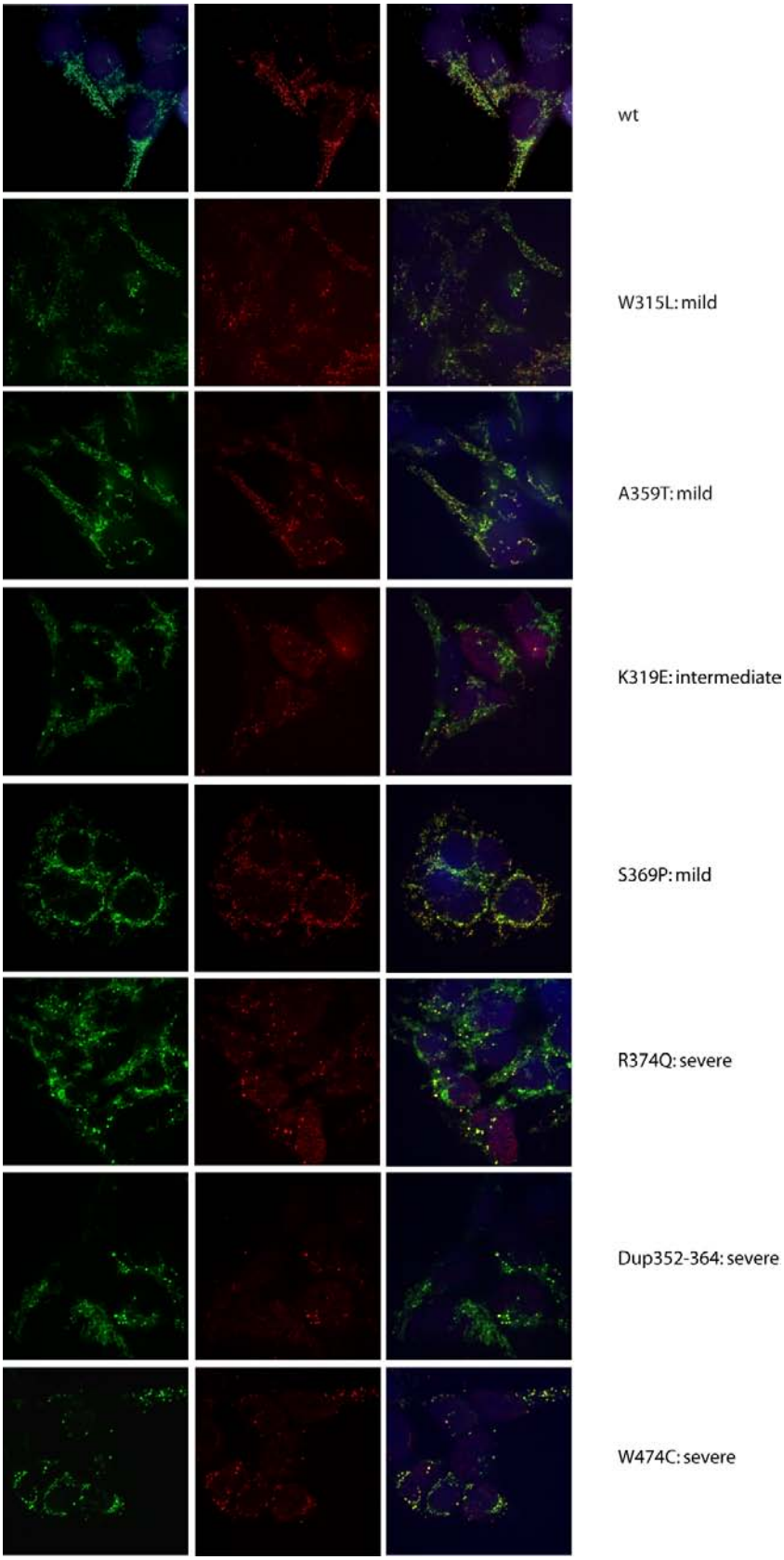


**Figure 5.12. The influence on nucleoid morphology of the adPEO mutants**.
The subcellular localization of the over-expressed Twinkle variants in HEK239e cells was determined by immunofluorescence (green) and compared to Mitotracker ®Red staining. The mutants cause mild to severe defects in nucleoid morphology.

### 5.3.3 Twinkle adPEO mutations cause a defect in mtDNA replication in both human cell culture and in a transgenic mouse model

Mitochondrial DNA replication was studied using the 2DNAGE method, which allows the visualisation of DNA replication intermediates (see Appendix 2 for the interpretation of 2DNAGE gels). Earlier studies carried out in the group have shown that structural mutations that completely abolish the helicase activity of Twinkle affect mtDNA replication in cultured cells leading to strong replication stalling and the accumulation of replication intermediates (Wanrooij et al. 2007). The adPEO mutants, with compromised helicase activity, affected replication to varying degrees compared to Myc-His-tagged wild-type Twinkle, whose over-expression had no influence on replication pattern or the abundance of replication intermediates apart from one species of molecules thought to be part of the termination process in the non-coding region of DNA (Wanrooij et al. 2007). Over-expression of the K319E led to a sharp accumulation of molecules on the y-arc and the double-stranded bubble-arc and a decrease in the levels of RNA rich intermediates. These findings are indicative of a strong effect on replication progression and were seen throughout the mitochondrial genome. A similar although milder replication stalling was induced when expressing R374Q, dup352–364 or W315L Twinkle variants. The S369P and A359T mutations had the mildest effect, although also they gave a clear replication stalling and a shift to less RNA containing intermediates. The W474C variant also caused the disappearance of RNA-rich intermediates and the accumulation of y-shaped molecules. However, in contrast to the other mutations studies, in the case of W474 bubble-containing intermediates did not accumulate, but vanished completely. (Figure 5.13.)

In cell culture the replication stalling observed when expressing Twinkle adPEO mutants led to rapid loss of mtDNA. But this effect has not been reported in adPEO patients. To determine whether similar phenomena as in cultured cells can found *in vivo*, we studied the mtDNA replication patterns of the Deletor mice, mice expressing a mutated Twinkle (Tyynismaa et al. 2005). These mice show mtDNA deletions in muscle at the age of 9-12 months. And deletions as well as DNA depletion can be detected in Deletor brain after one year of age. We studied the heart, liver, skeletal muscle, kidney and brain of animals of six weeks of age and

found abnormal replication patterns in all tissues except liver, in the absence of a decrease in mtDNA copy-number. With their age dependent increase in mtDNA deletions and histological features resembling those seen in patients, Deletor mice serve as an animal model for adPEO. Our similar findings in cultured cells and the tissues of Deletor mice demonstrate that the molecular defects caused by the Twinkle adPEO mutants can be studied in a cell culture model.

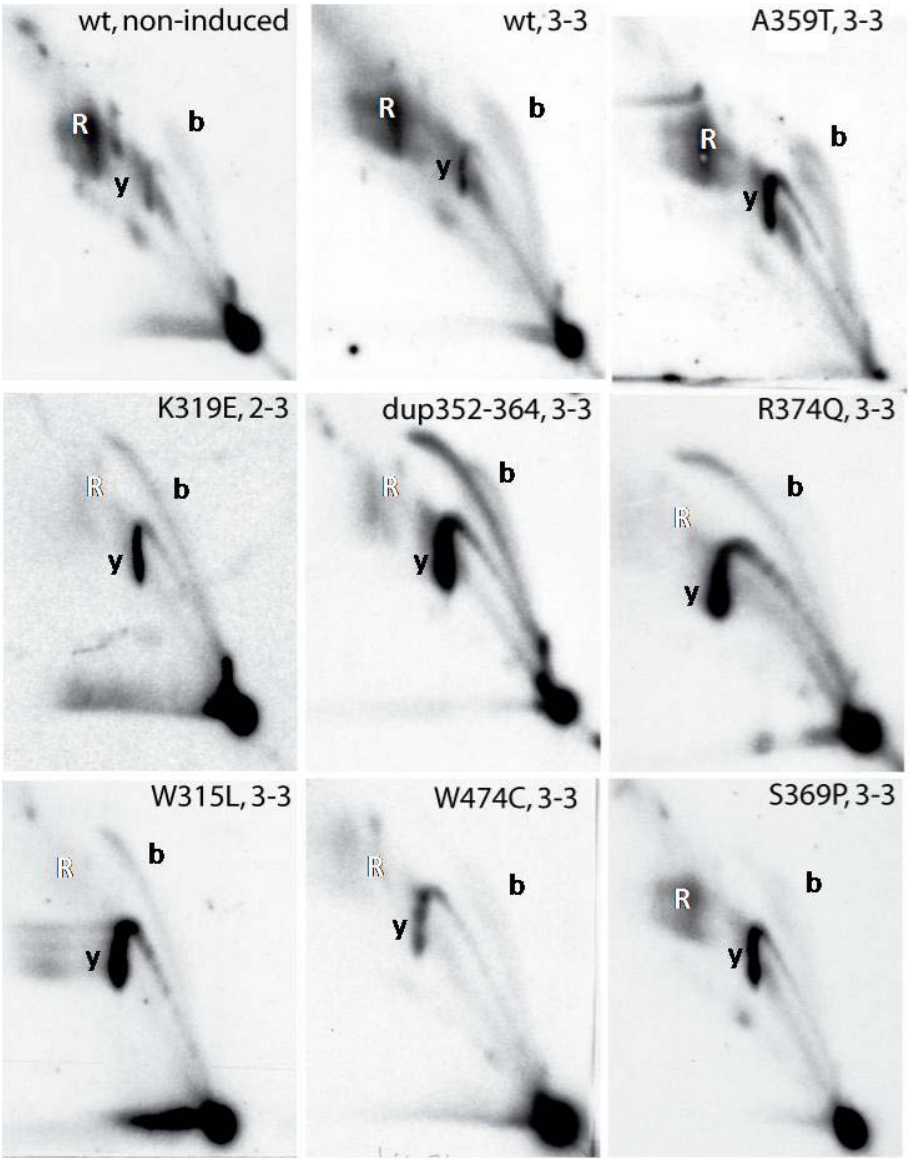


**Figure 5.13. mDNA replication intermediates seen in cell lines expressing adPEO mutants.**
The mtDNA of cells expressing Twinkle variants was analysed by 2DNAGE. Gene expression was induced with doxicycling (2–3: two days of induction with 3 ng/ml doxycycline; 3–3: three days induction with 3 ng/ml doxycycline), DNA was purified, digested with HincII and probed with a radiolabeled cytochrome b gene fragment (nt 14 846–15 357). The detection fragment includes the non-coding region of mtDNA, the cytochrome b, ND6, part of the ND5 gene and intervening tRNA genes (nt 13 636–1006). The upper two panels show a comparison of mtDNA replication in non-induced and Twinkle wild-type over-expressing cells. Over-expression of wild-type Twinkle did not change the replication pattern. In contrast the stronger disease mutations caused an accumulation of replication intermediates (y and b) and a decrease in all RITOLS related features (R).

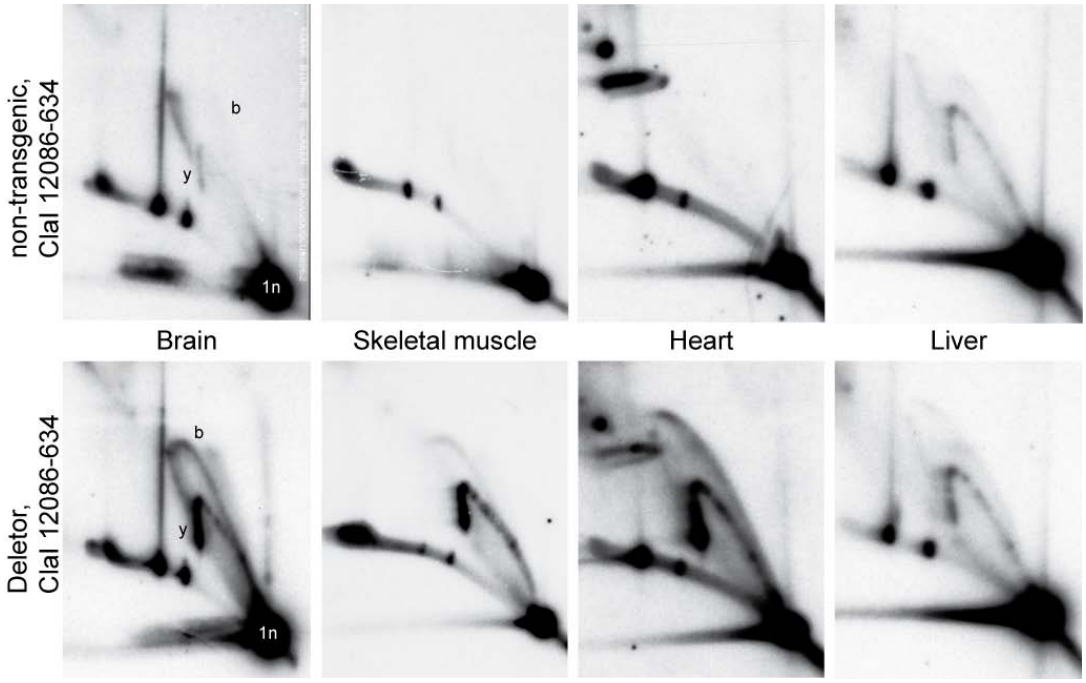


**Fig 5.x+4. mtDNA replication intermediates seen in tissues of wt and Deletor mice.**
Brain, skeletal muscle, heart and liver of 6-week-old transgenic mice harbouring the equivalent to the human dup352-364 mutant and non-transgenic siblings were analysed by 2DNAGE. The mitochondrial DNA was probed against the OH-containing ClaI fragment (nts 12086–634). Tissues from Deletor mice show, except for liver, a similar strong accumulation of replication intermediates as in cultured cells.

# 6. Discussion

## 6.1 Sirtuin biology

Due to their connection to the regulation of metabolism and lifespan SIR2-deacetylases are now receiving an increasing amount of attention. In recent years the field of sirtuin research has made several advances towards understanding the mechanism by which sirtuin action connects nutritional state to stress resistance and longevity. Mammals have at least seven different sirtuins, which have been shown to act on different substrates with different outcomes to substrate function. However, all sirtuin activity seems to connect to a common underlying theme of sensing and regulating energy state and stress responses. Mitochondria are the principal sites of cellular energy production. The mitochondrial sirtuins thus likely regulate core metabolic events.

### 6.1.1 SIRT3 in energy producing pathways

SIRT3 is known to influence acetyl-CoA production via the activation of Acetyl-CoA synthetase 2 (AceCS2) (Schwer et al. 2006, Hallows et al. 2006). AceCS2 is required for acetyl-CoA production from free acetate during the ketogenesis resulting from fasting. It has been proposed that by boosting AceCS2 activity SIRT3 increases the acetyl-CoA to CoA ratio (North and Sinclair 2006). The resulting increase in acetyl-CoA would feed the TCA cycle and induce glucose production from puryvate through gluconeogenesis. This inhibition of the pyruvate dehydrogenase complex would be augmented by the shift SIRT3 causes in the NAD:NADH ratio by consuming NAD. This way SIRT3 would promote gluconeogenesis during calorie restriction. We found that human SIRT3 interacts with enzymes of the β-oxidation pathway, which breaks down fatty-acids to ultimately form acetyl-CoA. Three enzymes, namely acyl-coA dehydrogenase (ACADM), acetyl-coA acyltransferase 2 (ACAA2) and short chain enoyl-coA

hydratase (SCEH), were also shown to be acetylated. Our results are in line with the view that hSIRT3 targets metabolic enzymes. Included in our findings on hSIRT interacting proteins were mitochondrial dehydrogenases, TCA cycle proteins and proteins of the beta-oxidation pathway. A significant number of our findings were shared with the screens for actylated proteins by Kim et al. and/or Choudhary et al. Although yeast two-hybrid screens are generally not recommended for the study of post-translational modifications, the above suggests that we might have picked-up actual acetylated and therefore credible interaction partners. This would suggest that within the context of a yeast-two-hybrid screen mitochondrial proteins could be targets of yeast acetyl transferases in the cytoplasm/nucleus, thus suggesting that these transferases are promiscuous with regard to their targets. This would also suggest that the majority of mitochondrial hSIRT3 partners identified here are potential acetylated proteins. This is at least in part substantiated by the fact that the ACADM isoform we identified was not identified as acetylated by Kim et al. or Choudhary et al. but is shown here to be actylated.

In addition, we measured an increase in acetyl-CoA levels in hSIRT3 over-expressing cells. Our findings support the view that SIRT3 regulates acetyl-CoA levels by targeting acetyl-CoA producing enzymes. We also found that co-expressed hSIR3 could deacetylate ACAA2 *in vivo*. This deacetylation also decreased the stability of ACAA2. At this point we cannot say whether this destabilising effect is directly due to the hSIRT3-mediated deacetylation of ACAA2, or if hSIRT3 activates e.g. a mitochondrial protease. Increrasing the amount of ACAA2 may be a means of feedback regulation of the beta-oxidation pathway, or it may play a part in determining the fatty-acid chain length-specify of the enzyme complexes.

SIRT3 can also deacetylate and activate isocitrate dehydrogenase 2, a key regulator for the flux through the TCA cycle (Schlicker et al. 2008). This further indicates that SIRT3 can control nutrient flux. This would then allow the production and targeting of glucose to dependant tissues under calorie restriction. Among the other proteins we found in a yeast-two-hybrid screen, were components of the electron transport chain (ETC) including dehydrogenases of Complex I and the alpha subunit of ATP synthase (Complex V). In agreement with our results, SIRT3 has also been shown to target the ETC in mice. SIRT3 -/- mice show an increase in acetylation of mitochondrial proteins (Lombard et al. 2007, Ahn et al. 2008). Among these proteins Ahn et al. found NDUFA9, which is part of Complex 1. SIRT3

mediated deacetylation of Complex 1 proved to be crucial for ATP production and SIRT3 -/- mice had decreased basal ATP levels (Ahn et al. 2008). SIRT3 can thus also influence ATP production via ETC proteins.

Lombard et al. in turn identified glutamate dehydrogenase as hyperacetylated in SIRT3 knock-out mice. GDH was also found to be a substrate for human SIRT3 *in vivo* and *in vitro* (Lombard et al. 2007). Deacetylation of GDH promoted the use of amino acids as fuel for the TCA cycle and ultimately ATP production (Lombard et al. 2007). This offers yet another mechanism by which SIRT3 can regulate energy production from different substrates. Interestingly, SIRT4 has an opposing effect on GDH, whose activity it inhibits via ADP-ribosylation (Haigis et al. 2006). Including our results in it, we present a supplemented version of the figure 11 shown in section 2 of the Literature Review to summarise the complementing and opposing effects of SIRT1, 3 and 4 on mitochondrial energy production.

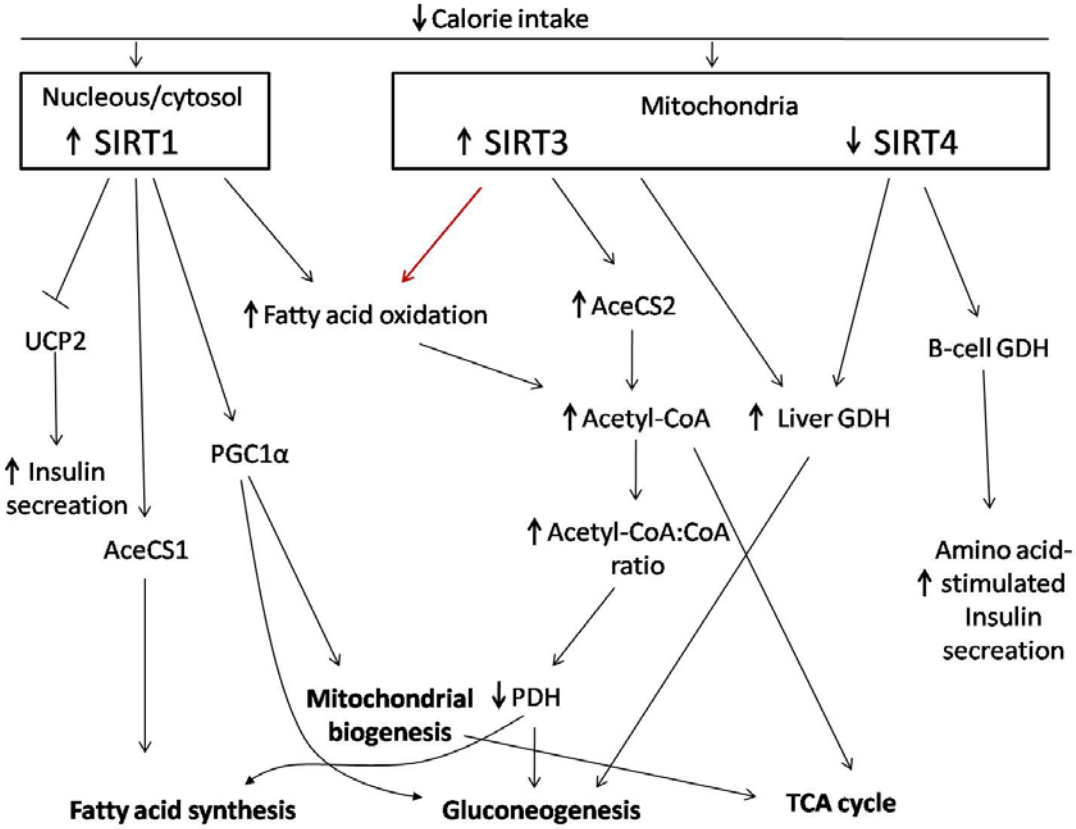


Figure 6.1. Complementing and opposing effects of SIRT1, SIRT3 and SIRT4 on energy producing pathways (adapted from North and Sinclair, 2006). In addition to its know roles in regulating Acetyl-CoA synthethase 2 (AceCS2) and glutamate dehydrogenase (GDH), we propose that SIRT3 can influence acetyl-CoA production by regulating beta-oxidation proteins.

The specific mechanisms of the connection between hSIRT3 over-expression and ACAA2 deacetylation and acetyl-CoA production still need to be addressed. At this point the functional consequences hSIRT3 has on both ACAA2 deacetylation and protein stability are unclear. Acetylation levels are decreased more than protein levels, so deacetylated protein may be more active but also more rapidly turned over. This may represent a mechanism of feed-back control, as ACAA2 catalyses the last step of the beta-oxidation spiral. Or the overall mechanism by which SIRT3 influences acetyl-CoA production is more complex and the outcome of hSIRT3 over-expression is a result of the combined control of many proteins and in many different pathways in an orchestrated manner. The HEK cells that we used are highly glycolytic, and it is unlikely that beta-oxidation is used for acetyl-CoA production under normal cell culture conditions to a great extent. Acetylation of beta-oxidation proteins could be detected more readily when cells were grown in low-glucose media supplemented with galactose. Attempts to measure beta-oxidation with palmitate using the Seahorse instrument (Seahorse Bioscience Inc) have been unsuccessful, since the HEK cell do not seem to take up the substrate. A different cell culture system and/or approach including differential levels of SIRT3 and beta-oxidation proteins will need to be tested to find ways of pin-pointing specific sites or regulation and measuring enzyme activities and metabolite production.

### 6.1.2 The subcellular location of SIRT3 in mouse and man

Although SIRT3 knock-out mice show a reduction in basal ATP levels (Ahn et al. 2008), they are phenotypically indistinguishable from wild type litter mates (Lombard et al. 2007, Ahn et al. 2008). The lack of any changes in body composition, oxygen consumption, activity levels or feeding behaviour is contradictory to the effect of over-expressing mSIRT3 in mouse adipocytes. Shi et al. demonstrated that enforced Sirt3 expression in brown adipocytes upregulated the expression of PGC-1α, UCP1 and a series of genes related to mitochondrial function (Shi et al. 2005). However, the over-expressed mSIRT3 was significantly shorter than its human counterpart, lacking 142 residues from its N-terminus. Being puzzled

about the discrepancy between the over-expression and knock-out phenotypes and about the seeming difference in length between these allegedly highly conserved proteins, we investigated the possibility of different mSIRT3 isoforms. And as is shown in the results section, an *in silico* analysis of available sequence data revealed the presence of longer mSIRT3 cDNAs, which we were also able to clone from mouse 3T3 cells. We demonstrate the existence and expression and clear mitochondrial localisation of an mSIRT3 variant, which corresponds in length to hSIRT3. Alternative splicing of this full length mRNA can lead to the translation of a shorter protein product, the one used by Shi et al. for over-expression studies. However, we show that this shorter form does not localise to mitochondria. This is in agreement with the observation that removal of the N-terminal portion abolishes the mitochondrial targeting of hSIRT3 (Cooper & Spelbrink, 2008). The low expression levels of the truncated mSIRT3 in our hands in several cell types and structural analysis (Jin et al. 2009) argue against its physiological relevance. However, we shall not exclude the possibility that the shorter non-mitochondrial form of mSIRT3 targets cytosolic proteins, since we did find cytosolic interaction partners in our yeast-two hybrid screen for hSIRT3. Perhaps a cytosolic isoform of SIRT3 offers a means of communication between cellular compartments. Still, due to the dramatic contradiction between the phenotype of mSIRT3 knock-out mice and over-expressing murine adipocytes, we are inclined to suspect that the mistargeted mSIRT3 over-expression simply mimicked SIRT1 over-expression (Rodgers et al. 2005).

Interestingly, mSIRT3 has a second methionine at position 15, which, as we show, can be used for translation initiation. This methionine is not present in human SIRT3 and could thus represent a species specific way of regulating mSIRT3 function. SIRT3 behaviour may also be tissue specific. SIRT3 has been shown to protect cardiomyocytes from stress-mediated apoptosis by deacetylating Ku70 (Sundaresan et al. 2008). Curiously, however, Ku70 is a nuclear protein. Gupta et al. report that while a shorter, 26kD form of SIRT3 is mitochondrial a longer 44kD form of the protein can be found in the nucleous of murine cardiomyocytes. If this is true, it is a demonstration of tissue and species specific differences in SIRT3 localisation and behaviour, since we have shown that at least hSIRT3 is exclusively mitochondrial.

The nuclear localisation of hSIRT3 has been suggested by Scher et al, who claimed that hSIRT3 is in fact a nuclear protein, which translocates to mitochondria upon cellular stress and when over-expressed (Scher et al. 2007). This result was contradictory to our observations, and could significantly influence functional studies. So we addressed the issue by firstly repeating the fractionation and localisation experiments described by Scher et al. We showed that in their crude nuclear isolation protocol a significant amount of unbroken cells remained in the nuclear pellet. The mitochondria of these cells then contaminated the nuclear fraction with mitochondrial proteins, including hSIRT3. A more thorough purification of nuclei on an iodixal gradient was required to remove mitochondrial contaminants. After this step, hSIRT3, neither endogenous nor over-expressed, was present in the nuclear fraction of HEK cells. The nuclear localisation of hSIRT3 as seen by microscopy is also subject to doubt, as we never saw any hSIRT3 signal in the nucleus, nor were we able to achieve nuclear retention of hSIRT3 with leptomycin B. The location of mitochondria in the close vicinity or above in a higher plane respective to the nucleolus may create the false impression of punctate nuclear expression. Although the methods employed by Gupta et al, in their study of murine cardiomyocytes are somewhat different to those used by Scher et al., we suggest caution when interpreting such fractionation and microscopy data, especially as the prevailing evidence, from both original observations (Schwer et al. 2002, Onyango et al. 2002, Michishita et al. 2005) and new reports (Lombard et al. 2007, Jin et al. 2009), is for the exclusive mitochondrial localisation of SIRT3 in mouse and man.

### 6.1.3 Mitochondrial acetylation

Perhaps because mitochondria have no histones as such, acetylation of mitochondrial proteins was largely disregarded. This was until a proteomics study reported the acetylation of 133 mitochondrial proteins (Kim et al. 2006). Evidently, acetylation is an important modification to mitochondrial proteins. And as the majority of the proteins reported by Kim et al. are metabolic enzymes they make potential sirtuin substrates. Accordingly, in our yeast-two-hybrid screen we found 29 SIRT3 interacting proteins, the majority of which were enzymes of central

metabolic pathways. A statistically significant 13 were included in the 133 acetylated proteins reported by Kim et al, and four of these were also found a later screen by Choudhary et al (Choudhary et al. 2009).

What is the significance of acetylation to the function of metabolic proteins in mitochondria? SIRT3 can remove acetyl groups thereby inducing the enzymatic activity of its known substrates. Acetylation is thus at least a way of regulating the activity of mitochondrial enzymes. We also found the co-expressing hSIRT3 with the beta-oxidation pathway enzyme ACAA2 decreased ACAA2 stability. Although deacetylation is known to influence protein degradation (Li et al. 2002), we cannot at this point say, if the hSIRT3 has a direct effect on ACAA2 or if it rather influences a mitochondrial protease.

So far, no mitochondrial acetyl transferase activity has been described. It is therefore unknown whether acetylation takes place outside or inside mitochondria and how and if proteins that are once deacetylated by SIRT3 become re-acetylated.

The large number of acetylated mitochondrial proteins and the fact that many of them have multiple acetylation sites raises the possibility of chemical acetylation. As its levels rise, acetyl-CoA may become incorporated into mitochondrial proteins thus repressing metabolic enzymes to down-regulate further acetyl-CoA production, when the electron-transport chain is amply fuelled. Simultaneously, high NADH levels and low NAD+ levels would suppress SIRT3 activity. A decrease or change in nutrient availability would then activate SIRT3 via an increase in NAD, and by deacetylating mitochondrial targets SIRT3 would promote energy production and the use of alternative metabolic pathways. Interestingly, a recent structural analysis of hSIRT3 showed, that the enzyme binds its acetylated substrate before the NAD co-factor (Jin et al. 2009). This would suggests, that an increase in mitochondrial protein acetylation is the primary trigger of hSIRT3 activity.

If the acetylation of mitochondrial proteins is a read-out of the metabolic state of the cell and if SIRT3 act as a master switch between metabolic “modes”, then the acetylation profile of metabolically compromised or SIRT3 deficient cells should be distinct from that of cells in a nutritionally normal state. Likewise, high metabolic and SIRT3 activity should be reflected in the acetylation of mitochondrial proteins. Studies in mice have shown that in the absence of SIRT3 mitochondrial proteins are hyperacetylated and ATP production is down to less than half of the levels in wild-type mice (Lombard et al. 2007, Ahn et al. 2008) . And conversely, calorie

restriction causes changes in the acetylation profile of mitochondrial proteins (Schwer et al. 2009). When mice were subjected to a calorie restricted diet mitochondrial acetylation in their brown adipose was markedly decreased. These mice also showed profound changes in liver mitochondrial acetylation. However, in liver, acetylation levels of most detected proteins were in fact increased despite the slight decrease in hSirt3 expression. This may be due to the different roles these tissues have in producing energy. Deacetylation of BAT mitochondrial proteins would promote beta-oxidation to release energy from stored lipids, whereas the hyperacetylation of mitochondrial proteins in the liver could promote glucose release by down-regulating other pathways. While calorie restriction has proven beneficial as measured by several attributes of metabolism, the absence of SIRT3 activity does not seem to be harmful for cells. Calorie restricted cells are pushed towards an overall more active metabolism as they strive to fuel obligate tissues with glucose. And this includes changes in mitochondrial acetylation. But cells seem to be able to maintain sufficient control of energy production without SIRT3. This may be due to sirtuin redundancy. Or perhaps the absence of sirtuin function only becomes apparent in certain tissues and/or under severe stress.

In an aging society that struggles against an increasing number in the incidences of type 2 diabetes and metabolic syndrome, it is tempting to speculate on the possibilities sirtuins may offer in counteracting these conditions and increasing a healthy lifespan. Boosting SIRT1 and SIRT3 activity could mimic the benefits of calorie restriction and direct metabolism towards the expenditure of fat depots even in the absence of glucose deprivation. hSIRT3 has indeed been associated with health benefits. Exercise can increase the epression of hSIRT and prevent its age associated decrease (Lanza et al. 2008). And variability in the hSIRT3 gene, which up-regulates SIRT3 expression, is enriched in long lived individuals (Rose et al., 2003, Bellizi et al., 2005). Some compounds that can potentially activate sirtuins, such as resveratrol, have been developed into commercially available products, but very little *in vitro* evidence let alone evidence on any beneficial effects they might have on human metabolism exists. The control of metabolism involves effectors on many levels, and although sirtuin research has been able to give important information on cellular responses to changes in nutritional state, it will require investigation into the biochemistry of many other compounds such as NAD, insulin

and ROS, to name a few, to unravel the complexities of metabolic control in relation to disease development and aging.

## 6.2 Mitochondrial DNA maintenance

The mitochondrial DNA codes for components of the electron transport chain and the number of mitochondrial genomes/mitochondrion reflects the energy needs of the cell. For its replication, transcription and repair the mtDNA is completely dependent on the protein products of nuclear genes. In proliferating cells the replication of mtDNA is synchronised with nuclear DNA replication and cell division. But in cells that no longer undergo mitosis, such as neurons and muscle cells, mtDNA replication is independent of the cell cycle. The molecular mechanisms of mtDNA maintenance are not fully understood and the regulation of e.g. replication is complicated by the involvement of nuclear genes. Mutations to mtDNA maintenance proteins cause syndromes, which often involve changes in mtDNA copy number or topology. These then ultimately lead to impaired energy production, which is often most detrimental to post-mitotic tissues. Also, changes in mitochondrial DNA and energy production are associated with aging in healthy individuals. Studying the behaviour of wild-type and mutated mtDNA maintenance proteins can help in understanding how situations of mtDNA derived energy deficiencies can arise.

### 6.2.1 Nucleoids

Contradictory to the previous view of “naked” mitochondrial genomes, mtDNA is now known to be associated with many proteins in complexes designated nucleoids. The composition and dynamics of nucleoids is a popular topic in the field of mtDNA research, and so far several proteins involved in mtDNA maintenance have been identified as part of the core nucleoid. However, little is known about the regulation of these protein-DNA interactions. Although mitochondria contain no histones, at least the mitochondrial transcription factor, Tfam has packaging properties. Tfam has in fact been shown to be acetylated in rat liver (Dinardo et al.

2003), but the significance of this was not addressed, nor are there similar reports for the human protein. But a very recent report describing the entire “acetolome” of a human cell lists the mitochondrial single-stranded binding protein (mtSSB) as acetylated (Choudhary et al. 2009). It is plausible to consider the possibility that the affinity of mitochondrial DNA binding proteins is regulated by acetylation-deacetylation in a manner analogous to nuclear chromatin remodelling. This was an underlying hypothesis when we set out to study the behaviour of the Twinkle helicase on a DNA template. Judging by the Twinkle amino acid sequence and comparing to known acetylation sites, Twinkle has several lysine residues, which could be targets for acetyl-transferases. However, to date, we have not been able to identify any acetylation sites. Instead, we were able to study the DNA binding properties of mutated Twinkle proteins, mutants that cause mtDNA deletions in the post-mitotic muscle of adPEO patients.

### 6.2.2 Understanding mitochondrial DNA maintenance in health and disease

Mutations in the mitochondrial DNA helicase cause neuro-muscular syndromes which arise from a mitochondrial energy deficiency, which is due to deletions in or depletion of the mitochondrial DNA. The severity of the disease depends on the type of the mutation: depletion syndromes manifest in early childhood, whereas deletions may gradually accumulate over the years in post-mitotic tissues until muscular and neurological symptomes appear typically in early adulthood. Autosomal dominant progressive ophthalmoplegia (adPEO) is a mitochondrial disease characterised by progressive external ophthalmoplegia, ptosis and myopathy. Symptoms appear in the mid-twenties and patients have multiple mitochondrial deletions, the number of which correlates with the age of onset and with the severity of the disease. The mechanism of how and at what rate mtDNA lesions accumulate is not known. Twenty-three Twinkle mutations have been identified as adPEO causing genes. In addition mutations in the catalytic subunit of the mitochondrial DNA polymerase gamma (POLGA) as well as the adenine nucleotide translocase (ANT) can cause adPEO.

### 6.2.3 Molecular features of Twinkle adPEO mutants

The underlying reason for the mtDNA deletions is in defective mtDNA maintenance in the case of Twinkle and POLG mutants, and nucleotide imbalances, which ultimately lead to mtDNA maintenance defects, in the case of ANT mutants. The biochemical properties of a number of Twinkle adPEO mutants have been studied *in vitro* and a mutant Deletor mouse, mimicking the tissue defects of adPEO patients, has been described. To further asses the properties of seven adPEO mutants, including previously uncharacterised ones, we created stable inducible cell lines with the Twinkle variants integrated into defined locations in their nuclear genomes. By measuring the copynumber and studying replication intermediates of the mutant over-expressing cells and by testing various biochemical properties of the purified mutant proteins *in vitro* we were able to show that the adPEO mutants cause a defect in mtDNA replication. Our data is largely in agreement with and augments existing data on the behaviour of adPEO mutants *in vitro* and in insect cells (Matsushima& Kaguni 2007, Korhonen et al. 2008)

Over-expression of all adPEO mutants led to replication stalling and a rapid drop in mtDNA levels. The situation was of course exaggerated, since the ratio of mutant to wild-type protein was approximately 4:1 (Wanrooij et al. 2007). However, replication intermediates could also be detected in the tissues of six-week-old Deletor mice, which don't produce detectable levels of mtDNA deletions until at nine months of age. Our cell culture system is therefore a valid model for studying the molecular events in adPEO. And in fact, the stronger adPEO mutants also showed a slowing down of mtDNA replication and a accumulation of of replication intermediates when expressed in a one-to-one ratio with endogenous wild-type Twinkle (data not shown).

The dominant negative effect of the adPEO mutants is due to the hexameric nature of the active enzyme. Even the presence of one mutated monomer can disturb the assembly and function of the holoenzyme. The co-existense of wild-type and mutant proteins in our preparations can explain the discrepancies between the *in vitro* studies performed by us and others (Korhonen et al. 2008). The baculovirus derived proteins used by Korhonen et al. were derived of any wild-type Twinkle. E.g in their hands the R374Q mutant remained monomeric, whereas we were able to obtain R374Q containing multimers, likely due to the presence of wild-type Twinkle

in the holoenzyme. Also observed differences in binding activity could be explained by differences in hexamerisation due to the source of the mutant protein. What we did find supprising though was the increased binding activity of the S369P mutant, compared to the decreased binding reported by Korhonen et al. (Korhonen et al. 2009). We also saw more nucloids in the S369P expressing cells, which was in contrast to all the other mutants, which had less nucloids than wild-type Twinkle expressing cells. It may be that the tight DNA binding of the S369P variant influences nucleoid segregation.

### 6.2.4 Consequences of replication stalling

In proliferating cells pauses in mitochondrial DNA replication should cause mtDNA depletion, as the rate of mtDNA replication can't keep up with cell division. This is what we observed in our Twinkle adPEO mutants cell lines, in which over-expression of the mutant helicase causes replication stalling. In adPEO patients affected cells are post-mitotic, and mtDNA replication is no longer coupled to the cell cycle. In this case mtDNA depletion will result, if the turnover of the DNA exceeds replication. AdPEO patients, however, have multiple mtDNA deletions instead of depletion, although deletions are preceeded by replication stalling, as was seen in the tissues of young Mutator mice. In contrast, we were not able to detect deletions in our cell culture model. It seems therefore, that the mitotic state of the cell determines the consequences of replication stalling. But the molecular mechanisms remain unclear. As is discussed in a recent review (Krishnan et al. 2008) pauses in replication could elicit an enhanced repair respons, which would then lead to deletion formation. Another scenario could be the focal depletion of mitochondrial DNA, which would be followed by rapid re-amplification favouring deleted molecules. In this case the mitochondrial turnover rate could also be significantly influenced by stalling. The time-dependent accumulation of mutations and the preceeding abnormal replication suggest that the cell counteracts the replication defects perhaps using several mechanisms, whose activity deteriotes with age.

In culutured cells replication stalling also caused an impairment of mtDNA transcription. Although RNA synthesis was observed to be hindered before the depletion of the mtDNA of cultured cells, it cannot be said at this point, whether the transcriptional defect precedes mtDNA deletion formation also in adPEO patients, and influences the pathophysiology of the disease.

.

# 7. Conclusions and perspectives

The acetylation of mitochondrial proteins is a new discovery, and with the identification of mitochondrial deacetylases, brings along a global mechanism for mitochondrial protein control. As is shown in this thesis and by the work of others sirtuin mediated deacetylation of mitochondrial proteins can control nutrient flux and energy production. A significant number of mitochondrial proteins have been identified as acetylated and we found that many of them interact with the mitochondrial sirtuin deacetylase hSIRT3. These interaction partners are mostly metabolic enzymes and our findings strengthen the view that hSIRT3 can influence energy producing pathways. hSIRT3 has previously been associated with the control of insulin secretion and the production of acetyl-CoA production from free acetate. This thesis adds the beta-oxidation pathway for the break-down of fatty-acids and subsequent acetyl-CoA production as a point of regulation for hSIRT3.

The subcellular localisation of SIRT3 in human and mouse has been a question of controversy as reports suggesting their non-mitochondrial targeting have been published. But the careful analysis of the expression profile and localisation of both proteins described here supports the exclusive mitochondrial localisation of both human and mouse SIRT3. The mitochondrial behaviour of the proteins may, however, differ between cell types and under different circumstances, especially since hSIRT3 itself is controlled by the availability of NAD. So far, we have only studied hSIRT3 in proliferating cells. SIRT3 knock-out mice have been described largely indistinguishable from wild-type animals, apart from hypeacetylation of mitochondrial proteins and a decrease in ATP production. Yet it would be interesting to futher determine metabolite levels and the acetylation pattern of SIRT3 substrates in different cell types grown in different nutrient conditions.

Acetylation is well-known for its role in regulating chromatin structure, and histones are an important target for many deacetylases. Although mitochondria contain DNA associated with proteins, little is known about the regulation of the dynamics of these nucleoid complexes. Acetylation could therefore take place on

nucloids proteins, such as the Twinkle helicase, which contains several putative acetylation sites in its amino acid sequence. This thesis includes an extensive study on the biochemical properties of mutant Twinkle variants, which result in impaired replication, abnormal nucleoid structures and mtDNA depletion. In light of the large amount of acetylated mitochondrial proteins and the analogy to nuclear chromatin remodelling, it would be interesting to look at post-translational modifications to Twinkle and other nucleoid proteins, and to study how they might influence DNA maintenance events.

Overall, the mitochondrial sirtuins and their targets as well as mtDNA maintenance events offer intriguing possibilities for studying different aspects of the control of energy production.

# Acknowledgements

This thesis work was carried out in the laboratory of Molecular Biology in the group of Mitochondrial DNA Maintenance at the Institute of Medical Technology, University of Tampere. The research was funded by the Tampere Graduate School in Biomedicine and Biotechnology (TGSBB), the Tampere University Support Fund, the Pirkanmaa Hospital District, the Emil Aaltonen Foundation, the Wihuri Foundation and the Finnish Cultural Foundation.

I want to thank the head of the Institute of Medical Technology for providing a dynamic and friendly working environment. And I want to thank the Tampere Graduate School in Biomedicine and Biotechnology for financial and educational support during the time I have worked on my thesis.

I am more than thankful to my supervisor Prof. Hans Spelbrink for all these years I have worked with him. Hans has taught me a great deal about research work, both practical laboratory work and scientific thinking. He has been invaluable in seeing through my publications, and I admire his scientific insight. I am grateful for his patience and flexibility and most of all for all the critical yet motivating discussions we've had. I am also deeply grateful for Prof. Howy Jacobs, who initially took me in as an undergraduate student and has kept on showing valuable interest in my work as a member of my thesis committee and as head of the FinnMit collaboration. The other member of my thesis committee, Prof. Anu Wartiovaara is also thanked for her advice and support. Anu and Dr. Brendan Battersby, the leaders of the Helsinki end of FinnMit are both thanked for all the FinnMit meetings I have been glad to participate in.

I want to express my sincere gratitude to my collaborators and co-authors. The SIRT3 mouse work was done at the Gladstone Institute of Virology and Immunology, University of California, San Francisco, USA and for this I am grateful to Dr. Jin-Yi Huang and Dr. Eric Verdin. The Deletor mouse, which was studied in the Twinkle work, was created by Dr. Henna Tyynismaa. Henna is also thanked for peer support. I thank Dr. Sjoerd Wanrooij for creating the inducible cell

lines. Special thanks to Paulina Wanrooij for the heroic YH2 hybrid screen, related cloning and useful pointers in writing the fourth article. Finally, Dr. Steffi Goffart is thanked for the tremendous amount of work she put into the Twinkle paper, but also for setting a good example, for the good company in the lab and for her friendship.

I thank the external reviewers of my thesis, Prof. José Antonio Enriquez and Prof. John M. Denu for carefully reading the manuscript and for making valuable comments. And I thank Prof. Mathias Ziegler for doing me the honour of being my opponent.

I'm also thankful for the educational and scientific influence of Prof. Markku Kulomaa, who supervised my Master's thesis in Jyväskylä, and has since moved to Tampere and has continued to be very supportive and encouraging. I am also most grateful to my post-doctoral supervisor Dr. Ian Holt for welcoming me into his lab, providing an interesting project and for helping in getting funding.

During my years in Howy&Hans lab I have had the honour of knowing and working with many wonderful and interesting people, and several of them have become my dear friends. Everyone is thanked for creating a great atmosphere and all the nice conversations and get-togethers. Specifically, I thank Outi Kurronen and Merja Jokela for their invaluable assistance with practical and administrative matters. Merja deserves special thanks for all the cell culture she did for me during the last stretch of in my lab work and for the analyses she did after I had left. I thank Anja Rovio for all her solid practical advice and her help and friendship, Tea Tuomela for caring and for many lovely chats, and Päivi Manninen for administrative help and advice. Fellow PhD students, some of who have already graduated, are thanked for sharing the ups and downs of the experience: Jaakko, for many interesting conversations from politics to wildlife; Anne, for sharing recipes and cooking together; Nina, for psychological support in the form of good, cleansing chats; Kia, for being such lovely company on our conference trip to the States and for the wonderful effort of making my graduation dress; Esko for being good company and always ready to help; Ernesto, Marina and finally Rimmy, for her long-lasting friendship, which I greatly cherish. Other researchers, including post-docs (Peter, Priit, Suvi, Eric, Alberto, Shanjun, Atshushi) are thanked for setting an example and for help and advice. The new Hanslab post-docs Lucia and Kirsi are thanked for continuing my projects and showing enthusiasm towards them. Other staff members, undergraduate students and civil servants who come and go

are thanked for keeping the lab running and for making the place interesting and lively. Of all the Glaswegian students, Rhoda, is especially thanked for the great cooking and Greek dancing.

During my PhD work I have had the privilege to supervise several skilled and motivated undergraduate students in the lab. All of them have played a part in contributing to the work and my own scientific growth. Special thanks to Alise Hyrskyluoto for her participation in the SIRT cell screen, which hopefully will soon find its way into a publication, too.

Former lab members are thanked for the good old times, which in many cases have become good present times, too. Sanna Marjavaara taught me a lot about life as a researcher when I first arrived in the lab. And I'm glad to remain in contact with her through the FinnMit collaboration. Mikko, who shared the sequencing experience with me back in the day, is thanked for all the great nights out in Helsinki. Lumikukka is mentioned here, as our first encounter was in the lab. We had so much fun then in the lab and on our crazy excursions. And today after many twist and turns of life, she and her family, Maria, Kaspar and my goddaughter Manta, are my dearest friends and I thank them all for bringing joy to my life, no matter how far apart we may be.

Other fellow researchers at the campus are thanked for help and advice with equipment, bureaucracy, the loan of reagents and simply nice conversations. Kati Pulkkinen is acknowledged for the peer support during the submission of our theses. Colleagues elsewhere are thanked for the likeminded company at meetings, the share of articles and protocols and contact over the internet.

Extracurricular activities have always been important for my social conscience and I thank the people from LAL, especially Suvi Liikkanen, for involving me in the union's activities. And I want to thank the people in Tampere who took part in starting up the local branch, LATTE. Special thanks to Susanna for her meticulous secretarial skills, but above all for her company and friendship in the lab, on the way cycling to and from the lab and outside the lab. And to Ulla for going along with ideas to organise activities for staff and students and for sharing the responsibility of student representative on the TGSBB board. Also Eloise Kok is thanked for her enthusiasm in organising student activities.

I want to thank C.C. Communications for giving me the opportunity to do some part time language teaching, while I wrote my thesis. If anything, it has certainly improved my writing. Many thanks also to all my wonderful students.

I want to thank my family and close relatives for showing interest in my work and for being such a colourful bunch of people. And I am so very grateful to Paula and David for housing and helping me both in Boston and in Cambridge. I also want to thank my godmothers, biologists Dr Mervi Sibakow, and Tuula Johansson for being important role models.

Thank you Seppo and Marita for all your invaluable help with our boat and in our home, for many conversations and for the relaxing times spent in Vaasa and its archipelago.

I am so lucky to have amazing friends, who have each in their own way made my life so good. Kaisa, Virpi, Marjukka, Niina, Suvi, Sanna, Ville-Veikko, thank you for talking, for listening, for laughing for understanding, for the nights out dancing, for the nights in talking or watching movies and for many outdoor activities. You are the best! I also want to thank all our friends in Turku for the excellent social events that prevented me from losing my mind while I was cooped up inside writing, and now for taking care of Pasi while I'm gone.

Äiti and Dad, thank you for putting me up and putting up with me while I was working on my thesis. Thank you for supporting and encouraging me in the choices I have made. And thank you for all your help in arranging the karonkka. For all this and more I thank you from the bottom of my heart.

Paul, thank for your camaraderie and friendship, for the jokes and the arguments; for being the best brother a sister could have.

And finally Pasi, thank you for being You: someone who urges me on, has faith and in me, and makes me smile and laugh. Thank you for teaching me so much, for being patient and for understanding. And thank you for the sailing. Thank you for making me so incredibly happy.

Cambridge, November 2009

Helen Cooper

# References


Afshar G and Murnane JP (1999): Characterization of a human gene with sequence homology to Saccharomyces cerevisiae SIR2. Gene 234**:**161–8.

Ahn BH, Kim HS, Song S, Lee IH, Liu J, Vassilopoulos A, Deng CX and Finkel T (2008): A role for the mitochondrial deacetylase Sirt3 in regulating energy homeostasis. Proc Natl Acad Sci U S A 105:14447-52.

Ahuja N, Schwer B, Carobbio S, Waltregny D, North BJ, Castronovo V, Maechler P and Verdin E (2007): Regulation of insulin secretion by SIRT4, a mitochondrial ADP-ribosyltransferase. J Biol Chem 282:33583-92.

Alam TI, Kanki T, Muta T, Ukaji K, Abe Y, Nakayama H, Takio K, Hamasaki N and Kang D (2003): Human mitochondrial DNA is packaged with TFAM. Nucleic Acids Res 31:1640-5.

Altschul SF, Gish W, Miller W, Myers EW and Lipman DJ (1990): Basic local alignment search tool. J Mol Biol 215:403-10.

Anderson RM, Bitterman KJ, Wood JG, Medvedik O, Cohen H, Lin SS, Manchester JK, Gordon JI and Sinclair DA (2002): Manipulation of a nuclear NAD+ salvage pathway delays aging without altering steady-state NAD+ levels. J Biol Chem 277:18881-90.

Anderson RM, Bitterman KJ, Wood JG, Medvedik O, Sinclair DA (2003): Nicotinamide and PNC1 govern lifespan extension by calorie restriction in Saccharomyces cerevisiae. 423:181-5.

Anderson S, Bankier AT, Barrell BG, de Bruijn MH, Coulson AR, Drouin J, Eperon IC, Nierlich DP, Roe BA, Sanger F, Schreier PH, Smith AJ, Staden R and Young IG (1981): Sequence and organization of the human mitochondrial genome. Nature 290: 457-65.

Andrews RM, Kubacka I, Chinnery PF, Lightowlers RN, Turnbull DM and Howell N (1999): Reanalysis and revision of the Cambridge reference sequence for human mitochondrial DNA. Nat Genet 23: 147.

Andziak B, O'Connor TP, and Buffenstein R (2005): Antioxidants do not explain the disparate longevity between mice and the longest-living rodent, the naked mole-rat. Mech Ageing Dev 126:1206-1212.

Avantaggiati ML, Ogryzko V, Gardner K, Giordano A, Levine AS and Kelly K (1997): Recruitment of p300/CBP in p53-dependent signal pathways. Cell 89:1175–84.

Baloh RH, Salavaggione E, Milbrandt J and Pestronk A (2007): Familial parkinsonism and ophthalmoplegia from a mutation in the mitochondrial DNA helicase twinkle. Arch Neurol; 64: 998-1000.

Bellizzi D, Rose G, Cavalcante P, Covello G, Dato S, De Rango F, Greco V, Maggiolini M, Feraco E, Mari V, Franceschi C, Passarino G, and De Benedictis G (2005): A novel VNTR enhancer within the SIRT3 gene, a human homologue of SIR2, is associated with survival at oldest ages. Genomics 85:258-63.

Bergstrom RW, Wahl PW, Leonetti DL and Fujimoto WY (1990): Association of fasting glucose levels with a delayed secretion of insulin after oral glucose in subjects with glucose intolerance. J Clin Endocrinol Metab 71:1447–53.

Bertram L, Blacker D, Mullin K, Keeney D, Jones J, Basu S, Yhu S, McInnis MG, Go RC, Vekrellis K, Selkoe DJ, Saunders AJ and Tanzi RE (2003): Evidence for genetic linkage of Alzheimer's disease to chromosome 10q. Science 290:2302-3.

Bhakat KK, Hazra TK and Mitra S (2004): Acetylation of the human DNA glycosylase NEIL2 and inhibition of its activity. Nucleic Acids Res 32:3033–39.

Bhakat KK, Mokkapati SK, Boldogh I, Hazra TK and Mitra S (2006): Acetylation of human 8-oxoguanine-DNA glycosylase by p300 and its role in 8-oxoguanine repair in vivo. Mol Cell Biol 26:1654–1665.

Birky CW (2001): The inheritance of genes in mitochondria and chloroplasts: laws, mechanisms, and models. Annual Review of Genetics 35:125–148.

Blander G, Kipnis J, Leal JF, Yu CE, Schellenberg GD, and Oren M (1999):Physical and Functional Interaction between p53 and the Werner's Syndrome Protein J Biol Chem 274:29463-69.

Blander G, Zalle N, Daniely Y, Taplick J, Gray MD and Oren M (2002): DNA damage-induced translocation of the Werner helicase is regulated by acetylation. J Biol Chem 277:50934-40.

Blander G and Guarente L (2004): The Sir2 family of protein deacetylases. Annu Rev Biochem 73:417-35.

Bogenhagen DF, Pinz KG and Perez-Jannotti RM (2001): Enzymology of mitochondrial base excision repair. Prog Nucleic Acid Res Mol Biol 68:257-71.

Bogenhagen DF, Rousseau D and Burke S (2008): The layered structure of human mitochondrial DNA nucleoids. J Biol Chem 283: 3665-75.

Bohr VA (2005): Deficient DNA repair in the human progeroid disorder, Werner syndrome. Mutat Res 577:252–59.

Bordone L, Motta MC, Picard F, Robinson A, Jhala US, Apfeld J, McDonagh T, Lemieux M, McBurney M, Szilvasi A, Easlon EJ, Lin SJ and Guarente L (2006): Sirt1 regulates insulin secretion by repressing UCP2 in pancreatic beta cells. PLoS Biol 4:e31.

Bowmaker M, Yang MY, Yasukawa T, Reyes A, Jacobs HT, Huberman JA and Holt IJ. Mammalian mitochondrial DNA replicates bidirectionally from an initiation zone. J Biol Chem 278:50961-9

Brachmann CB, Sherman JM, Devine SE, Cameron EE, Pillus L and Boeke JD(1995): The SIR2 gene family, conserved from bacteria to humans, functions in silencing, cell cycle progression, and chromosome stability. Genes Dev 9:2888-902.

Brewer BJ and Fangman WL (1987): The localization of replication origins on ARS plasmids in S. cerevisiae. Cell 3:463-71.

Brunet A, Sweeney LB, Sturgill JF, Chua KF, Greer PL, Lin Y, Tran H, Ross SE, Mostoslavsky R, Cohen HY, Hu LS, Cheng HL, Jedrychowski MP, Gygi SP, Sinclair DA, Alt FW and Greenberg ME (2004): Stress-dependent regulation of FOXO transcription factors by the SIRT1 deacetylase. Science 303:2011-5.

Bua E, McKiernan SH and Aiken JM (2004): Calorie restriction limits the generation but not the progression of mitochondrial abnormalities in aging skeletal muscle. FASEB J 3:582-4.

Bürkle A (2001): Physiology and pathophysiology of poly(ADribosyl)ation.Bioessays 23:795-806.

Cheng HL, Mostoslavsky R, Saito S, Manis JP, Gu Y, Patel P, Bronson R, Appella E, Alt FW and Chua KF (2003). Developmental defects and p53 hyperacetylation in Sir2 homolog (SIRT1)-deficient mice. Proc Natl Acad Sci U S A 100:10794-9.

Choudhary C, Kumar C, Gnad F, Nielsen ML, Rehman M, Walther TC, Olsen JV and Mann M (2009): Lysine acetylation targets protein complexes and co-regulates major cellular functions. Science 325:834-40.

Church GM and Gilbert W (1984): Genomic sequencing. Proc Natl Acad Sci U S A 81:1991-5.

Clancy DJ, Gems D, Harshman L. G., Oldham S, Stocker H, Hafen E, Leevers SJ and Partridge L. (2001): Extension of life-span by loss of CHICO, a *Drosophila* insulin receptor substrate protein. Science 292, 104–6.

Clayton DA (1982): Replication of animal mitochondrial DNA. Cell 28:693-705.

Coffey G, Lakshmipathy U and Campbell C. (1999): Mammalian mitochondrial extracts possess DNA end-binding activity, Nucleic Acids Res**. 27** 3348–54.

Cohen HY, Miller C, Bitterman KJ, Wall NR, Hekking B, Kessler B, Howitz KT, Gorospe M, de Cabo R and Sinclair DA (2004): Calorie restriction promotes mammalian cell survival by inducing the SIRT1 deacetylase. Science 305:390-2.

Cook DG, Leverenz JB, McMillan PJ, Kulstad JJ, Ericksen S, R. A. RA, Schellenberg GD, Jin LW, Kovacina KS, and Craft S (2003): Reduced hippocampal insulin-degrading enzyme in late-onset Alzheimer's disease is associated with the apolipoprotein E-epsilon4 allele. American Journal of Pathology 162:313.

Cooper HM and Spelbrink JN (2008). The human SIRT3 protein deacetylase is exclusively mitochondrial. Biochem J 411:279-85.

Cooper HM, Huang JY, Verdin E and Spelbrink JN (2009): A new splice variant of the mouse SIRT3 gene encodes the mitochondrial precursor protein. PLoS ONE 4:e4986.

D'Aurelio M, Gajewski CD, Lin MT, Mauck WM, Shao LZ, Lenaz G, Moraes CT and Manfredi G (2004): Heterologous mitochondrial DNA recombination in human cells. Hum Mol Genet 13:3171-9.

Deng CX (2009): SIRT1, is it a tumor promoter or tumor suppressor? Int J Biol Sci. 5:147-52.

Dimauro S and Davidzon G (2005): Mitochondrial DNA and disease. Ann Med 37:222-32.

Dinardo MM, Musicco C, Fracasso F, Milella F, Gadaleta MN, Gadaleta G, Cantatore P (2003): Acetylating and level of mitochondrial transcription factor A in several organs of young and old rats. Biochem Biophys Res Commun 301:187-91.

Dryden SC, Nahhas FA, Nowak JE, Goustin AS and Tainsky MA (2003): Role for human SIRT2 NAD-dependent deacetylase activity in control of mitotic exit in the cell cycle. Mol Cell Biol 23:3173-85.

Eaton S, Bartlett K and Pourfarzam M (1996): Mammalian mitochondrial beta-oxidation. Biochem J 320:345-57.

Espinosa JM and Emerson BM (2001) Transcriptional regulation by p53 through intrinsic DNA/chromatin binding and site-directed cofactor recruitment. Mol Cell 8: 57–69.

Farge G, Pham XH, Holmlund T, Khorostov I and Falkenberg M (2007) The accessory subunit B of DNA polymerase gamma is required for mitochondrial replisome function. Nucleic Acids Res 35:902-11.

Farge G, Holmlund T, Khvorostova J, Rofougaran R, Hofer A and Falkenberg M (2008): The N-terminal domain of TWINKLE contributes to single-stranded DNA binding and DNA helicase activities. Nucleic Acids Res 36:393-403.

Farris W, Mansourian S, Chang Y, Lindsley L, Eckman EA, Frosch MP, Eckman CB, Tanzi RE, Selkoe DJ and Guenette S (2003). Insulin-degrading enzyme regulates the levels of insulin, amyloid beta-protein, and the beta-amyloid precursor protein intracellular domain in vivo. Proc Natl Acad Sci U S A 100:4162-7.

Ferrannini E (1998): Insulin resistance versus insulin deficiency in non–insulin-dependent diabetes mellitus: problems and prospects. Endocr Rev 19:477–90.

Fisher RP and Clayton DA (1988): Purification and characterization of human mitochondrial transcription factor 1. Mol Cell Biol 8**:**3496-509.

Fleming JE, Reveillaud I and Niedzwiecki A (1992): Role of oxidative stress in Drosophila aging. Mutat Res 275:267-279.

Frazier AE, Kiu C, Stojanovski D, Hoogenraad NJ and Ryan MT (2006): Mitochondrial morphology and distribution in mammalian cells. Biol Chem 387:1551-8.

Friedman DB and Johnson TE. (1988): A mutation in the age-1 gene in *Caenorhabditis elegans* lengthens life and reduces hermaphrodite fertility. Genetics 118, 75–86.

Friedman KL, Brewer BJ. Analysis of replication intermediates by two-dimensional agarose gel electrophoresis. Methods Enzymol 262:613-27.

Frye RA (2000): Phylogenetic classification of prokaryotic and eukaryotic Sir2-like proteins. Biochem Biophys Res Commun 273:793-8.

Fujino T, Kondo J, Ishikawa M, Morikawa K and Yamamoto TT (2001): Acetyl-CoA synthetase 2, a mitochondrial matrix enzyme involved in the oxidation of acetate. J Biol Chem. 276:11420-6.

Gaikwad A, Long DJ 2nd, Stringer JL and Jaiswal AK (2001): In vivo role of NAD(P)H:quinone oxidoreductase 1 (NQO1) in the regulation of intracellular redox state and accumulation of abdominal adipose tissue. J Biol Chem 276:22559-64.

Garsin, DA, Villanueva JM, Begun J, Kim DH, Sifri CD, Calderwood SB, Ruvkun G and Ausubel FM (2003): Long-lived *C. elegans* daf-2 mutants are resistant to bacterial pathogens. Science 300:1921

Garrido N, Griparic L, Jokitalo E, Wartiovaara J, van der Bliek AM, Spelbrink JN (2003): Composition and dynamics of human mitochondrial nucleoids. Mol Biol Cell 14:1583-96.

Gerhart-Hines Z, Rodgers JT, Bare O, Lerin C, Kim SH, Mostoslavsky R, Alt FW, Wu Z and Puigserver P (2007): Metabolic control of muscle mitochondrial function and fatty acid oxidation through SIRT1/PGC-1alpha. EMBO J 26:1913-23.

Goffart S, Martinsson P, Malka F, Rojo M and Spelbrink JN (2007): The Mitochondria of Cultured Mammalian cells. In: Leister D, Herrman JM, editors. Mitochondria Practical Protocols, vol 372 Humana press. pp. 17–32.

Goldstein BJ (2002): Insulin resistance as the core defect in type 2 diabetes mellitus. Am J Cardiol. 90:3G-10G.

Gray MD, Shen JC, Kamath-Loeb AS, Blank A, Sopher BL, Martin GM, Oshima J and Loeb LA (2007). The Werner syndrome protein is a DNA helicase. Nat Genet 17;100-3.

Gray MD, Wang L, Youssoufian H, Martin GM and Oshima J (1998): Werner helicase is localized to transcriptionally active nucleoli of cycling cells. Exp Cell Res 242:487-94.

Graziewicz MA, Longley MJ and Copeland WC (2006): DNA polymerase gamma in mitochondrial DNA replication and repair. Chem Rev 106: 383-405.

Gu W and Roeder RG (1997): Activation of p53 sequence-specific DNA binding by acetylation of the p53 C-terminal domain. Cell 90:595–06.

Haigis MC, Mostoslavsky R, Haigis KM, Fahie K, Christodoulou DC, Murphy AJ, Valenzuela DM, Yancopoulos GD, Karow M, Blander G, Wolberger C, Prolla TA, Weindruch R, Alt FW and Guarente L (2006): SIRT4 inhibits glutamate dehydrogenase and opposes the effects of calorie restriction in pancreatic beta cells. Cell 126:941-54.

Hakonen AH, Heiskanen S, Juvonen V, Lappalainen I, Luoma PT, Rantamaki M, Goethem GV, Lofgren A, Hackman P, Paetau A, Kaakkola S, Majamaa K, Varilo T, Udd B, Kaariainen H, Bindoff LA and Suomalainen A (2005) Mitochondrial DNA polymerase W748S mutation: a common cause of autosomal recessive ataxia with ancient European origin. Am J Hum Genet. 77:430–441.

Hakonen AH, Isohanni P, Paetau A, Herva R, Suomalainen A and Lönnqvist T (2007). Recessive Twinkle mutations in early onset encephalopathy with mtDNA depletion. Brain 130:3032-40.

Hakonen AH, Goffart S, Marjavaara S, Paetau A, Cooper H, Mattila K, Lampinen M, Sajantila A, Lönnqvist T, Spelbrink JN and Suomalainen A (2008). Infantile-onset spinocerebellar ataxia and mitochondrial recessive ataxia syndrome are associated with neuronal complex I defect and mtDNA depletion. Hum Mol Genet 17:3822-35.

Hallows WC, Lee S and Denu JM (2006): Sirtuins deacetylate and activate mammalian acetyl-CoA synthetases. Proc Natl Acad Sci U S A 103:10230-5.

Hari R, Burde V and Arking R (1998): Immunological confirmation of elevated levels of CuZn superoxide dismutase protein in an artificially selected long-lived strain of Drosophila melanogaster. Exp Gerontol 33:227-37.

Hasan S, Stucki M, Hassa PO, Imhof R, Gehrig P, Hunziker P, Hubscher U, and Hottiger MO (2001): Regulation of human flap endonuclease-1 activity by acetylation through the transcriptional coactivator p300. Mol Cell 7:1221–1231.

Hasan S, El-Andaloussi N, Hardeland U, Hassa PO, Bürki C, Imhof R, Schär P and Hottiger MO (2002):. Acetylation regulates the DNA end-trimming activity of DNA polymerase beta. Mol Cell 10:1213–22.

He J, Mao CC, Reyes A, Sembongi H, Di Re M, Granycome C, Clippingdale AB, Fearnley IM, Harbour M, Robinson AJ, Reichelt S, Spelbrink JN, Walker JE and Holt IJ (2007): The AAA+ protein ATAD3 has displacement loop binding properties and is involved in mitochondrial nucleoid organization. J Cell Biol 176:141-6.

Hsieh P (2001): Molecular mechanisms of DNA mismatch repair. Mutation research 486:71–87.

Hirano M, Marti R, Ferreiro-Barros C, Vilà MR, Tadesse S, Nishigaki Y, Nishino I and Vu TH (2001). Defects of intergenomic communication: autosomal disorders that cause multiple deletions and depletion of mitochondrial DNA. Semin Cell Dev Biol 12:417–427.

Hirschey MD, Shimazu T, Huang JY and Verdin E (2009): Acetylation of mitochondrial proteins. Methods Enzymol 457:137-47.

Holmlund T, Farge G, Pande V, Korhonen J, Nilsson L and Falkenberg M (2009): Structure-function defects of the twinkle amino-terminal region in progressive external ophthalmoplegia. Biochim Biophys Acta 1792:132-9.

Holloszy JO (1998): Longevity of exercising male rats: effect of an antioxidant supplemented diet. Mech Ageing Dev 100:211-19.

Holt IJ, Lorimer HE and Jacobs HT (2000): Coupled leading- and lagging-strand synthesis of mammalian mitochondrial DNA. Cell 100:515-24.

Holzenberger M, Dupont J, Ducos B, Leneuve P, Geloen A, Even PC, Cervera P and Le Bouc Y (2003): IGF-1 receptor regulates lifespan and resistance to oxidative stress in mice. Nature 421: 182–87.

Huang S, Li B, Gray MD, Oshima J, Mian IS and Campisi J (1998): The premature ageing syndrome protein, WRN, is a 3'-->5' exonuclease. Nat Genet 20:114-6.

Hudson G, Deschauer M, Busse K, Zierz S and Chinnery PF (2005): Sensory ataxic neuropathy due to a novel C10Orf2 mutation with probable germline mosaicism. Neurology 64: 371-3.

Iborra FJ, Kimura H and Cook PR (2004): The functional organization of mitochondrial genomes in human cells. BMC Biol 2:9.

Imai S, Armstrong CM, Kaeberlein M and Guarente L (2000): Transcriptional silencing and longevity protein Sir2 is an NAD-dependent histone deacetylase. Nature 403:795-800.

Inoue T, Hiratsuka M, Osaki M and Oshimura M (2007): The molecular biology of mammalian SIRT proteins: SIRT2 in cell cycle regulation. Cell Cycle 6:1011-8.

Inoue T, Nakayama Y, Yamada H, Li YC, Yamaguchi S, Osaki M, Kurimasa A, Hiratsuka M, Katoh M and Oshimura M (2009): SIRT2 downregulation confers resistance to microtubule inhibitors by prolonging chronic mitotic arrest. Cell Cycle 8:1279-91.

Jensen M, Leffers H, Petersen JH, Nyboe Andersen A, Jorgensen N, Carlsen E, Jensen TK, Skakkebaek NE and Rajpert-De Meyts E (2004): Frequent polymorphism of the mitochondrial DNA polymerase gamma gene (POLG) in patients with normal spermiograms and unexplained subfertility. Hum. Reprod 19**:**65–70.

Jeong J, Juhn K, Lee H, Kim SH, Min BH, Lee KM, Cho MH, Park GH and Lee KH (2007): SIRT1 promotes DNA repair activity and deacetylation of Ku70. Exp Mol Med 39:8-13.

Jin L, Wei W, Jiang Y, Peng H, Cai J, Mao C, Dai H, Choy W, Bemis JE, Jirousek MR, Milne JC, Westphal CH and Perni RB (2009): Crystal Structures of Human SIRT3 Displaying Substrate-induced Conformational Changes. J Biol Chemm284:24394-405.

Kaeberlein M, McVey M and Guarente L (1999): The SIR2/3/4 complex and SIR2 alone promote longevity in Saccharomyces cerevisiae by two different mechanisms. Genes Dev 13:2570-80.

Kaeberlein M, Kirkland KT, Fields S and Kennedy BK (2004): Sir2-independent life span extension by calorie restriction in yeast. PLoS Biol 9:E296.

Kanfi Y, Shalman R, Peshti V, Pilosof SN, Gozlan YM, Pearson KJ, Lerrer B, Moazed D, Marine JC, de Cabo R and Cohen HY (2008): Regulation of SIRT6 protein levels by nutrient availability. FEBS Lett 582:543-8.

Karmakar P and Bohr VA (2005): Cellular dynamics and modulation of WRN protein is DNA damage specific. Mech Ageing Dev 126:1146-58.

Kaufman BA, Durisic N, Mativetsky JM, Costantino S, Hancock MA, Grutter P and Shoubridge EA (2007): The mitochondrial transcription factor TFAM coordinates the assembly of multiple DNA molecules into nucleoid-like structures. Mol Biol Cell 18:3225-36.

Kawahara TL, Michishita E, Adler AS, Damian M, Berber E, Lin M, McCord RA, Ongaigui KC, Boxer LD, Chang HY and Chua KF (2009):. SIRT6 links histone H3 lysine 9 deacetylation to NF-kappaB-dependent gene expression and organismal life span. Cell 136:62-74.

Kim SC, Sprung R, Chen Y, Xu Y, Ball H, Pei J, Cheng T, Kho Y, Xiao H, Xiao L, Grishin NV, White M, Yang XJ and Zhao Y (2006): Substrate and functional diversity of lysine acetylation revealed by a proteomics survey. Mol Cell 23:607-18.

Klass MR (1983) A method for the isolation of longevity mutants in the nematode *Caenorhabditis elegans* and initial results. Mech Ageing Dev 22:279–286.
Kompare M and Rizzo WB (2008): Mitochondrial fatty-acid oxidation disorders. Semin Pediatr Neurol 15:140-9.

Koubova J, Guarente L. How does calorie restriction work? Genes Dev 2003;17:313-21.

Korhonen JA, Gaspari M and Falkenberg M (2003): TWINKLE Has 5' -> 3' DNA helicase activity and is specifically stimulated by mitochondrial single-stranded DNA-binding protein. J Biol Chem 278:48627-32.

Korhonen JA, Pham XH, Pellegrini M and Falkenberg M (2004): Reconstitution of a minimal mtDNA replisome in vitro. EMBO J 23:2423-9.

Korhonen JA, Pande V, Holmlund T, Farge G, Pham XH, Nilsson L and Falkenberg M (2008): Structure-function defects of the TWINKLE linker region in progressive external ophthalmoplegia. J Mol Biol 377: 691-705.

Koskinen T, Sainio K, Rapola J, Pihko H and Paetau A (1994b): Sensory neuropathy in infantile onset spinocerebellar ataxia (IOSCA). Muscle Nerve 17: 509-15.

Koskinen T, Santavuori P, Sainio K, Lappi M, Kallio AK and Pihko H (1994a): Infantile onset spinocerebellar ataxia with sensory neuropathy: A new inherited disease. J Neurol Sci 121: 50-6.

Koskinen T, Valanne L, Ketonen LM, Pihko H (1995): Infantile-onset spinocerebellar ataxia: MR and CT findings. AJNR Am J Neuroradiol 16:1427-33.

Kraytsberg Y, Schwartz M, Brown TA, Ebralidse K, Kunz WS, Clayton DA, Vissing and Khrapko K (2004): Recombination of human mitochondrial DNA. Science 304:981.

Krishnan KJ, Reeve AK, Samuels DC, Chinnery PF, Blackwood JK, Taylor RW, Wanrooij S, Spelbrink JN, Lightowlers RN and Turnbull DM (2008): What causes mitochondrial DNA deletions in human cells? Nat Genet 40:275-9.

Kujoth GC, Hiona A, Pugh TD, Someya S, Panzer K, Wohlgemuth SE, Hofer T, Seo AY, Sullivan R, Jobling WA, Morrow JD, Van Remmen H, Sedivy JM, Yamasoba T, Tanokura M, Weindruch R, Leeuwenburgh C and Prolla TA (2005): Mitochondrial DNA mutations, oxidative stress, and apoptosis in mammalian aging. Science 309:481-4.

Lanza IR, Short DK, Short KR, Raghavakaimal S, Basu R, Joyner MJ, McConnell JP and Nair KS (2008): Endurance exercise as a countermeasure for aging. Diabetes. 57:2933-42.

Larsen P L (1993): Aging and resistance to oxidative damage in Caenorhabditis elegans. Proc Natl Acad Sci U S A 90:8905-09.

Larsson NG, Wang J, Wilhelmsson H, Oldfors A, Rustin P, Lewandoski M, Barsh GS and Clayton DA (1998): Mitochondrial transcription factor A is necessary for mtDNA maintenance and embryogenesis in mice. Nat Genet 18:231-36.

LeCluyse E, Bullock P, Madan A, Carroll K and Parkinson A (1999): Influence of extracellular matrix overlay and medium formulation on the induction of cytochrome P-450 2B enzymes in primary cultures of rat hepatocytes. Drug Metab Dispos 27: 909–15.

Lecrenier N, Van Der Bruggen P and Foury F (1997): Mitochondrial DNA polymerases from yeast to man: a new family of polymerases. Gene 185:147-52.

Legros F, Malka F, Frachon P, Lombes A and Rojo M (2004): Organization and dynamics of human mitochondrial DNA. J Cell Sci 117: 2653-62.

Li M, Luo J, Brooks CL and Gu W (2002): Acetylation of p53 inhibits its ubiguition by Mdm2. J Biol Chem 52:50607–11.

Libert S, Chao Y, Zwiener J and Pletcher SD (2008): Realized immune response is enhanced in long-lived puc and chico mutants but is unaffected by dietary restriction. Mol. Immunol. 45:810–817.

Lin SJ, Defossez PA and Guarente L (2000): Requirement of NAD and SIR2 for life-span extension by calorie restriction in Saccharomyces cerevisiae. Science 289:2126-8.

Lin SJ, Kaeberlein M, Andalis AA, Sturtz LA, Defossez PA, Culotta VC, Fink GR and Guarente L (2002): Calorie restriction extends Saccharomyces cerevisiae lifespan by increasing respiration. Nature 418:344-8.

Lin SJ, Ford E, Haigis M, Liszt G and Guarente L (2004): Calorie restriction extends yeast life span by lowering the level of NADH. Genes Dev 18:12-6.

Lipman, RD, Bronson RT, Wu D, Smith DE, Prior R, Cao G, Han SN, Martin KR, Meydani SN and Meydani M (1998). Disease incidence and longevity are unaltered by dietary antioxidant supplementation initiated during middle age in C57BL/6 mice. Mech Ageing Dev 103:269-284.

Liszt G, Ford E, Kurtev M and Guarente L (2005): Mouse Sir2 homolog SIRT6 is a nuclear ADP-ribosyltransferase. J Biol Chem 280:21313-20.

Liu Y, Kao HI and Bambara RA (2004): Flap endonuclease 1: a central component of DNA metabolism. Annu Rev Biochem 73:589–615.

Lombard DB, Alt FW, Cheng HL, Bunkenborg J, Streeper RS, Mostoslavsky R, Kim J, Yancopoulos G, Valenzuela D, Murphy A, Yang Y, Chen Y, Hirschey MD, Bronson RT, Haigis M, Guarente LP, Farese RV Jr, Weissman S, Verdin E and Schwer B (2007): Mammalian Sir2 homolog SIRT3 regulates global mitochondrial lysine acetylation. Mol Cell Biol 27:8807-14.

Longley MJ, Ropp PA, Lim SE and Copeland WC (1998): Characterization of the native and recombinant catalytic subunit of human DNA polymerase gamma: identification of residues critical for exonuclease activity and dideoxynucleotide sensitivity. Biochemistry 37:10529-39.

Longley MJ, Graziewicz MA, Bienstock RJ and Copeland WC (2005): Consequences of mutations in human DNA polymerase γ Gene 354:125–31.

Longley MJ, Clark S, Yu Wai Man C, Hudson G, Durham SE, Taylor RW, Nightingale S, Turnbull DM, Copeland WC and Chinnery PF (2006): POLG2 disrupts DNA polymerase gamma subunits and causes progressive external ophthalmoplegia. Am. J. Hum. Genet 78:1026–1034.

Lombard DB, Chua KF, Mostoslavsky R, Franco S, Gostissa M and Alt FW (2005): DNA repair, genome stability, and aging. Cell 120:497–512.

Lombard DB, Alt FW, Cheng HL, Bunkenborg J, Streeper RS, Mostoslavsky R, Kim J, Yancopoulos G, Valenzuela D, Murphy A, Yang Y, Chen Y, Hirschey MD, Bronson RT, Haigis M, Guarente LP, Farese RV Jr, Weissman S, Verdin E and Schwer B (2007): Mammalian Sir2 homolog SIRT3 regulates global mitochondrial lysine acetylation. Mol Cell Biol 27:8807-14.

Lombard DB, Schwer B, Alt FW and Mostoslavsky R (2008): SIRT6 in DNA repair, metabolism and ageing. J Intern Med 263:128-41.

López-Lluch G, Hunt N, Jones B, Zhu M, Jamieson H, Hilmer S, Cascajo MV, Allard J, Ingram DK, Navas P and de Cabo R (2006): Calorie restriction induces mitochondrial biogenesis and bioenergetic efficiency. Proc Natl Acad Sci U S A. 103:1768-73.

Lopez-Torres M, Gredilla R, Sanz A and Baria G (2002): Influence of aging and long-term caloric restriction on oxygen radical generation and oxidative DNA damage in rat liver mitochondria. Free Radic Biol Med 32:882-9.

Luo J, Nikolaev AY, Imai S, Chen D, Su F, Shiloh A, Guarente L and Gu W (2001): Negative control of p53 by Sir2alpha promotes cell survival under stress. Cell 107:137–48.

Luoma P, Melberg A, Rinne JO, Kaukonen JA, Nupponen NN, Chalmers RM, Oldfors A, Rautakorpi I, Peltonen L, Majamaa K, Somer H and Suomalainen A (2004): Parkinsonism, premature menopause, and mitochondrial DNA polymerase gamma mutations: clinical and molecular genetic study. Lancet 364:875–82.

Luong A, Hannah VC, Brown MS and Goldstein JL (2000): Molecular characterization of human acetyl-CoA synthetase, an enzyme regulated by sterol regulatory element-binding proteins. J Biol Chem 275:26458–66.

MacCay CM, Cromwell MF and Maynard LA (1935):. The effect of retarded growth upon the lengh of life span and ultimate body size. J Nutr 10:63-79.

Mason PA, Matheson EC, Hall AG and Lightowlers RN (2003): Mismatch repair activity in mammalian mitochondria Nucleic Acids Res **31**:1052–1058.

Marciniak RA, Lombard DB, Johnson FB and Guarente L (1998): Nucleolar localization of the Werner syndrome protein in human cells. Proc Natl Acad Sci U S A 95:6887-92.

Martin GM (2005): Genetic modulation of senescent phenotypes in Homo sapiens. Cell 120:523–32.

Matsushima Y and Kaguni LS (2007): Differential phenotypes of active site and human autosomal dominant progressive external ophthalmoplegia mutations in Drosophila mitochondrial DNA helicase expressed in Schneider cells. J Biol Chem 282:9436-44.

McBurney MW, Yang X, Jardine K, Hixon M, Boekelheide K, Webb JR, Lansdorp PM and Lemieux M (2003): The mammalian SIR2alpha protein has a role in embryogenesis and gametogenesis. Mol Cell Biol 23:38–54.

McCulloch V, Seidel-Rogol BL and GS Shadel **(**2002): A human mitochondrial transcription factor is related to RNA adenine methyltransferases and binds *S*-adenosylmethionine. Mol Cell Biol 22**:**1116-25.

Magni G, Amici A, Emanuelli M, Raffaelli N and Ruggieri S (1999): Enzymology of $NAD^+$ synthesis. Adv. Enzymol. Relat. Areas Mol Biol 73:135–82.

Malka F, Auré K, Goffart S, Spelbrink JN and Rojo M (2007): The Mitochondria of Cultured Mammalian cells. In: Leister D, Herrman JM, editors. Mitochondria Practical Protocols, vol 372 Humana press. pp. 3–16.

Michishita E, Park JY, Burneskis JM, Barrett JC and Horikawa I (2005): Evolutionarily conserved and nonconserved cellular localizations and functions of human SIRT proteins. Mol Biol Cell 16:4623-35.

Miller BC, Eckman EA, Sambamurti K, Dobbs N, Chow KM, Eckman CB, Hersh LB and Thiele DL (2003): Amyloid-beta peptide levels in brain are inversely correlated with insulysin activity levels in vivo. Proc Natl Acad Sci U S A 100:6221-6.

Mostoslavsky R, Chua KF, Lombard DB, Pang WW, Fischer MR, Gellon L, Liu P, Mostoslavsky G, Franco S, Murphy MM, Mills KD, Patel P, Hsu JT, Hong AL, Ford E, Cheng HL, Kennedy C, Nunez N, Bronson R, Frendewey D, Auerbach W, Valenzuela D, Karow M, Hottiger MO, Hursting S, Barrett JC, Guarente L,

Mulligan R, Demple B, Yancopoulos GD and Alt FW (2006): Genomic instability and aging-like phenotype in the absence of mammalian SIRT6. Cell 124:315–29.

Motta MC, Divecha N, Lemieux M, Kamel C, Chen D, Gu W, Bultsma Y, McBurney M and Guarente L (2004): Mammalian SIRT1 represses forkhead transcription factors. Cell 116:551-63.

Muftuoglu M, Kusumoto R, Speina E, Beck G, Cheng WH and Bohr VA (2008): Acetylation regulates WRN catalytic activities and affects base excision DNA repair. PLoS ONE 3:e1918.

Murakami E, Feng JY, Lee H, Hanes J, Johnson KA and Anderson KS (2003): Characterization of novel reverse transcriptase and other RNA-associated catalytic activities by human DNA polymerase gamma: importance in mitochondrial DNA replication. J Biol Chem 278:36403-9.

Nakagawa T, Lomb DJ, Haigis MC and Guarente L (2009) SIRT5 deacetylates carbamoyl phosphate synthetase 1 and regulates the urea cycle. Cell 137:560-70.

Naviaux RK, Nyhan WL, Barshop BA, Poulton J, Markusic D, Karpinski NC and Haas RH (1999): Mitochondrial DNA polymerase gamma deficiency and mtDNA depletion in a child with Alpers' syndrome. Ann Neurol 45:54–58.

Nikali K, Suomalainen A, Saharinen J, Kuokkanen M, Spelbrink JN, Lönnqvist T and Peltonen L (2005): Infantile onset spinocerebellar ataxia is caused by recessive mutations in mitochondrial proteins twinkle and twinky. Hum Mol Genet 14: 2981-90.

North BJ, Marshall BL, Borra MT, Denu JM and Verdin E (2003): The human Sir2 ortholog, SIRT2, is an NAD+-dependent tubulin deacetylase. Mol Cell 11:437–444.

North BJ and Verdin E (2004): Sirtuins: Sir2-related NAD-dependent protein deacetylases. Genome Biol 5:224.

North BJ and Sinclair DA (2007): Sirtuins: a conserved key unlocking AceCS activity. Trends Biochem Sci 32:1-4.

Oberdoerffer P, Michan S, McVay M, Mostoslavsky R, Vann J, Park SK, Hartlerode A, Stegmuller J, Hafner A, Loerch P, Wright SM, Mills KD, Bonni A, Yankner BA, Scully R, Prolla TA, Alt FW and Sinclair DA (2008): SIRT1 redistribution on chromatin promotes genomic stability but alters gene expression during aging. Cell 135:907-18.

Ojala D, Montoya J and Attardi G (1981): tRNA punctuation model of RNA processing in human mitochondria. Nature 290: 470-4.

Onyango P, Celic I, McCaffery JM, Boeke JD and Feinberg AP (2002): SIRT3, a human SIR2 homologue, is an NAD-dependent deacetylase localized to mitochondria. Proc Natl Acad Sci U S A 99:13653-8.

Orr W C and Sohal R S (1994): Extension of life-span by overexpression of superoxide dismutase and catalase in Drosophila melanogaster Science 263:1128-30.

Pagnamenta AT, Taanman JW, Wilson CJ, Anderson NE, Marotta R, Duncan AJ, Bitner-Glindzicz M, Taylor RW, Laskowski A, Thorburn DR and Rahman S (2006): Dominant inheritance of premature ovarian failure associated with mutant mitochondrial DNA polymerase gamma. Hum Reprod 21:2467–73.

Palmer JP, Benson JW, Walter RM and Ensinck JW (1979): Arginine-stimulated acute phase of insulin and glucagon secretion in diabetic subjects. J Clin Invest 58:565–570.

Parisi MA, Xu B and Clayton DA **(**1993): A human mitochondrial transcriptional activator can functionally replace a yeast mitochondrial HMG-box protein both in vivo and in vitro. Mol. Cell. Biol 13**:**1951-1961.

Parkes TL, Elia AJ, Dickinson D, Hilliker AJ, Phillips JP and Boulianne GL (1998): Extension of Drosophila lifespan by overexpression of human SOD1 in motorneurons. Nat Genet 19:171-174.

Perrod S, Cockell MM, Laroche T, Renauld H, Ducrest AL, Bonnard C and Gasser SM (2001): A cytosolic NAD-dependent deacetylase, Hst2p, can modulate nucleolar and telomeric silencing in yeast. EMBO J **20**:197–209.

Pfister JA, Ma C, Morrison BE and D'Mello SR (2008): Opposing effects of sirtuins on neuronal survival: SIRT1-mediated neuroprotection is independent of its deacetylase activity. PLoS ONE 3:e4090.

Pfluger PT, Herranz D, Velasco-Miguel S, Serrano M and Tschöp MH (2008): Sirt1 protects against high-fat diet-induced metabolic damage. Proc Natl Acad Sci U S A 105:9793-8.

Pohjoismäki JL, Wanrooij S, Hyvärinen AK, Goffart S, Holt IJ, Spelbrink JN and Jacobs HT (2006): Alterations to the expression level of mitochondrial transcription factor A, TFAM, modify the mode of mitochondrial DNA replication in cultured human cells. Nucleic Acids Res 34:5815-28.

Pohjoismäki JL, Goffart S, Tyynismaa H, Willcox S, Ide T, Kang D, Suomalainen A, Karhunen PJ, Griffith JD, Holt IJ and Jacobs HT (2009): Human Heart Mitochondrial DNA Is Organized in Complex Catenated Networks Containing Abundant Four-way Junctions and Replication Forks. J Biol Chem 284:21446-57.

Revollo JR, Grimm AA and Imai S (2004): The NAD biosynthesis pathway mediated by nicotinamide phosphoribosyltransferase regulates Sir2 activity in mammalian cells. J Biol Chem 279:50754-63.

Richardson A (1985): The effect of age and nutrition on protein synthesis by cells and tissues fron mammals. In Handbook on Nutrition in the Aged, W.R. Atson, ed. (Boca Raton, Florida: CRC Press), pp. 31-48.

Robberson DL, Kasamatsu H and Vinograd J (1971): Replication of mitochondrial DNA. Circular replicative intermediates in mouse L cells. Proc Natl Acad Sci U S A 69:737-41.

Rodgers JT, Lerin C, Haas W, Gygi SP, Spiegelman BM and Puigserver P (2005): Nutrient control of glucose homeostasis through a complex of PGC-1alpha and SIRT1. Nature 434:113-8.

Roe CR and Ding J (2001): Mitochondrial fatty acid disorders, in. In: Scriver CR, Beaudet AL and Sly WS, Editors, The Metabolic & Molecular Bases of Inherited Disease (ed 8), McGraw-Hill, New York, NY 2297–326.

Rogina B, Helfand SL and Frankel S (2002): Longevity regulation by Drosophila Rpd3 deacetylase and caloric restriction. Science 298:1745.

Rogina B and Helfand SL (2004): Sir2 mediates longevity in the fly through a pathway related to calorie restriction. Proc Natl Acad Sci U S A 101:15998-6003.

Rongvaux A, Andris F, Van Gool F and Leo O (2003): Reconstructing eukaryotic NAD metabolism. Bioessays 25:683-90.

Ropp PA and Copeland WC (1996): Cloning and characterization of the human mitochondrial DNA polymerase, DNA polymerase gamma. Genomics 36:449-58.

Rose G, Dato S, Altomare K, Bellizzi D, Garasto S, Greco V, Passarino G, Feraco E, Mari V, Barbi C, BonaFe M, Franceschi C, Tan Q, Boiko S, Yashin AI and De Benedictis G (2003): Variability of the SIRT3 gene, human silent information regulator Sir2 homologue, and survivorship in the elderly. Exp Gerontol 38:1065-70.

Rovio AT, Marchington DR, Donat S, Schuppe HC, Abel J, Fritsche E, Elliott DJ, Laippala P, Ahola AL, McNay D, Harrison RF, Hughes B, Barrett T, Bailey DM, Mehmet D, Jequier AM, Hargreave TB, Kao SH, Cummins JM, Barton DE, Cooke HJ, Wei YH, Wichmann L, Poulton J, Jacobs HT (2001): Mutations at the mitochondrial DNA polymerase (POLG) locus associated with male infertility. Nat Genet 29:261–2.

Rusche LN, Kirchmaier AL and Rine J (2003): The establishment, inheritance, and function of silenced chromatin in Saccharomyces cerevisiae. Annu Rev Biochem 72:481-516.

Sarzi E, Goffart S, Serre V, Chrétien D, Slama A, Munnich A, Spelbrink JN and Rötig A (2007): Twinkle helicase (PEO1) gene mutation causes mitochondrial DNA depletion.Ann Neurol. 62:579-87.

Selman C, Lingard S, Choudhury AI, Batterham RL, Claret M, Clements M, Ramadani F, Okkenhaug K, Schuster E, Blanc E, Piper MD, Al-Qassab H, Speakman JR, Carmignac D, Robinson IC, Thornton JM, Gems D, Partridge L and Withers DJ (2008): Evidence for lifespan extension and delayed age-related biomarkers in insulin receptor substrate 1 null mice. FASEB J 22:807–818.

Scher MB, Vaquero A and Reinberg D (2007): SirT3 is a nuclear NAD+-dependent histone deacetylase that translocates to the mitochondria upon cellular stress. Genes Dev 21:920-8.

Schlicker C, Gertz M, Papatheodorou P, Kachholz B, Becker CF and Steegborn C (2008): Substrates and regulation mechanisms for the human mitochondrial sirtuins Sirt3 and Sirt5. J Mol Biol 382:790-801.

Schriner SE, Ogburn CE, Smith AC, Newcomb TG, Ladiges WC, Dolle ME, Vijg J, Fukuchi K and Martin GM. (2000). Levels of dna damage are unaltered in mice overexpressing human catalase in nuclei. Free Radic Biol Med 29:664-673.

Schriner SE, Linford NJ, Martin GM, Treuting P, Ogburn CE, Emond M, Coskun PE, Ladiges W, Wolf N, Van Remmen H, Wallace DC and Rabinovitch PS (2005): Extension of murine life span by overexpression of catalase targeted to mitochondria, Science 308**:**1909–1911.

Schwartz M and Vissing J (2002): Paternal inheritance of mitochondrial DNA. N Engl J Med. 347:576-80.

Schwer B, North BJ, Frye RA, Ott M and Verdin E (2002): The human silent information regulator (Sir)2 homologue hSIRT3 is a mitochondrial nicotinamide adenine dinucleotide-dependent deacetylase. J Cell Biol 158:647-57.

Schwer B, Bunkenborg J, Verdin RO, Andersen JS and Verdin E (2006): Reversible lysine acetylation controls the activity of the mitochondrial enzyme acetyl-CoA synthetase 2. Proc Natl Acad Sci U S A. 103:10224-9.

Schwer B, Eckersdorff M, Li Y, Silva JC, Fermin D, Kurtev MV, Giallourakis C, Comb MJ, Alt FW and Lombard DB (2009): Calorie Restriction Alters Mitochondrial Protein Acetylation. DB. Aging Cell. 2009 Jul 9. [Epub ahead of print]

Sedding DG (2008): FoxO transcription factors in oxidative stress response and ageing--a new fork on the way to longevity? Biol Chem 389:279-83.

Shi T, Wang F, Stieren E and Tong Q (2005): SIRT3, a mitochondrial sirtuin deacetylase, regulates mitochondrial function and thermogenesis in brown adipocytes. J Biol Chem 280:13560-7.

Shuldiner AR, Yang R and Gong D-W (2001): Resistin, obesity, and insulin resistance: the emerging role of the adipocyte as an endocrine organ. N Engl J Med 345 1345–46.

Skutches CL, Holroyde CP, Myers RN, Paul P and Reichard GA (1979): Plasma acetate turnover and oxidation. J Clin Invest 64:708-13.

Sohal RS and Weindruch R (1996): Oxidative stress, caloric restriction, and aging. Science 273:59-63.

Sohal RS, Mockett RJ and Orr WC (2002): Mechanisms of aging: an appraisal of the oxidative stress hypothesis. Free Radic Biol Med 33:575-86.

Spelbrink JN, Toivonen JM, Hakkaart GA, Kurkela JM, Cooper HM, Lehtinen SK, Lecrenier N, Back JW, Speijer D, Foury F and Jacobs HT (2000): In vivo functional analysis of the human mitochondrial DNA polymerase POLG expressed in cultured human cells. J Biol Chem 275:24818-28.

Spelbrink JN, Li FY, Tiranti V, Nikali K, Yuan QP, Tariq M, Wanrooij S, Garrido N, Comi G, Morandi L, Santoro L, Toscano A, Fabrizi GM, Somer H, Croxen R, Beeson D, Poulton J, Suomalainen A, Jacobs HT, Zeviani M and Larsson C (2001): Human mitochondrial DNA deletions associated with mutations in the gene encoding twinkle, a phage T7 gene 4-like protein localized in mitochondria. Nat Genet 28: 223-31.

Starai VJ, Celic I, Cole RN, Boeke JD and Escalante-Semerena JC (2002): Sir2-dependent activation of acetyl-CoA synthetase by deacetylation of active lysine. Science **298**:2390–92.

Sugden MC, Howard RM, Munday MR and Holness MJ (1993): Mechanisms involved in the coordinate regulation of strategic enzymes of glucose metabolism. Adv Enzyme Regul 33:71-95.

Sundaresan NR, Samant SA, Pillai VB, Rajamohan SB and Gupta MP (2008): SIRT3 is a stress-responsive deacetylase in cardiomyocytes that protects cells from stress-mediated cell death by deacetylation of Ku70. Mol Cell Biol 28:6384-401.

Suomalainen A, Majander A, Wallin M, Setälä K, Kontula K, Leinonen H, Salmi T, Paetau A, Haltia M, Valanne L, Lonnqvist J, Peltonen L and Somer H (1997): Autosomal dominant progressive external ophthalmoplegia with multiple deletions of mtDNA: clinical, biochemical, and molecular genetic features of the 10q-linked disease. Neurology 48:1244-53.

Szekely AM, Chen YH, Zhang C, Oshima J and Weissman SM (2000): Werner protein recruits DNA polymerase delta to the nucleolus. Proc Natl Acad Sci 97:11365-70.

Tanner KG, Landry J, Sternglanz R and Denu JM (2000): Silent information regulator 2 family of NAD- dependent histone/protein deacetylases generates a unique product, 1-O-acetyl-ADP-ribose. Proc Natl Acad Sci U S A 97:14178-82.

Tatar M., Kopelman A, Epstein D, Tu M P, Yin C M and Garofalo R S (2001): A mutant *Drosophila* insulin receptor homolog that extends life-span and impairs neuroendocrine function. Science 292:107–10.

Thyagarajan R, Padua A and Campbell C (1996): Mammalian mitochondria possess homologous recombination activity, J. Biol. Chem. **271**:27536–43.

Tissenbaum HA and Guarente L (2001): Increased dosage of a sir-2 gene extends lifespan in Caenorhabditis elegans. Nature 410:227-30.

Trifunovic A, Wredenberg A, Falkenberg M, Spelbrink JN, Rovio AT, Bruder CE, Bohlooly-Y M, Gidlöf S, Oldfors A, Wibom R, Törnell J, Jacobs HT and Larsson NG (2004): Premature ageing in mice expressing defective mitochondrial DNA polymerase. Nature 429:417-23.

Trifunovic A, Hansson A, Wredenberg A, Rovio AT, Dufour E, Khvorostov I, Spelbrink JN, Wibom R, Jacobs HT and Larsson NG (2005): Somatic mtDNA mutations cause aging phenotypes without affecting reactive oxygen species production. Proc Natl Acad Sci U S A 102:17993-8.

Tyynismaa H, Sembongi H, Bokori-Brown M, Granycome C, Ashley N, Poulton J, Jalanko A, Spelbrink JN, Holt IJ and Suomalainen A (2004): Twinkle helicase is essential for mtDNA maintenance and regulates mtDNA copy number. Hum Mol Genet 13:3219-27.

Tyynismaa H, Mjosund KP, Wanrooij S, Lappalainen I, Ylikallio E, Jalanko A, Spelbrink JN, Paetau A and Suomalainen A (2005): Mutant mitochondrial helicase Twinkle causes multiple mtDNA deletions and a late-onset mitochondrial disease in mice. Proc Natl Acad Sci U S A Dec 102:17687-92.

Van Goethem G, Dermaut B, Löfgren A, Martin JJ, Van Broeckhoven C. Mutation of POLG is associated with progressive external ophthalmoplegia characterized by mtDNA deletions. Nat. Genet 2001;28:211–12.

Van Goethem G, Schwartz M, Lofgren A, Dermaut B, Van Broeckhoven C and Vissing J (2003): Novel POLG mutations in progressive external ophthalmoplegia mimicking mitochondrial neurogastrointestinal encephalomyopathy. Eur J Hum Genet 11: 547–49.

Van Remmen H, Ikeno Y, Hamilton M, Pahlavani M, Wolf N, Thorpe SR, Alderson NL, Baynes JW, Epstein CJ, Huang TT, Nelson J, Strong R and Richardson A. (2003). Life-long reduction in MnSOD activity results in increased DNA damage and higher incidence of cancer but does not accelerate aging. Physiol Genomics 16:29-37.

Vakhrusheva O, Smolka C, Gajawada P, Kostin S, Boettger T, Kubin T, Braun T and Bober E (2008): Sirt7 increases stress resistance of cardiomyocytes and prevents apoptosis and inflammatory cardiomyopathy in mice. Circ Res 102:703-10.

Vaziri H, Dessain SK, Ng Eaton E, Imai SI, Frye RA, Pandita TK, Guarente L and Weinberg RA (2001): hSIR2(SIRT1) functions as an NAD-dependent p53 deacetylase. Cell 107:149–59.

Vijg, J (2000): Somatic mutations and aging: a re-evaluation. Mutation research 447:117–35.

Walker RL, Anziano P and Meltzer PS (1997): A PAC containing the human mitochondrial DNA polymerase gamma gene (POLG) maps to chromosome 15q25. Genomics 40:376-8.

Wanrooij S, Luoma P, van Goethem G, van Broeckhoven C, Suomalainen A and Spelbrink JN (2004): Twinkle and POLG defects enhance age-dependent accumulation of mutations in the control region of mtDNA. Nucleic Acids Res 32:3053-64.

Wanrooij S, Goffart S, Pohjoismäki JL, Yasukawa T and Spelbrink JN (2007): Expression of catalytic mutants of the mtDNA helicase Twinkle and polymerase POLG causes distinct replication stalling phenotypes. Nucleic Acids Res 35:3238-51.

Wanrooij S, Fusté JM, Farge G, Shi Y, Gustafsson CM and Falkenberg M (2008): Human mitochondrial RNA polymerase primes lagging-strand DNA synthesis in vitro. Proc Natl Acad Sci U S A 105:11122-7.

Warram JH, Martin BC, Krolewski AS, Soeldner JS and Kahn CR (1990): Slow glucose removal rate and hyperinsulinemia precede the development of type II diabetes in the offspring of diabetic parents. Ann Intern Med 113:909–15.

Westerheide SD, Anckar J, Stevens SM Jr, Sistonen L and Morimoto RI (2009): Stress-inducible regulation of heat shock factor 1 by the deacetylase SIRT1. Science 323:1063-6.

Wilkinson A, Day J and Bowater R (2001): Bacterial DNA ligases. Mol Microbiol 40:1241-8.

Wood JG, Rogina B, Lavu S, Howitz K, Helfand SL, Tatar M and Sinclair D (2004): Sirtuin activators mimic caloric restriction and delay ageing in metazoans. Nature 430:686-9. Erratum in: Nature. 2004;431:107.

Wu Z, Puigserver P, Andersson U, Zhang C, Adelmant G, Mootha V, Troy A, Cinti S, Lowell B, Scarpulla RC and Spiegelman BM (1999): Mechanisms controlling mitochondrial biogenesis and respiration through the thermogenic coactivator PGC-1. Cell 98:115-24.

Yakubovskaya E, Chen Z, Carrodeguas JA, Kisker C and Bogenhagen DF (2006): Functional human mitochondrial DNA polymerase gamma forms a heterotrimer. J Biol Chem 281: 374-82.

Yakubovskaya E, Lukin M, Chen Z, Berriman J, Wall JS, Kobayashi R, Kisker C and Bogenhagen DF (2007) The EM structure of human DNA polymerase gamma reveals a localized contact between the catalytic and accessory subunits. EMBO J 26: 4283-91.

Yang H, Yang T, Baur JA, Perez E, Matsui T, Carmona JJ, Lamming DW, Souza-Pinto NC, Bohr VA, Rosenzweig A, de Cabo R, Sauve AA and Sinclair DA (2007): Nutrient-sensitive mitochondrial NAD+ levels dictate cell survival**.** Cell 130:1095-107.

Yasukawa T, Yang MY, Jacobs HT and Holt IJ (2005): A bidirectional origin of replication maps to the major noncoding region of human mitochondrial DNA. Mol Cell 18:651-62.

Yasukawa T, Reyes A, Cluett TJ, Yang MY, Bowmaker M, Jacobs HT and Holt IJ (2006): Replication of vertebrate mitochondrial DNA entails transient ribonucleotide incorporation throughout the lagging strand. EMBO J 25:5358-71.

Yu CE, Oshima J, Wijsman EM, Nakura J, Miki T, Piussan C, Matthews S, Fu YH, Mulligan J, Martin GM and Schellenberg GD. (1996): Positional Cloning of the Werner's Syndrome Gene. *Science* 5259:258-62.

Zeviani M, Servidei S, Gellera C, Bertini E, DiMauro S and DiDonato S (1989): An autosomal dominant disorder with multiple deletions of mitochondrial DNA starting at the D-loop region. Nature 339:309–11.

Zsurka G, Kraytsberg Y, Kudina T, Kornblum C, Elger CE, Khrapko K and Kunz WS (2005): Recombination of mitochondrial DNA in skeletal muscle of individuals with multiple mitochondrial DNA heteroplasmy. Nat Genet 37:873-7.

# Appendices

## Appendix 1

A list of all proteins found to interact with BD-hSirt3 in the yeast two-hybrid library screen. The second column states the GI number of the protein in the NCB1 Protein database (plain letters) on in the Nucleotide database (*italics*). The third column give the number of clones recovered in the screen.

| Protein | gi number | Total |
|---|---|---|
| 43kD acetylcholine receptor-associated protein | 19310213 | 2 |
| *Acetyl-coenzyme A acetyltransferase 1* | 4557237 | 1 |
| *Acetyl-coenzyme A acyltransferase 2* | 12804931 | 5 |
| Actin, α-1, skeletal muscle | 56204816 | 177 |
| Actinin, α 2 | 4501893 | 1 |
| *Acyl-coA dehydrogenase,C-4 to C-12 straight chain* | 4557231 | 1 |
| Adenylate kinase 1 | 4502011 | 1 |
| *Adenylate kinase 2* | 7524346 | 5 |
| Aldolase A | 169877049 | 95 |
| Amyotrophic lateral sclerosis 2 (ALS2CR2) | 60551806 | 1 |
| Ankyrin repeat domain 9 | 22748713 | 1 |
| Aryl hydrocarbon receptor interacting protein(AIP) | 4502009 | 3 |
| Arylsulfatase A (ARSA) | 6005990 | 1 |
| Asparagine synthetase, variants 1-3 | 34452703/19718774 | 3 |
| ATPase, H+-transporting, lysosomal, V1 subunit,G isoform | 4757818 | 1 |
| ATPase, H+-transporting, lysosomal, V1 subunit,H isoform | ntd 47717099 | 1 |
| *ATPase, mitochondrial F1 complex,alpha subunit* | 15030240 | 1 |
| Barrier to autointegration factor 1 | 4502389 | 1 |
| BRCA1-associated protein-1 | ntd 19718752 | 2 |
| C 20 orf 166 | ntd 51371944 | 2 |
| C6 orf 82 | ntd 62526025 | 1 |
| Candidate tumor suppressor in ovarian cancer2 | 18201880 | 1 |
| Carboxylesterase 2(intestine, liver)? | ntd 56788327 | 4 |
| Catalase | 4557014 | 1 |
| CGI-112 protein/ c14 orf122 | 12803345 | 1 |
| Chaperonin containing TCP1 subunit 7 (eta) | 5453607 | 3 |
| Collagen, alpha 1, type XV | 18641350 | 1 |
| Collagen, type IV, alpha 2 | 17986277 | 1 |
| Creatine kinase, muscle | 21536288 | 34 |
| CTD small phosphatase1 isoform2 | 32813443 | 1 |
| Cystatin C | 4503107 | 5 |
| Cytochrome b5 reductase 3 | ntd 70908371 | 1 |
| *Cytochrome c oxidase deficient homolog1* | 4759068 | 2 |

| | | |
|---|---|---|
| *Cytochrome c oxidase subunit III* | 51657746 | 3 |
| DAZ associated protein 2 (DAZAP2) | 7661886 | 2 |
| DEAD/H box polypeptide 32 | 20336300 | 1 |
| *Deoxyguanosine kinase, mitochondrial* | 23503050 | 1 |
| Deoxyhypusine synthase, (isoform a) | 4503325 | 1 |
| Dishevelled, dsh homolog 1 | ntd 59894797 | 1 |
| Dual specificity phosphatase,muscle restricted | 56117818 | 1 |
| Dynein, cytoplasmic, heavy polypeptide 1 | 33350932 | 2 |
| EEFIA1 protein | 15214751 | 1 |
| *Electron-transfer flavoprotein,alpha* | 4503607 | 3 |
| *Electron-transferring-flavoprotein dehydrogenase* | 4758312 | 1 |
| Enolase 3 | 16554592 | 15 |
| *Enoyl coenzyme A hydratase 1,short chain, mitochondrial* | 14286220 | 6 |
| Eukaryotic translation initiation factor 3,subunit 5 epsilon | ntd 4503518 | 2 |
| Eukaryotic trl initiation factor 2B,4, delta | 41281817 | 1 |
| Eukaryotic trl intiation factor 4 gamma1 (EIF4G1) | 38201618 | 1 |
| F-box protein 42 | 62955044 | 1 |
| Ferritin, light polypeptide | ntd 56682960 | 7 |
| FGF receptor 1, transcript variant 9 (2,4,3,1..) | ntd 13186248 | 1 |
| FLJ11200, hypothetical protein | 48146673 | 2 |
| FLJ20850 hypothetical protein | ntd 15082339 | 2 |
| *Fumarate hydratase = fumarase* | 19743875 | 1 |
| General transcription factor IIIc,polyp.1, alpha,22kDa | ntd 4753160 | 1 |
| GGI-128 protein (hypothetical?) | 12804621 | 1 |
| Glutamate-ammonia ligase (glutamine synthetase) | 74271826 | 2 |
| Glutamic-pyruvate transaminase | ntd 4885350 | 2 |
| Glyceraldehyde-3-phosphate dehydrogenase | 7669492 | 63 |
| Glycogen phosphorylase,muscle | ntd 5032008 | 1 |
| Guanidinoacetate N-methyltransferase | 4503909 | 5 |
| Guanylate kinase 1 | 4504221 | 1 |
| Heat shock 27 kDa protein family,member 7 | ntd 34147560 | 3 |
| Heat shock 27kDa protein 1 | 15126735 | 1 |
| *Hydroxyacyl dehydrogenase, subunit B* | 4504327 | 12 |
| Hypothetical protein FLJ10916/LOC55258 | 40538796 | 1 |
| Hypothetical protein LOC124402 | 21687062 | 1 |
| Hypothetical protein LOC200942 | 27734909 | 1 |
| Hypothetical protein LOC205251 | ntd 28372544 | 5 |
| Hypothetical protein LOC55004 | 8923579 | 1 |
| Hypothetical protein LOC80208 | 33636748 | 1 |
| ISOC2 protein (=isochrismatase) | 16878298 | 3 |
| Koyt binding protein 1 | 20149229 | 2 |
| Kruppel-like factor 13 | ntd 37693994 | 3 |
| Lactate dehydrogenase A | 5031857 | 9 |
| Lamin A/C (LMNA) | 27436947 | 2 |
| *Malate dehydrogenase, mitochondrial* | 21735621 | 1 |
| Mannosidase, alpha, class 2B, member 1 | 51873064 | 1 |
| Matrix remodelling associated 6 | 38648826 | 2 |
| *Mercaptopyruvate sulfurtransferase* | ntd 17511725 | 2 |
| Metallothionein 2A | 5174764 | 8 |
| Methylenetetrahydrofolate dehydrogenase 2-like | ntd 62243411 | 2 |
| Mitogen-activated protein kinase kinase 7(MAPK7) | 40806198 | 1 |
| MURR1 | 22749079 | 1 |
| MutL protein homolog 1 variant; mRNA | ntd 62897178 | 1 |
| Myelin basic protein | ntd 68509939 | 1 |

| | | |
|---|---|---|
| Myosin light chain-2 | 7689897 | 1 |
| Myozenin 1 | 10864053 | 4 |
| *N-acylsphingosine amidohydrolase 2 (mt ceramidase)* | 9845267 | 3 |
| NAD(P)H dehydrogenase,quinone2 | 4505417] | 1 |
| *NADH dehydrogenase (ubiquinone) Fe-S protein 8* | 4505371 | 3 |
| *NADH dehydrogenase (ubiquinone) Fe-S protein3(NDUFS3)* | 4758788 | 1 |
| NADH dehydrogenase (ubiquinone)1 alpha subcomplex 10 | 4758768 | 1 |
| *NADH dehydrogenase (ubiquinone)1alpha subcomplex7* | 4826850 | 1 |
| *NADH dehydrogenase ubiquinone 1 β subcomplex 10* | 4758774 | 51 |
| *NDUFA13/GRIM19* | (14327930/)21361822 | 6 |
| *Nipsnap homolog 1* | ntd 4505398 | 1 |
| Nodal modulator 1 (or 2) | ntd 51944952 | 2 |
| Nuclear prelamin A recognition factor-like | 11968051 | 1 |
| Nucleoside diphosphate kinase type 6 | 5031951 | 1 |
| Phosphatidic acid phosphatase type2 domain containing3 | ntd 34147435 | 1 |
| Phosphoglucomutase1 (PGM1 protein) | 45768704 | 2 |
| Phytanoyl-CoA dioxygenase domain-containing1 (PHYHD1) | 55859583 | 1 |
| PP14397 | 33341770 | 1 |
| PPGB | 56001073 | 1 |
| Proteasome beta 1 subunit | 12653473 | 6 |
| Proteasome beta 5 subunit | 4506201 | 2 |
| Proteasome inhibitor subunit 1 | 30581145 | 1 |
| Proteasome α 7 subunit | 23110948 | 2 |
| *Pyruvate dehydrogenase (lipoamide) beta* | 4505687 | 1 |
| Pyruvate kinase, muscle | ntd 33286421 | 5 |
| Radical S-adenosyl methionine domain containing1(RSAD1) | ntd 8922910 | 1 |
| Rhomboid, veintlet-like 7 (RHBDL7) | 46255831 | 1 |
| Ribonucleoside-diphosphate reductase,M1 chain | 4506749 | 3 |
| Ribosomal protein SA (RPSA),transcript variant 1 | 9845502 | 1 |
| Ring finger protein 123/ubiquitin ligase | 37588869/53766621 | 1 |
| Sarcoglycan, alpha | 4506911 | 1 |
| SCIRP10-related protein | 7019545 | 1 |
| Serpin peptidase inhibitor, clade H (hsp47) member 1 | 47124471 | 1 |
| Similar to AC1147 | 51464624 | 1 |
| Single immunoglobulin&toll-interleukin1receptor(TIR)domain | 11141876 | 1 |
| *SLC25A3 (Solute carrier family25(mitochondrial) member 3* | 30802109 | 13 |
| Solute carrier family 44 member 2 | 31377726 | 1 |
| Sphingomyelin phosphodiesterase1,acid lysosomal isoform1 | 62089136 | 1 |
| *Succinate dehydrogenase complex, subunit B,iron-sulfur* | 8979800 | 1 |
| *Sulfide dehydrogenase like* | 10864011 | 1 |
| Supervillin(SVIL), mRNA | ntd 11496981 | 1 |
| Tax1 binding protein 3 | 62339397 | 1 |
| Telethonin (=titin-cap) | 4507435 | 20 |
| Tetraspanin 7 | 21265104 | 1 |
| THAP domain containing 8 | 22749337 | 3 |
| Thimet oligopeptidase (metalloproteinase) | 1030054 | 1 |
| Thioredoxin-like 3 | 37087933 | 2 |
| *Thiosulfate sulfurtransferase* | 17402865 | 2 |
| Thyroid hormone receptor,alpha isoform1 | ntd 62088271 | 1 |

| | | |
|---|---|---|
| Tropomyosin 2 (=beta), transcript variant 1 | ntd 47519592 | 2 |
| Troponin I, cardiac | 30141910 | 3 |
| Troponin T type 3(skeletal,fast) | ntd 5803202 | 1 |
| Ubiquilin 4 | 55663556 | 1 |
| *Ubiquinol-cyt c reductase core protein I* | 46593007 | 9 |
| Ubiquitin-associated protein (NAG20) | ntd 7948992 | 1 |
| Ubiquitin-associated protein 1 (UBAP1) | ntd 22212941 | 1 |
| WD and tetratricopeptide repeats 1 (WDTC1) | ntd 22095348 | 2 |
| Vesicle amine transport protein 1 | ntd 1698398 | 1 |
| *Voltage-dependent anion channel 1* | 4507879 | 1 |
| Zinc finger protein 650 | ntd 40255162 | 1 |

# Appendix 2

## 2DNAGE methodology and interpretation

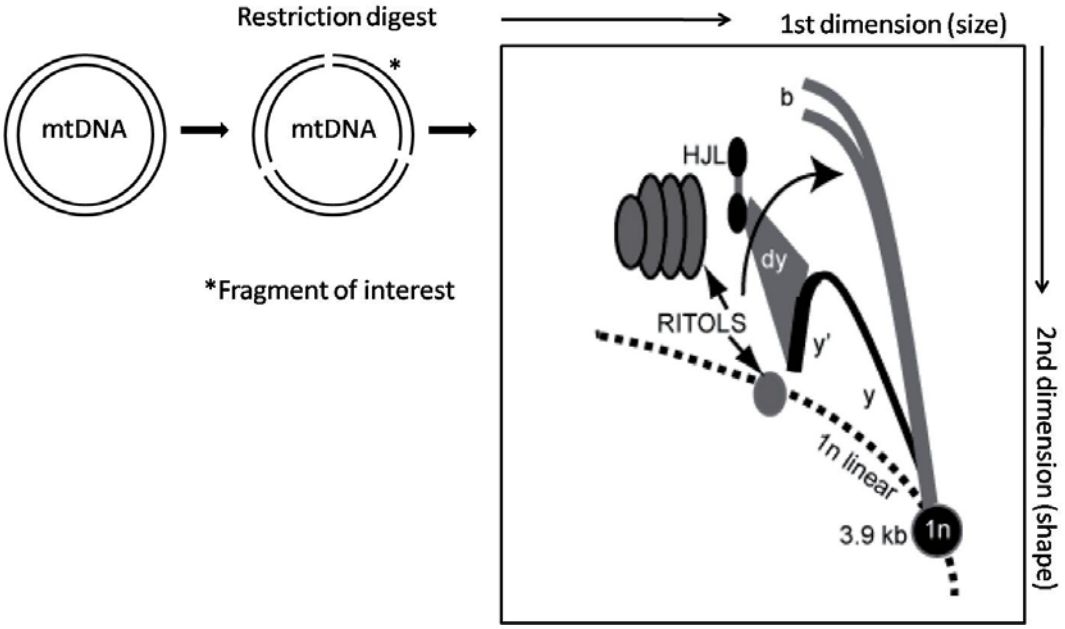


DNA is digested with restriction enzymes to obtain fragments containing regions of interest. In the first dimension, which is run without ethidium bromide (EtBr), molecules separate by size. After the 1st dimension run the gel in stained with EtBr and individual lanes are cut out, rotated 90° and a second gel is cast around them. In the 2nd dimension run, this includes EtBr, molecules separate by size and shape. Gels are blotted and the resulting membranes a probed for the fragment of interest with complementary radio-labelled DNA oligos.

Fragments of different size and shapes migrate at different positions in the 2nd dimension. Linier single stranded fragments cluster in the 1n spot, whereas molecules that contain replication forks travel along the y-arc. y and y' indicate ascending and descending parts of the y arc, respectively, and (dy) indicates double-Y structures typical for the termination of replication. These will eventually form resolution intermediates resembling Holliday junctions (HJL-Holliday junction like molecules). Molecules that contain replication bubbles migrate along the bubble arc (b). Other higher molecular weight fragments arise from the failure to cut RNA–DNA hybrids at a restriction site, these as well as the RNA-rich bubble arcs are marked as RITOLS (RNA Incorporation Through Out the Lagging Strand).

# Original communications

BJ www.biochemj.org

Biochem. J. (2008) **411**, 279–285 (Printed in Great Britain) doi:10.1042/BJ20071624



# The human SIRT3 protein deacetylase is exclusively mitochondrial

Helen M. COOPER and Johannes N. SPELBRINK[1]

Institute of Medical Technology and Tampere University Hospital, Tampere, Finland

It has recently been suggested that perhaps as many as 20 % of all mitochondrial proteins are regulated through lysine acetylation while SIRT3 has been implicated as an important mitochondrial protein deacetylase. It is therefore of crucial importance that the mitochondrial localization of potential protein deacetylases is unambiguously established. Although mouse SIRT3 was recently shown to be mitochondrial, HsSIRT3 (human SIRT3) was reported to be both nuclear and mitochondrial and to relocate from the nucleus to the mitochondrion upon cellular stress. In the present study we show, using various HsSIRT3 expression constructs and a combination of immunofluorescence and careful subcellular fractionation, that in contrast with earlier reports HsSIRT3 is exclusively mitochondrial. We discuss possible experimental explanations for these discrepancies. In addition we suggest, on the basis of the analysis of public genome databases, that the full-length mouse SIRT3 protein is a 37 kDa mitochondrial precursor protein contrary to the previously suggested 29 kDa protein.

Key words: deacetylase, immunofluorescence, import, leptomycin B, mitochondrial, sirtuin.

## INTRODUCTION

An important aspect of the regulation of chromatin remodelling and consequently gene expression involves post-translational modifications of histones, abundant nuclear DNA-binding proteins with regulatory and packaging functions [1,2]. These modifications include phosphorylation, methylation and acetylation. Acetylation of lysine residues involves HATs (histone acetyl transferases) such as p300/CBP [CREB (cAMP-response-element-binding protein)-binding protein], whereas deacetylation involves HDACs (histone deacetylases). HDACs can be divided into three distinct families based on their domain architecture, and originally based on similarity with yeast HDACs [3]. Class I and II HDACs share similar catalytic domains, whereas the Class III 'Sir' or SIRT (sirtuin) family of deacetylases are catalytically distinct and depend on $NAD^+$ as a cofactor. Although the names suggest that HDACs are specific for histones, this is not the case. Indeed, many proteins have been identified as targets of HATs and HDACs, many of them transcription factors, but also, for example, the cytoplasmic protein tubulin, a major structural component of the microtubular network [4]. In addition, in recent years acetylation/deacetylation has been shown to play an important role in protein stability [5].

The deacetylase SIRT3, as well as SIRT4 and 5, were recently identified as mitochondrial members of the Sir family of deacetylases [6–8], which suggested the possibility of acetylated mitochondrial protein substrates. A recent proteomics approach to identify lysine-acetylated proteins indeed has suggested that as many as 20 % of all mitochondrial proteins are regulated by lysine acetylation [9]. The first bona fide HsSIRT3 (human SIRT3) substrate to be identified was the mitochondrial acetyl-CoA synthetase or AceCS2 (mitochondrial acetyl-CoA synthetase 2) [10,11] and further work has now shown that SIRT3 in mouse is a global mitochondrial deacetylase involved in the regulation of steady-state acetylation levels of many proteins [12]. Whereas SIRT3 is a deacetylase, SIRT4 has been shown to be an ADP-ribosylase functioning in the regulation of insulin secretion [13,14]. The identification of SIRT3 and SIRT4 substrates and the involvement of SIRT1 in e.g. the metabolic syndrome has suggested roles of several SIRT proteins in the regulation of whole organism metabolism in response to food availability [15–18]. Finally, both SIRT3 and 4 but not SIRT5 have been implicated in nutrient sensing via mitochondrial $NAD^+$ levels [19].

In order to understand the consequences of mitochondrial protein acetylation and deacetylation it is of crucial importance to unambiguously establish the mitochondrial localization of HDACs. The HsSIRT3 has an additional 142 amino acids at its N-terminus. Although the mouse protein is exclusively mitochondrial [12], it was recently suggested that the N-terminal extension of HsSIRT3 mediates an initial localization to the nucleus [20] and mitochondrial relocation occurs upon stress, induced by its own overexpression, by UV damage or etoposide. A second family II HDAC, HDAC7 has been shown to be localized in the inner mitochondrial membrane and nucleus and to relocate to the cytoplasm upon apoptosis inducing stress [21]. In the present study we re-address the issue of HsSIRT3 nuclear localization by using similar approaches [20] and show, contrary to the original publication, that HsSIRT3 is exclusively mitochondrial similar to the mouse protein.

## MATERIALS AND METHODS

### Reagents and antibodies

All common reagents used in the present study were of analytical grade. LMB (leptomycin B) was purchased from Sigma and Optiprep™ (Iodixanol) was from Axis-Shield. Antibodies used in the present study were as follows: anti-HDAC7 (sc-11421) and anti-SIRT3 (sc-49744) were from Santa Cruz Biotechnology; anti-(c-Myc) 9E10 monoclonal antibody was from Roche Molecular Biochemicals; anti-FLAG M2 monoclonal antibody was from Sigma; anti-HA (haemagglutinin) monoclonal antibody HA.11

Abbreviations used: AceCS2, mitochondrial acetyl CoA synthetase 2; EST, expressed sequence tag; FCS, foetal calf serum; HA, haemagglutinin; HAT, histone acetyl transferase; HDAC, histone deacetylase; HEK, human embryonic kidney; HsSIRT3, human SIRT3; LMB, leptomycin B; mtCOXII, cytochrome *c* oxidase subunit II; PFA, paraformaldehyde; P2HA, HA-tagged POLG2; POLG2, polymerase $\gamma$ accessory subunit; siRNA, small interfering RNA; SIRT, sirtuin; U2OS, U2 osteosarcoma.

[1] To whom correspondence should be addressed (email hans.spelbrink@uta.fi).

was from Covance; anti-SIRT3 was from Abcam (40006); anti-mtCOXII (cytochrome *c* oxidase subunit II), Alexa Fluor® 488 or 568 secondary antibodies were from Invitrogen. HDAC1 and nucleoporin antibodies were from Santa Cruz Biotechnology and Zymed respectively (gifts from Keijo Viiri, Institute of Medical Technology, Tampere, Finland). HsSIRT3 siRNAs (small interfering RNAs) and non-targeting siRNAs were from Dharmacon as follows: HsSIRT3 #1 (D-004827-01), CAACGUCACUCACUACUUUUU; HsSIRT3 #2 (D-004827-02), GAACUCCCAUUCUUCUUUCUU; HsSIRT3 #4 (D-004827-04), GGAGUGGCCUGUACAGCAAUU; and non-targeting (D-00121-01-05), UAGCGACUAACACAUCAA.

### Cloning of expression constructs

Full-length HsSIRT3 was originally obtained by RT (reverse transcriptase)-PCR using highly purified HeLa mRNA, and cloned in pcDNA3.1(−)/Myc-His A (Invitrogen) using NotI and BamHI. Truncated (Δ1–142) HsSIRT3–Myc–His and HsSIRT3–FLAG were obtained by PCR amplification from the original full-length construct and cloned either into pcDNA3.1(−)/Myc-His A or pcDNA5/FRT/TO (for FLAG) (Invitrogen). The FLAG epitope was introduced at the C-terminus by PCR and followed immediately by a stop-codon (all primer sequences can be obtained upon request). All constructs were fully verified by sequencing.

### Stable inducible cell lines, transient transfections and siRNA transfections

Stable inducible cell lines expressing HsSIRT3–FLAG and POLG2 (polymerase $\gamma$ accessory subunit)–HA were generated and maintained as previously described [22]. To induce expression, the indicated amount of doxycycline (Sigma) was added to the growth medium from an ethanol stock, and cells were processed for further analyses following the required induction. U2OS (U2 osteosarcoma) and HeLa cells were maintained in DMEM (Dulbecco's modified Eagle's medium) (Cambrex Bioscience) with 2 mM L-glutamine (Cambrex Bioscience) and 10 % FCS (foetal calf serum; Euroclone). For immunofluorescence, cells were transfected using TransIT®-LT1 transfection reagent (Mirus) according to the manufacturer's protocol and 1 $\mu$g of plasmid per 6-well plate well. LMB was added as required at 5 ng/ml 2–3 h prior to processing for immunofluorescence or Western blot analysis. For the RNAi (RNA interference), cells were transfected with a total of 420 pmol siRNAs/10 cm plate, either a combination of three HsSIRT3-specific siRNAs or a single non-targeting siRNA, using Lipofectamine™ 2000 reagent at 30 $\mu$l/420 pmol RNA according to the manufacturer's protocol. Cells were grown for 48 h after transfection.

### Immunofluorescence

For immunofluorescent detection, cells were grown on coverslips in 6-well plates. Following transfection for 1–2 days and LMB treatment, cells were fixed using either 3.3 % PFA (paraformaldehyde) in cell culture medium for 25 min or in methanol for 5 min at −20 °C [23]. This was followed by three washes in PBS and lysis for 10 min with 0.5 % Triton X-100 in PBS/10 % FCS after PFA fixation. No lysis step was performed after methanol fixation. Primary and secondary antibodies were incubated at the recommended concentrations in PBS/10 % FCS for 1 h or overnight. Mitotracker® Red CMXRos treatment was performed prior to fixation essentially as described previously [24]. Slides were mounted using ProLong® Gold antifade with DAPI (4′,6-diamidino-2-phenylindole; Invitrogen). Image acquisition using confocal microscopy was carried out as described [25], using an Andor iXon DV885 EMCCD camera and the Andor iQ software (Andor). Images were further processed using Photoshop CS2.

### Subcellular fractionation and Western blot analysis

Cells were isolated by centrifugation (300 ***g*** for 3 min at 4 °C) and washed once with ice-cold PBS. For hypotonic lysis, the cell pellet was resuspended by gentle pipetting in 2–3 vol. of ice-cold homogenization buffer [4 mM Tris/HCl (pH 7.8), 2.5 mM NaCl, 0.5 mM $MgCl_2$ and 0.1 mM PMSF], kept on ice for 6 min, then homogenized in a glass homogenizer with 20–25 strokes of a tight-fitting pestle. Disruption of the cells was monitored by microscopy. A one-ninth volume of 2 M sucrose, 10 mM Tris/HCl and 1 mM EDTA (pH 7.8) was added following lysis and nuclei and cell debris were pelleted by centrifugation at 1200 ***g*** for 3 min at 4 °C. Mitochondria from the post-nuclear supernatants were recovered by centrifugation at 12 000 ***g*** for 3 min at 4 °C. Mitochondrial pellets were washed once with 1 ml of ice-cold sucrose wash solution [0.25 M sucrose, 25 mM KCl, 5 mM $MgCl_2$ and 20 mM Tricine/KOH (pH 7.8)] and the mitochondrial pellet was lysed for 15 min on ice in 50 mM Tris/HCl (pH 7.5), 300 mM NaCl, 1 mM EDTA and 1 % Triton X-100. An equal volume of 2× Laemmli sample buffer was added and the sample was denatured at 95 °C for 5 min prior to SDS/PAGE. Following hypotonic lysis, nuclear pellets were either extracted first by 0.5 % Nonidet P40 in 50 mM Tris/HCl (pH 7.5) and 150 mM NaCl, again pelleted and extracted with 20 mM Tris/HCl (pH 7.9), 25 % glycerol, 0.42 M NaCl, 1.5 mM $MgCl_2$, 0.2 mM EDTA, 0.1 mM PMSF and 0.5 mM DTT (dithiothreitol) [26] for 20 min and centrifuged at 20 000 ***g*** for 30 min. Alternatively, the low-speed pellet obtained from hypotonic lysis was further purified on a 25 %/30 %/35 % Optiprep gradient to obtain purer nuclear fractions free of whole cell and mitochondrial contaminations according to the manufacturer's protocol, and then extracted by high salt as above. Western blot analysis by ECL (enhanced chemiluminescence) was performed essentially as described previously [27]. Western blot analysis used pre-stained broad-range markers from Bio-Rad. Peroxidase-coupled secondary anti-mouse or anti-rabbit was obtained from Vector Laboratories. In some instances the Supersignal® West Femto Maximum kit (Pierce) was used for detection according to the manufacturer's protocol. Detection and quantification used a Bio-Rad Chemi Doc XRS system.

## RESULTS AND DISCUSSION

As has been reported previously by others [6,8] we observed a clear mitochondrial localization of HsSIRT3 upon transient or stable overexpression in various human cell lines, including HeLa, U2OS and HEK (human embryonic kidney)-293 FlpIn™ TREx™ a stable inducible cell line engineered to express HsSIRT3–FLAG. It has been suggested that overexpression is enough to induce HsSIRT3 translocation from the nucleus to the mitochondria [20] but that preventing nuclear export by inhibition of CRM1 (chromosome region maintenance 1) by LMB would retain the protein in the nucleus. We chose to similarly test LMB in combination with immunofluorescence in U2OS cells following transient transfection of various HsSIRT3 expression plasmids because these cells spread well and have a large surface area of cytoplasm. In addition, an advantage of using transient transfection is that a large variation can be observed in expression levels with cells expressing the recombinant protein at high levels but also with cells in which the protein is expressed at levels just above the detection limit. Thus cells not treated with LMB showed

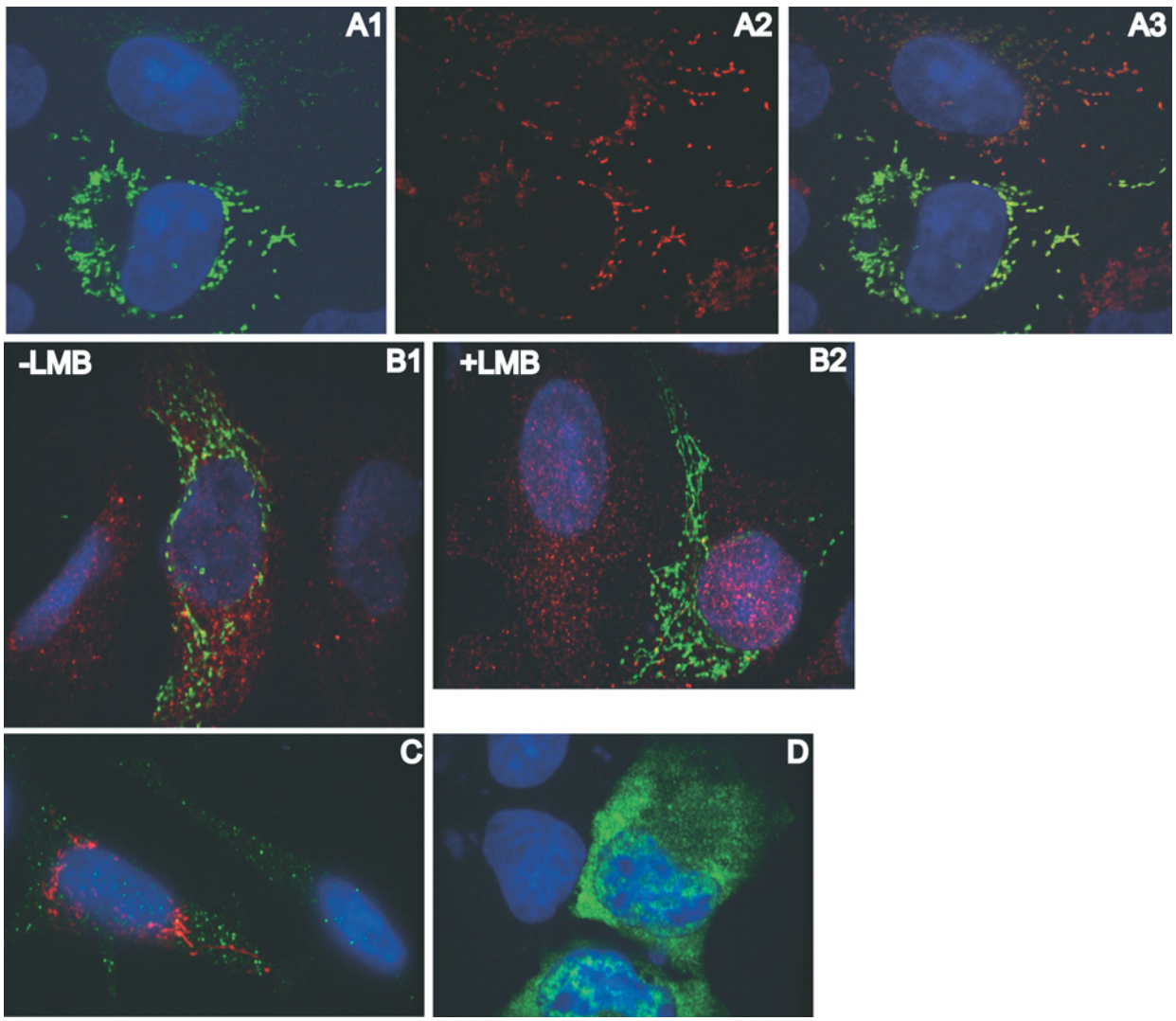


**Figure 1 Overexpressed HsSIRT3 is mitochondrial irrespective of expression level or presence of LMB**

HsSIRT3–FLAG was expressed in human U2OS cells following transient transfection (**A**1–**A**3). At 2 days following transfection, cells were stained with Mitotracker® Red (**A**2) and processed for immunofluorescence using an anti-FLAG antibody (**A**1). A merge image is shown in (**A**3). The results show that, irrespective of expression levels, HsSIRT3–FLAG is mitochondrially localized. (**B**1–**B**2) U2OS cells were transfected as in (**A**) and treated (**B**2) for 2–3 h with 5 ng/ml LMB. HsSIRT3–FLAG is shown as green fluorescence while endogenous HDAC7, which was used to show that LMB is an effective inhibitor of nuclear export in these cells, is shown as red fluorescence. Results show that LMB had no discernible effect on HsSIRT3–FLAG localization, whereas it showed a clear increase in the HDAC7 nuclear signal compared with non-LMB-treated cells. Similar results were observed for HeLa cells treated with LMB (**C** and results not shown; HsSIRT3–FLAG shown as red fluorescence and HDAC7 as green fluorescence) although the LMB effect on HDAC7 in this case was not as clear, but reproducible. Of particular note in this image is the clustering of mitochondria in the nuclear periphery in LMB-treated HeLa cells, giving the false impression that some of the red fluorescence is nuclear. (**D**) Human SIRT3 Δ1–142 with a Myc tag was transiently transfected in U2OS cells. Immunofluorescence showed that this protein is located in the cytoplasm and at high expression levels, as shown here, also in the nucleus.

a clear mitochondrial localization of HsSIRT3 irrespective of the level of expression or the epitope tag, being either the FLAG or Myc epitope (Figure 1, A1–A3, and results not shown). Treatment of these cells with LMB did not show any evidence of a nuclear fluorescent signal suggestive of nuclear retention of HsSIRT3 (Figure 1, B1 and B2). We used a commercial antibody against HDAC7 in co-staining to demonstrate the efficacy of the LMB treatment showing a clear redistribution of HDAC7 from mostly cytoplasmic to mostly nuclear, as previously observed [28]. Similar results were observed using HeLa cells although results were sometimes more difficult to interpret due to clustering of mitochondria in the nuclear periphery (Figure 1C). Unfortunately commercial antibodies against HsSIRT3 worked very poorly in immunofluorescence unless the protein was overexpressed, suggesting that endogenous HsSIRT3 expression levels were relatively low in the cells examined. Finally, we transfected cells to express an HsSIRT3 variant that lacked the first 142 amino acids previously suggested to be important for initial nuclear localization where it was suggested to be processed prior to mitochondrial re-localization [20]. Our hypothesis was that if indeed the full-length protein is processed in the nucleus to yield a protein that is mitochondrial-import competent, deletion of the first 142 amino acids should result in a protein that is mainly mitochondrial. In addition, it has been suggested that mouse SIRT3 starts at the equivalent of human $Met^{143}$ [29,30], but is nevertheless a mitochondrial protein [12] (see below). However, the results (Figure 1D) show that the human variant lacking amino acids 1–142 is present in the cytoplasm and, at high expression levels, also in the nucleus. LMB treatment of these cells did not alter this distribution (results not shown). Co-staining

with Mitotracker® CMXRos did not show any evidence of mitochondrial targeting of truncated HsSIRT3 (results not shown).

To corroborate further the immunofluorescence experiments we relied on Western blot analysis and careful subcellular fractionation. Although the use of a hypotonic lysis method to obtain mitochondrial fractions from cultured cells is common practice, it is not appropriate to use the resulting nuclear pellet without further purification, as in the earlier demonstration of nuclear localization of HsSIRT3 [20]. The problem is that the nuclear fraction resulting from hypotonic lysis typically contains 20–30 % unbroken cells and has a considerable mitochondrial contamination that is not always clear in a subsequent high-salt extraction because many mitochondrial contaminants, especially membrane proteins, will be in the unused pellet following centrifugation of the high-salt extract. To illustrate this problem we repeated essentially the same procedure as previously published [20], and furthermore tried to remove the nuclear mitochondrial contamination from the nuclear pellet by an additional Nonidet P40 detergent extraction which is a detergent commonly used to prepare crude nuclear fractions from whole cells. The results in Figure 2(A) show that it is essentially impossible to avoid a mitochondrial contamination of a crude nuclear fractionation, even following an additional Nonidet P40 step. Apart from cells overexpressing HsSIRT3–FLAG we used a cell line engineered to express an HA-tagged version of the accessory subunit of mitochondrial DNA polymerase $\gamma$ POLG2 (termed P2HA), which is a well-established mitochondrial protein [31]. Although with immunofluorescence this protein is clearly mitochondrial, the use of the crude isolation method also shows this protein to be present in all fractions including the high-salt 'nuclear' extract.

To obtain a clean nuclear fraction we subjected the low-speed nuclear pellet fractions of hypotonic lysates to a further purification step using an iodixanol gradient fractionation. Because nuclei are of considerably higher density than mitochondria and whole cells, this procedure yields a very pure nuclear fraction essentially free from mitochondrial contaminants. The resulting fraction was again subjected to a high-salt extraction and the various fractions were subjected to Western blot analysis. Using inducible HEK-293 FlpIn™ TREx™ cells this furthermore allowed us to use very short induction times similar to the immunofluorescence approach previously used [20] which suggested that short induction showed apparent nuclear HsSIRT3 localization. Both the tagged overexpressed HsSIRT3 as well as the endogenous protein were detected with commercial SIRT3 antibodies. The results (Figure 2B) unambiguously demonstrate that both HsSIRT3–FLAG and endogenous HsSIRT3 are mitochondrially localized with no evidence of protein residing in the nucleus. Similar results were also obtained with regular HEK-293 cells not engineered to overexpress any protein (results not shown). Enrichment of typical nuclear proteins in the iodixanol nuclear fraction was demonstrated by reprobing membranes for HDAC1 (Figure 2B) and e.g. nucleoporin (results not shown) showing that the high-salt extraction had worked. Neither the short induction times nor LMB treatment (results not shown) had any effect on the above results. Strong overexpression for a longer period (2–3 days) or for 1–1.5 h showed the presence of the 44 kDa precursor HsSIRT3–FLAG protein. This was detected with the FLAG antibody but more importantly also with one of the commercial HsSIRT3 antibodies, showing that this antibody is capable of detecting also the endogenous precursor protein. The precursor form of HsSIRT3–FLAG was clearly detectable in the mitochondrial lysates but was not observed on any occasion in clean nuclear extracts. A potential precursor form of the endogenous protein was not observed on any occasion in the nuclear fraction. In fact, like most inducible systems, the cell-culture

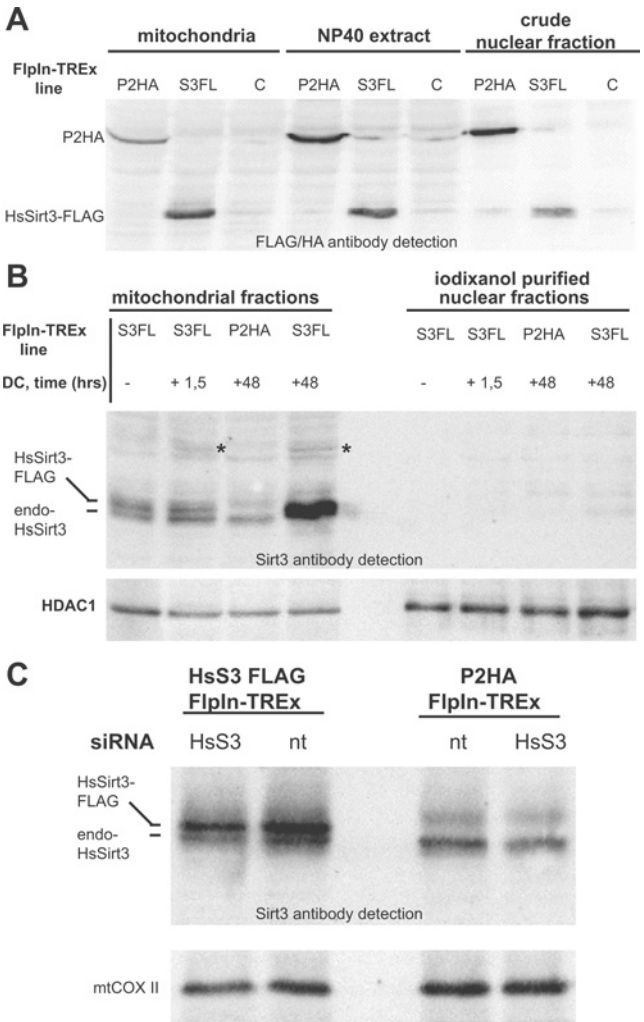


**Figure 2 The precursor and processed form of overexpressed HsSIRT3, as well as endogenous HsSIRT3, is exclusively mitochondrial**

(**A**) HEK-293 FlpIn-TREx cells were induced for 2 days with 5 ng/ml doxycyclin to overexpress either HsSIRT3–FLAG (S3FL), POLG2–HA (P2HA) or nothing and a crude mitochondrial fraction was prepared, the low-speed 'nuclear' pellet obtained after hypotonic lysis was first extracted with a small volume of Nonidet P40 lysis buffer (NP40 extract) and the resulting pellet of this NP40 extract was subjected to high-salt extraction (nuclear fraction). The results illustrate the problem of obtaining a clean nuclear extract using this crude isolation procedure as even the well-established mitochondrial POLG2 protein is found in all fractions: any conclusions based on this method regarding potential nuclear localization of proteins are unwarranted. (**B**) Purification of mitochondrial fractions by hypotonic lysis and subsequent nuclear fractionation using an iodixonal step-gradient. Indicated cell lines were non-induced (−) or induced (+) with 5 ng/ml doxycyclin (DC) for the indicated time in hours. Equivalent amounts of the starting material for the mitochondrial and nuclear fraction were loaded in each lane on to a single gel. Membranes were probed with various antibodies starting with the Santa Cruz HsSIRT3 polyclonal antibody. Indicated are mature HsSIRT3–FLAG and endogenous HsSIRT3 (based on the experiment shown in **C**) and based on their mobility which was just below a 30 kDa marker band. The asterisk indicates the HsSIRT3–FLAG precursor protein that was observed at variable levels in mitochondrial fractions and with various induction levels and times. A short 1.5 h induction also showed this precursor in the mitochondrial fraction but not in the nuclear fraction even upon long exposure of the membranes (results not shown). These results are in clear contradiction with published results [20] and do not show any evidence of nuclear HsSIRT3–FLAG or of endogenous HsSIRT3 in cells that weakly or do not at all overexpress HsSIRT3–FLAG (lanes labelled P2HA). (**C**) HsSIRT3 siRNA (HsS3) or non-targeting siRNA (nt) had the desired effect of reducing both the overexpressed HsSIRT3–FLAG protein and the tentatively assigned endogenous HsSIRT3 band both in HsSIRT3–FLAG and in P2HA expressing HEK-293 FlpIn-TREx cells. The knockdown effect was confirmed by reprobing the membrane for a mitochondrial marker protein mtCOXII. Observed knockdown after 48 h was typically 30–40 %. In similar experiments, the same siRNA oligonucleotides resulted in increased acetylation of overexpressed AceCS2–FLAG compared with nt-treated controls, as previously shown by others [10] (results not shown).

system used in the present study is slightly leaky resulting in steady-state HsSIRT3–FLAG in non-induced cells that is comparable with endogenous HsSIRT3 steady-state levels (see below). Non-induced cells that continuously express HsSIRT3–FLAG at very low levels did not show the HsSIRT3–FLAG precursor form in their mitochondrial (or nuclear) extracts, but only upon a short 1–1.5 h induction the precursor form became visible in the mitochondrial lysates but not in the nuclear lysates and without a visible increase in the processed form. These results show that the precursor is generally short-lived (not visible in the 'leaky' non-induced cells but visible after short induction) and mitochondrially targeted where it is further processed to yield the mature protein as previously suggested [6].

To demonstrate that the band tentatively assigned to the endogenous HsSIRT3 is indeed HsSIRT3, we treated cells with HsSIRT3 siRNA. Figure 2(C) shows that in cells overexpressing HsSIRT3–FLAG, siRNA treatment for 48 h had the desired effect of knocking down HsSIRT3–FLAG expression, albeit modestly. Furthermore, the same treatment in regular HEK-293 cells increased acetylation of AceCS2 as detected by an anti-acetyl lysine antibody, as previously described [10] (results not shown). Treatment of siRNA and subcellular fractionation followed by Western blot analysis showed that the assigned endogenous mitochondrial HsSIRT3 band was indeed HsSIRT3.

Combining the above results unequivocally demonstrates the mitochondrial localization of HsSIRT3 and suggests that processing of the full-length protein very probably takes place in the mitochondrion. There are various explanations for the discrepancy of our results with the previously published results [20]. First, as we have shown in the present study, the subcellular fractionation previously used to obtain a nuclear fraction was flawed in that any crude nuclear fraction derived from hypotonic lysis will still contain both whole cells and mitochondria. Furthermore, the use of an antibody marker to detect a mitochondrial membrane protein is not appropriate to exclude contamination from the nuclear high-salt extract. Secondly, the previous paper relied heavily on an antibody that was specific for the N-terminus of HsSIRT3 but the specificity of that antibody for HsSIRT3 was not adequately demonstrated and various appropriate immunofluorescence controls were lacking. For example, an HsSIRT3 siRNA experiment to demonstrate a reduction in or complete loss of the nuclear fluorescent signal assumed to be from the precursor form of HsSIRT3 was not shown. Finally, some of the images that appear to suggest nuclear retention of signal upon LMB treatment could be explained by clustering of a mitochondrial signal around and on top of the nucleus.

One of the premises to suggest that HsSIRT3 behaves differently has been the absence of an N-terminal extension in the predicted mouse SIRT3 protein [20,29,30], i.e. the mouse protein has been predicted to start at the methionine residue equivalent to human $Met^{143}$. Since the human and mouse protein are very highly conserved from $Met^{143}$ onward and we have not seen any evidence of mitochondrial localization of a truncated human variant starting at $Met^{143}$ (Figure 1D) we questioned the original mouse protein prediction and its localization [29,30]. In addition both the human and mouse proteins when starting at $Met^{143}$ have a very poor mitochondrial targeting prediction. For these reasons we searched the mouse genome initially using the mouse cDNA sequence coding for the 29 kDa SIRT3. This analysis using the *ab initio* RNA database yielded several predicted mRNAs from the Celera mouse genome (the sequence is provided in Supplementary Figure 1 at http://www.BiochemJ.org/bj/411/bj4110279add.htm) that when translated would give a larger protein more compatible with the full-length human protein. Using this prediction we looked for confirmation in the EST (expressed sequence tag) databases by using the 5′ end of the cDNA up to and including the equivalent of the human $Met^{143}$ codon. This confirmed that the predicted mRNAs that would code for a larger mouse SIRT3 protein do exist *in vivo* (as also shown in Supplementary Figure 1). It should be noted here that the larger protein variant was originally also predicted by Yang et al. [29] but was discarded on the basis of it being rare and on a poor alignment with the predicted full-length human protein. For reasons unknown, this alignment did not take into consideration the possibility of large gaps. Instead it was proposed that the major SIRT3 mRNA in mouse would be created by an eight nucleotide extension to the mRNA derived from the 5′ end of exon 2. ESTs that agree with this can indeed be found in abundance, but curiously the intron–exon boundary resulting from the eight nucleotide extension of exon 2 of mouse SIRT3 is less a consensus boundary than is the one without this extension. Since the SIRT3 genomic region is gene-dense we suggest that the abundant ESTs with the eight nucleotide extension result from (pre)-mRNA of the gene adjacent to mouse SIRT3, coding for a 26S proteasomal subunit and transcribed in the opposite orientation.

When we searched for protein homologues using our prediction for the mouse full-length protein the best hits were with various predicted mammalian SIRT3 proteins such as those from horse, pig and cow. Sequence alignment of these proteins showed an excellent alignment (Figure 3), with all proteins having a predicted N-terminal stretch of 75–77 amino acids prior to the equivalent of human $Met^{143}$. In addition, all proteins had an excellent prediction for mitochondrial localization. Of the various proteins in the alignment, the mouse protein is the only one to have a second methionine residue 14 amino acids downstream of the first methionine residue that we assign in the present study as $Met^{1}$. Further experiments are required to test whether $Met^{1}$ or the downstream methionine ($Met^{15}$) is preferentially used.

In conclusion, based on experimental data we show in the present study the unambiguous and exclusive localization of HsSIRT3 in mitochondria. In addition, based on the reanalysis of the mouse SIRT3 gene and transcripts we suggest that mouse SIRT3 has an N-terminal mitochondrial targeting sequence similar to that predicted for other mammals, but shorter than the human protein. This is supported by the observation that a truncated human protein that starts at the previously predicted mouse N-terminus is not mitochondrially targeted despite a high degree of similarity with the mouse protein from this residue onwards. Nevertheless, the endogenous mouse protein has been demonstrated unequivocally to be mitochondrial [12]. Our results greatly simplify various ambiguous published results relating to the function of the SIRT3 protein and should help in clarifying its potential roles in metabolism. First, based on data from the present study, there is no support for a nuclear function of HsSIRT3. Secondly, the effects of mouse SIRT3 overexpression on, for example, PGC1$\alpha$ (peroxisome-proliferator-activated receptor $\gamma$ co-activator 1$\alpha$) in brown adipocytes [30] is probably an artefact caused by the overexpression of a truncated mouse SIRT3 that is targeted not to mitochondria but to the cytoplasm. Although Shi et al. [30] did show apparent co-localization with the mitochondrial dye Mitotracker®, this appears to be an experimental artefact, possibly caused by severe overexpression, since the Mitotracker® staining does not actually show a typical mitochondrial network as normally seen with mouse 3T3 cells that were used in that study. Finally, as an additional cautionary note, the HDAC7 antibody used in the present study was identical with the antibody used by Bakin et al. [21], who suggested a mitochondrial localization of HDAC7. Our immunofluorescence results in U2OS cells (Figure 1, B1–B2) and similar results obtained using C4-2 cells (results not shown) showed nuclear/cytoplasmic localization

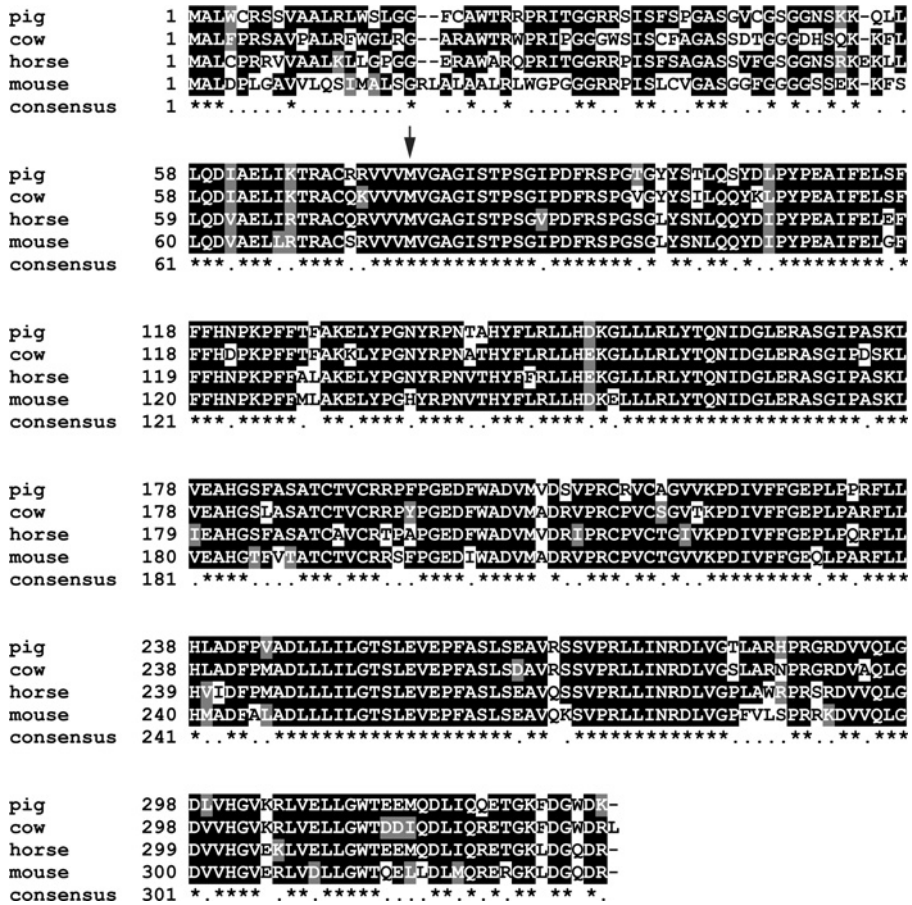


**Figure 3 The predicted mouse SIRT3 is highly similar to the predicted proteins from cow, pig and horse**

The predicted mouse SIRT3 protein based on the predicted cDNA sequence in Supplementary Figure 1 (at http://www.BiochemJ.org/bj/411/bj4110279add.htm) was BLASTp searched against the non-redundant NCBI protein database (http://www.ncbi.nlm.nih.gov/blast/Blast.cgi). A multiple sequence alignment (using the ClustalW server at http://www.ebi.ac.uk/) is shown with the best-matching proteins predicted for horse (accession XP_001489390), pig (NP_001103527) and cow (XP_879073). The arrow indicates the methionine residue equivalent to HsSIRT3 $Met^{143}$. This is also the residue originally predicted to be the start of the mouse protein (for details see [20,29,30] and the main text). A multiple sequence alignment including the human and chicken proteins is shown in Supplementary Figure 2 (at http://www.BiochemJ.org/bj/411/bj4110279add.htm).

of HDAC7 and thus also seem to contradict this previous report. In addition, when we expressed in various cell lines an HDAC7–FLAG variant of essentially the same sequence as reported [21] we see the same nuclear/cytoplasmic pattern as observed with the endogenous protein and the same LMB responsiveness. Nevertheless, since in our opinion it is difficult to exclude fully a mitochondrial localization of at least a minor fraction of HDAC7 we are hesitant to exclude fully a mitochondrial role for this protein.

We would like to acknowledge Outi Kurronen and Merja Jokela (Institute of Medical Technology, Tampere, Finland) for their skilful technical assistance, Howy Jacobs (Institute of Medical Technology, Tampere, Finland), Anu Wartiovaara-Suomalainen and Brendan Battersby (Biomedicum, University of Helsinki, Helsinki, Finland) for many discussions, Sjoerd Wanrooij (currently at the Karolinska Institute, Stockholm, Sweden) for his help in creating the inducible HsSIRT3 and POLG2 cell lines and Fenne Koning (currently at the Faculty of Biology, University of Utrecht, Utrecht, The Netherlands) for the initial characterization of the HsSIRT3 siRNAs used in the present study. This research was financially supported by the Academy of Finland (Grants 110689, 103213 and CoE funding), the Sigfrid Juselius Foundation, Tampere University Hospital Medical Research Fund and the University of Tampere.

## REFERENCES

1 Strahl, B. D. and Allis, C. D. (2000) The language of covalent histone modifications. Nature **403**, 41–45

2 Marmorstein, R. (2001) Protein modules that manipulate histone tails for chromatin regulation. Nat. Rev. Mol. Cell Biol. **2**, 422–432

3 Marmorstein, R. (2001) Structure of histone deacetylases: insights into substrate recognition and catalysis. Structure **9**, 1127–1133

4 Kouzarides, T. (2000) Acetylation: a regulatory modification to rival phosphorylation? EMBO J. **19**, 1176–1179

5 Freiman, R. N. and Tjian, R. (2003) Regulating the regulators: lysine modifications make their mark. Cell **112**, 11–17

6 Schwer, B., North, B. J., Frye, R. A., Ott, M. and Verdin, E. (2002) The human silent information regulator (Sir)2 homologue hSIRT3 is a mitochondrial nicotinamide adenine dinucleotide-dependent deacetylase. J. Cell Biol. **158**, 647–657

7 Onyango, P., Celic, I., McCaffery, J. M., Boeke, J. D. and Feinberg, A. P. (2002) SIRT3, a human SIR2 homologue, is an NAD-dependent deacetylase localized to mitochondria. Proc. Natl. Acad. Sci. U.S.A. **99**, 13653–13658

8 Michishita, E., Park, J. Y., Burneskis, J. M., Barrett, J. C. and Horikawa, I. (2005) Evolutionarily conserved and nonconserved cellular localizations and functions of human SIRT proteins. Mol. Biol. Cell **16**, 4623–4635

9 Kim, S. C., Sprung, R., Chen, Y., Xu, Y., Ball, H., Pei, J., Cheng, T., Kho, Y., Xiao, H., Xiao, L. et al. (2006) Substrate and functional diversity of lysine acetylation revealed by a proteomics survey. Mol. Cell **23**, 607–618

10 Schwer, B., Bunkenborg, J., Verdin, R. O., Andersen, J. S. and Verdin, E. (2006) Reversible lysine acetylation controls the activity of the mitochondrial enzyme acetyl-CoA synthetase 2. Proc. Natl. Acad. Sci. U.S.A. **103**, 10224–10229

11 Hallows, W. C., Lee, S. and Denu, J. M. (2006) Sirtuins deacetylate and activate mammalian acetyl-CoA synthetases. Proc. Natl. Acad. Sci. U.S.A. **103**, 10230–10235

12 Lombard, D. B., Alt, F. W., Cheng, H. L., Bunkenborg, J., Streeper, R. S., Mostoslavsky, R., Kim, J., Yancopoulos, G., Valenzuela, D., Murphy, A. et al. (2007) Mammalian Sir2 homolog SIRT3 regulates global mitochondrial lysine acetylation. Mol. Cell. Biol. **27**, 8807–8814
13 Haigis, M. C., Mostoslavsky, R., Haigis, K. M., Fahie, K., Christodoulou, D. C., Murphy, A. J., Valenzuela, D. M., Yancopoulos, G. D., Karow, M., Blander, G. et al. (2006) SIRT4 inhibits glutamate dehydrogenase and opposes the effects of calorie restriction in pancreatic $\beta$-cells. Cell **126**, 941–954
14 Ahuja, N., Schwer, B., Carobbio, S., Waltregny, D., North, B. J., Castronovo, V., Maechler, P. and Verdin, E. (2007) Regulation of insulin secretion by SIRT4, a mitochondrial ADP-ribosyltransferase. J. Biol. Chem. **282**, 33583–33592
15 Guarente, L. (2006) Sirtuins as potential targets for metabolic syndrome. Nature **444**, 868–874
16 Haigis, M. C. and Guarente, L. P. (2006) Mammalian sirtuins: emerging roles in physiology, aging, and calorie restriction. Genes Dev. **20**, 2913–2921
17 Lagouge, M., Argmann, C., Gerhart-Hines, Z., Meziane, H., Lerin, C., Daussin, F., Messadeq, N., Milne, J., Lambert, P., Elliott, P. et al. (2006) Resveratrol improves mitochondrial function and protects against metabolic disease by activating SIRT1 and PGC-1$\alpha$. Cell **127**, 1109–1122
18 Gerhart-Hines, Z., Rodgers, J. T., Bare, O., Lerin, C., Kim, S. H., Mostoslavsky, R., Alt, F. W., Wu, Z. and Puigserver, P. (2007) Metabolic control of muscle mitochondrial function and fatty acid oxidation through SIRT1/PGC-1$\alpha$. EMBO J. **26**, 1913–1923
19 Yang, H., Yang, T., Baur, J. A., Perez, E., Matsui, T., Carmona, J. J., Lamming, D. W., Souza-Pinto, N. C., Bohr, V. A., Rosenzweig, A. et al. (2007) Nutrient-sensitive mitochondrial $NAD^+$ levels dictate cell survival. Cell **130**, 1095–1107
20 Scher, M. B., Vaquero, A. and Reinberg, D. (2007) SirT3 is a nuclear $NAD^+$-dependent histone deacetylase that translocates to the mitochondria upon cellular stress. Genes Dev. **21**, 920–928
21 Bakin, R. E. and Jung, M. O. (2004) Cytoplasmic sequestration of HDAC7 from mitochondrial and nuclear compartments upon initiation of apoptosis. J. Biol. Chem. **279**, 51218–51225
22 Wanrooij, S., Goffart, S., Pohjoismaki, J. L., Yasukawa, T. and Spelbrink, J. N. (2007) Expression of catalytic mutants of the mtDNA helicase Twinkle and polymerase POLG causes distinct replication stalling phenotypes. Nucleic Acids Res. **35**, 3238–3251
23 Malka, F., Auré, K., Goffart, S., Spelbrink, J. N. and Rojo, M. (2007) The mitochondria of cultured mammalian cells. I. Analysis by immunofluorescence microscopy, histochemistry, subcellular fractionation and cell fusion. In Mitochondria Practical Protocols, vol. 372 (Leister, D. and Herrmann, J.M., eds), pp. 3–16, Humana Press
24 Goffart, S., Martinsson, P., Malka, F., Rojo, M. and Spelbrink, J. N. (2007) The mitochondria of cultured mammalian cells. II. Expression and visualization of exogenous proteins in fixed and live cells. In Mitochondria Practical Protocols, vol. 372 (Leister, D. and Herrmann, J.M., eds), pp. 17–32, Humana Press
25 Garrido, N., Griparic, L., Jokitalo, E., Wartiovaara, J., Van Der Bliek, A. M. and Spelbrink, J. N. (2003) Composition and dynamics of human mitochondrial nucleoids. Mol. Biol. Cell **14**, 1583–1596
26 Dingham, J. D., Lebovitz, R. M. and Roeder, R. G. (1983) Accurate transcription initiation by RNA polymerase II in a soluble extract from isolated mammalian nuclei. Nucleic Acids Res. **11**, 1475–1489
27 Spelbrink, J. N., Toivonen, J. M., Hakkaart, G. A., Kurkela, J. M., Cooper, H. M., Lehtinen, S. K., Lecrenier, N., Back, J. W., Speijer, D., Foury, F. and Jacobs, H. T. (2000) *In vivo* functional analysis of the human mitochondrial DNA polymerase POLG expressed in cultured human cells. J. Biol. Chem. **275**, 24818–24828
28 Kao, H.-Y., Verdel, A., Tsai, C.-C., Simon, C., Juguilon, H. and Khochbin, S. (2001) Mechanism for nucleocytoplasmic shuttling of histone deacetylase 7. J. Biol. Chem. **276**, 47496–47507
29 Yang, Y. H., Chen, Y. H., Zhang, C. Y., Nimmakayalu, M. A., Ward, D. C. and Weissman, S. (2000) Cloning and characterization of two mouse genes with homology to the yeast Sir2 gene. Genomics **69**, 355–369
30 Shi, T., Wang, F., Stieren, E. and Tong, Q. (2005) SIRT3, a mitochondrial Sirtuin deacetylase, regulates mitochondrial function and thermogenesis in brown adipocytes. J. Biol. Chem. **280**, 13560–13567
31 Kaguni, L. S. (2004) DNA polymerase $\gamma$, the mitochondrial replicase. Annu. Rev. Biochem. **73**, 293–320

Received 30 November 2007/21 January 2008; accepted 23 January 2008
Published as BJ Immediate Publication 23 January 2008, doi:10.1042/BJ20071624

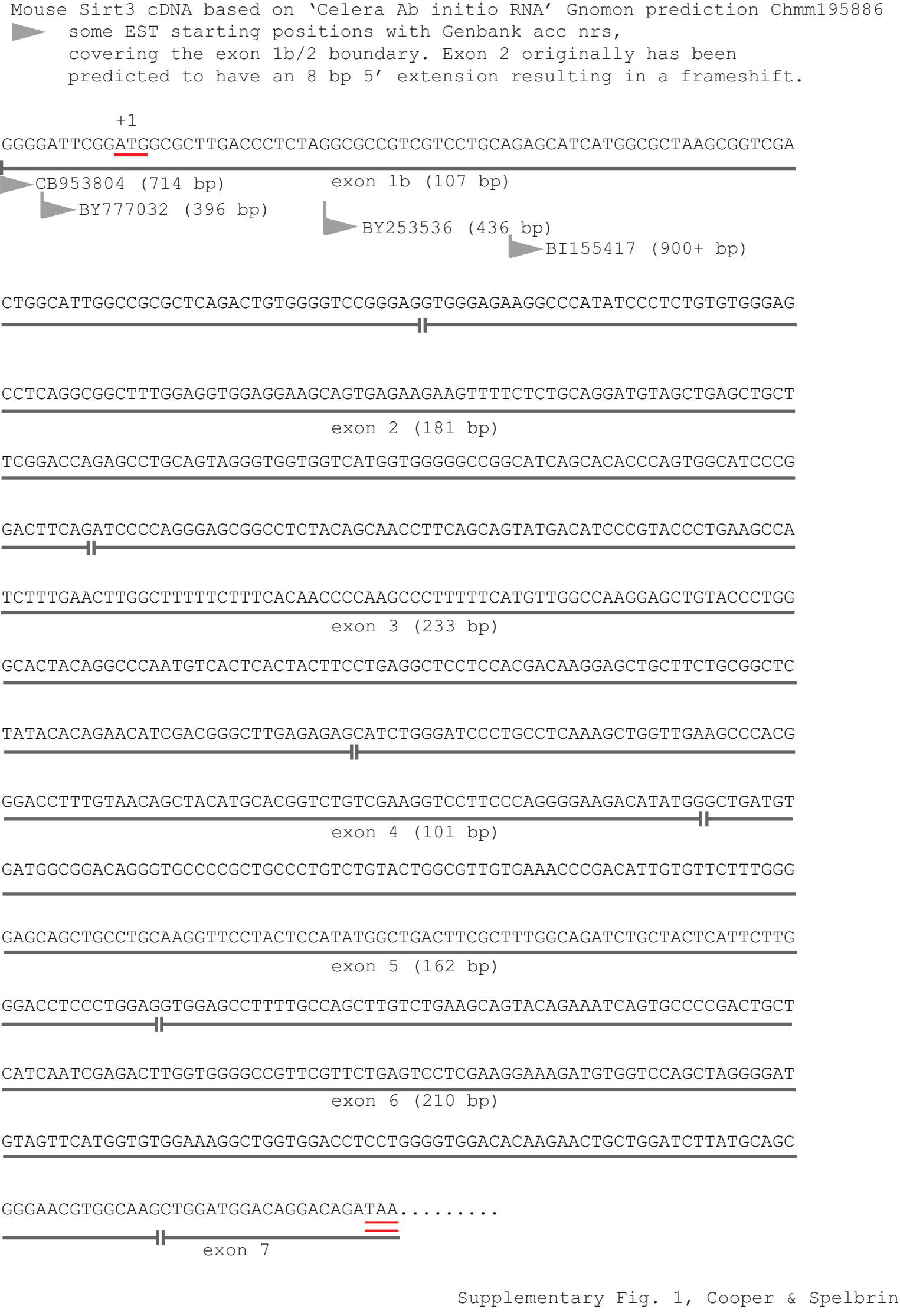


Supplementary Fig. 1, Cooper & Spelbrink

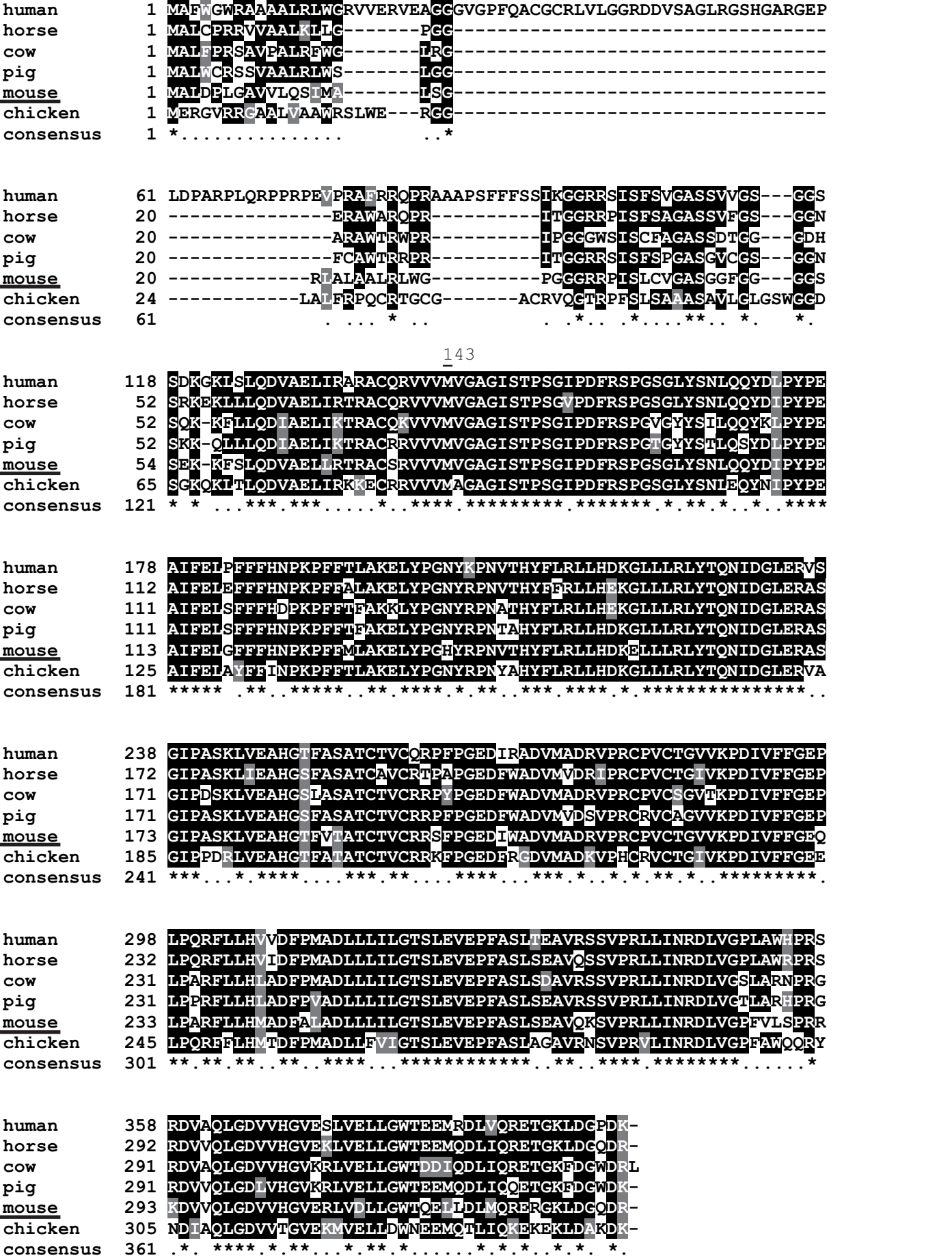


Supplementary Fig. 2, Cooper & Spelbrink

*Human Molecular Genetics, 2009, Vol. 18, No. 2* **328–340**
*doi:10.1093/hmg/ddn359*
*Advance Access published on October 29, 2008*

# Twinkle mutations associated with autosomal dominant progressive external ophthalmoplegia lead to impaired helicase function and *in vivo* mtDNA replication stalling

**Steffi Goffart[1], Helen M. Cooper[1], Henna Tyynismaa[2,3], Sjoerd Wanrooij[1,†], Anu Suomalainen[2,3] and Johannes N. Spelbrink[1,*]**

[1]Institute of Medical Technology and Tampere University Hospital, Biokatu 6, 33014, Tampere, Finland, [2]Research Program of Molecular Neurology, Biomedicum-Helsinki, University of Helsinki, Helsinki, Finland and [3]Department of Neurology, Helsinki University Central Hospital, Helsinki, Finland

Received September 19, 2008; Revised and Accepted October 27, 2008

**Mutations in the mitochondrial helicase Twinkle underlie autosomal dominant progressive external ophthalmoplegia (PEO), as well as recessively inherited infantile-onset spinocerebellar ataxia and rare forms of mitochondrial DNA (mtDNA) depletion syndrome. Familial PEO is typically associated with the occurrence of multiple mtDNA deletions, but the mechanism by which Twinkle dysfunction induces deletion formation has been under debate. Here we looked at the effects of Twinkle adPEO mutations in human cell culture and studied the mtDNA replication in the Deletor mouse model, which expresses a dominant PEO mutation in Twinkle and accumulates multiple mtDNA deletions during life. We show that expression of dominant Twinkle mutations results in the accumulation of mtDNA replication intermediates in cell culture. This indicated severe replication pausing or stalling and caused mtDNA depletion. A strongly enhanced accumulation of replication intermediates was evident also in six-week-old Deletor mice compared with wild-type littermates, even though mtDNA deletions accumulate in a late-onset fashion in this model. In addition, our results in cell culture pointed to a problem of transcription that preceded the mtDNA depletion phenotype and might be of relevance in adPEO pathophysiology. Finally, *in vitro* assays showed functional defects in the various Twinkle mutants and broadly agreed with the cell culture phenotypes such as the level of mtDNA depletion and the level of accumulation of replication intermediates. On the basis of our results we suggest that mtDNA replication pausing or stalling is the common consequence of Twinkle PEO mutations that predisposes to multiple deletion formation.**

## INTRODUCTION

Mitochondrial diseases manifest with a broad spectrum of symptoms but frequently involve skeletal muscle and/or the nervous system. Diseases with mitochondrial DNA (mtDNA) mutations are quite frequent, with prevalences of ~1:11 000 in North-Eastern England (1) and 1:6000 for a single-point mutation A3243G in Finland (2). mtDNA disease can be split into two groups. A first group comprises diseases caused by primary mtDNA mutations that lead to impairment of respiratory function. A second group is often referred to as mtDNA maintenance diseases, as the underlying cause is a dysfunction of the replication and maintenance machinery of mtDNA, encoded by nuclear genes, that leads to a secondary loss or damage of the mitochondrial genome and subsequent mitochondrial dysfunction. These disorders have also been

*To whom correspondence should be addressed Tel: +358 335518598; Fax: +358 335517710; Email: hans.spelbrink@uta.fi
†Present address: Department of Medical Biochemistry and Cell Biology, Göteborg University, Göteborg, Sweden.

shown to be common in the population, with carrier frequencies for single mutations reaching 1:100 in some populations (3,4). The most severe examples of mtDNA maintenance dysfunction are early-onset, recessively inherited syndromes characterized by severe mtDNA depletion in one or more tissues, such as the Alpers-Huttenlocher syndrome associated with mutations in the mtDNA polymerase gamma catalytic subunit POLG1 (5,6). In contrast, autosomal progressive external ophthalmoplegia (PEO) is late-onset form of mtDNA maintenance disease. It affects mainly the function of skeletal muscles, initiating with weakness of the extra-ocular muscles during adulthood. Patients with autosomal PEO do not typically show loss of mtDNA in tissues analyzed (7–9). Instead, large deletions of mtDNA accumulate in post-mitotic tissues over time and the appearance of a considerable amount of deletions is associated with the onset and progression of symptoms (9).

Several essential proteins for mtDNA maintenance have been described and characterized. The mitochondrial polymerase gamma (PolG) functions as a heterotrimer consisting of a catalytic alpha and two accessory beta subunits in mammals (10,11). Polymerase gamma is assumed to be the replicative polymerase in mitochondria. Mutations in the alpha subunit cause mtDNA depletion syndromes (MDS) like Alpers-Huttenlocher, SANDO (sensory-atactic neuropathy, dysarthria and ophthalmoplegia) or MIRAS (mitochondrial recessive ataxia syndrome) (3,12), but are also associated with recessive and sporadic forms of PEO (13–15). Only one mutation of the beta subunit associated with PEO has been described to date (16). Twinkle, a hexameric DNA helicase of the RecA superfamily (17,18), is thought to be the replicative helicase of mtDNA, as it functions together with PolG and single-stranded DNA binding protein (mtSSB) in a minimal mtDNA replisome (19), while catalytic mutations or RNAi cause mtDNA depletion (20–22) in human and insect cell culture. To date and to our knowledge, 23 mutations in the Twinkle gene (PEO1) have been shown to be associated with PEO, and PEO1 mutations were recently shown to be the most prevalent cause of adPEO in Italy (18,23). A single recessive mutation (Y508C) has been uniquely identified in Finland and associates with infantile onset spinocerebellar ataxia. The same mutation was recently identified in a compound heterozygous configuration with a A318T mutation in two siblings with a severe MDS (24). A second recessive T457I mutation was identified homozygous in a family with MDS (25).

While MDS might be caused by a complete impairment of replication due to a non-functional component of the replication machinery, the precise molecular mechanism(s) for the creation and slow accumulation of mtDNA deletions in PEO is unknown. The Deletor mice, expressing an adPEO mutation, a 13 amino acid duplication in the Twinkle linker region equivalent to human amino acid 352–364, accumulate substantial amounts of mtDNA deletions in the skeletal muscle and show similar histological features as the human patients, but are functionally only mildly affected (26). This mouse clearly proves that impaired Twinkle function is the underlying cause of mtDNA deletions and respiratory chain dysfunction and provides an excellent tool to study disease progression. However, studies focusing in the actual molecular mechanism of mtDNA deletion formation is hindered by the fact that the deletions accumulate only slowly *in vivo*. In this study, we therefore used cultured human cells to study the effects of different Twinkle PEO mutations on mtDNA replication. We show that PEO mutations impair the helicase activity of Twinkle and lead to mtDNA replication stalling or pausing and reduced mitochondrial transcript levels. Similarly, already in young Deletor mouse tissues, we observed accumulation of replication intermediates, indicative of pausing. Since mtDNA deletions in the Deletor model accumulate only in a late-onset fashion, this could suggest that early problems in mtDNA replication predispose to the accumulation of deletions later in life. We hypothesize that the accumulation of replication intermediates can mediate an enhanced formation of mtDNA deletions allowing for their later accumulation in adult tissues in PEO patients.

## RESULTS

### Expression of dominant Twinkle PEO mutations in proliferating cells leads to mtDNA depletion

In order to study the effect of Twinkle mutations found in patients suffering from adPEO in a reduced cell model, we established stable HEK293 Flp-In™ T-REx™ cell lines expressing human Twinkle variants containing a C-terminal Myc-His tag. This system has the advantage of allowing controllable expression of transgenes in a proliferating human cell background, and as the endogenous Twinkle gene is unaffected, resembles under conditions of low induction, the heterozygous situation in patients with PEO (22).

Seven adPEO-related mutations of Twinkle causing mild to severe symptoms were chosen, including several mutations in the linker region of Twinkle (dup352–364, A359T, S369P, R374Q), two mutations located in the N-terminal domain in close proximity to the linker region (W315L, K319E) and one mutation in the helicase domain (W474C) (see Fig. 1A for an overview). All mutations showed expression levels comparable to transgenic wild-type Twinkle-Myc-His, and overexpression could be modulated in a range from 1- to 20-fold over the endogenous wild-type Twinkle (Fig. 1B, and not shown). Overexpression of wild-type Twinkle resulted in a slight but statistically significant copy-number increase, as previously observed (22). In contrast, depletion of mtDNA levels was observed after expression of all adPEO mutations after thee days (Fig. 2A). The level of depletion depended on the mutation. The point mutations K319E located at the end of the N-terminal domain as well as the R374Q mutation in the linker region reduced mtDNA levels to 25% within three days, indicating the complete absence of successful replication. Expression of the 13 amino acid duplication within the linker region also depleted mtDNA levels more than half, while the remaining mutants caused a less severe drop of mtDNA copy-number to 60–76%. None of the mutants caused an increase of mtDNA copy-number when expressed for several days, but for the milder mutations S369P and A359T an initial increase in mtDNA levels after one to two days of expression could sometimes be observed.

Interestingly, mtDNA transcript levels were also affected by Twinkle mutations (Fig. 2B). After two days of overexpression,

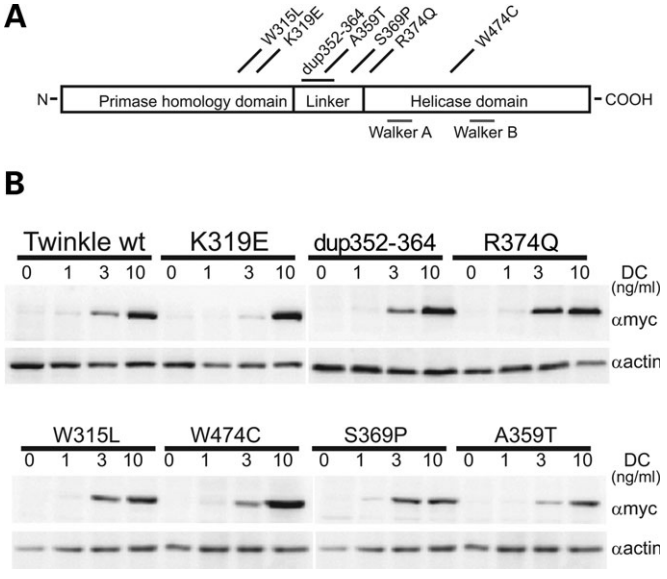


**Figure 1.** Expression of Twinkle adPEO mutations in HEK293 Flp-In$^{TM}$ T-REx$^{TM}$ cells. (**A**) Schematic presentation of the human Twinkle protein and localization of the adPEO-related mutations investigated in this study. Most mutations are located at the end of the N-terminal domain or in the linker region of Twinkle, only the W474C point mutation lies within the helicase domain. (**B**) Expression levels of adPEO Twinkle variants. Expression was induced for three days with the indicated amounts of doxycycline (DC) and protein expression was analyzed by western blot analysis against the myc-tagged Twinkle variants. At 1 ng/ml DC no increase in transgene expression could be observed, although mild effects on mtDNA replication were already detectable (data not shown). Maximal expression was reached with 10 ng/ml DC.

steady-state transcript levels of all analyzed H-strand transcripts were strongly reduced. The reduction of H-strand transcripts was stronger than the observed mtDNA copy-number depletion after two days of expression (Fig. 2A), indicating that the negative effect of Twinkle dysfunction on transcription precedes the depletion of mtDNA and is not due to reduced mtDNA template levels. The reduction in mitochondrial transcript levels appeared to cause a deficiency of mitochondrial respiration indicated by increased acidification of the cell culture medium (not shown).

## adPEO mutations affect nucleoid structure

The mtDNA nucleoids in cells overexpressing Twinkle variants for three days were visualized using immunocytochemistry against DNA and the Twinkle protein tag. Twinkle wild-type and W315L (Fig. 3 and Supplementary Material, Fig. S2) co-localized with mtDNA in a pattern of small punctate structures that we have previously found to constitute mtDNA nucleoids (27). The Twinkle variants K319E, R374Q and dup352–364, and A359T to a lesser extent, showed a more uniform mitochondrial matrix staining, but clearly also nucleoid-like spots based on their co-localization with mtDNA. The nucleoids in the K319E, R374Q, W474C and dup352–364 expressing cell lines appeared larger in size and fewer in number compared with wild-type. Finally, the S369P mutation co-localized well with mtDNA similar to W315L. Based on the mtDNA antibody, the number of mtDNA foci

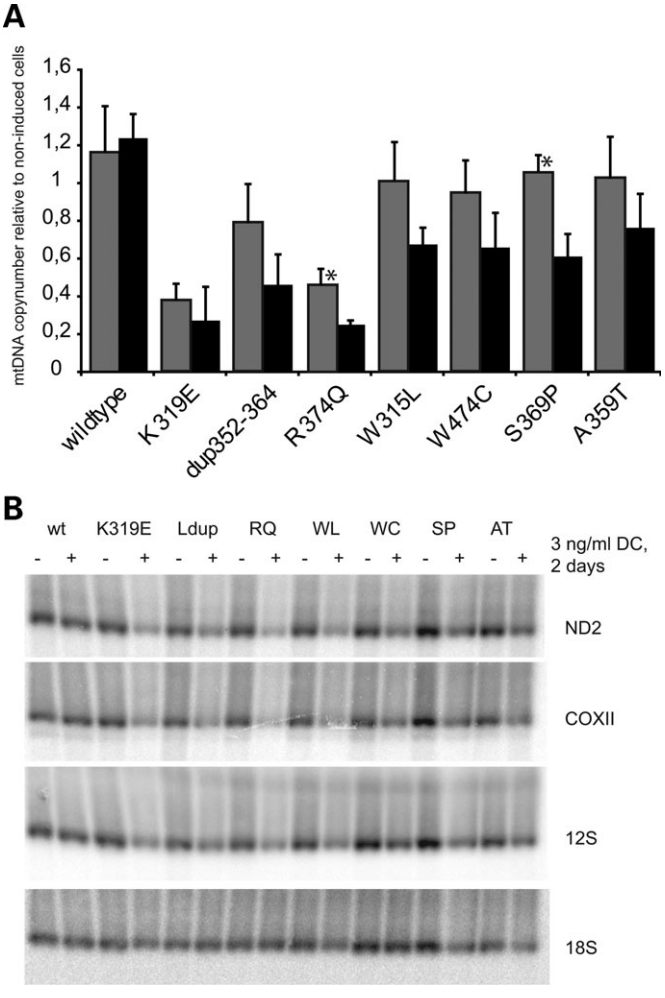


**Figure 2.** Mutant expression causes rapid mtDNA copynumber and transcript level depletion. (**A**) While overexpression of wild-type Twinkle transiently increased the relative copynumber of mtDNA per cell, expression of adPEO variants lead to rapid mtDNA depletion. The loss of mtDNA correlated approximately with the severity of the biochemical and replication defects measured in this study. MtDNA levels of cells induced with 3 ng/ml doxycycline for two days (grey bars) or three days (black bars) were quantified by duplex Taqman PCR and normalized to non-induced cells of the same cell line. Four to six independently isolated samples were measured in triplicate with the exception of the two samples indicated with an asterisk that were isolated twice and measured in triplicate. Similar results were obtained by Southern blot analysis (not shown). Error bars show the standard deviation. (**B**) Also the steady-state levels of mtDNA transcripts were decreased upon Twinkle mutant expression, while the overexpression of wild-type Twinkle and the resulting mtDNA increase did not change transcript levels. RNA from cells grown for two days with or without 3 ng/ml DC was analysed by Northen blot using probes against several mitochondrial transcripts as indicated and 18S rRNA. Note that the decrease in transcripts occurred in advance of mtDNA depletion (Fig. 2A). No effect on protein levels of representative, nuclear encoded, respiration complex subunits were detected by western blot analysis after 3 days (data not shown). Ldup refers to dup352–364.

seemed normal in cells overexpressing W315L and A359T or even increased for S369P. All the other mutations lead to a reduced number of spots, which could be expected from the copy-number determination of these mutants. Based on the observed effects we have categorized the severity of the nucleoid phenotype as mild for mutants showing no or a

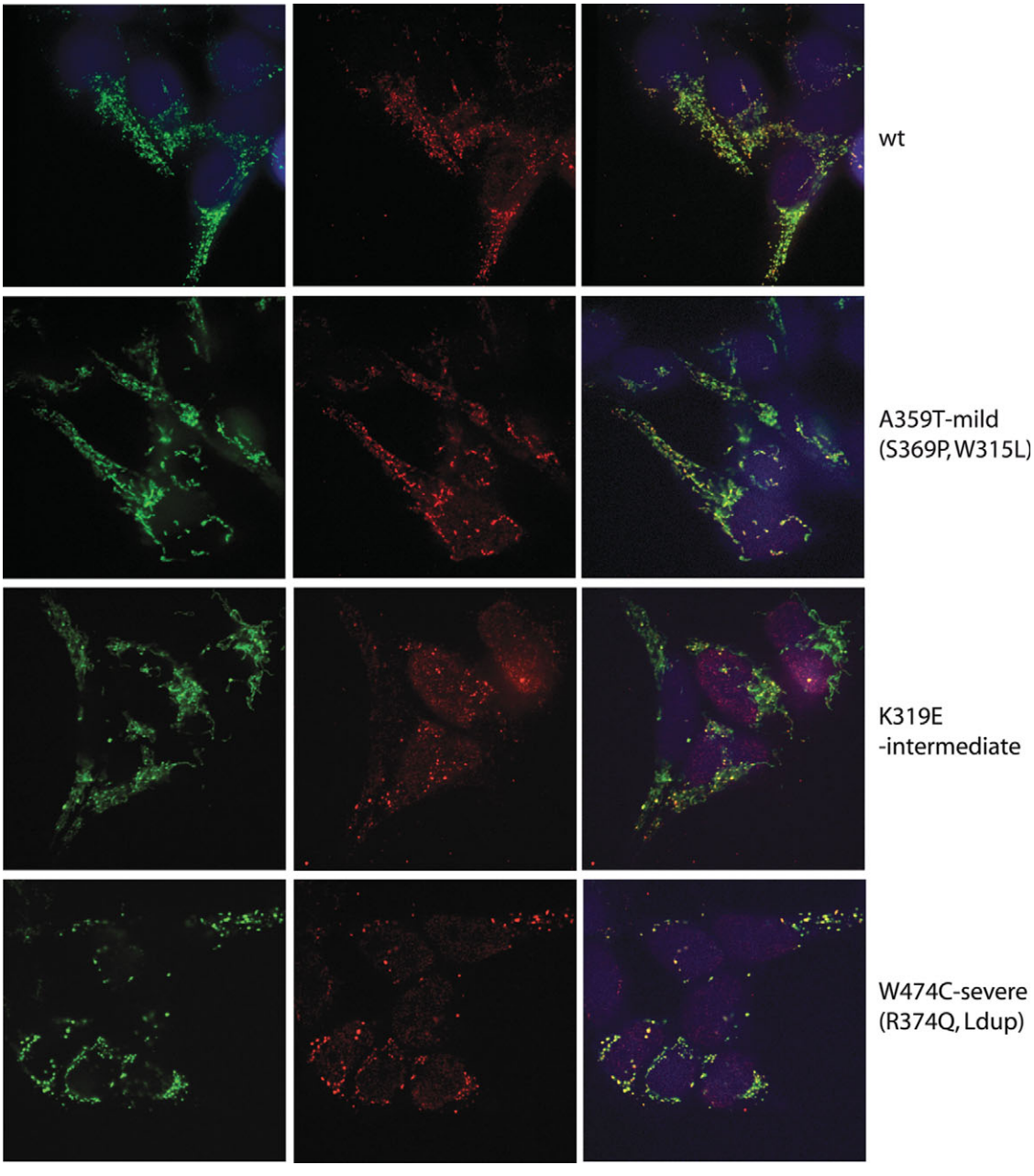


**Figure 3.** Some adPEO Twinkle mutants alter the localization of the protein in mtDNA nucleoids. The subcellular localization of the Twinkle variants was determined by immunofluorescence. While wild-type Twinkle co-localized with mtDNA in punctate nucleoids within mitochondria, the disease variants K319E Twinkle variants localized only partially with nucleoids, a proportion of the protein was diffusely localized in the mitochondrial lumen, while the nucleoids often appeared enlarged (similar results were observed with the R374Q and dup 352–364 mutants; Supplementary Material, Fig. S2). The W474C variant caused aggregation of nucleoids without a more diffuse distribution of the protein, while the A359T mutation decreased the Twinkle localization in nucleoids without altering their size and number extensively. The effects of expression of the various mutants were categorized as mild, moderate and severe as indicated in the Figure. Cells were induced with 3 ng/ml doxycycline for 3 days, immunocytochemistry was performed using specific antibodies against the myc-tagged Twinkle variants (green) and DNA (red). Images were taken with the same settings for exposure, laser intensity, etc. and in addition were processed for brightness and contrast in the same manner. All mutants are shown in Supplementary Material, Fig. S2.

limited effect on nucleoid structure and number based on the mtDNA immunofluorescence (A359T, W315L, S369P), moderate (K319E) and severe (R374Q, dup352–364, W474C) and show one example each in Figure 3, A359T, K319E and W474C respectively, while all mutants are shown in Supplementary Material, Fig. S2. Particularly interesting is the observation that especially for the Dup 352–364 and the W474C one can observe a mosaic pattern of cells with some cells being devoid entirely of the strong mtDNA positive foci, whereas other cells of the same culture still showed nucleoid structures. As the cell line used ensures single insertion of the transgene in the genome and similar expression levels in all cells studied, this variability in cell phenotypes could be indicative of an mtDNA segregation defect.

### *In vitro* enzyme activities of mutated Twinkle are impaired

For *in vitro* assays, wild-type and mutant variants of Twinkle were purified from crude mitochondrial fractions with a single-step procedure using TALON® $Co^{2+}$ affinity resin (see also Materials and Methods). TALON affinity resin eluates were routinely checked using Coomassie staining (Supplementary Material, Fig. S1), and showed a high level of purification of the Twinkle protein using this single-step procedure. Specific activity of the wild-type Twinkle protein (specified as the concentration of Twinkle that gives 50% unwinding activity at a given substrate concentration) purified in this manner seems very similar to that observed with enzyme purified using a baculovirus expression system (28,29), although a precise comparison is not possible since we have used less DNA substrate and measured at 37°C compared with 32°C used by Korhonen *et al*. Using approximately 5-fold less M13 substrate we find 50% unwinding activity with ∼25 fmol of purified Twinkle, whereas Korhonen *et al*. reaches 50% unwinding activity at ∼1.2 pmol of purified Twinkle (28) and at slightly less than half that concentration in a later publication that used an improved protocol to purify the enzyme (29). Given that we used less substrate, our purified Twinkle is five to ten times more active which seems in very good agreement given that we measure the activity at 37°C and not at 32°C. For each repeat of the various *in vitro* assays, −80°C frozen aliquots were first re-analyzed by Coomassie staining to estimate the protein concentration of each sample using BSA as a standard, to ensure the same concentration of wild-type and mutant proteins were being used.

Twinkle is a low-processive helicase *in vitro* and alone can unwind only short stretches of up to 25 nucleotides. In our hands, the highest activity is achieved when 3 mM UTP is used as an energy source, but also ATP, GTP and dGTP can drive the unwinding reaction. As the natural concentrations of these nucleotides within mitochondria are not known, we measured the helicase activity of the wild-type Twinkle and the various mutants separately with all four nucleotides (Fig. 4A). All mutants had reduced unwinding activity compared with the wild-type protein. The helicase activity of K319E and R374Q was reduced to <20%with all nucleotides, consistent with the strong depletion observed with these mutants in cell culture. However, the Dup 352–364 mutant had ∼70% remaining helicase activity, when GTP was used as an energy source. The relative helicase activity was considerably lower with dGTP and UTP. The W315L and W474C mutations showed an ∼70% reduction in helicase activity irrespective of the nucleotide used. The S369P showed a considerable reduction in helicase activity despite its mild effect on mtDNA copy-number. The mutation with the smallest effect on mitochondrial copy-number, A359T, also had near to normal helicase activities.

As the nucleotide concentration of 3 mM is saturating and might conceal any alteration in nucleotide affinity in Twinkle, we measured helicase activities of some mutations with UTP, ATP and GTP over a broader range of nucleotide concentrations. While the unwinding activity was reduced gradually with reduced nucleotide concentrations, no mutant showed a clear change in nucleotide kinetics (not shown).

The binding of Twinkle to single-stranded DNA *in vitro* was evaluated by electromobility shift assay described recently by Farge *et al*. (30). (Fig. 4B). The G575D mutation affecting the DNA binding domain of Twinkle (22) was used as a control and gave <25% binding efficiency. Also the adPEO mutations K319E, dup352–364 and W315L had clearly reduced binding affinities, while no clear effect was seen with R374Q and A359T. As the only variant of those investigated, the S369P mutation increased the affinity to ssDNA by 50% compared with wild-type.

The majority of adPEO mutations are located close to or in the linker region of Twinkle. The homologous region in T7 was

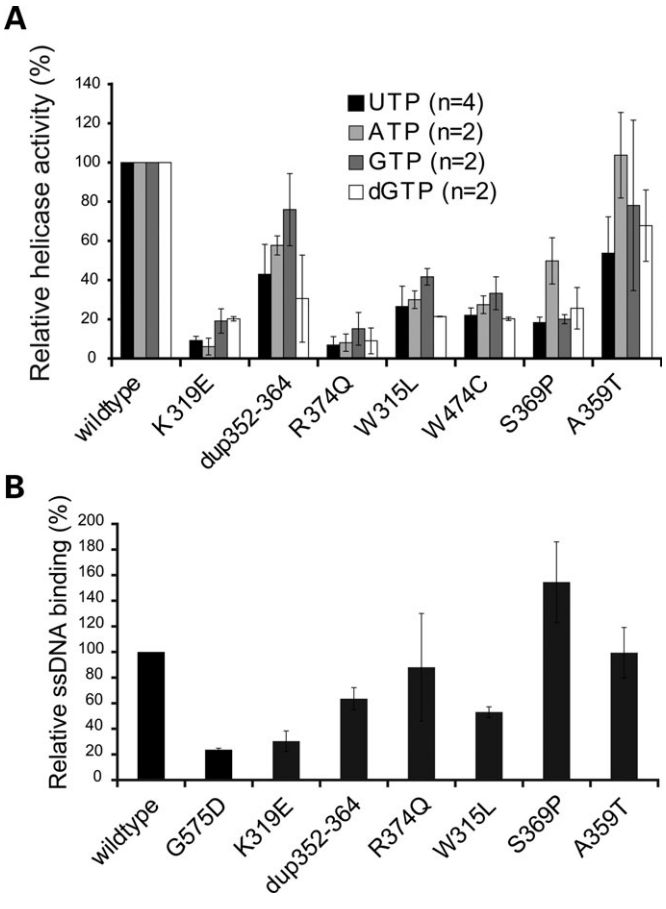


**Figure 4.** AdPEO mutations affect the unwinding and ssDNA binding activity of Twinkle. (**A**) Purified protein extracts of the various Twinkle mutations showed clearly reduced maximal unwinding activity in *in vitro* assays using an M13-based substrate. Most adPEO mutants had less than 25% remaining unwinding activity with UTP, while dup352–364 and A359T were around 50% active compared with wild-type protein ($P < 0.05$ for dup 352–364 and A359T, $P < 0.01$ for all others). Other nucleotides (ATP, GTP and dGTP) stimulated the unwinding activity of Twinkle to a lesser extend, but were giving approximately similar decreases for the mutants, only A359T exhibited full activity with ATP. (**B**) Twinkle ssDNA binding assays were performed essentially as described previously (30) (see also Materials and Methods). We used the G575D mutation previously described by us (22) as an additional control as this mutation was expected to have clearly reduced DNA affinity and indeed showed very poor binding even compared with the various adPEO Twinkle mutants. Of the adPEO mutants, K319E, dup352–364 and W315L showed reduced binding, whereas R374Q and A359T showed near normal ssDNA affinity. The S369P in our hands showed a moderately increased binding. Note that the W474C is not shown because this protein with several repeated isolations gave spurious results. Binding is expressed relative to the binding of the wild-type protein set at 100%.

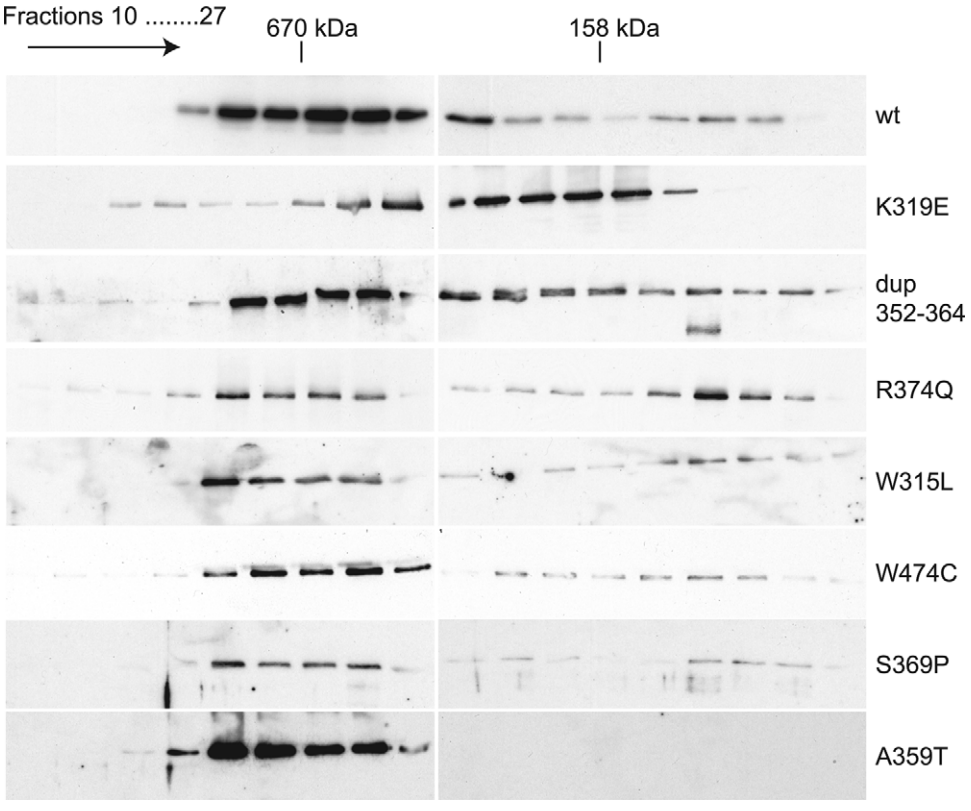


**Figure 5.** Some adPEO mutations decrease the stability of Twinkle hexamers. Gel filtration chromatography of purified Twinkle proteins indicated the formation of hexameric complexes in both wild-type and mutant proteins. The same results were obtained in the presence or absence of $Mg^{2+}$ ions and under salt conditions from 100 to 500 mM NaCl (data not shown). The partial delay and the extensive trailing during the chromatography run indicated the relative instability of the hexamers of K319E, R374Q and dup352–364. Following gel filtration all collected fractions were concentrated and analyzed by western blot analysis as detailed in Materials and Methods.

shown to be important for subunit interaction and formation of a functional hexamer (31). Therefore, to investigate whether also in Twinkle the reduction in helicase activity and DNA binding are caused by impaired oligomerization, we analyzed the multimeric state of Twinkle with isolated proteins *in vitro* using a similar chromatographic approach, as described previously (29). As already described by Farge *et al*. (30), wild-type Twinkle forms hexamers even under high ionic-strength conditions and in the absence of any nucleotide. Using similar conditions, all proteins bearing adPEO mutations formed hexamers, although differences in the degree of oligomerization could readily be detected. Wild-type Twinkle, A359T, W474C, W315L and S369P were mostly eluted at high molecular weight in agreement with normal multimer stability (Fig. 5). The R374Q, K319E and dup352–364 appeared less stable, but in all three cases high molecular weight multimers could still be detected. These results, as far as they involve the analysis of the same mutations, are largely in agreement with Korhonen *et al*. (29) (see Discussion). Similar results were obtained using glutaraldehyde crosslinking (not shown).

### Twinkle adPEO mutations cause mtDNA replication stalling in cell culture

As we described earlier, structural mutations that abolish the helicase activity of Twinkle affected replication of mtDNA in cultured cells and led to strong replication stalling and the accumulation of replication intermediates (22). To test whether the reduced helicase activity of Twinkle adPEO variants impaired mtDNA replication in a similar way, we analyzed the mtDNA replication pattern of cultured cells expressing wild-type and mutant Twinkle variants using two-dimensional DNA gel electrophoresis (Fig. 6). The expression of Myc-His-tagged wild-type Twinkle on top of the endogenous Twinkle levels did not influence the replication pattern or the abundance of replication intermediates except for one species of molecules believed to be part of the termination process in the non-coding region of mtDNA (22). In contrast, a strong effect was visible when Twinkle K319E was expressed in a similar fashion. Low expression levels of Twinkle K319E lead to the appearance of a sharp double-stranded bubble-arc in a fragment containing the non-coding region of mtDNA, while the club-headed double bubble-arc typical for RNA-rich initiation intermediates was reduced. At the same time, the abundance of incompletely digested intermediates containing RNA or single-stranded patches was decreased. With higher expression levels these intermediates vanished completely, with the y- and bubble-arc remaining as the only visible features. This effect could be observed also in other parts of the mitochondrial genome, indicating a general problem with replication fork progression. At full expression levels also the y-shaped intermediates were decreased, indicating an accumulation of replicating molecules shortly after initiation. This change resembled the

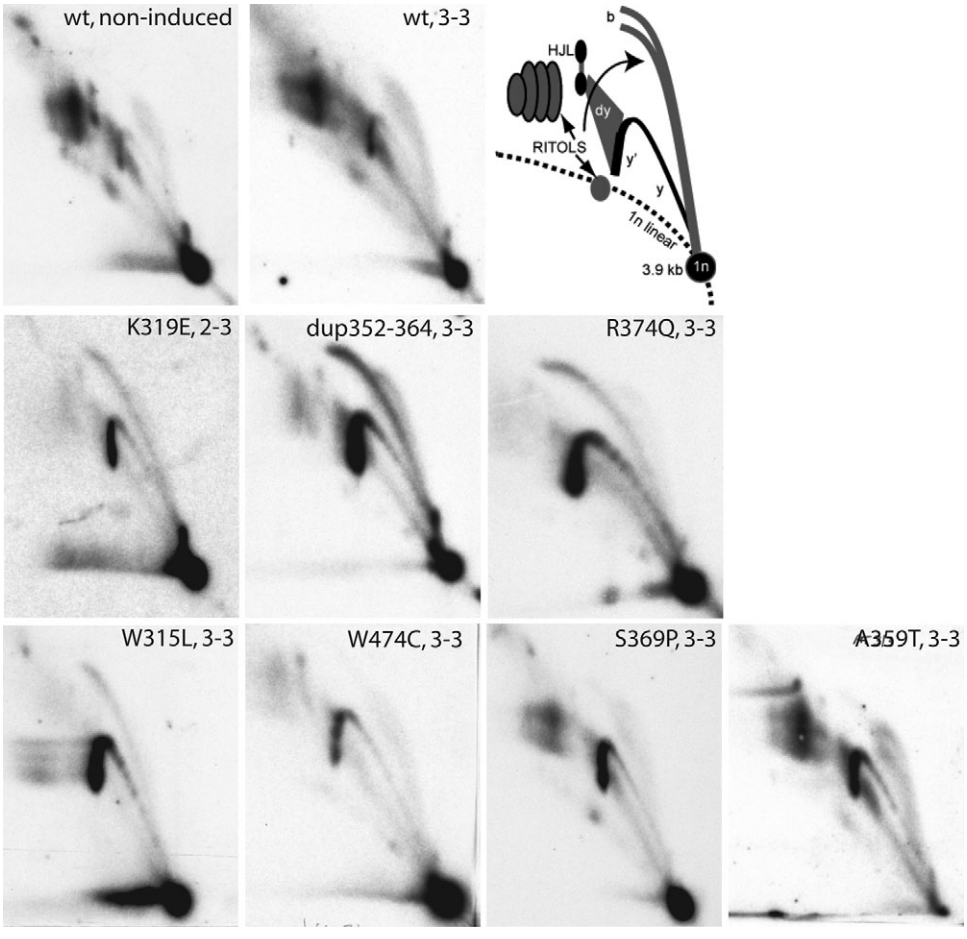


**Figure 6.** MtDNA replication is stalling upon Twinkle mutant expression. 2DNAGE analysis of mtDNA replication intermediates from cells expressing Twinkle variants for two to three days (2−3: two days of induction with 3 ng/ml doxycycline; 3−3: three days induction with 3 ng/ml doxycycline). 2DNAGE samples for all panels consisted of purified mtDNA digested with HincII and probed with a radiolabeled cytochrome b gene fragment (nt 14 846−15 357). The detected fragment includes the non-coding region of mtDNA, the cytochrome b, ND6, part of the ND5 gene and intervening tRNA genes (nt 13 636−1006). The upper two panels show a comparison of mtDNA replication in non-induced and Twinkle wild-type overexpressing cells and the interpretation based on earlier 2DNAGE analysis of mtDNA RIs (22). 1n, 3.9 kb non-replicating *Hin*cII fragment. b, bubble arcs. MtDNA bubble arcs are usually very sensitive to RNase H due to the presence of patches of RNA−DNA especially on the lagging strand; therefore a second, degraded bubble arc is visible in cells incorporating RNA into the lagging strand. *y* and *y*′ indicate ascending and descending parts of the *y* arc and (d*y*) indicates double-Y structures typical for the termination region of replication. These will eventually form resolution intermediates resembling Holliday junctions (HJL-Holliday junction like molecules). Other higher molecular weight fragments arise from the failure to cut RNA−DNA hybrids at a restriction site, these as well as the RNA-rich bubble arcs are marked as RITOLS (RNA Incorporation ThroughOut the Lagging Strand). Overexpression of wild-type Twinkle did not change the replication pattern, the only notable difference was a reproducible reduction in one of the HJL RIs as described earlier. In contrast the stronger disease mutations caused accumulation of replication intermediates on the *y*- and bubble arc (*y* and *b*) and a decrease in all RITOLS related features. The milder disease mutations S359P and A369T had only a moderately enhanced descending *y*-arc (*y*′) (note that the 1n spot in the A359T panel has run of the gel). The helicase domain mutation W474C was exceptional as no bubble arc, indicating initiation in the non-coding region, was clearly visible, while similar to other strong mutants RITOLS had almost completely disappeared. This was even more clearly visible after induction with 10 ng/ml DC for three days as is illustrated in Supplementary Material, Fig. S3.

effect of catalytically inactive Twinkle mutations described by Wanrooij *et al*. (22).

A similar although milder replication stalling was induced when expressing R374Q, dup352−364 or W315L Twinkle variants; while molecules on the y- and double-stranded bubble-arc strongly accumulated, the levels of RNA-rich intermediates decreased. Expression of the Twinkle S369P and A359T mutations had the mildest effect, although also they resulted in clear replication stalling and a shift to less RNA-containing intermediates.

The W474C variant, the only helicase domain mutation analyzed had a different effect: also here RNA-rich intermediates vanished and y-shaped molecules accumulated upon expression, but in contrast to the previously described mutants bubble-containing intermediates did not accumulate, but vanished completely (Fig. 6 and Supplementary Material, Fig. S3).

## Transgenic animals expressing an adPEO Twinkle variant show impaired replication already at young age

Although the replication stalling that is observed when expressing Twinkle adPEO mutants in cell culture leads to rapid loss of mtDNA, this effect has not been reported in adPEO patients. To determine whether similar phenomena as in cultured cells are found *in vivo*, we studied the mtDNA

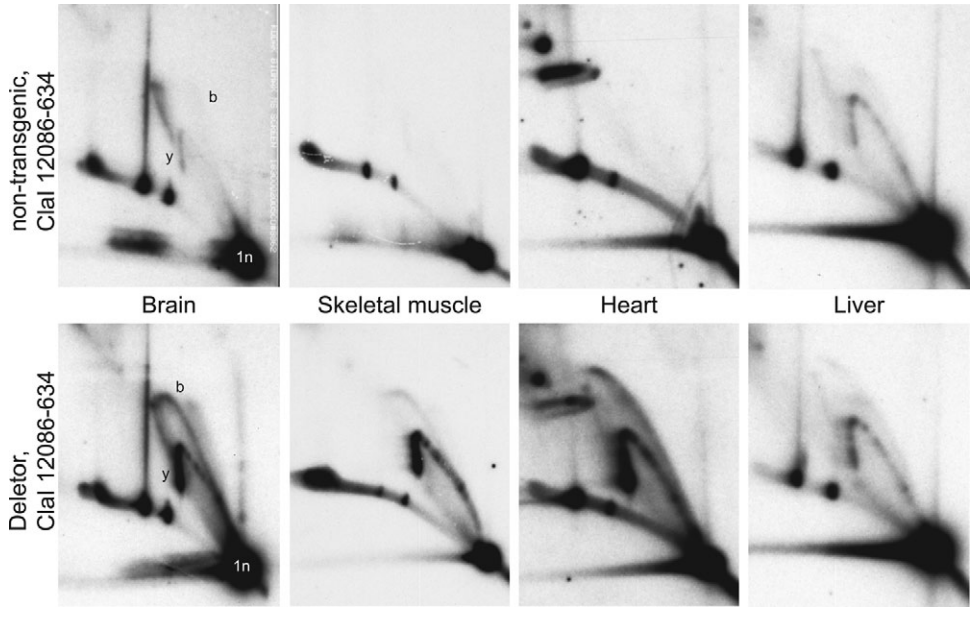


**Figure 7.** Deletor mice expressing the mouse variant of dup352–364 Twinkle also show mtDNA replication stalling. 2DNAGE analysis of brain, skeletal muscle, heart and liver mtDNA from young Deletor mice expressing the mouse Twinkle mutation equivalent to the human dup352–364 Twinkle variant show, except for liver, a similar strong accumulation of replication intermediates on both y- and bubble arc as in cultured cells. MtDNA was isolated from 6-week-old transgenic mice and non-transgenic siblings and probed against the OH-containing ClaI fragment (nts 12086–634). A similar replication stalling as observed in brain was also observed in kidney (data not shown).

replication patterns of the Deletor mice. In Deletor muscle, the first histological signs of disease and detectable amounts of mtDNA deletions appear at the age of 9–12 months. Similarly, in Deletor brain, multiple mtDNA deletions as well as depletion are becoming apparent after approximately one year of age (26 and unpublished data). Since the number of replicating mtDNA molecules is low in mice of old age, we studied the heart, liver, skeletal muscle, kidney and brain of animals of six weeks of age. The expression levels of the transgenic mutant Twinkle compared with the endogenous wild-type Twinkle mRNA were between 13 and 59% depending on the tissue. All these tissues at this age, including brain, showed normal mtDNA copy-number levels. In contrast, the analysis of replication patterns showed a striking accumulation of replication intermediates in mutant animals in all tissues examined except for liver. In the liver, the effect of transgene expression on the accumulation of replication intermediates was rather mild. Figure 7 shows the comparison for brain, muscle, heart and liver mtDNA with the mutant transgene expression level measured to be 39, 59, 45 and 16% of the endogenous transcript level. The results for kidney (13% of endogenous transcript level) were very similar to those observed for brain (not shown). Similar results were obtained for three different Deletor founder lines (26) (not shown), demonstrating that the observed effect was not a consequence of the transgene insertion sites. Also, transgenic overexpression of wild-type Twinkle at much higher levels (20) only showed a slight quantitative change in replication intermediates in all tissues (not shown) except in heart where also qualitative changes were observed (Pohjoismäki *et al*., manuscript submitted) that were however not seen in the Deletor mouse heart.

## DISCUSSION

Mutations in the mtDNA helicase Twinkle are one of the major causes of adPEO (18,23). Understanding how Twinkle mutations cause mitochondrial dysfunction and multiple mtDNA deletions in post-mitotic tissues in patients is one of the primary goals in studying the effects of Twinkle mutants using a combination of *in vitro* assays, cell culture and animal models. Using these approaches we show here that the Twinkle adPEO mutations cause a defect in mtDNA replication both in human cell culture and in a transgenic mouse model (26), resulting in the accumulation of replication intermediates, indicative of replication pausing/stalling. In addition, we suggest that replication stalling can also result in a mitochondrial transcription defect. Although the defects of several of the mutations we studied are largely in agreement with recent studies using both *in vitro* assays and insect cell culture (21,29), we here extend these findings by studying additional mutants in human cell culture, and show that the cell culture findings are relevant for the disease pathogenesis, as they can be replicated *in vivo*, in the Deletor mice.

### Oligomerization

As Twinkle PEO is a dominantly inherited disease, the mutations are heterozygous and the mutant protein coexists with the wild-type protein. Therefore, adPEO Twinkle variants are assumed to be dominant negative and to impair the function of wild-type Twinkle by interaction, which requires co-hexamerization. We show here that the Twinkle mutants K319E, dup352–364 and R374Q resulted in a moderate to severe decrease of hexamer formation under all tested

conditions, although some ability to form multimers was maintained. This is in apparent contrast with a recent study (29) who found that several mutations including the R374Q studied caused the helicase to be completely monomeric. In seeming agreement with our results, the *Drosophila* R341Q mutant, analogous to R374Q in humans, expressed and isolated from *Drosophila* Schneider S2 cells retained the ability to form multimers using glycerol-gradient sedimentation (21), although the resolution of these experiments makes it difficult to assess to what extent hexamers were stable.

The apparent discrepancy of identical mutations showing different multimerization abilities can be explained by the different origin of the proteins in our study and that of Korhonen *et al*. (29). In the latter study, human Twinkle variants were expressed in the cytosol of insect cells using baculovirus which also ensures that the isolated mutant proteins are free from any wild-type Twinkle. However, it was shown clearly that co-expression with the wild-type form increased the ability to form hexamers of otherwise monomeric mutant protein, such as the R374Q mutant (29). In contrast, the proteins used in our study are expressed in the mitochondria of human cells that do contain functional wild-type Twinkle. Although the mutant form is overexpressed to a great extent, a small proportion of the extracted Twinkle hexamers does contain one or more subunits of the wild-type Twinkle. This might be especially the case for the R374Q variant that in the studied cells was expressed at normal levels, but consistently gave low yields when isolated. The diffuse mitochondrial signal in immunocytochemistry supports the possibility of increased destabilization of this variant that might lead to the selective purification of heteromultimers containing wild-type Twinkle. The same argument can be applied to the expression of the R341Q *Drosophila* Twinkle protein (21), as previously discussed (29). A second difference that might apply to this discussion is that the localization of Twinkle variants in mitochondria allows for potential post-translational modification that may influence and regulate the activity of Twinkle *in vivo*. Mitochondrial chaperones that could assist in protein stability and folding could also influence the ability of mutants to form multimers. In conclusion, based on the present and previous studies (21,29), the lost ability of some of the mutant Twinkle PEO variants to form multimers in their pure form does not reflect the *in vivo* ability of the protein to interact with wild-type Twinkle, the situation found in heterozygous PEO patients. Clearly, the presence of wild-type Twinkle rescues a quarternary structural defect of several mutant Twinkle variants to the extent that a heteromultimeric complex can be formed that is still able to perform its function to some degree in mtDNA replication. The lost ability to form homomultimers for some of the mutants does suggest that either heteromultimer formation can be less efficient, perhaps even to the extent that there is a preferential formation of wild-type-only multimers, or that heteromultimers form that are, for example, less processive or that are defective in the coupling of nucleotide hydrolysis with DNA unwinding. It is again important to note here that the nucleotide binding and hydrolysis pocket of ring helicases is formed at the interface of subunits (see 32, for a review). Any disturbance by mutation, however subtle, could be anticipated to affect the hydrolysis cycle and its mechanistic coupling to DNA unwinding, thus resulting in a less-effective enzyme.

### Helicase activity and DNA binding

As described earlier, Twinkle has affinity both to single-stranded and double-stranded DNA (30). We measured the affinity of purified protein to a single-stranded DNA substrate and found reduced binding for the mutations K319E, dup352–364 and W315L, in agreement with their reduced helicase activity (all three) and hexamerization (K319E and dup352–364). Surprisingly, in our hands the S369P variant had a clearly increased affinity to ssDNA in contrast to the results of Korhonen *et al*. (29), who reported a decreased binding affinity for the same variant. As we found an increased amount of mtDNA nucleoids in cells expressing this variant in contrast to other variants showing less nucleoids, the tight binding of S369P Twinkle to mtDNA might influence the segregation of nucleoids. The observed differences in binding activity compared with Korhonen *et al*. could be explained as described above for hexamerization. The unwinding ability of all mutations *in vitro* was diminished compared with wild-type Twinkle. Depending on the oligonucleotide used as energy source the range of residual activity ranged from $<10$ to 76% remaining activity, but all mutations had $<55\%$ maximal activity with UTP.

### mtDNA replication in human cells expressing Twinkle mutants and in Deletor mice

As all available *in vitro* assays for Twinkle function have the disadvantage of working with a relatively inactive enzyme, we studied the effect of adPEO variants on mtDNA replication directly under physiological conditions. When expressed approximately in a one-to-one ratio with wild-type Twinkle, the 'strong' mutations showed a slowing-down of mtDNA replication rate and an accumulation of replication intermediates (not shown). Under these conditions, comparable to the situation in patients, mtDNA depletion is not detected, indicating that the slow replication is still sufficient to keep mtDNA copy-numbers normal. When mutant levels are increased, the stalling is increased and results in reduced mtDNA levels. This might explain why only the relatively mild A359T mutation has been seen as homozygous in patients: a severely deleterious Twinkle variant would lead to mtDNA loss already early in the development. We used the exaggerated situation of a mutant to wild-type ratio of ca. 4:1 (22) to study the immediate effect on the replication machinery in detail. All mutations localized in or close to the linker domain, except for the A359T, caused relatively severe replication stalling over the whole length of mtDNA. The observed stalling/pausing phenotypes with most of the adPEO Twinkle mutants are entirely consistent with our previous analysis of catalytic and structural mutations in the Twinkle protein (22); all of the Twinkle mutants except for the W474C mutant (see later) showed more or less severe accumulation of what we previously showed to be mostly double-stranded DNA bubble and y-shaped replication intermediates, while at the same time there was a strong reduction in the

RNA-containing RITOLS intermediates. Overexpression of wild-type Twinkle, even at full induction, did not substantially modify the types of replication intermediates observed, such as RITOLS, though there did appear to be a small increase in y-shaped replication intermediates (for a more extensive comparison of the effects of wild-type and mutant proteins on replication intermediates, we have also included a Supplementary Material, Fig. S3 comparing effects at different levels of induction). It should be pointed out again here that overexpression of all mutants resulted in a more or less severe drop in mtDNA levels, while no such drop was observed for the wild-type protein even at full induction. For a discussion of the implications of the stalling/pausing phenotype of Twinkle mutants with reference to the mechanisms of mtDNA replication we refer to our previous paper (22). The W474C mutation localized in the helicase domain of Twinkle showed a slightly different effect on replication. The stalling effect was limited to the non-coding region, while replication in other parts of the mtDNA seemed to be normal (not shown). Analysis of an OH-containing fragment showed that only y-shaped replication intermediates accumulated, while bubble intermediates, indicative of replication initiation, were reduced or absent. This suggests a specific effect of this mutation on the initiation in the non-coding region of mtDNA, while elongation elsewhere seemed to be less affected.

Analysis of various tissues of six-week-old Deletor mice showed strong accumulation of replication intermediates compared with non-transgenic littermates. This was a surprising finding, since multiple mtDNA deletions are only detectable in animals older than approximately nine months of age (26), thus suggesting that perhaps the critical events that in later live result in the typical molecular phenotype of PEO occur at a much earlier age when mtDNA replication is still frequent. Similarly, depletion of brain mtDNA is apparent in older mice (26) but not in the 6-week-old animals, yet replication intermediates clearly accumulated at this stage already. Finally, multiple mtDNA deletions accumulate in muscle, heart and brain but not in liver and kidney (26 and unpublished data), yet 6-week-old kidney also showed clear signs of replication stalling similar to what was observed in brain. These differences could be explained by variable degrees of self-regenerating capacity or apoptosis resistance of the various tissues, but remain still to be clarified.

## Transcription

The expression of Twinkle mutations in human cells impaired not only replication, but also the transcription of mtDNA. Already after 2 days of expression the steady-state levels of H-strand transcripts were depleted, an effect that clearly preceded the depletion of mtDNA. The impairment of RNA synthesis might be due to several mechanisms. Firstly, as replication is severely slowed down, an increasing number of mtDNA molecules are in the state of replication. The increased presence of replisomes on the mtDNA could cause a collision of replication and transcription machineries and abort successful transcription. Secondly, a change in mtDNA topology was observed upon the expression of mutant Twinkle. The proportion of relaxed molecules increased, while supercoiled mtDNA molecules were less abundant (unpublished data). At this point, however, the exact cause and effect relationship is unclear. It remains to be determined whether in adPEO patients a defect in the mitochondrial transcription precedes the accumulation of multiple deletions and could in fact contribute to the pathophysiology of adPEO by inducing an oxidative phosphorylation deficiency.

## Can we understand the functional consequences of replication stalling in proliferating cells versus post-mitotic tissues?

In proliferating cells mtDNA replication needs to keep pace with the mitochondrial and cellular proliferation rate. Thus, if mtDNA replication significantly pauses or stalls without immediately affecting cell proliferation one can expect a drop in mtDNA copy-number and this is exactly what is observed when we overexpress Twinkle mutants (this study and 22), POLG1 mutants (22) and, for example, wild-type TFAM (33) or when we knock-down Twinkle expression (20). It is unclear at the moment what happens with stalled replication forks during cell division, but expression of Twinkle PEO mutants in cultured cells does not seem to result in mtDNA deletions (none could be detected, neither by Southern blot analysis nor by long range PCR, unpublished data), which is in line with our previous observations with cultured adPEO patient cells (unpublished data). One might expect that a failure to complete replication would result in a failure to divide nucleoids resulting in enlarged nucleoid structures and a mosaic cell distribution of nucleoids. This is indeed one of the phenotypes of some of our Twinkle variants in cell culture. In contrast, in post-mitotic tissues the situation is different as mtDNA replication is no longer coupled to the cell cycle. Presumably in this case it is the balance between mitochondrial (DNA) turnover and replication that determines whether there will be a net loss of mtDNA copy-number. How this different requirement for mtDNA replication might cause multiple deletions to accumulate remains a matter of speculation but we can envisage several scenarios. First, the persistent presence of stalled/paused replication forks could elicit an mtDNA repair response similar to SOS responses resulting in the recruitment of specific repair proteins. We recently discussed a scenario of how enhanced rates of mtDNA repair could result in enhanced rates of deletion formation (34). A second scenario that cannot be excluded at this point would be frequent focal depletion of mtDNA followed by reamplification. Especially in a situation where replication is frequently paused due to a partially defective replication machinery, this could favour the amplification of mtDNA deletions that naturally occur at low frequencies. Finally, and in line with the previous suggestion, replication stalling might induce an increased rate of mitochondrial (DNA) turnover, for example, via mitophagy (see also 26), combined with an increased rate of replication in order to maintain normal mtDNA steady-state levels. The observation that replication intermediates abnormally accumulate in tissues of young mice but multiple deletions and depletion are only observed in much older animals could suggest that one or several mechanisms to efficiently deal with mtDNA replication problems are in place and that the later onset mtDNA defects are a

direct consequence of an age-associated deterioration of these repair mechanisms. We are currently pursuing the various possibilities suggested here.

## MATERIALS AND METHODS

### Cloning of expression constructs

The full-length cDNA of Twinkle variants were originally cloned in the pcDNA3.1(-)/Myc-His A (Invitrogen), as previously described (18,35). All constructs were re-cloned in the pcDNA5/FRT/TO vector (Invitrogen) taking advantage of two *Pme*I restriction sites flanking the multiple cloning sites of the original pcDNA3 vector and the target vector. The resulting fusion proteins contained the sequence of the respective proteins followed by an Myc-His tag. All resulting plasmid constructs were confirmed by DNA sequencing.

### Creation and maintenance of stable transfected inducible expression cell lines

Stable cell lines expressing various Twinkle mutants upon induction were created as described (22) using the Flp-In™ T-Rex™ 293 host cell line (Invitrogen), an HEK293 variant containing a Flip recombination site at a transcriptionally active locus. The resulting cells were grown in DMEM medium (Sigma) supplemented with 10% FCS (Sigma), 1 mM L-glutamine, 50 μg/ml uridine (Sigma), 150 μg/ml Hygromycin and 15 μg/ml Blasticidin in a 37°C incubator at 8.5% $CO_2$. To test cell lines for mosaic expression of transgenes, which is a common problem with inducible cell lines that are generated by allowing for random integration, we routinely tested all cell lines using immunofluorescence (as described below). All cell lines tested in this manner showed that >99% of cells were positive for expression and that the protein was correctly localized in mitochondria. Even at maximal induction levels there was no evidence of mistargeting.

To induce expression the indicated amount of doxycycline (DC) (Sigma) was added to the growth medium, and cells were processed for further analyses. With longer than 2 day induction, medium was refreshed every 2 days.

### Mouse tissue collection

All animal procedures were performed according to protocols approved by the ethical boards for animal experimentation of the National Public Health Institute and Helsinki University (agreement number STU575A/2004) and all experiments were done in accordance with good practice of handling laboratory animals and of genetically modified organisms. The generation and the phenotypes of the Deletor and the wild-type Twinkle overexpressor mice have been previously described (20,26). The mice were housed in a humidity- and temperature-controlled environment with free access to chow and water. Mouse tissue samples were carefully dissected and immediately processed for DNA extraction.

### Western blots

Cell lysates were prepared and analyzed for protein expression by immunoblotting after SDS–PAGE (35). A primary monoclonal c-myc (Roche Molecular Biochemicals) antibody was used for detection of recombinant proteins. Detection of actin (polyclonal antibody from Novus Biologicals) was used as a loading control. Peroxidase-coupled secondary antibody horse-anti-mouse or goat-anti-rabbit was obtained from Vector Laboratories. Enhanced Chemiluminescence detection was done essentially as described (35).

### Southern blots

The mtDNA levels per cell and the conformation of mtDNA were analyzed by one-dimensional agarose gels and Southern blotting. Total DNA was extracted from cells by proteinase K digest and Phenol–Chloroform extraction. mtDNA levels were analyzed by separating 2 μg of *Hin*dIII digested total DNA on a 0.6% agarose gel in TBE. For conformational studies, 1 μg of DNA was digested with *Bgl*II that does not cut mtDNA, and separated over a 0.4% agarose gel in TBE without ethidium bromide. All gels were blotted and hybridized with $^{32}$P-labelled DNA probes containing the D-loop region (nts 16341–151) or part of the cytochrome b sequence (nts 14846–15357) of human mtDNA. The signal was quantified by phosphorimager and for mtDNA copy-number determination normalized against the signal for 18S rDNA.

### Northern blots

RNA for northern blot analysis was extracted with Trizol (Sigma) using the manufacturer's recommendations. 4 μg of total RNA per sample was run on a 1% agarose MOPS/formaldehyde gel, blotted and hybridized using standard techniques (36). Blots were probed with ca. 500 bp double-stranded DNA probes radioactively labelled by random-primed labelling. Exposures were performed using a phosphorimager (Storm 840, Molecular Dynamics).

### Quantitative PCR

The copy-number of mtDNA per cell was determined essentially as described (22). Total cellular DNA was extracted by Proteinase K digest and isopropanol precipitation, and copy-numbers of cytochrome b (mtDNA) and APP (nuclear DNA) were determined in a Taqman assay on an Abiprism 7000 (Applied Biosciences, Foster City, CA, USA) using plasmids containing the amplicons as standards.

### Immunocytochemistry

Immunofluorescent detection was done as described previously (37) using a monoclonal anti-DNA antibody AC-30-10 (PROGEN, Shingle Springs, CA, USA) and a monoclonal c-myc antibody (Roche Molecular Biochemicals) as primary antibodies. Secondary antibodies were anti-mouse IgG-Alexa-Fluor®488 (Invitrogen, myc) and anti-mouse IgM-Alexa Fluor®568 (DNA). Image acquisition using confocal microscopy was done as described (37).

### Protein extraction, helicase, ssDNA binding and oligomerization assays

*In vitro* assays for determination of helicase activities were performed with highly enriched Twinkle preparations derived from 293 Flp-In™ T-REx™ cells. Cells induced for 36 h were disrupted after short cytochalasin treatment (38); mitochondria were isolated using differential centrifugation and sucrose gradient purification and then lyzed and sonicated in high salt buffer (50 mM $KH_2PO_4$, pH 7.4, 1 M NaCl, 0.05% Triton X-100, 10 mM Imidazol, 7 mM β-mercaptoethanol). The lysate was incubated with TALON $Co^{2+}$ affinity resin (Clontech) for 1 h at 4°C, the resin was washed twice each with high and low salt buffer (25 mM Tris pH 7.6, 200 mM NaCl, 100 mM L-arginine, pH 7.6, 40 mM Imidazol, 10% glycerol, 7 mM β-mercaptoethanol) and His-tagged proteins binding to the resin were isolated with elution buffer containing 25 mM Tris pH 7.6, 200 mM NaCl, 100 mM L-arginine, pH 7.6, 200 mM Imidazol, 50% glycerol. Protein extracts were aliquoted, shock frozen in liquid nitrogen and stored at −80°C. The concentration of Twinkle in the eluate was judged by SDS–PAGE and Coomassie Brilliant blue staining using BSA as a reference. Typically 100 mg mitochondrial wet weight yielded 2–4 μg of Twinkle protein.

Helicase assays were performed as described (22) with a radioactively end-labelled 60 nt oligonucleotide hybridized to M13 (+) ssDNA, forming a 20 nt double-stranded stretch with a 40 nts 5′ end overhang. The reaction conditions were essentially as described previously (22), but the reaction mix did not contain other DNA besides the substrate which was used at a concentration of ∼3 fmol. UTP, ATP, GTP or dGTP were added at 3 mM, if not indicated otherwise. Short-term oligomerization of isolated Twinkle variants *in vitro* was tested by crosslinking the protein with low concentrations of glutaraldehyde followed by separation on an SDS–PAGE and western blotting. Ca. 20 ng of Twinkle protein was diluted in 20 μl of oligomerization buffer (25 mM Tris–HCl pH 7.6, 100 mM L-arginine, pH 7.6, 1 mM DTT, 10% glycerol) containing either 50 mM NaCl (helicase conditions) or 400 mM NaCl (high salt conditions). Glutaraldehyde measuring 0.02% was added and the reaction mix incubated for 5 min at room temperature. The crosslinking was stopped by adding 10 μl of SDS-containing sample buffer and directly heat-denatured for 10 min at 95°C. The denatured sample was separated on a 3–8% Tris–Acetate gel (NuPAGE, Invitrogen) and Twinkle proteins were detected by regular western blotting.

The stability of Twinkle hexamers was analyzed by gel filtration. 100 ng of purified twinkle were separated over a Sephadex 200 10/300GL column (GE healthcare) in high salt buffer (25 mM Tris–HCl pH 7.6, 400 mM NaCl, 100 mM L-arginine pH 7.6, 5 mM EDTA, 10% glycerol), proteins from 0.5 ml fractions were precipitated with deoxycholate and TCA and analyzed by western blot using the anti-myc antibody.

Binding of Twinkle wild-type and mutant protein to a ssDNA oligonucleotide was essentially performed as described previously (30), but with the exception that we used the following oligo nucleotide primer: CT TCC TGG CTT GCT TTG GCT GAG CCA AAA in stead of an oligodT primer; reactions were done in 20 μl with a protein concentration of 50–100 ng as judged by Coomassie staining. Binding was quantified by phosphorimaging and is expressed as the level of binding relative to the wild-type protein.

### Brewer-Fangman 2D neutral/neutral agarose electrophoresis

Mitochondrial nucleic acids were extracted using cytochalasine (Sigma-Aldrich) as described (38). Purified mtDNA was digested with *Hin*cII (human) or *Cla*I (mouse). The fragments were separated by 2DNAGE as described (39,40) and the gels were blotted and hybridized with a $^{32}$P-labelled DNA probe for human mtDNA nts 14846–15357 or mouse mtDNA nts 16356–136.

## SUPPLEMENTARY MATERIAL

Supplementary Material is available at *HMG* online.

## ACKNOWLEDGEMENTS

We are very grateful for suggestions and many discussions we have had with the Ian Holt laboratory (Cambridge, UK) and with Howy Jacobs and Jaakko Pohjoismäki.

*Conflict of Interest statement*. None declared.

## FUNDING

This work was supported by the Academy of Finland [110689, 103213 and CoE funding to J.N.S.]; Sigrid Juselius Foundation [to A.S. and J.N.S.]; the University of Helsinki [to A.S.]; the EU sixth Framework Programme for Research, Priority 1 'Life sciences, genomics and biotechnology for health [LSHM-CT-2004-503116 to J.N.S. and S.G.]; and the Tampere University Hospital Medical Research Fund [9G072, 9H079 to J.N.S., 9H102 to H.M.C.]. Funding to Pay the Open Access Charge was provided by the Academy of Finland.

## REFERENCES

1. Schaefer, A.M., Blakely, E.L., He, L., Whittaker, R.G., Taylor, R.W., Chinnery, P.F. and Turnbull, D.M. (2008) Prevalence of mitochondrial DNA disease in adults. *Ann. Neurol.*, **63**, 35–39.
2. Majamaa, K., Moilanen, J.S., Uimonen, S., Remes, A.M., Salmela, P.I., Karppa, M., Majamaa-Voltti, K.A., Rusanen, H., Sorri, M., Peuhkurinen, K.J. *et al.* (1998) Epidemiology of A3243G, the mutation for mitochondrial encephalomyopathy, lactic acidosis, and strokelike episodes: prevalence of the mutation in an adult population. *Am. J. Hum. Genet.*, **63**, 447–454.
3. Hakonen, A.H., Heiskanen, S., Juvonen, V., Lappalainen, I., Luoma, P.T., Rantamaki, M., Goethem, G.V., Lofgren, A., Hackman, P., Paetau, A. *et al.* (2005) Mitochondrial DNA polymerase W748S mutation: a common cause of autosomal recessive ataxia with ancient European origin. *Am. J. Hum. Genet.*, **77**, 430–441.
4. Winterthun, S., Ferrari, G., He, L., Taylor, R.W., Zeviani, M., Turnbull, D.M., Engelsen, B.A., Moen, G. and Bindoff, L.A. (2005) Autosomal recessive mitochondrial ataxic syndrome due to mitochondrial polymerase gamma mutations. *Neurology*, **64**, 1204–1208.
5. Naviaux, R.K. and Nguyen, K.V. (2004) POLG mutations associated with Alpers' syndrome and mitochondrial DNA depletion. *Ann. Neurol.*, **55**, 706–712.

6. Chinnery, P.F. and Zeviani, M. 155th ENMC workshop: Polymerase gamma and disorders of mitochondrial DNA synthesis, 21–23 September 2007, Naarden, The Netherlands. *Neuromuscul. Disord.*, **18**, 259–267.
7. Zeviani, M., Servidei, S., Gellera, C., Bertini, E., DiMauro, S. and DiDonato, S. (1989) An autosomal dominant disorder with multiple deletions of mitochondrial DNA starting at the D-loop region. *Nature*, **339**, 309–311.
8. Suomalainen, A., Majander, A., Haltia, M., Somer, H., Lonnqvist, J., Savontaus, M.-L. and Peltonen, L. (1992) Multiple deletions of mitochondrial DNA in several tissues of a patient with severe retarded depression and familial progressive external opthalmoplegia. *J. Clin. Invest.*, **90**, 61–66.
9. Suomalainen, A., Majander, A., Wallin, M., Setala, K., Kontula, K., Leinonen, H., Salmi, T., Paetau, A., Haltia, M., Valanne, L. *et al.* (1997) Autosomal dominant progressive external ophthalmoplegia with multiple deletions of mtDNA: clinical, biochemical, and molecular genetic features of the 10q-linked disease. *Neurology*, **48**, 1244–1253.
10. Yakubovskaya, E., Chen, Z., Carrodeguas, J.A., Kisker, C. and Bogenhagen, D.F. (2006) Functional human mitochondrial DNA polymerase gamma forms a heterotrimer. *J. Biol. Chem.*, **281**, 374–382.
11. Yakubovskaya, E., Lukin, M., Chen, Z., Berriman, J., Wall, J.S., Kobayashi, R., Kisker, C. and Bogenhagen, D.F. (2007) The EM structure of human DNA polymerase gamma reveals a localized contact between the catalytic and accessory subunits. *Embo J.*, **26**, 4283–4291.
12. Van Goethem, G., Martin, J.J., Dermaut, B., Lofgren, A., Wibail, A., Ververken, D., Tack, P., Dehaene, I., Van Zandijcke, M., Moonen, M. *et al.* (2003) Recessive POLG mutations presenting with sensory and ataxic neuropathy in compound heterozygote patients with progressive external ophthalmoplegia. *Neuromuscul. Disord.*, **13**, 133–142.
13. Van Goethem, G., Dermaut, B., Lofgren, A., Martin, J.J. and Van Broeckhoven, C. (2001) Mutation of POLG is associated with progressive external ophthalmoplegia characterized by mtDNA deletions. *Nat. Genet.*, **28**, 211–212.
14. Lamantea, E., Tiranti, V., Bordoni, A., Toscano, A., Bono, F., Servidei, S., Papadimitriou, A., Spelbrink, H., Silvestri, L., Casari, G. *et al.* (2002) Mutations of mitochondrial DNA polymerase gammaA are a frequent cause of autosomal dominant or recessive progressive external ophthalmoplegia. *Ann. Neurol.*, **52**, 211–219.
15. Agostino, A., Valletta, L., Chinnery, P.F., Ferrari, G., Carrara, F., Taylor, R.W., Schaefer, A.M., Turnbull, D.M., Tiranti, V. and Zeviani, M. (2003) Mutations of ANT1, Twinkle, and POLG1 in sporadic progressive external ophthalmoplegia (PEO). *Neurology*, **60**, 1354–1356.
16. Longley, M.J., Clark, S., Yu Wai Man, C., Hudson, G., Durham, S.E., Taylor, R.W., Nightingale, S., Turnbull, D.M., Copeland, W.C. and Chinnery, P.F. (2006) Mutant POLG2 disrupts DNA polymerase gamma subunits and causes progressive external ophthalmoplegia. *Am. J. Hum. Genet.*, **78**, 1026–1034.
17. Leipe, D.D., Aravind, L., Grishin, N.V. and Koonin, E.V. (2000) The bacterial replicative helicase DnaB evolved from a RecA duplication. *Genome Res.*, **10**, 5–16.
18. Spelbrink, J.N., Li, F.Y., Tiranti, V., Nikali, K., Yuan, Q.P., Tariq, M., Wanrooij, S., Garrido, N., Comi, G., Morandi, L. *et al.* (2001) Human mitochondrial DNA deletions associated with mutations in the gene encoding Twinkle, a phage T7 gene 4-like protein localized in mitochondria. *Nat. Genet.*, **28**, 223–231.
19. Korhonen, J.A., Pham, X.H., Pellegrini, M. and Falkenberg, M. (2004) Reconstitution of a minimal mtDNA replisome *in vitro*. *Embo J.*, **23**, 2423–2429.
20. Tyynismaa, H., Sembongi, H., Bokori-Brown, M., Granycome, C., Ashley, N., Poulton, J., Jalanko, A., Spelbrink, J.N., Holt, I.J. and Suomalainen, A. (2004) Twinkle helicase is essential for mtDNA maintenance and regulates mtDNA copy number. *Hum. Mol. Genet.*, **13**, 3219–3227.
21. Matsushima, Y. and Kaguni, L.S. (2007) Differential phenotypes of active site and human autosomal dominant progressive external ophthalmoplegia mutations in *Drosophila* mitochondrial DNA helicase expressed in Schneider cells. *J. Biol. Chem.*, **282**, 9436–9444.
22. Wanrooij, S., Goffart, S., Pohjoismaki, J.L., Yasukawa, T. and Spelbrink, J.N. (2007) Expression of catalytic mutants of the mtDNA helicase Twinkle and polymerase POLG causes distinct replication stalling phenotypes. *Nucleic Acids Res.*, **35**, 3238–3251.
23. Virgilio, R., Ronchi, D., Hadjigeorgiou, G.M., Bordoni, A., Saladino, F., Moggio, M., Adobbati, L., Kafetsouli, D., Tsironi, E., Previtali, S. *et al.* (2008) Novel Twinkle (PEO1) gene mutations in mendelian progressive external ophthalmoplegia. *J. Neurol.*, First published on June 30, 2008, 10.1007/s00415–008–0926–3.
24. Hakonen, A.H., Isohanni, P., Paetau, A., Herva, R., Suomalainen, A. and Lonnqvist, T. (2007) Recessive Twinkle mutations in early onset encephalopathy with mtDNA depletion. *Brain*, **130**, 3032–3040.
25. Sarzi, E., Goffart, S., Serre, V., Chretien, D., Slama, A., Munnich, A., Spelbrink, J.N. and Rotig, A. (2007) Twinkle helicase (PEO1) gene mutation causes mitochondrial DNA depletion. *Ann. Neurol.*, **62**, 579–587.
26. Tyynismaa, H., Mjosund, K.P., Wanrooij, S., Lappalainen, I., Ylikallio, E., Jalanko, A., Spelbrink, J.N., Paetau, A. and Suomalainen, A. (2005) Mutant mitochondrial helicase Twinkle causes multiple mtDNA deletions and a late-onset mitochondrial disease in mice. *Proc. Natl. Acad. Sci. USA*, **102**, 17687–17692.
27. Garrido, N., Griparic, L., Jokitalo, E., Wartiovaara, J., Van Der Bliek, A.M. and Spelbrink, J.N. (2003) Composition and dynamics of human mitochondrial nucleoids. *Mol. Biol. Cell*, **14**, 1583–1596.
28. Korhonen, J.A., Gaspari, M. and Falkenberg, M. (2003) TWINKLE Has 5′ ->3′ DNA helicase activity and is specifically stimulated by mitochondrial single-stranded DNA-binding protein. *J. Biol. Chem.*, **278**, 48627–48632.
29. Korhonen, J.A., Pande, V., Holmlund, T., Farge, G., Pham, X.H., Nilsson, L. and Falkenberg, M. (2008) Structure-function defects of the TWINKLE linker region in progressive external ophthalmoplegia. *J. Mol. Biol.*, **377**, 691–705.
30. Farge, G., Holmlund, T., Khvorostova, J., Rofougaran, R., Hofer, A. and Falkenberg, M. (2008) The N-terminal domain of TWINKLE contributes to single-stranded DNA binding and DNA helicase activities. *Nucleic Acids Res.*, **36**, 393–403.
31. Guo, S., Tabor, S. and Richardson, C.C. (1999) The linker region between the helicase and primase domains of the bacteriophage T7 gene 4 protein is critical for hexamer formation. *J. Biol. Chem.*, **274**, 30303–30309.
32. Donmez, I. and Patel, S.S. (2006) Mechanisms of a ring shaped helicase. *Nucleic Acids Res.*, **34**, 4216–4224.
33. Pohjoismaki, J.L., Wanrooij, S., Hyvarinen, A.K., Goffart, S., Holt, I.J., Spelbrink, J.N. and Jacobs, H.T. (2006) Alterations to the expression level of mitochondrial transcription factor A, TFAM, modify the mode of mitochondrial DNA replication in cultured human cells. *Nucleic Acids Res.*, **34**, 5815–5828.
34. Krishnan, K.J., Reeve, A.K., Samuels, D.C., Chinnery, P.F., Blackwood, J.K., Taylor, R.W., Wanrooij, S., Spelbrink, J.N., Lightowlers, R.N. and Turnbull, D.M. (2008) What causes mitochondrial DNA deletions in human cells? *Nat Genet.*, **40**, 275–279.
35. Spelbrink, J.N., Toivonen, J.M., Hakkaart, G.A., Kurkela, J.M., Cooper, H.M., Lehtinen, S.K., Lecrenier, N., Back, J.W., Speijer, D., Foury, F. *et al.* (2000) *In vivo* functional analysis of the human mitochondrial DNA polymerase POLG expressed in cultured human cells. *J. Biol. Chem.*, **275**, 24818–24828.
36. Church, G.M. and Gilbert, W. (1984) Genomic sequencing. *Proc. Natl. Acad. Sci. USA*, **81**, 1991–1995.
37. Cooper, H.M. and Spelbrink, J.N. (2008) The human Sirt3 protein deacetylase is exclusively mitochondrial. *Biochem J.*, **411**, 279–285.
38. Yasukawa, T., Yang, M.Y., Jacobs, H.T. and Holt, I.J. (2005) A bidirectional origin of replication maps to the major noncoding region of human mitochondrial DNA. *Mol. Cell*, **18**, 651–662.
39. Friedman, K.L. and Brewer, B.J. (1995) Analysis of replication intermediates by two-dimensional agarose gel electrophoresis. *Methods Enzymol.*, **262**, 613–627.
40. Brewer, B.J. and Fangman, W.L. (1987) The localization of replication origins on ARS plasmids in *S. cerevisiae*. *Cell*, **51**, 463–471.

## Supplementary Material

**Supplementary Figure 1:** Purity of wild type and mutant proteins following full induction of expression in 293 Flp-In™ T-REx™ cells, mitochondrial isolation and subsequent TALON resin purification. The samples represented here stained with Coomassie Brilliant Blue show the typical purity of protein from this single-step isolation procedure and used in the various in vitro assays described in the main text. Abbreviations are as described in the main text.

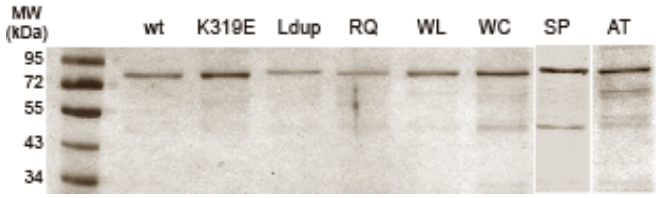


**Supplementary Figure 2:**

The subcellular localization of the Twinkle variants was determined by immunofluorescence. While wildtype Twinkle (not shown) and the W315L mutant co-localized with mtDNA in punctate nucleoids within mitochondria, the disease variants K319E, R374Q and dup 352-364 Twinkle variants all localized only partially with nucleoids, a proportion of the protein was diffusely localized in the mitochondrial lumen, while the nucleoids often appeared enlarged. The W474C variant caused aggregation of nucleoids without a more diffuse distribution of the protein, while the A359T mutation decreased the Twinkle localization in nucleoids without impairing their size. S369P Twinkle cells appeared normal as wildtype and W315L Twinkle, but had an elevated

number of nucleoids. Cells were induced with 3ng/ml doxycycline for 3 days, immunocytochemistry was performed using specific antibodies against the myc-tagged Twinkle variants (green) and DNA (red). Images were taken with the same settings for exposure, laser intensity, etc. and in addition were processed for brightness and contrast in the same manner.

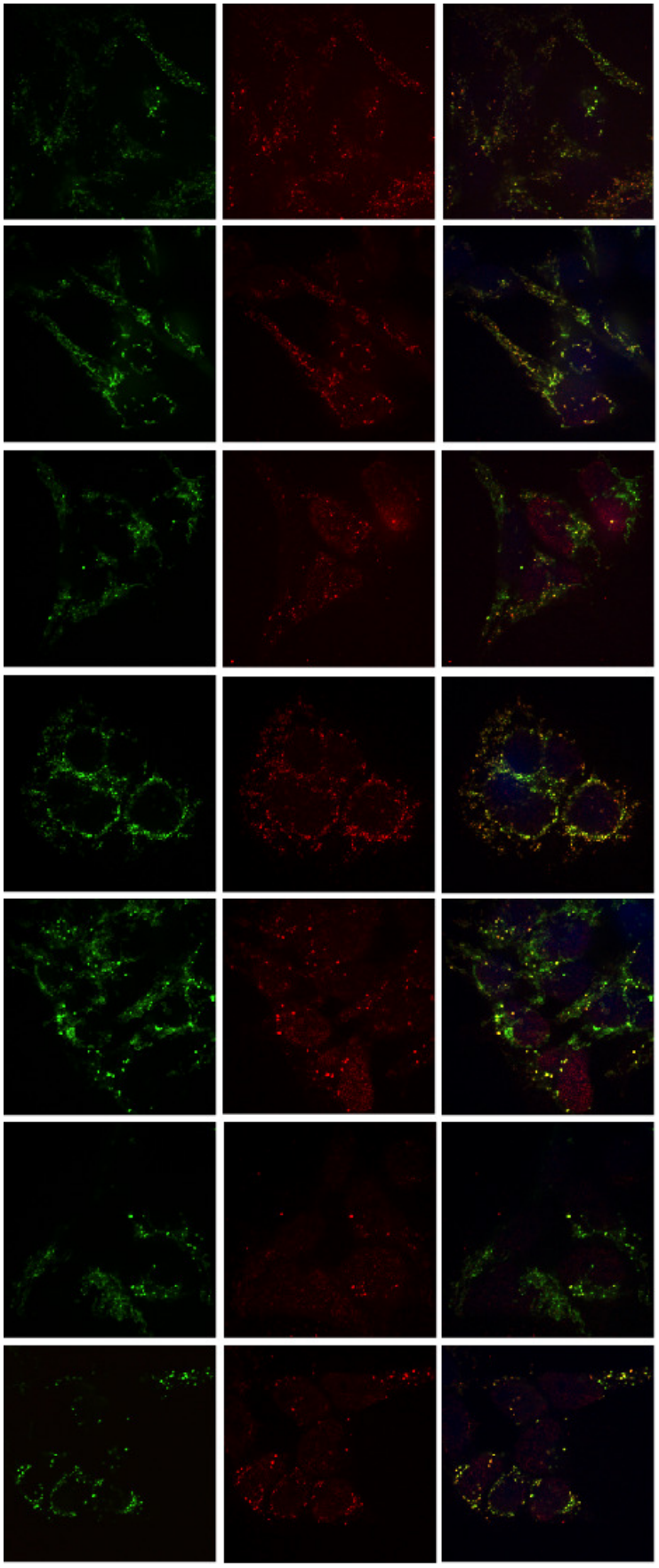
W315L
A359T
K319E
S369P
R374Q
Dup352-364
W474C

**Supplementary Figure 3:** Clear differences in replication intermediates (RIs) isolated from wild type and mutant induced 293 Flp-In™ T-REx™ cells are apparent both at lower and higher than 3 ng/ml doxycycline (DC) concentrations. (A) shows the comparison of RIs of two of the more severe mutants at low induction (1 ng/ml DC) with modest induction (3 ng/ml DC) of wild type (wt) Twinkle. (2-3: 2 days of induction with 3 ng/ml DC; 2-1: 2 days induction with 1 ng/ml DC; 3-1: 3 days induction with 1 ng/ml DC). As is clearly illustrated here for the dup352-364 and K319E mutants, even weak induction resulted in a relative decrease in RITOLS intermediates and the accumulation of both a sharply defined bubble arc and descending y intermediates, that based on our previous work (Wanrooij et al., 2007, Ref 22 of the main text) are dsDNA intermediates and clear signs of replication pausing/stalling. (B) shows the comparison of RIs of fully induced wild type Twinkle with fully induced expression of several of the mutants. The results shown here, again clearly illustrate the differences in the accumulation of RIs between wild type Twinkle and the various mutants. Two example illustrate this: first, the mutation that by all biochemical measures is mild still show signs of reduced Ritols intermediates and accumulation of (dsDNA) bubble and descending y intermediates compared to wild type Twinkle. Second, whereas full induction of wild type Twinkle still shows a pattern of RIs that is essentially identical to non-induced cells except for the dy intermediates (see Figure 6 and Legend), both low and more strongly, high induction of dup352-364, shows loss of RITOLS and a very prominent accumulation of a dsDNA bubble arc and descending y intermediates. Finally, and as commented on in the main text and in Fig 6+Legend of the main text, the W474C mutation is the only mutant that deviates from the general pattern in that it does not accumulate bubble RIs upon overexpression. (2-10: 2 days of induction with 10 ng/ml DC; 3-10: 3 days induction with 10 ng/ml DC).

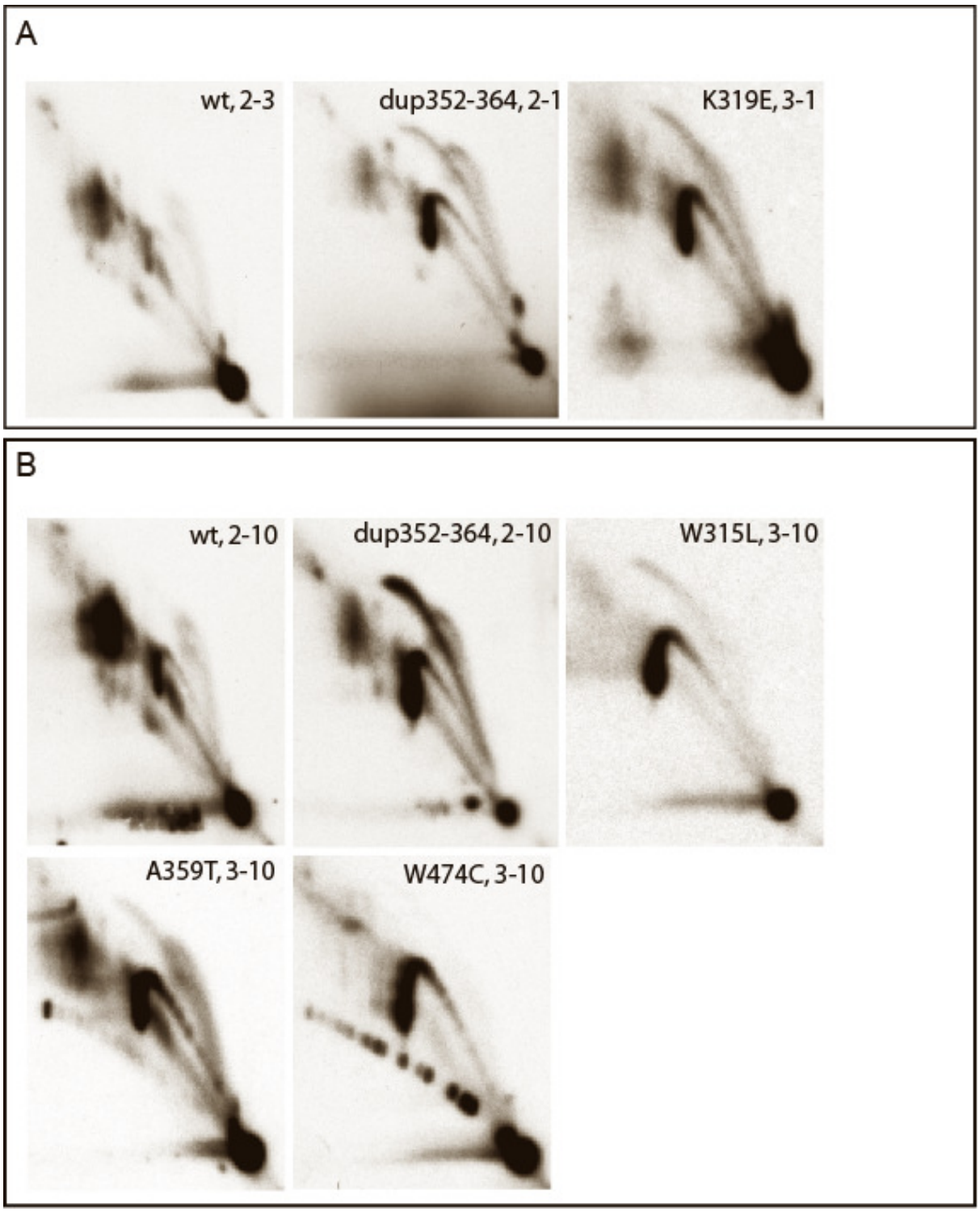
A
wt, 2-3
dup352-364, 2-1
K319E, 3-1
B
wt, 2-10
dup352-364, 2-10
W315L, 3-10
A359T, 3-10
W474C, 3-10

OPEN ACCESS Freely available online

PLoS one

# A New Splice Variant of the Mouse SIRT3 Gene Encodes the Mitochondrial Precursor Protein

**Helen M. Cooper[1☯], Jing-Yi Huang[2☯], Eric Verdin[2], Johannes N. Spelbrink[1]***

**1** University of Tampere, Institute of Medical Technology and Tampere University Hospital, Tampere, Finland, **2** Gladstone Institute of Virology and Immunology, University of California San Francisco, San Francisco, California, United States of America

## Abstract

***Background:*** Mammals have seven NAD-dependent protein deacetylases. These proteins, called sirtuins, are homologous to yeast Sir2, and are emerging as important regulators of lifespan and intermediary metabolism. Three mammalian sirtuins, SIRT3-5 are mitochondrial. Sirtuins are highly conserved between species, yet mouse SIRT3 was reported to be markedly shorter than its human counterpart and to lack the N-terminal mitochondrial targeting signal present in the human protein.

***Results:*** We have isolated a novel mouse SIRT3 splice variant. This cDNA contains two translation initiation codons upstream of the originally reported start site. We show, using immunofluorescence and protein expression analysis that these longer variants are expressed and efficiently targeted to mitochondria, and that the processed forms of these longer variants are identical in size to the endogenous mouse SIRT3. We also show that the previously described form of SIRT3 is not mitochondrial.

***Conclusions:*** Our observations point to a high level of conservation of SIRT3 as a mitochondrial protein in mice and human and indicate that several previous studies, which addressed mouse Sirt3 function, need to be re-evaluated.

**Citation:** Cooper HM, Huang J-Y, Verdin E, Spelbrink JN (2009) A New Splice Variant of the Mouse SIRT3 Gene Encodes the Mitochondrial Precursor Protein. PLoS ONE 4(3): e4986. doi:10.1371/journal.pone.0004986

**Editor:** Grzegorz Kudla, University of Edinburgh, United Kingdom

**Received** December 1, 2008; **Accepted** February 14, 2009; **Published** March 31, 2009



**Funding:** This work was supported by the Academy of Finland [110689, 103213 and CoE funding to JNS]; Sigrid Juselius Foundation [to J.N.S.]; and the Tampere University Hospital Medical Research Fund [9J119 to J.N.S., 9H102 to H.M.C.]. J-Y.H is supported by a postdoctoral fellowship from the Larry L. Hillblom Foundation and E.V. is supported by the J. David Gladstone Institutes. The funders had no role in study design, data collection and analysis, decision to publish, or preparation of the manuscript.

**Competing Interests:** The authors have declared that no competing interests exist.

* E-mail: hans.spelbrink@uta.fi

☯ These authors contributed equally to this work.

## Introduction

The yeast 'silent information regulator' Sir2 is an NAD-dependant deacetylase with a role in regulating longevity in response to nutrient availability [1]. Members of the Sir2 family are conserved from yeast to man and regulate metabolic responses in several organisms. Seven Sir2-homologs have been identified in humans and three of these *sirtuins*, SIRT3, SIRT4 and SIRT5 are targeted to mitochondria [2]. The mouse counterparts of human SIRT3, 4 and 5 (mSIRT3, 4, 5) also show mitochondrial localization [3,4,5]. The human SIRT3 (hSIRT3) deacetylates the mitochondrial acetyl-CoA synthetase, AceCS2 [6,7], and, in human, SIRT3 and, in mouse, both SIRT3 and SIRT4, interact with glutamate dehydrogenase [5,8,9]. SIRT3, 4 and 5 knock-out mice show no evident phenotype, except for hyperacetylation of mitochondrial proteins in the absence of SIRT3 [5]. Curiously, and unexpectedly for a mitochondrial protein, over-expression of mSIRT3 in mouse adipocytes led to increased expression of several mitochondria-related proteins such as uncoupling protein UCP1, and to an increase in cellular respiration [3].

Despite a high degree of conservation between the mouse and human sirtuins, the reported mouse SIRT3 cDNA encodes a protein that lacks most of the mitochondrial targeting signal present in the human protein. Questions whether SIRT3 is truly mitochondrial [10] and whether the existing mSIRT3 cDNA is complete have therefore been raised.

We set out to look for novel transcripts of mSIRT3. An *in silico* analysis of mSIRT3 cDNA sequences predicted the presence of a splice variant that introduces two potential translational start sites [11] upstream of the one described previously [3,12]. These potential start sites Met1 and Met15, correspond to Met1 and Tryp15, respectively, in the human SIRT3 gene. Here we describe the localization and proteolytic processing of the newly predicted proteins from cDNAs cloned from mouse 3T3 cells and compare their subcellular localization to the protein expressed from the existing mSIRT3 cDNA. In 3T3 cells and primary mouse hepatocytes the two longer mSIRT3 isoforms M1 and M2, beginning from Met1 and Met15, respectively, are mitochondrial and are both proteolytically processed to a form that corresponds in size to endogenous mSIRT3. The previously reported mSIRT3 isoform, which was over-expressed in mouse adipocytes, and was previously reported to be mitochondrial [3], shows a distinct cytoplasmic distribution that is not consistent with mitochondrial localization. Moreover, it is shorter in size than the endogenous, processed mSIRT3.

## Results and Discussion

The mSIRT3 isoform predicted by Yang et al., [12] and used in over-expression studies by Shi et al., [3] begins from a methionine codon corresponding to position 143 in the human SIRT3 amino acid sequence. This implies that the mouse SIRT3 protein is significantly shorter than its human counterpart. In a previous study [11], we questioned the mitochondrial localization of this truncated protein, examined the available mSIRT3 sequence data and found evidence of a SIRT3 splice variant that included two potential translational start sites at Met1 and Met15, corresponding to Met1 and Tryp15 of the human SIRT3 gene. Here, using a specific oligo that overlapped with the mSIRT3 stop codon, we made cDNA from polyA RNA isolated from mouse NIH3T3 fibroblasts. Subsequent PCR and cloning using the same reverse oligo and a forward oligo complementary to the region of exon 1B containing the predicted M1 start codon [11] yielded 2 distinct cDNAs. These two cDNAs are distinguished by the insertion of an additional 8 bp at the 5′extremity of exon 2 in splice variant 2 (Figure 1). This 8 bp is present in the originally suggested major mRNA/cDNA suggested by Yang et al., [12]. It would theoretically induce a frameshift in the translation of mSIRT3 initiated at the level of either Met 1 or Met 15 resulting in termination of translation at codon 66. In our hands, cloning and sequencing of 17 randomly selected cDNA clones yielded 9 clones without the 8 bp insertion (Genbank accession FJ621493), thus coding for the predicted full length protein, while 8 clones had the 8 bp insertion predicted to cause premature termination at codon 66. These findings suggest that at least in 3T3 cells both splice variants were present in roughly equal proportions.

To further study the different mSIRT3 proteins encoded by these different cDNAs, we generated three constructs. Two distinct constructs were generated from splice variant 1 using in the first case Met1, and in the second case Met15 as the initiation codon (primers 1F and 2F, Figure 1). The third construct was generated from splice variant 2 but using primer 1F (see Fig. 1). It thus included the Met 1 and Met15 initiation codons as well as the frameshift sequence leading to termination at codon 66. Translation from the mRNA of the splice variant 2 construct should yield an mSIRT3 protein which starts at the equivalent of the human Met143 (mSIRT3 Met78) and lacks a mitochondrial leader peptide. The protein products encoded by the three constructs will hereafter be referred to as M1, M2 and M3, respectively (see also Fig. 1). All three constructs included a 3′ in frame sequence for the FLAG epitope-tag.

To determine the subcellular localization of the different mSIRT3 isoforms, we used immunofluorescence in transiently transfected cells. Both M1 and M2 showed clear mitochondrial localization in 3T3 cells (Fig 2 a,b), which was further confirmed by co-staining with Mitotracker® Red. Despite the presence of two ATGs followed by a stop codon at position 66, the M3 construct generated a protein, which was detected using the FLAG antiserum. This would indicate that the cDNA encoded a protein starting at the third methionine. The protein encoded by this construct, called M3, showed a non-mitochondrial uniform cytosolic and sometimes nuclear staining with some clusters in case of (rare) high levels of over-expression (Fig 2c). Based on the immunofluorescence, M3 was generally expressed at lower levels than M1 and M2 and a much lower number of cells could be identified as clearly positive. We conclude that the proteins M1 and M2, starting from translational start sites at Met1 and Met15, respectively, yield proteins that are mitochondrial, whereas the shorter M3, which is the previously predicted full-length mouse Sirt3 protein, is not targeted to mitochondria.

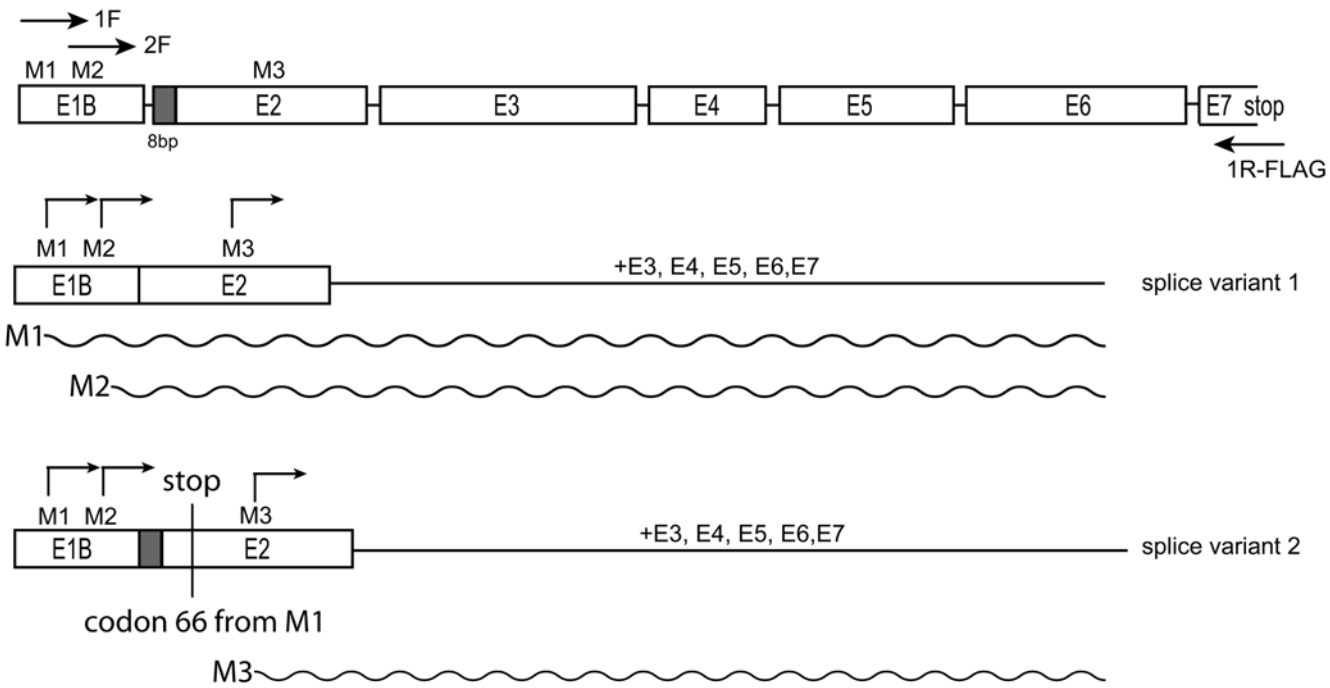


**Figure 1. Schematic representation of the coding sequence of mSIRT3 splice variants.** Met1 (M1) and Met15 (M2) are in exon 1B (E1B) (nomenclature according to Yang et al., [12]), Met78 (M3, equivalent to M143 in hSIRT3) in exon 2 (E2). M1 and M2 were cloned from cDNA derived from mouse NIH3T3 cells using exon 1B specific forward primers (1F and 2F in picture) and a reverse primer that included the sequence for the FLAG epitope-tag, binding at exon 7. Similarly, the second splice variant that can only result in an mSIRT3 protein when translation initiates at the third ATG (for M3) was obtained using the 1F and reverse oligo. Predicted proteins M1, M2 and M3 are indicated with a wave-line.
doi:10.1371/journal.pone.0004986.g001

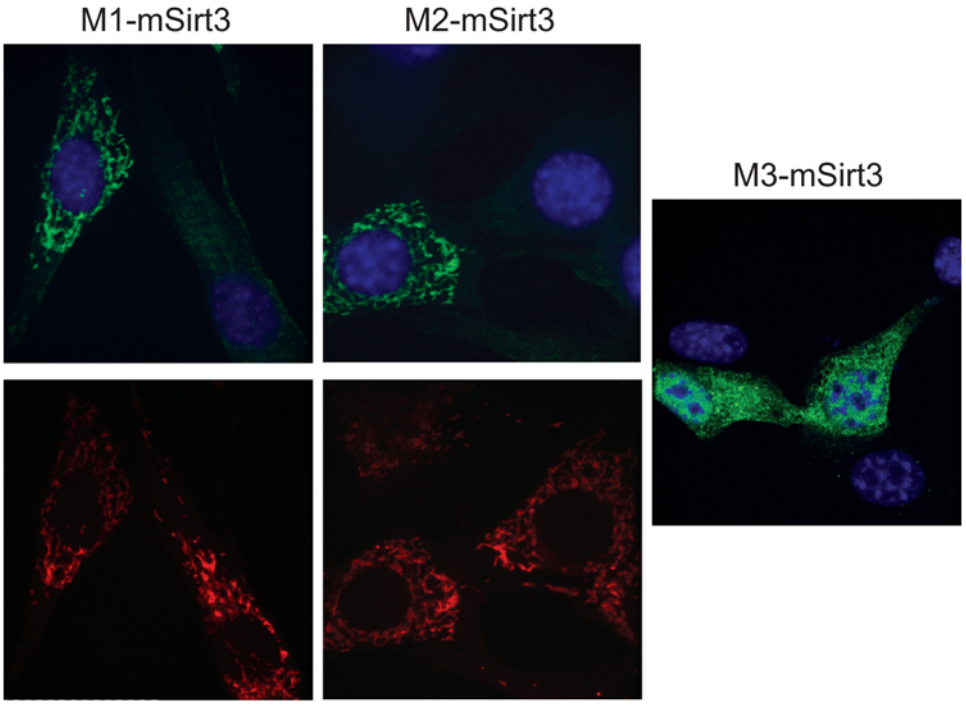


**Figure 2. Mouse SIRT3 variants M1 and M2 show mitochondrial localization, whereas M3 does not.** Three FLAG-tagged mSIRT3 variants M1, starting at Met1 (A), M2, starting at Met15 (B) and M3, starting at Met78 (C), were over-expressed in mouse 3T3 cells. Two days after transfection, proteins were detected by immunofluorescence with an anti-FLAG antibody. The results show that M1 and M2 give a typically mitochondrial localization pattern, upper panel (confirmed by Mitotraker® Red staining, lower panel). M3, on the other hand is more uniformly distributed in the cytoplasm and does not show mitochondrial localization.
doi:10.1371/journal.pone.0004986.g002

We studied the expression profile of the mSIRT3 isoforms by Western blot using either an antibody against the FLAG epitope tag for the detection of over-expressed FLAG-tagged variants or an antibody specific for mouse SIRT3 for the detection of endogenous and over-expressed proteins. Human SIRT3 has previously been shown to be cleaved into an enzymatically active form by mitochondrial processing peptidase MPP [13]. Expression from both the M1 construct (starting at Met1) and the M2 construct (starting at Met15) could be detected as 2 major forms: an uncleaved precursor (indicated by arrows 'M1' and 'M2', respectively) and an identical processed form (indicated by 'proM1–2'), which corresponded in size to the endogenous protein (including the epitope tag). This expression pattern was seen upon over-expression in 3T3 cells (Fig 3A, right part for 'endogenous Kozak'), and was more clearly visible in mouse hepatocytes (Fig 3B) as well as in human embryonal kidney (HEK) 293T cells (Fig 3C). The M2 variant seemed to be processed more efficiently than M1. This conclusion is based on the observation that the ratio of the cleaved form versus the uncleaved precursor appeared higher for M2 compared to M1 in all cell types examined. Especially in 3T3 and HEK293 cells, the precursor protein from the M2 construct was often barely visible (see panels 3A and C) unless expression was boosted by replacing the endogenous sequence upstream of the start codon by a consensus Kozak sequence, as can be seen in the left part of Figure 3A. Introduction of the consensus Kozak, in particular into the M2 construct, helped to clearly identify the precursor and cleaved form of the M2 protein in 3T3 cells. The full-length M1-encoding vector also gave rise to a protein, which was the same size as the precursor protein expressed from the M2-encoding vector. This observation suggests that translation also initiated at Met15 in the M1 construct; at low levels in 3T3 cells and mouse hepatocytes but seemingly at much higher levels in HEK293 cells. Accumulation of uncleaved precursor was also clearly detected in human cells over-expressing full length hSIRT3 (Fig 4 and not shown), suggesting that this is not a peculiarity of the mouse SIRT3 protein but rather something that SIRT3 proteins from various species have in common.

Detection of the M3 variant in total lysates and mitochondrial fractions from 3T3 cells was weak at best (Fig 3A and Fig S1). This is in agreement with the poor expression observed by immunofluorescence. Detection was more clear in total lysates from mouse hepatocytes and HEK293 cells (Fig 3B and C). The corresponding human variant of the protein (translation from M143) was not enriched in mitochondrial fractions and was shown to be non-mitochondrial by immunofluorescence ([11], Fig. 4 and not shown). The FLAG-tagged mSIRT3 M3 protein in mouse hepatocytes migrated on SDS-PAGE as a single band which was, despite the tag, smaller than endogenous (untagged) mSIRT3 (Figure 3B, compare bands indicated by 'M3' and 'endogenous' respectively). Furthermore, over-expression of non-tagged versions of M1 and M2 in 293T cells showed processed proteins larger than the FLAG-tagged M3 but identical in size to endogenous mouse liver SIRT3. These results raise significant questions regarding the physiological significance of the splice variant coding for the mouse SIRT3 protein variant M3.

Sir2-orthologues are well conserved from yeast to man. The identification of a mouse SIRT3 cDNA encoding a mSIRT3 protein significantly smaller than its human counterpart raised the possibility that the reported [12] mouse SIRT3 cDNA was incomplete. Careful analyses of available sequence data led to the discovery of putative longer mSIRT3 transcripts. We have confirmed our *in silico* findings [11] by cloning longer mSIRT3

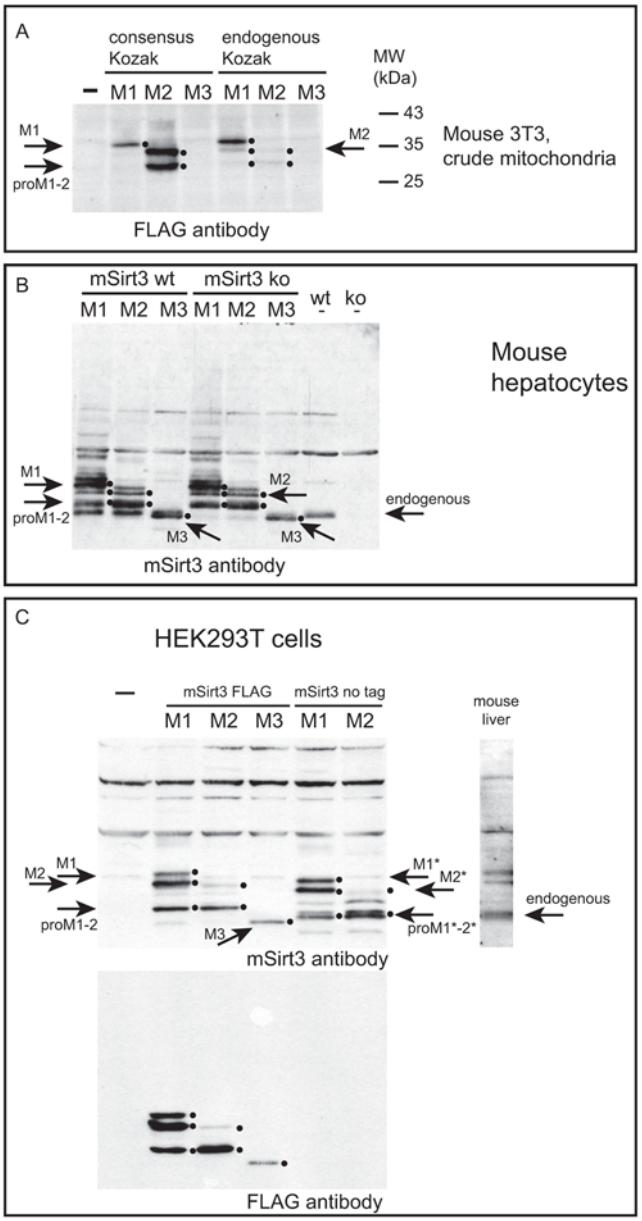


**Figure 3. Over-expressed variants M1 and M2 appear in two forms.** FLAG-tagged mSIRT3 variants M1, M2 and M3 were expressed in 3T3 cells (A) and primary mouse hepatocytes from both wild type and ko-mice (B) while both FLAG-tagged M1–3 and untagged M1 and M2 were expressed in HEK293T cells (C). Crude mitochondrial lysates (3T3 cells, panel A) or total cell lysates (mouse hepatocytes and HEK293T cells, panels B and C) were analysed by western blot with an anti-FLAG antibody and an antibody against mSIRT3 as indicated in the various panels. In an attempt to boost expression, all three variants were also analyzed in 3T3 cells only, using constructs into which we introduced a consensus Kozak sequence, 5′CCACC (using PCR cloning), immediately upstream the respective ATG for M1–3 (Left part of panel A). A mouse liver extract was run alongside the HEK293T derived samples (panel C) to denote the size of endogenous mSIRT3 (indicated by →'endogenous'). Similarly, non-transfected wild-type (wt) and mSirt3 knock-out (ko) mouse hepatocytes were run along transfected samples to clearly detect the endogenous protein (panel B, →'endogenous'). In all cases both M1 and M2 constructs yielded an un-processed precursor (indicated by →M1 and M2 for the FLAG tagged protein, and →M1* and M2* for the untagged variants) and a processed mature protein (indicated by→proM1–2, and →proM1*–2*), the latter corresponding in size to the endogenous mSIRT3 (panel C). Translation of M2 but not M1 or M3, was greatly improved with the consensus Kozak sequence (panel A). M2 was processed more efficiently than M1 (all three panels). M2 processing may even account for all of the processed over-expressed protein in M1 lanes, since the M1 construct was also transcribed to yield a band the size of M2 in all cell types (all panels). In each panel we have emphasized detected proteins using small dots right from the appropriate bands. Over-expressed M3 is shorter than endogenous mSIRT3 and was undetected or only weakly detected in 3T3 total cell lysates (Figure S1 and not shown) or 3T3 mitochondrial lysates (panel A and not shown), but could clearly be detected in mouse hepatocytes and HEK293 cells (panels B and C, indicated by →M3). Membranes for total and mitochondrial 3T3 lysates were also analysed for a control cytoplasmic and mitochondrial protein in particular to illustrate the quality of the mitochondrial fractions (Figure S1).
doi:10.1371/journal.pone.0004986.g003

cDNAs. We made DNA constructs with different transcriptional start sites and show here that the longer mSIRT3 variants, M1 and M2 beginning at Met1 and Met15, respectively, are targeted to mitochondria. M3, the previously predicted full length protein, which begins at Met78 of the newly identified full length protein M1, does not localize to mitochondria.

Interestingly, human SIRT3 does not have a methionine at position 15, nor do other studied mammalian SIRT3 cDNAs. Since we observed that translation using the M1 construct yielded both the M1 and M2 precursor in varying amounts depending on the cell type used (Fig 3), it is conceivable that the choice of the mSIRT3 translation initiation site (Met1 vs. Met15) described here serves a regulatory role resulting in the expression of proteins with differing levels of proteolytic processing in mitochondria. Studying the physiological consequences of over-expressing M1 and M2 may help in elucidating possible different physiological roles for different SIRT3 forms.

## Materials and Methods

### Reagents and antibodies

All reagents used in this study were of analytical grade. Anti-c-Myc 9E10 monoclonal antibody was purchased from Roche Molecular Biochemicals. Anti-FLAG M2 monoclonal antibody was purchased from Sigma. Anti-hSIRT3 was purchased from Santa Cruz. Anti-mSIRT3 serum was homemade [5].

### Cloning

Mouse NIH3T3 total RNA was isolated using Trizol reagent (Invitrogen) and was enriched for polyA RNA using the Oligotex® kit (Qiagen). First strand cDNA synthesis (Superscript II kit, Invitrogen) used an mSIRT3 specific oligo including a restriction (NotI) and FLAG epitope sequence as follows: NotI/FLAG-mSirt3R-5′-GCA TGC GGC CGC TCA CTT ATC GTC GTC ATC CTT GTA ATC TCT GTC CTG TCC ATC CAG C-3′. PCR amplification of cDNA used the NotI/FLAG-mSirt3R and one of the following forward oligos to amplify cDNA from the M1 or M2 codon from within exon 1B (see Fig. 1 and main text): HindIII-M1-mSirt3- 5′-CTT AAG CTT ATT CGG ATG GCG CTT GAC CC-3′; HindIII-M2-mSirt3- 5′-CTT AAG CTT AGC ATC ATG GCG CTA AGC GG-3′. PCR used standard conditions with Pfu polymerase and the amplified cDNA was initially cloned using Zero-blunt cloning (Invitrogen), and selected clones partially sequenced to identify those cDNAs that did or did not include the 8 bp extension to exon 2 (see Fig. 1). Fully sequenced clones for both splice variants were subsequently recloned into pcDNA5/FRT/TO (Invitrogen) using the HindIII/NotI restriction sites. All subsequent recloning, e.g. to introduce a consensus Kozak and/or stop codon used these original clones and

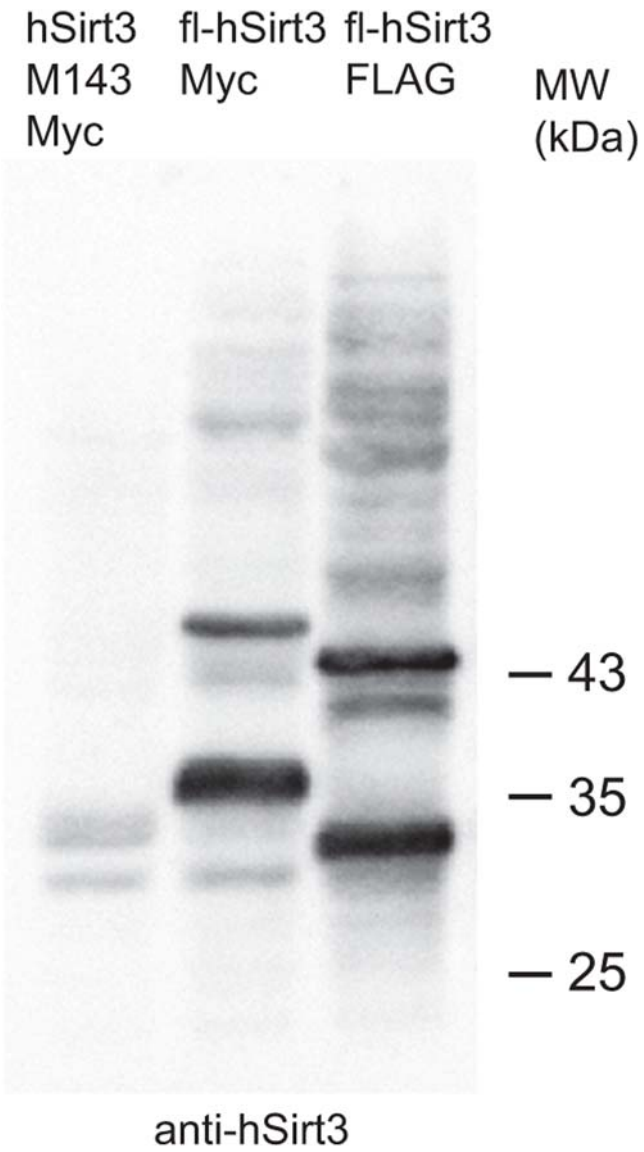


**Figure 4. Human SIRT3 corresponds in its expression pattern to mSIRT3.** Full length (fl) MycHis (Myc) and FLAG tagged versions of hSIRT3, or a truncated MycHis tagged version starting at Met143 (M3 in mouse) were expressed in human HEK293 EBNA cells and crude mitochondrial fractions were prepared for Western blot analysis using an hSIRT3 antibody. The results show that the truncated version is only weakly detected in the mitochondrial fraction in agreement with its mostly cytoplasmic localization [11]. Over-expression of the full length proteins shows the clear presence of both the precursor and mature forms of hSIRT3.
doi:10.1371/journal.pone.0004986.g004

standard PCR and cloning methods. All constructs were completely sequence verified.

## Cell culture and transfections

HEK293T cells and NIH3T3 cells were grown in DMEM (Dulbecco's modified Eagle's medium) (Sigma) with 2 mM L-glutamine (Cambrex Biosciences) and 10% FCS (foetal calf serum) (Euroclone) unless stated otherwise. For immunofluorenscence cells were transfected using Lipofectamine$^{TM}$2000 transfection reagent (Invitrogen) according to the manufacturer's instructions and using 1 μg of DNA per well on a 6-well plate. For Western blot analysis cells were similarly transfected using Lipofectamine$^{TM}$2000 with 3 μg of DNA per 10 cm plate.

Mouse hepatocytes were isolated from H129sv male mice according to a two-step collagenase perfusion technique described by LeCluyse et al [14]. Briefly, the liver was flushed via the portal vein with a calcium-chelating buffer for 3 to 5 min, followed by perfusion with collagenase, for an additional 8 min. At the end of the digestion, the liver was removed and transferred to a sterile dish and minced thoroughly with scissors. Purified isolates contained 88% hepatocytes. Purified hepatocytes in hepatocyte plating medium containing 5% fetal bovine serum, insulin-transferrin-selenium-G (1×), 50 U/ml penicillin/streptomycin, and 2 mM L-glutamine, were seeded onto culture dishes pre-coated with collagen type I. Hepatocytes were allowed to attach at 37°C for 2 to 3 h in a humidified chamber gassed with 95% air and 5% $CO_2$ and transfected with different mouse SIRT3 expression constructs using Lipofectamine$^{TM}$2000. 24 hours after transfection, cell lysates were prepared by directly adding 1× SDS sample buffer to the cells.

## Animals

All animal experiments were carried out under protocols approved by the Committee on Animal Research at the University of California, San Francisco.

## Immunofluorescence

For immunofluorescent detection, cells were grown on coverslips in 6 well plates. Following transfection for 1–2 days cells were fixed using either 3.3% PFA (paraformaldehyde) in cell culture medium for 25 min or in methanol for 5 min at −20°C [15]. This was followed by three washes in PBS and lysis for 10 min with 0.5% Triton X-100 in PBS/10% FCS after PFA fixation. No lysis step was performed after methanol fixation. Primary and secondary antibodies were incubated at recommended concentrations in PBS/10% FCS for 1 h or overnight. Mitotracker® Red CMXRos treatment was performed prior to fixation essentially as described previously [16]. Slides were mounted using ProLong® Gold antifade with DAPI (4_,6- diamidino-2phenylindole; Invitrogen). Image acquisition using confocal microscopy was carried out as described [17], using an Andor iXon DV885 EMCCD camera and the Andor iQ software (Andor). Images were further processed using Photoshop CS2.

## Western Blotting

After detaching NIH3T3 cells and HEK293T cells were isolated by centrifugation (1200 rpm for 2 min at +4°C) and washed once with ice-cold PBS. For isolation of crude mitochondrial fractions by hypotonic lysis and differential centrifugation, the cell pellet was resuspended by gentle pipetting in 2–3 vol of ice-cold homogenization buffer [4 mM Tris/HCl (pH 7.8), 2.5 mM NaCl, 0.5 mM MgCl2 and 0.1 mM PMSF], kept on ice for 6 min, then homogenized in a glass homogenizer with 20–25 strokes of a tight-fitting pestle. Disruption of the cells was monitored by microscopy. A one-ninth volume of 10×homogenization buffer was added following lysis and nuclei and cell debris were pelleted by centrifugation at 1200 ***g*** for 3 min at 4°C. Mitochondria from the post-nuclear supernatants were recovered by centrifugation at 12000 ***g*** for 3 min at 4°C. Mitochondrial pellets were washed once with 1 ml of ice-cold PBS and the mitochondrial pellet was lysed 15 min on ice in 50 mM Tris/HCl (pH 7.5), 150 mM NaCl, 1 mM EDTA and 1%Triton X-10. An equal volume of 2× Laemmli sample buffer was added and the sample was denatured at 95°C for 5 min prior to SDS/PAGE. Western blot analysis by ECL (enhanced chemiluminescence) was performed essentially as

described previously [18]. Western blot analysis used pre-stained broad-range markers from Fermentas. Peroxidase-coupled secondary anti-mouse and anti-rabbit antibodies were obtained from Vector Laboratories. In some instances the Supersignal® West Femto Maximum kit (Pierce) was used for detection according to the manufacturer's protocol. Detection and quantification used a Bio-Rad Chemi Doc XRS system.

## Supporting Information

**Figure S1** FLAG-tagged mSIRT3 variants M1, M2 and M3 expressed in 3T3 cells. (A) Similar amounts of total cell and crude mitochondrial lysates from cells expressing mSirt3 variants M1-3 from plasmids with endogenous Kozak sequences 5′ of the respective ATG start codons. (B) Samples from cells expressing mSirt3 variants M1-3 from plasmids with consensus Kozak sequences 5′ of the respective ATG start codons. To illustrate the quality of mitochondrial lysates, membranes were reprobed to detect the cytosolic marker protein gamma-Actin (polyclonal antibody from Novus Biologicals) and the mitochondrial marker protein subunit I of cytochrome c oxidase (COXI, monoclonal antibody from Invitrogen). These results illustrate the poor expression of the M3 variant in 3T3 cells as it is not clearly visible in mitochondrial nor in total cell lysates. The only modest enrichment of the mSirt3 proteins in the mitochondrial lysates is typical for transient over-expression of mitochondrial proteins. Transient expression in our experience always results in a mosaic of expressing cells with a considerable population of cells expressing transgenes at such high levels that they show cytosolic clustering (reminiscent of inclusion body formation in bacterial expression) and aberrant targeting. Marked arrows are as in Figure 3.

Found at: doi:10.1371/journal.pone.0004986.s001 (0.08 MB PDF)

## Author Contributions

Conceived and designed the experiments: HMC JYH EV JNS. Performed the experiments: HMC JYH JNS. Analyzed the data: HMC JYH EV JNS. Wrote the paper: HMC EV JNS.

## References


1. Kaeberlein M, McVey M, Guarente L (1999) The SIR2/3/4 complex and SIR2 alone promote longevity in Saccharomyces cerevisiae by two different mechanisms. Genes Dev 13: 2570–2580.
2. Michishita E, Park JY, Burneskis JM, Barrett JC, Horikawa L (2005) Evolutionarily conserved and nonconserved cellular localizations and functions of human SIRT proteins. Mol Biol Cell 16: 4623–4635.
3. Shi T, Wang F, Stieren E, Tong Q (2005) SIRT3, a mitochondrial sirtuin deacetylase, regulates mitochondrial function and thermogenesis in brown adipocytes. J Biol Chem 280: 13560–13567.
4. Nakamura Y, Ogura M, Tanaka D, Inagaki N (2008) Localization of mouse mitochondrial SIRT proteins: shift of SIRT3 to nucleus by co-expression with SIRT5. Biochem Biophys Res Commun 366: 174–179.
5. Lombard DB, Alt FW, Cheng HL, Bunkenborg J, Streeper RS, et al. (2007) Mammalian Sir2 homolog SIRT3 regulates global mitochondrial lysine acetylation. Mol Cell Biol 24: 8807–8814.
6. Hallows WC, Lee S, Denu JM (2006) Sirtuins deacetylate and activate mammalian acetyl-CoA synthetases. Proc Natl Acad Sci U S A 103: 10230–10235.
7. Schwer B, Bunkenborg J, Verdin RO, Andersen JS, Verdin E (2006) Reversible lysine acetylation controls the activity of the mitochondrial enzyme acetyl-CoA synthetase 2. Proc Natl Acad Sci U S A 103: 10224–10229.
8. Schlicker C, Gertz M, Papatheodorou P, Kachholz B, Becker CF, et al. (2008) Substrates and Regulation Mechanisms for the Human Mitochondrial Sirtuins Sirt3 and Sirt5. J Mol Biol 382: 790–801.
9. Haigis MC, Mostoslavsky R, Haigis KM, Fahie K, Christodoulou DC, et al. (2006) SIRT4 inhibits glutamate dehydrogenase and opposes the effects of calorie restriction in pancreatic beta cells. Cell 126: 941–954.
10. Scher MB, Vaquero A, Reinberg D (2007) SirT3 is a nuclear NAD+-dependent histone deacetylase that translocates to the mitochondria upon cellular stress. Genes Dev 21: 920–928.
11. Cooper HM, Spelbrink JN (2008) The human SIRT3 protein deacetylase is exclusively mitochondrial. Biochem J 411: 279–785.
12. Yang YH, Chen YH, Zhang CY, Nimmakayalu MA, Ward DC, et al. (2000) Cloning and characterization of two mouse genes with homology to the yeast Sir2 gene. Genomics 69: 355–369.
13. Schwer B, North BJ, Frye RA, Ott M, Verdin E (2002) The human silent information regulator (Sir)2 homologue hSIRT3 is a mitochondrial nicotinamide adenine dinucleotide-dependent deacetylase. J Cell Biol 158: 647–657.
14. LeCluyse E, Bullock P, Madan A, Carroll K, Parkinson A (1999) Influence of extracellular matrix overlay and medium formulation on the induction of cytochrome P-450 2B enzymes in primary cultures of rat hepatocytes. Drug Metab Dispos 27: 909–915.
15. Malka F, Auré K, Goffart S, Spelbrink JN, Rojo M (2007) The Mitochondria of Cultured Mammalian cells. In: Leister D, Herrman JM, eds. Mitochondria Practical Protocols, vol 372 Humana press. pp 3–16.
16. Goffart S, Martinsson P, Malka F, Rojo M, Spelbrink JN (2007) The Mitochondria of Cultured Mammalian cells. In: Leister D, Herrman JM, eds. Mitochondria Practical Protocols, vol 372 Humana press. pp 17–32.
17. Garrido N, Griparic L, Jokitalo E, Wartiovaara J, van der Bliek AM, et al. (2003) Composition and dynamics of human mitochondrial nucleoids. Mol Biol Cell 14: 1583–1596.
18. Spelbrink JN, Toivonen JM, Hakkaart GA, Kurkela JM, Cooper HM, et al. (2000) In vivo functional analysis of the human mitochondrial DNA polymerase POLG expressed in cultured human cells. J Biol Chem 275: 24818–24828.